TOTAL BODY KINETICS. OUR WINDOW INTO THE SYNERGIES OF HUMAN MOVEMENT

David A. Winter
Department of Kinesiology
University of Waterloo
Waterloo, Ont. CANADA

INTRODUCTION

The famous Russian scientist, Bernstein, in his inciteful predictions (1967) regarding total body motor control, postulated the "principle of equal simplicity" where "it would be incredibly complex to control each and every muscle." Our challenge, as researchers, is to see how the CNS actually controls a 3D multisegment system towards a common goal or goals. Gait is a particularly demanding movement in terms of complimentary and competitive goals; the stance and swing limbs appear to have separate agendas and the large common segment (H.A.T) joining the two lower limbs must be balanced against large perturbing forces.

OUR FIRST CHALLENGE - RECOGNIZE REDUNDANCY AND IDENTIFY COMMON GOALS

Before we attempt to pinpoint synergies we must recognize the anatomical organization of the neuromuscular system. It is a huge converging system starting with the individual motor unit, then to a recruitment strategy to generate individual muscle tension, then the algebraic contributions of each agonist and antagonist to individual joint moments and finally to synergistic combinations of moments-of-force. Such a converging system is highly redundant and again Bernstein (1967) observed that "the coordination of a movement is the process of mastering redundant degrees of freedom and its conversion to a controlled system" To identify what degrees of freedom are being mastered is our goal. It does not come easily and often requires years of observation of both normal and pathological movement. The value of studying pathological movement is that the CNS has had to adapt the kinetic patterns and by scrutinizing the changed patterns we can often identify a synergistic pattern. Also, by applying controlled perturbations to the movement we can identify synergistic responses (cf. Horak and Nashner, 1986)

EXAMPLES OF TOTAL LIMB OR TOTAL BODY SYNERGIES

Three quite different examples are presented to demonstrate synergies present during standing and walking. The first was identified 15 years ago (Winter, 1980) and has subsequently been expanded and explained (Winter, 1984). The second is a total body response to a potential trip (Eng, et al. 1994) and the third is the total body's balance response in the frontal plane during quiet and perturbed standing (Winter, et al. 1993)

SUPPORT SYNERGY

The notion of a total limb support synergy during stance phase of gait resulted from a major adaptation that was seen in a knee replacement patient. For years prior to her surgery the pain due to osteoarthritis had forced her not to use her quadriceps during weight bearing. She compensated by using her hip extensors and achieved a safe weight bearing. This adaptive trade-off was part of a total limb defence against collapse and was quantified as a support moment, $M_s = M_h + M_k + M_a$, where extensor moments are positive. A positive and somewhat invariable M_s is seen in all normals and patients. On repeat trials of the same subject we see low variability in M_s in the presence of high variability in M_h and M_k (Winter, 1984). Such findings demonstrate the tremendous redundancy of the many flexors/extensors at all three joints which is mastered by a single kinetic pattern, M_s. The reasons for the high variability in M_h are the demands of balance of the large H.A.T. segment on a stride-to-stride basis. Thus the support synergy is a CNS response to keep the vertical support

constant at the same time as responding to the variable stride-to-stride demands of H.A.T balance.

TRIPPING RESPONSE

The goal of the CNS during swing is to achieve a safe and efficient trajectory of the foot. Thus a safe toe clearance and a gentle heel contact are the goals. Our biomechanical analysis of the degrees of freedom in the stance and swing limbs reveals that six angular changes have major influences over the toe clearance (Winter, 1992). Thus we would predict that any or all of the muscles controlling those joints could respond in a trip during swing. In actual fact four of the six muscle groups responded together in a total "elevator strategy" when a trip was induced early in swing (Eng, et al. 1994) The swing knee flexors, the stance hip abductors and the stance ankle plantarflexors all responded with the shortest latencies to extend the stance limb, raise the pelvis and flex the swing limb. Interestingly, the swing tibialis anterior, traditionally responsible for toe clearance was not only late but inconsistent in its response. The swing hip flexors responded consistently but with a longer latency than the first three muscles. If the trip were induced late in swing the response changed completely, no longer was an elevator response the goal of the CNS, rather an extensor response was evident showing that these synergic responses were phase dependent.

MEDIAL-LATERAL BALANCE DURING STANDING

Quiet standing has been heavily researched in the anterior/posterior (A/P) direction and an ankle strategy was evident during quiet standing and low level platform perturbations However, a hip strategy is utilized when the ankle cannot act (Horak and Nashner, 1986) Most researchers have assumed that M/L balance is also controlled at the ankle during quiet stance A biomechanical analysis of frontal plane balance shows there are four control sites two sets of ankle invertors/evertors and two sets of hip abd/adductors Theoretically, each site can control equally well However, our anatomy demonstrates a major conflict when the ankle invertors/evertors act because they also have dominant responsibilities as dorsiflexors and plantarflexors. Also, because of the narrow width of the feet the maximum ankle inversion/eversion moment is about 10 N.m, whereas the hip abd/adductors can generate 150 N m Thus biomechanics and anatomy predicts that the only independent control of M/L balance would be a hip load/unload mechanism by the hip abd/adductors (Winter, et al. 1993) Only through the use of two force platforms can we see this motor action, as one limb loads by a few % the opposite limb unloads by exactly the same %. Thus the centre of pressure (COP) movement between the two feet moves solely because of hip motor action and not because of COP changes under each foot.

REFERENCES

Bernstein, NA (1967). The coordination and regulation of movements Pergamon Press, Oxford.

Eng, JJ, Winter, DA, Patla, AE (1994) Neuromuscular strategies for recovery from a trip in early and late swing during human walking. Exp. Brain Res. 102, 339-349

Horak, FB, Nashner, LM (1986). Central programming of postural movements: adaptation to altered support surface configurations. J Neurophysiol 55, 1369-1381

Winter, DA (1980). Overall principle of lower limb support during stance phase of gait J Biomech. 13, 923-927

Winter, DA (1984). Kinematic and kinetic patterns in human gait. Variability and compensating effects. Hum. Movement Sci 3, 51-76.

Winter, DA (1992). Foot trajectory in human gait - a precise and multifactorial motor control task. Phys. Therap. 72, 45-56.

Winter, DA, Prince, F, Stergiou, P, Powell, C (1993) M/L and A/P motor responses associated with COP changes in quiet standing. Neurosci. Res. Commun. 12, 141-148, 1993.

FUNCTIONAL ADAPTATION OF BONE TO PHYSIOLOGICAL AND MECHANICAL STIMULI

Ronald F. Zernicke, Ted S. Gross, and Stefan Judex
Department of Surgery, McCaig Centre for Joint Injury and Arthritis
University of Calgary, Calgary, Canada

In the last three decades, great emphasis has been placed on understanding the ability of bone to alter its mass and morphology in response to physiological and mechanical stimuli. In that light, here, we focus on how selected stimuli (diet, exercise, vascular response) initiate and mediate adaptation in the skeleton.

In the healthy adult skeleton, a coordinated interplay (remodeling) occurs between osteoclasts and osteoblasts, in which the bone-resorbing osteoclasts are first recruited, and then followed by the recruitment and differentiation of osteoblasts to fill in the newly excavated surface.[4] As the primary reservoir of body calcium, the skeleton must fulfill dual—at times antagonistic—roles in maintaining the metabolic homeostasis and structural integrity of the body. A variety of imbalanced systemic states (vitamin D deficiency, hyperparathyroidism, menopause) affect recruitment and activity of osteoclasts and osteoblasts, and, as a result, dramatically influence skeletal mass. Obviously, dietary calcium plays a central role in skeletal health[7], but recently, we examined other influences of diet on bone.[9,13,14,15] Both short-term[9,13] and long-term[14] exposure to high fat and sucrose (HFS) diets markedly influence rat axial and appendicular bone mechanical integrity. After 2 yr on either an HFS diet or a low-fat complex-carbohydrate (LFCC) diet, we found that the vertebrae of rats on the HFS diet withstood significantly smaller loads and compressional stress and were significantly less stiff than LFCC vertebrae. Also, the femoral necks from the HFS rats withstood significantly smaller mechanical stress and had an increased ratio of trabecular-to-cortical bone. In immature vertebrae and femoral necks in trained versus untrained rats fed either a recommended- or high-protein diet, we[15] found that coupling high dietary protein with exercise attenuated the adverse affects of strenuous exercise on immature rat bone, particularly in the weight bearing femoral neck.

In adults, long-term training elevates bone mass, but the specific parameter responsible for controlling that adaptation has not been identified. Numerous mechanical parameters have been proposed, including: strain magnitude[12], frequency[11], and history[2] and strain energy density.[8] Recently Gross and colleagues[5] applied exogenous loads to turkey radii and found that sites of periosteal new bone formation correlated poorly with sites of peak strain magnitude, but strongly related to sites with large circumferential strain gradients. We are now measuring strain gradients generated during normal locomotion and identifying changes in stimuli related to running speed, to predict sites of exercise-induced adaptation. Three triple rosette strain gages are attached to the medial, lateral, and anterior cortices of the diaphyseal tarsometatarsus (TMT) in mature White Leghorn roosters, as they walk and run on a treadmill. Using linear beam theory, the distribution of longitudinal normal strain acting on the mid diaphysis cross-section is determined. The cortex is divided into 12 equal-angle pie sectors, and the circumferential strain gradient within each sector is calculated. We are finding that despite a 3-fold increase in locomotor speed, peak compressive and tensile strains and the location of the neutral axis vary little during the stance phase of each gait (**FIG 1**), but maximum strain gradient magnitudes are non uniform in distribution (**FIG 2**). The range of functionally induced gradients is not altered by running speed. We are also investigating whether uphill or downhill running more substantially alters these gradients, thereby providing a larger stimulus for adaptation.

While mechanical stimuli undoubtedly play a vital role in skeletal adaptation, profound vascular adaptation (hyperemia, angiogenesis) also plays a role. Cellular and molecular data indicate that endothelial cells, if stimulated by fluid flow, express peptides that act directly upon bone cell populations, or alternatively, as paracrine regulators of bone cell activity.[1,10] Thus, endothelial cells (through a flow mediated pathway) may play an active—rather than passive—role in regulating bone cell activity.[3] To examine this hypothesis, we assessed the relation between bone blood flow and bone structural integrity following joint injury in mature female New Zealand white rabbits (n=8 ACL transection, n=8 sham surgery).[6] Post surgery, rabbits ambulated either 14 or 48 wk, and then anesthesia was induced and colored microspheres were injected into the left ventricle. Cylindrical bone cores (3 x 6 mm) from the medial condyle of the each right femur were mechanically tested, the number of spheres trapped within the remaining subchondral bone was assessed, and standardized blood flow was determined. The 14 wk joint laxity was associated with a 76% *increase* in experimental bone blood flow and a 34% *decrease* in bone stiffness (blood flow and stiffness, r = –0.9). After 48 wk of joint laxity, mean flow in the ACL transected femurs was elevated 25% compared to sham controls. Stiffness in the 48 wk ACL group was degraded 54% in comparison with shams, but no significant correlation persisted between these measures. Thus, enhanced blood flow may more actively mediate tissue adaptation immediately post-trauma, and we are currently analyzing data at 2 and 6 wk post-injury to verify this hypothesis.

Our research highlights the interactive cellular, physiological, and mechanical facets of skeletal adaptation. By better understanding these facets of skeletal adaptation, more specific information may emerge to treat bone loss pathologies.

References

1) Alam *Endocrin* 130:3617;1992. **2)** Carter *J Biomech* 20:1095;1987. **3)** Fiorelli *J Bone Miner Res* 9:329;1994. **4)** Frost *Calcif Tissue Res,* 3:211;1969. **5)** Gross *Trans Orthop Res Soc* 19: 278;1994. **6)** Gross *Trans Orthop Res Soc* 20:795;1995. **7)** Heaney *Calcif Tissue Int* 49:S42;1991. **8)** Huiskes *J Biomech* 20:1135;1987. **9)** Li *Calcif Tissue Int* 47:308;1990. **10)** MacIntyre *Proc Natl Acad Sci* 88:2936;1994. **11)** McLeod *J Biomech* In press. **12)** Rubin *Calcif Tissue Int* 37: 411;1985. **13)** Salem *Am J Physiol* 262:R318; 1992. **14)** Zernicke *Bone* In press. **15)** Zernicke *Med Sci Sports Exerc* In press.

Acknowledgment

Supported in part by The Alberta Heritage Foundation for Medical Research, The Arthritis Society of Canada, The Medical Research Council of Canada, and The Natural Sciences and Engineering Research Council of Canada.

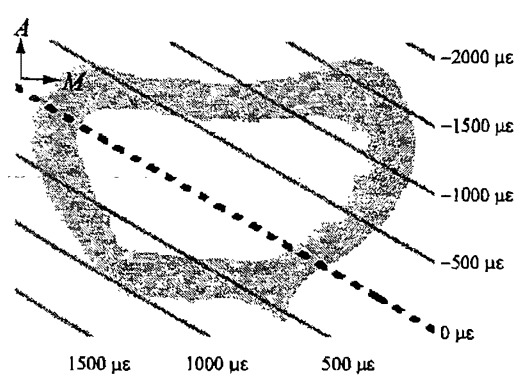

Fig 1. Diaphyseal cross section of TMT. (Anterior=A; Medial=M). Compression (–) and tension (+) strain isopleths are shown, along with the neutral axis (dashed line).

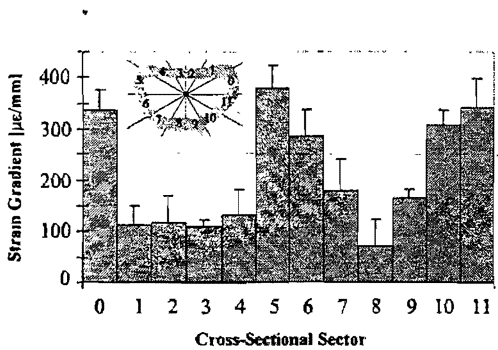

Fig 2. Maximum circumferential strain gradients *vs* TMT cross sectional sectors (12 equal-angle pie sectors) during a rooster step cycle.

Biomechanics of Knee Ligament Healing, Repair, and Reconstruction

Woo SL-Y, Chan SS, Yamaji T, Livesay GA
Musculoskeletal Research Center, Department of Orthopaedic Surgery,
University of Pittsburgh, Pittsburgh PA

Knee ligaments are tough bands of fibrous tissue that connect the femur to the tibia. Their nonlinear tensile properties are uniquely suited for maintaining smooth joint kinematics and limiting excessive joint motion. Nevertheless, the anterior cruciate ligament (ACL) and the medial collateral ligament (MCL) are frequently injured, accounting for 90% of all ligament injuries in young and active individuals.

The biomechanical properties of knee ligaments are generally determined in tension. Because these structures are relatively short and broad, their tensile properties must be derived from the testing of a bone-ligament-bone complex; femur-ACL-tibia complex (FATC), or femur-MCL-tibia complex (FMTC). With the introduction of video technology and improved methods of determining cross-sectional area, the structural properties of the complex, represented by the load-elongation curve, and the mechanical properties of the ligament substance, represented by the stress-strain curve, can be obtained from a single uniaxial tensile test [14] Ligaments also exhibit viscoelastic, or time- and history-dependent, behavior as a result of interactions between collagen, proteoglycan molecules, water, and other structural components in the tissue. Therefore, the loading and unloading curves do not follow the same path and form a hysteresis loop due to energy dissipation. Additionally, ligaments display typical stress-relaxation behavior.

In our laboratory, we have examined the effects of several physiologic factors on the basic biomechanical properties of ligaments using the rabbit MCL as a model. These studies have elucidated important biologic factors that affect the biomechanical properties; they include maturation and aging, immobilization/mobilization of the joint, and tension and exercise, all of which affect ligament remodeling [16]. We also have reported on experimental factors that significantly affect the ligament properties, including temperature, strain rate, ligament orientation and state of ligament hydration [16].

Armed with basic science data, our laboratory during the last decade has focused on (1) MCL repair and healing and (2) ACL reconstruction. Because the MCL is able to repair itself after an injury, it serves as a good model to study ligament healing. Earlier models had successfully tested MCL healing after a simple surgical transection [2, 5, 8]. Our recent work has concentrated on a clinically relevant model whereby "mop-end" types of tears in the ligament substance were created with concomitant damage to the insertion sites [13]. We have used such an injury model in rabbits to compare repair versus nonrepair of the rupture After histologic confirmation of insertion-site damage, biomechanical evaluation revealed that all MCLs were well healed 12 weeks after injury. However, the ligament substance and the insertion sites healed at asynchronous rates. At 6 weeks after injury, the ligament substance was stronger than the insertion sites. With time, the latter gained strength, and by 52 weeks, all tensile failures occurred in the midsubstance, confirming that the insertion sites were stronger. Moreover, although strength and function of the injured FMTC were totally recovered by 52 weeks, histologic and biomechanical results indicated that the properties of the healed ligament material remained inferior. We also found that primary repair had no advantage over nonoperative treatment [12].

The model was extended to address whether the MCL needs to be repaired in a combined ACL and MCL injury after surgical reconstruction of the ACL. We found that although MCL repair reduced varus-valgus laxity and improved structural properties of the FMTC in the first 12 weeks, the long-term effects of MCL repair were diminished by 52 weeks. Further, the stiffness of the FMTC and modulus of the MCL did not differ significantly between the repair and nonrepair groups. We concluded that in a combined ACL and MCL injury, primary MCL repair provides little or no benefit [9, 17].

In contrast to the MCL, midsubstance ACL injuries have limited healing ability. Hence, when the ACL of a young, active patient is torn, it is generally reconstructed with an autograft or allograft. However, the appropriate choices for both the replacement graft and the surgical technique are still

hotly debated. Two types of information are needed to answer these questions: (1) What is the tensile response of the ACL?, and (2) How does it function within the joint? Our laboratory determined the tensile properties of the human FATC while maintaining proper anatomic alignment, and documented a significant effect of specimen age and orientation of these properties [15].

Recently, we have focused on the determination of the *in-situ* force within the ACL using a universal force-moment sensor (UFS) [4]. This sensor is capable of measuring the three forces and three moments applied to the knee during testing, and with incremental dissection and appropriate mathematics, the magnitude and direction of *in-situ* forces in the human ACL can be calculated. The primary advantage of this approach is that it requires neither surgical intervention nor the use of mechanical devices attached to or near the ACL. Moreover, no *a priori* assumption is needed for the directions of *in-situ* forces. Essentially, a known loading condition is applied to the intact joint, and the joint motion is recorded. All supporting structures in the knee except the ACL are then dissected away, and the previous path of joint motion is reproduced. The outputs of the UFS in the second test then represent the contribution of the ACL to the intact joint by the principle of superposition Under 1 degree-of-freedom (DOF) anterior tibial loading of the intact joint, *in-situ* forces in the ACL were higher than the applied drawer force. The direction of this force corresponded approximately to the insertion angle of the anteromedial (AM) portion of the ACL on the tibial plateau. We also found that the AM portion supports approximately 95% of the total *in-situ* force in the ACL for this loading condition [6].

To extend our methodology to include multiple-DOF joint motion, we are utilizing a robotic manipulator [3]. The primary advantage of this approach is that the robot can learn and reproduce more complex motions of the knee. Using force-moment control, an unconstrained (5-DOF) anterior-posterior load is applied to the knee while the robot records joint motion. After all structures (except the ACL) are removed, the robot reproduces the identical path of intact joint motion. As discussed previously, the *in-situ* force in the ACL (magnitude and direction) then can be determined using superposition [4, 6] Thus, our combined UFS and robotics approach is a powerful tool for characterizing the *in-situ* force in the ACL under a variety of external loading conditions.

Better understanding of the properties of normal ligaments and the changes associated with injury, healing, repair, and reconstruction are important to guide the clinical management of ligament injuries. Recent advances have been made using growth factors and gene therapy to improve the quality of healing tissue [1, 10, 11] and using robotics technology to evaluate the contributions of normal and reconstructed ligaments to joint stability. Future studies should additionally consider muscle stabilization [7] and then can address the important need for the development of rehabilitation protocols. These studies will provide important information that the clinician can use to make better choices regarding surgical technique as well as subsequent rehabilitation protocols and eventually lead to improved clinical care for injuries of the MCL and ACL.

Acknowledgments

Some of the cited work was done in collaboration with the colleagues of the senior author while he was at the University of California, San Diego. The financial support of NIH grant #AR-39683 and #AR-41820 are gratefully appreciated.

References

1) Batten ML and Dahners LE: *Trans ORS*, **20**:37, 1995.
2) Frank C, Woo SL-Y, Amiel D and Harwood F: *Am. J. Sports Med.*, **11**(379-389), 1983
3) Fujie H, Arai S, Woo SL-Y, Livesay GA and Mabuchi K: *J. Biomech. Eng.*, **115**:211-217, 1993
4) Fujie H, Livesay GA, Woo SL-Y, Kashiwaguchi S and Blomstrom GL: *J. Biomech. Eng.*, **117**:1-7, 1995.
5) Horwitz MT: *Arch Surg*, **38**:946-954, 1939
6) Livesay GA, Fujie H, Kashiwaguchi S, Blomstrom G and Woo SL-Y: *Trans ORS*, **18**:1, 1993
7) More RC, Karras BT, Neiman R, Fritschy D, Woo SLY and Daniel DM: *Am. J. Sports Med.*, **21**: 231-237, 1993
8) O'Donoghue DH, Rockwood CA, Zaricznyj B and Kenyon R: *J. Bone Joint Surg.*, **43**:1167-1178, 1961.
9) Ohno K, Pomaybo AS, Schmidt CC, Levine RE, Ohland KJ and Woo SL-Y:*Trans ORS*, **19**:619, 1994.
10) Otani K, Nita I, Macaulay W, Georgescu HI, Mueller GM, Robbins PD and Evans CH:*Trans ORS*, **20**:227, 1995
11) Weiss JA, Beck CL, Levine RE and Greenwald RM:*Trans ORS*, **20**:159, 1995
12) Weiss JA, Ohland KJ, Anderson DR and Woo SL-Y: in *First World Congress of Biomechanics*. La Jolla, CA, 1990.
13) Weiss JA, Woo SL-Y, Ohland KJ and Horibe S: *J. Orthop. Res.*, **9**:516-528, 1991
14) Woo SL-Y, Gomez MA, Seguchi Y, Endo C and Akeson WH: *J. Orthop. Res.*, **1**:22-29, 1983.
15) Woo SL-Y, Hollis JM, Adams DJ, Lyon RM and Takai S: *Am. J. Sports Med.*, **19**(217-225), 1991
16) Woo SL-Y, Smith BA and Johnson GA: in Knee Surgery, Williams & Wilkins, Baltimore, MD, 1994
17) Yamaji T, Pomaybo AS, Levine RE, Ohno K, Schmidt CC and Woo SL-Y: *Trans ORS*, **20**:626, 1995

Muscle architecture and muscle function in human

Tetsuo Fukunaga
Department of Life Sciences
University of Tokyo
Komaba,Meguro,Tokyo,JAPAN

Introduction;

A force produced by skeletal muscle is transmitted to bone by tendon, performing a joint movement Muscle fibers are tied up in a fascicle which connect tendon and aponeurosis Thus, to estimate noninvasively the functional characteristics of muscle fiber *in vivo* we have to consider such architectural factors as length and angle of the fascicle, moment arm of joint, total cross-sectional area of muscle fibers in parallel (physiological cross-sectional area,PCSA). Recently developed imaging technique such as MRI and ultrasonography make possible to estimate directly and noninvasively the architecture of muscle-tendon complex Purpose of the present study is to observe a dynamics of the muscle-tendon complex in human extremity by means of MR and ultrasonic imaging techniques, and to make it clear the relation between the architecture and the function of human muscles

(1)Visualization of intramuscular excursion during joint action;

The intramuscular excursion of the human tibialis anterior (TA) was observed by the real-time ultrasonic method. The tester visually confirmed the echoes reflected from the aponeurosis and interspaces among fascicles in the TA (Kuno and Fukunaga,1995) The cross point (η) between two echoes; one echo from the deep aponeurosis and the other from fascicles, was easily determined on the ultrasonogram. During dorsi and plantar flexion without additional load the η moved completely in phase with the angular change of the ankle joint, giving the (displacement/angular change) of 47mm/radian, which was equivalent to the functional moment arm observed by MRI (Rugg,1989).

(2)Fascicle length changes due to joint angle;

Fascicle length in vastus lateralis estimated by ultrasonography was about 100 mm at the knee joint extended full (0°) without muscle contraction, and it increased to 130 mm (+30%) at knee flexed position (110°). If the knee angle was changed from 0 to 110° with the contraction of 10% MVC the increment of fascicle length was more than the muscle relaxed, i.e. the length increased by 70%, from 70 mm (0°) to 120 mm (110°) This differences of length between relaxed and tensed would be due to the flabbiness (large compliance) of fascicles when the muscle is relaxed, especially when the knee is extended.

(3)Muscle fiber pennation angles are greater in hypertrophied than in normal muscles;

The pennation angles which was estimated as angles between ultrasonic echoes from the interspaces of fascicles and from the aponeurosis of long heads of triceps brachii were in the range of 15 and 53° (about 40° for bodybuilder and about 20° for normal)(Kawakami et al, 1993). Significant differences were observed between normal subjects and highly trained bodybuilders in muscle thickness and pennation angles, suggesting that muscle hypertrophy involves and increase in fiber pennation angles.

(4)Muscle-tendon length shortened during isometric action;

An elastic component of muscle is stretched by the contraction force of muscle. It was observed clearly that in the TA muscle the insertion point (η) of fascicles onto the aponeurosis moved during static action at the ankle joint fixed, i.e the η shifted

proximally according to the increasing dorsiflexion force. Notably, the moved distance of η (δL) and the dorsiflexion force (δF) relationship was quadratic in nature ($\delta F = k \delta L^2$, k=0.6-2.2, r=0.99, n=9), which curve was similar to that of the isolated tendon.

(5)Contribution of tendon elasticity in human movement;

When a repetitive ankle bending exercises in a standing position was performed with different frequencies the relation between the length changes in the fiber (l_f) and the muscle-tendon complex (l_{oi}) of triceps surae was affected by the frequencies, i e at low frequency the l_f and l_{oi} changed in phase, while at high frequencies above 160 times/min the l_f and l_{oi} changed almost 180^0 out of phase with each other. This suggest that even if the muscle tendon complex was lengthened at high frequencies of bending, the fiber activated not eccentrically but concentrically, which was also confirmed by EMG recordings

(6)Are specific tension same in different muscle groups?

Reported specific tension measurements for human muscle vary widely (20-90 N/cm^2). This variability would be due, at least in part to the determination of the PCSA (Fukunaga et al 1992). Even if the specific tension was estimated by using the newest imaging techniques for various muscle groups, it was observed still so many scatters of the specific tension as 20(plantarflexor and knee extensor), 25(dorsiflexor), 65(elbow flexor and extensor) N/cm^2 This discrepancy may be due to other factors as neural mechanism than muscle-tendon architecture.

(7)Resistance training induces architectural changes in muscle;

When a human elbow extensor muscle was trained 16 weeks with resistance exercise the muscle architecture changed remarkably, i e the PCSA increased by 33% , accompanying 29% increment of fascicle angle, while the length of fascicle didn't change. The specific tension decreased after training Increase in fascicle angles implies the occurrence of changes in muscle architecture, which might have contributed to the increase in muscle volume while giving a negative effect on force-generating properties of muscle

(8)Space flight cause more muscle atrophy than bed rest?

By 14 days of space flight the PCSA of leg muscles reduced remarkably, i e the PCSAs of knee extensor, flexor muscles, and triceps surae decreased by about 15%, except for dorsiflexor muscle In the case of 20 days of bed rest, however, the decrement of muscle PCSA was lower than the space flight, i e the knee extensor and flexor muscles indicated significant decrease of 5-8%, and the plantar flexor muscles by 10% These results suggest that there is variability of muscle atrophy in the muscle groups after space flight or bed rest, and it may be considered that the space flight effect more on muscle atrophy than the bed rest

References;

Fukunaga,T.,R.Roy,F.Schellock,J.Hodgson,M.Day,P.Lee,H.Kwong and R.Edgerton;Physiological cross-sectional area of human leg muscles based on magnetic resonance imaging *J.Orthopaedic Res.*10,926-934,1992

Kawakami,Y.,T.Abe and T.Fukunaga;Muscle-fiber pennation angles are greater in hypertrophied than in normal muscles *J.Appl.Physiol.*76,2740-2744,1993

Kawakami,Y.,K.Nakazawa,T.Fujimoto,D.Nozaki,M.Miyashita and T.Fukunaga;Specific tension of elbow flexor and extensor muscles based on magnetic resonance imaging *Eur J.Appl.Physiol.*68,139-147,1994

Kuno,S and T.Fukunaga;Measurement of muscle fibre displacement during contraction by real-time ultrasonography in humans *Eur J.Appl.Physiol.*70,45-48,1995

Rugg,S.,R.Gregor,B.Mandelbaum,L.Chui;In vivo moment arm calculations at the ankle using magnetic resonance imaging *J.Biomech.*23,495-501,1990

NONINVASIVE APPROACH TO MOTOR UNIT CHARACTERIZATION: MUSCLE STRUCTURE, MEMBRANE DYNAMICS AND NEURONAL CONTROL

G. Rau, C. Disselhorst-Klug, J. Silny

Helmholtz-Institute for Biomedical Engineering
Aachen, University of Technology
Pauwelsstr. 20, 52074 Aachen, Germany

INTRODUCTION

The standard surface-EMG reflects, due to its low spatial resolution, the compound activity of a high number of motor units (MUs). Therefore, detailed information about structural and functional characteristics of the muscle, like the functional anatomy, the excitation spread or the innervation pattern, can not be gained from the standard surface-EMG. However, this information formes the basis for detailed interpretations of the surface-EMG signal and, thus, of the physiological and pathological properties.

A novel, noninvasive EMG-procedure with a high spatial resolution (HSR-EMG) allows in contrast to the standard surface-EMG the detection of the single MU activity during voluntary contraction. By this approach the HSR-EMG provides information about the structural and functional characteristics as well as a deeper insight in the active state of the muscle. Examples will demonstrate the potential and the limitations of this method.

METHODS

The HSR-EMG procedure is based on a spatial sampling of the potential distribution generated on the skin surface by the excitation of the MUs. Therefore, a special two-dimensional multi-electrode array with an interelectrode distance adjusted to the spatial gradient of the potential distribution (2.5 - 5 mm depending on the investigated muscle) is used (Fig.1). The spatial resolution of the recording setup has been improved by a weighted summation of five adjacent EMG-leads forming the filter which are arranged crosswise (NDD-filter) (Fig.1)[1,2]. This spatial filtering of the potential distribution performed in this way enhances the electrical activity of MUs located directly beneath the center of the filter and reduces the activity of more distantly located sources. In this way, the activities of MUs located close to the skin surface and therefore close to the electrode array become detectable in a noninvasive way [1,2].

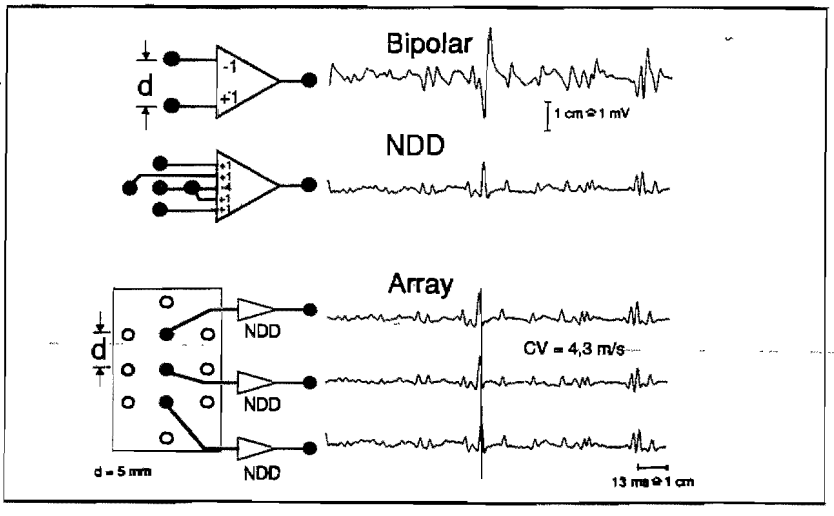

Fig.1: Comparison between a bipolar and a NDD-filtered channel. A series connection of NDD-filters (in this case three) allows the determination of the excitation spread in single MUs.

From one spatially filtered channel the activities of single MUs can be recorded as a function of time. To get additional information about the excitation spread along the muscle fibres of single MUs, electrode arrays are used which provide several NDD-filtered channels in a lined row orientated in parallel to the muscle fibres (Fig.1) [1,2]. In this way the noninvasive recording of the excitation spread along single MUs becomes possible [1,2].

APPLICATIONS

The HSR-EMG procedure allows a noninvasive determination of different essential structural and functional characteristics of the muscle. From the direction of the excitation spread in single MUs information about the functional anatomy of the investigated muscle can be gained: The orientation of the muscle fibres can be determined and additionally the endplate region can be localized with an accuracy lower than the interelectrode distance of the electrode array. When using various sizes of electrode arrays different muscle groups or functional units of the muscle can be distinguished.

The knowledge about the excitation spread allows the calculation of the conduction velocity in single MUs. Additionally, the membrane dynamics as well as the muscle fibre geometry (e.g. fibre diameter) which affect the excitation spread can be examined in this noninvasive way.

- Since the HSR-EMG allows the detection of the single MUs activity even during maximal voluntary contraction of the muscle, the procedure is well suited for investigations of the innervation pattern of the muscle. The firing rate of single MUs as well as their recruitment can be determined by the HSR-EMG in a noninvasive way.

Combining this procedure with other approaches like the MU triggered sampling principle [3], the understanding of the active state of MUs could be further extended.

CONCLUSION

Since the conventional surface-EMG is highly affected by the structural and functional characteristics of the muscle, the information about these characteristics is essential for a correct interpretation of the surface-EMG signal. The noninvasive HSR-EMG procedure allows in contrast to the standard surface-EMG the determination of the functional anatomy of the muscle, the examination of the excitation spread as well as the investigation of the neuronal control of the muscle.

REFERENCES

[1] Reucher H., Silny J., Rau G 1987 Spatial Filtering of Noninvasive Multielectrode EMG Part I: Introduction to Measuring Technique and Application; Part II: Filterperformance in Theory and Modelling.
IEEE Trans. on Biomed. Eng. BME-34, No. 2, 98-105.

[2] Reucher H., Rau G., Silny J 1987 Spatial Filtering of Noninvasive Multielectrode EMG Part I: Introduction to Measuring Technique and Application; Part I: Introduction to Measuring Technique and Applications.
IEEE Trans on Biomed. Eng. BME-34, No. 2, 106-113.

[3] Roeleveld K , Stegeman D F., Vingerhoets H.M , v Oosterom A. 1994 Representation of Motor Units in the Surface Electromyogram.
Proceedings of the 10th Congress of ISEK, 140 - 141

NEURAL ADAPTATIONS WITH CHRONIC PHYSICAL ACTIVITY

Roger M. Enoka
Department of Biomedical Engineering, Cleveland Clinic Foundation,
Cleveland, Ohio 44195, USA

Although the role of neural mechanisms in the adaptations that accompany chronic physical activity has been controversial, there is now substantial evidence that they are at least as important as the changes that occur in the musculoskeletal system. Evidence in favor of a significant role for neural mechanisms has been accumulated from a variety of chronic activities, including aging, cross education, immobilization, and strength training. However, the actual nature of the adaptations that occur within the nervous system has been difficult to determine, largely due to technical limitations. The presentation will first review some of the evidence for neural mechanisms and then consider what is known about the form of these adaptations.

THE CASE FOR NEURAL ADAPTATIONS

Perhaps the most familiar evidence indicating a role for neural adaptations is the gain in strength that occurs in the first few weeks of a strength-training program (Moritani & deVries, 1979). When a naive person performs strengthening exercises, the initial increase in strength is often accompanied by a comparable increase in EMG, but this precedes a significant change in muscle size (Narici et al., 1989). Such a time course suggests a prominent role for neural adaptations. This possibility was underscored by the observation that a 4-week training program of imagined contractions resulted in an increase in MVC force (Yue & Cole, 1992). The magnitude of the increase in MVC force produced with the imagined contractions was less than that achieved by the subjects who actually performed the training program, but it was nonetheless significantly greater than that measured in those subjects who did not train. Because the increase in strength occurred without accompanying EMG or force during training, the effect must have been due to adaptations in the nervous system, probably involving reorganization of the descending drive from suprasegmental centers.

TYPES OF NEURAL ADAPTATIONS

Although such observations implicate the nervous system, much of the evidence is inferential (e.g., the strength training adaptations) and definitive studies are lacking. The actual form of the neural adaptations that mediate these effects is largely unknown.

1. Maximality of Neural Drive

   At least since Belanger & McComas (1981), results with the superimposition technique have indicated that maximum activation of a muscle by voluntary command is difficult and that this difficulty varies across muscles. Recent data suggests that subjects can maximally activate the elbow flexor muscles, but that this only occurs in about 10% of the maximum voluntary contraction (MVC) trials (Allen et al., 1995). Furthermore, periods of reduced use, such as limb immobilization, cause marked reductions in the ability of individuals to maximally activate a muscle by voluntary command (Duchateau & Hainaut, 1987). However, new opportunities with magnetic resonance (MR) imaging suggest that MVC force with the knee extensors can be achieved by activating only 75% of the cross-sectional area of the quadriceps femoris muscle (Adams et al., 1993). This is consistent with the finding that sensory feedback can increase MVC force, even in highly trained strength athletes (Howard & Enoka, 1991).

2. Specificity of Neural Drive

   The adaptations that can be attributed to changes in neural drive appear to be specific for a task but not focused exclusively on the motor neuron pool of the prime mover muscle. Examples of task-specific adaptations in neural drive include the velocity-dependent effect of isokinetic training that occurs for both intended (but blocked) and actual isokinetic contractions (Behm & Sale, 1993), the increase in strength (MVC force) that can be achieved with imagined contractions (Yue & Cole, 1992), and differences in the EMG amplitude for intended concentric and eccentric

contractions (Grabiner et al., 1995). However, strength training of one limb, either by voluntary activation or by electrical stimulation, results in significant increases in strength of the contralateral limb (Enoka, 1988). This cross-education effect suggests that the neural adaptations are not limited to the motor neurons that innervate the prime mover muscle.

3. Pattern of Neural Drive

Because the neural adaptations cannot be explained solely by changes in the quantity of neural drive (EMG) to a muscle, there must also be qualitative changes in the input. At a global level, this is evident by a reduction in coactivation (Carolan & Cafarelli, 1992) and an improved coordination among synergists (Rutherford & Jones, 1986) with strength training. One mechanism thought to mediate some of these effects is motor unit synchronization (Milner-Brown et al., 1975), although this remains speculative. Other potential mechanisms include changes in reflex excitability and in the discharge of motor units (Sale, 1988).

The nervous system has remarkable adaptive capabilities. Some of the alterations in performance that occur as a consequence of chronic activity patterns are undoubtedly mediated by changes that occur in the nervous system.

References

Adams GR, Harris RT, Woodard D, Dudley GA: Mapping of electrical muscle stimulation using MRI. *J Appl Physiol* 74: 532-537, 1993.

Allen GM, Gandevia SC, McKenzie DK: Reliability of measurements of muscle strength and voluntary activation using twitch interpolation. *Muscle Nerve* in press.

Behm DG, Sale DG: Intended rather than actual movement velocity determines velocity-specific training response. *J Appl Physiol* 74: 359-368, 1993.

Belanger AY, McComas AJ: Extent of motor unit activation during effort. *J Appl Physiol* 51: 1131-1135, 1981.

Carolan B, Cafarelli E: Adaptations in coactivation after isometric resistance training. *J Appl Physiol* 73: 911-917, 1992.

Duchateau J, Hainaut K: Electrical and mechanical changes in immobilized human muscle. *J Appl Physiol* 62: 2168-2173, 1987.

Enoka RM: Muscle strength and its development: new perspectives. *Sports Med* 6: 146-168, 1988.

Grabiner MD, Owings TA, George MR, Enoka RM: Eccentric contractions are specified *a priori* by the CNS. *XVth Congr Int Soc Biomech* Jyväskylä, Finland, July 2-6, 1995.

Howard JD, Enoka RM: Maximum bilateral contractions are modified by neurally mediated interlimb effects. *J Appl Physiol* 70: 306-316, 1991.

Milner-Brown HS, Stein RB, Lee RG: Synchronization of human motor units: possible roles of exercise and supraspinal reflexes. *Electroenceph Clin Neurophysiol* 38: 245-254, 1975.

Moritani T, deVries HA: Neural factors versus hypertrophy in the time course of muscle strength gain. *Amer J Phys Med* 58: 115-130, 1979.

Narici MV, Roi GS, Landoni L, Minetti AE, Ceretelli P: Changes in force, cross-sectional area, and neural activation during strength training and detraining of the human quadriceps. *Eur J Appl Physiol* 59: 310-319, 1989.

Rutherford OM, Jones DA: The role of learning and coordination in strength training. *Eur J Appl Physiol* 55: 100-105, 1986.

Sale DG: Neural adaptation to resistance training. *Med Sci Sports Exerc* 20: S135-S145, 1988.

Yue G, Cole KJ: Strength increases from the motor program: a comparison of training with maximal voluntary and imagined muscle contractions. *J Neurophysiol* 67: 1114-1123, 1992.

BIOMECHANICS OF LOW BACK INJURY

Stuart M. McGill
Occupational Biomechanics and Safety Laboratories, Department of Kinesiology, University of Waterloo, Waterloo, Ontario, Canada

How can a person hurt their back picking up a pencil from the floor after lifting safely all day? How does low back injury occur from sitting? Why do we pressurize the abdominal cavity upon exertion? Is it better to stoop or squat during lifting? Should the spine be in a flexed posture or in a neutral posture upon exertion? Is compression the most important loading variable when considering injury? These are all important and fascinating questions related to mechanics of normal low back function and of injury. While it is currently popular to state that psychosocial components factor heavily in several aspects of occupational low back pain, there is no dispute that injury must result from excessive loading of a particular tissue. In fact, it is the characteristics of the load itself (load rate, mode of load-compression, bending, torsion, shear, etc.) and properties of the tissue which determines the type and extent of the tissue damage. **The purpose of this keynote lecture is to update ISB delegates, who are experts in a variety of areas in biomechanics, on some of the issues associated with the biomechanics of low back injury.** While several issues will be discussed in the lecture only a few will be introduced here.

What really causes injury? Injury occurs when the magnitude of load applied to a tissue exceeds the failure tolerance. Despite the tendency for many people to cite a single event that caused their injury, in reality their injury was more likely the result of cumulative microtramma associated with repeated and prolonged loading. Tissue tolerance is modulated by many factors including age, gender, and load factors (repetition, duration, and rate of application) to name a few. Combining biomechanical modelling techniques to obtain the load-time histories on each tissue with studies of tissue mechanics and structural architecture is a powerful approach for analyzing injury mechanisms, assessing the risk, and planning avoidance strategies.

The anatomical design of the various tissues of the low back contain many subtleties that both work to support loads in a safe way but may lead to tissue overload if the advantages in design go unrecognized. For example, some have implicated anterior-posterior shear forces as a potential injury mechanism (e.g., Troup, 1976). It is interesting that the major lumbar extensors create large posterior shear forces upon activation while the interspinous ligament causes anterior shear forces when stretched in fully flexed postures (Heylings, 1978) This is one example where spine posture determines the interplay between passive tissues and muscles which ultimately modulates the risk of several types of injury. Furthermore, it is the opinion of this author that far too much effort has been devoted to the issue of whether it is better to stoop or squat when lifting to reduce the risk of injury. Given the wide variety in dimensions of objects to be lifted, one sometimes has to employ one method over another to get the object close and reduce the reaction moment arm. A much larger issue is the curvature of the spine which must be separated from hip rotation when discussing "trunk angle". Trunk angle simply affects the magnitude of the moment while spine posture determines the distribution of loads among the passive tissues and muscles and in fact the ultimate strength of some of the load bearing structures.

Reasonable interpretation and assessment of injury mechanisms requires the acquisition of tissue load-time histories in vivo. The approach that I took with my colleague Bob Norman several years ago was to develop a model that incorporated sufficient anatomical detail and that used a strategy of obtaining tissue loads that was sensitive to the individual ways people support their spines (e.g., McGill and Norman, 1986; McGill, 1992) For this reason,

traditional optimization approaches were forgone in favour of utilizing biological signals of multichannel EMG to assist in assigning muscle forces At the same time measurement of 3D spine displacement is used to obtain passive tissue loads once the range of motion/passive resistance has been calibrated. In this way, full credit is given to muscle co-contraction during complex tasks together with enabling analysis of the subtle differences that lead to overload and injury of a particular tissue A major assumption with this approach has been to use surface electrodes to represent deep muscle activity Recently we have attempted to justify this assumption and have concluded that deep muscles appear to have synergists that are myoelectrically accessible on the surface

Explaining injuries when forceful exertions are required have been attempted to varying degrees of success - but at least it follows intuition that high loads can cause injury. **Far more curious is the case where one "throws his back out" when picking up a pencil** Recent work by my graduate student and colleague Jacek Cholewicki, demonstrated that when the reaction moments are small, and muscle forces are correspondingly low, the risk of instability and short column buckling is much higher It would appear that it is much more likely that a motor control error, resulting in an inappropriate, but small and temporary, muscle force could cause local joint motion sufficient to create overload in a single tissue

The spine has a memory. Its viscoelastic structures react to load in a way that depends on the previous loading history For example, prolonged sitting in a flexed posture stretches the posterior passive tissues which require up to half an hour to restore normal joint stiffness (McGill and Brown, 1992) This knowledge may be used by those responsible for organizing manual work to minimize the risk of injury Several other biomechanically justifiable guidelines to minimize the risk of injury at work will be introduced in this lecture

What are the major "hot" issues for the immediate future? Certainly the currently used, single values for occupational spine load exposure are woefully inadequate in the field of reducing the risk of injury. A load-time integral, that is sensitive to the direction and mode of loading, age, gender, load repetition, load duration, number and duration of rest breaks, etc. is needed. As well, the field of rehabilitation requires better functional diagnoses of low back injury Only then will clinicians be better able to optimize programs to strengthen tissues without exacerbating the real injury or structural weakness.

The spine is a wonderfully complex structure that will continue to cause sufficient problems which in turn will motivate clever minds to determine how it works and how to minimize the risk of injury The young ISB members - the consummate biomechanists, who are conversant in functional anatomy, mechanics, motor control and principles of instrumentation will enjoy a lifetime of most pleasurable and satisfying work in assisting the great majority of us who suffer back injury. Much remains to be done.

References:

Heylings, D. (1978) Supraspinous and Interspinous ligaments of the human lumbar spine, J. Anat., 123: 127-131.

McGill, S.M. and Norman, R.W. (1986) Partitioning of the L4/L5 dynamic moment into disc, ligamentous, and muscular components during lifting, Spine, 11(7), 666-678.

McGill, S.M. and Brown, S (1992) Creep response of the lumbar spine to prolonged full flexion, Clin. Biomech., 7: 43-46.

McGill, S.M. (1992) A myoelectrically based dynamic 3D model to predict loads on lumbar spine tissues during lateral bending, J. Biomech.

Troup, J.D.G (1976) Mechanical factors in Spondylolisthesis and Spondylolysis, Clin Orthop. Rel. Res., 117: 59-67.

CURRENT ISSUES IN MECHANICS OF ATHLETIC ACTIVITIES

Roger Bartlett

Division of Sport Science, The Manchester Metropolitan University, Alsager, UK.

INTRODUCTION

There are many topics in the study of strenuous sporting activity which biomechanists would consider to be important issues - that is contentious matters th decision of which has significant consequences. This presentation will focus on son of these current issues, chosen to illustrate the range of sports biomechanists activiti from applied through to fundamental research. The intention of the presentation is n to resolve these issues, but to stimulate debate on them by standing aside from everyday research and looking at these issues from a broader perspective.

APPLIED ISSUES

There is some controversy about the contribution which biomechanists hav made to improvements in the performance of athletes or reductions in the occurrenc in injury. It is possible to cite a great deal of anecdotal evidence of useful contributic in both respects at the elite level, and far less at the non-elite level. Biomechanists h played an important role in the understanding of technique, for example the generati of propulsive forces in swimming. There have also been important contributions to tl understanding of the causes of injury, as exemplified by the identification of the injurious mixed technique in cricket fast bowling (e.g. Elliott *et al*., 1992). However, there is a paucity of research to establish whether any improvements in the performances of individual athletes have been the result of biomechanical analysis o some other factor such as motivation. Nor is there a great deal of evidence of whethe identification by biomechanists of risk factors in injury has led to any reduction in th occurrence of injury. Many biomechanists are proud of their contribution to sport through applied research and yet such issues have not been adequately addressed.

Far too much applied research, such as projects at the Olympic Games, is simply never used in the field or communicated appropriately to athletes and coaches This is partly because insufficient attention is given to optimisation of the process of feedback of biomechanical information to coaches and athletes. As Gregor *et al.* (1991) pointed out, the focus has been on what is provided not how. Whilst the latter does involve aspects of motor learning (Hay, 1991), it also falls within the domain of the sports biomechanist. Such collaborative, interdisciplinary work, to improve the application of research into practice, should form a greater focus of our activity.

FUNDAMENTAL ISSUES

As Cappozzo (1983) identified for the non-use of gait evaluation by clinical practitioners, there are both practical and fundamental, theory based issues. Much applied sports biomechanics research and servicing also poses fundamental research questions. Arising from the issue of how best to utilise and feedback biomechanical information are many concerns of fundamental research relating to how movement is coordinated. The coordination of segment, joint and muscle actions are held to be crucial to the successful execution of sports skills. However, there has been far too little systematic research in this area, and more is needed if sports movements are to be fully explained and not simply measured, described and modelled (e.g. Norman, 1989)

The identification of the optimal movements for an athlete is crucial for performance and injury prevention. Do we really know, for example, what makes an athlete throw further, even in terms of descriptive variables, let alone the mechanisms which generate the movement? Questions remain as to which of the many possible

variables are most important and, more fundamentally, how such movements are controlled. There remains a need for both experimental and theoretical approaches to these problems. Whilst developments in technology may enable the acquisition of much larger amounts of experimental data on individual athletes, great care will have to be taken in the design of such experiments and, particularly, in the statistical analysis of the data obtained from them (e.g. Zatsiorsky and Fortney, 1993).

It is unlikely that statistical modelling will supersede the current use of computer simulation models. One of the major problems in such modelling of sports movements is that too many of the models used are divorced from the real world. There are still many unresolved issues in this area, relating to model complexity, simulation evaluation, what muscle models are needed for specific sports and the customisation of whole body models (Yeadon and Challis, 1994).

The whole process 'from muscles to the movement pattern' (Nelson and Zatsiorsky, 1994) is also of major relevance, including the issue of muscle redundancy and how best to tackle it. Much research has focussed on the stretch-shorten cycle (e.g. Komi, 1984), although its exact importance in comparison with the concentric mechanism remains open to debate. The role of two-joint muscles has received much attention in the literature but there is no complete consensus on this topic, as evidenced by van Ingen Schenau (1989) and the variety of responses to his target article in an area of fundamental importance to the biomechanics and motor control of sports movements.

CONCLUSIONS

There remain many unresolved issues in the biomechanics of athletic activities, many of which overlap with other disciplines (e.g. Nigg, 1993). Research to address these important applied and fundamental issues will increasingly become more question than discipline orientated, will focus more on mechanisms than description, and will involve multidisciplinary teams of researchers.

REFERENCES

Cappozzo, A. (1983). Considerations on clinical gait evaluation. *J Biomechs*, **16**, 302.

Elliott, B.C., Hardcastle, P.H., Burnett, A.F. and Foster, D.H. (1992). The influence of fast bowling and physical factors on radiological features in high performance young fast bowlers. *Sports Med, Train and Rehab*, **3**, 113-130.

Gregor, R.J., Broker, J.P. and Ryan, M. (1991). Performance feedback and new advances. In R.W. Christina and H.M. Eckert (eds.) *Enhancing Human Performance in Sport. New Concepts and Developments*, pp. 19-32. Champaign: Human Kinetics.

Hay, J.G. (1991). Reaction to performance feedback: advances in biomechanics. In R.W. Christina and H.M. Eckert (eds.) *Enhancing Human Performance in Sport: New Concepts and Developments*, pp. 33-37. Champaign: Human Kinetics.

Komi, P.V. (1984). Physiological and biomechanical correlates of muscle function. In R.L. Terjung (ed.) *Exercise & Sport Sciences Revs*, **12**, 81-121. Lexington: Collamore.

Nelson, R.C. and Zatsiorsky, V.M. (1994). Sports biomechanics. *Sp Sci Revs*, **3**, 1-7.

Nigg, B.M. (1993). Sports science in the twenty-first century. *J Sport Sci*, **11**, 343-347.

Norman, R.W. (1989). A barrier to understanding human motion mechanisms: a commentary. In J.S. Skinner, C.B. Corbin, D.M. Landers, P.E. Martin and C.L. Wells (eds.) *Future Directions in Exercise and Sport Science Research*, pp. 151-161. Champaign: Human Kinetics.

Van Ingen Schenau, J.G. (1989). From rotation to translation: constraints on multi-joint movements and the unique action of bi-articular muscles. *Hum Move Sci*, **8**, 301-338.

Yeadon, M.R. and Challis, J.H. (1994). The future of performance-related sports biomechanics research. *J Sport Sci*, **12**, 3-32.

Zatsiorsky, V.M. and Fortney, V.L. (1993). Sport biomechanics 2000. *J Sport Sci*, **11**, 279-283.

DEVELOPMENT OF GAIT AND PHYLOGENY OF HUMAN QUADRUPEDAL WALKING

M. Abe, H. Morishita[1] , T. Suzuki[2] and R. Sasaki[3]
College of Liberal Arts and Sciences, Kitasato University, Sagamihara, Japan
[1]Laboratory of Human Movement, Ochanomizu University, Tokyo, Japan
[2]College of Education, Akita University, Akita, Japan
[3]Institute of Physical Education, Keio University, Yokohama, Japan

INTRODUCTION

Animal quadrupedal walking has been reported to be diagonal sequence (DS) gait (Left Hind-Right Fore-RH-LF) for nonhuman primates and lateral sequence (LS) gait (LH-LF-RH-RF) for nonprimate mammals (1,2). Hildebrand (2) thought phylogeny of quadrupedal locomotion by means of graphic method of animal's gait.

Abe et al. (3) reported creeping on hands and knees (Figure 1.) and walking on hands and feet (Figure 2.) of human differ in gait development by kinematics method. The former has a period where leaving and touching-ground do not coincide with each other, and human may possess motor program of DS gait because walking on hands and feet shows DS gait in both leaving and touching-ground regardless of ages.

As for gait graph of human quadrupedal walking, Hildebrand (1) reported creeping on hands and knees of infants and walking on hands and feet of 6 to 11 ages and Sparrow (4) reported creeping on hands and knees of infants and walking on hands and feet of adults. Some questions still remained to be discussed, however, in the results of creeping on hands and knees of Sparrow (4).

The purpose of the present study were applying the graphic method to the development of human quadrupedal walking gait and considering phylogeny of quadrupedal locomotion.

Figure 1. creeping on hands and knees

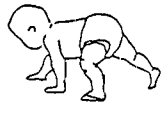

Figure 2. walking on hands and feet

METHODS

The subjects were 15 infants under one year old, 100 children aged 1 to 5 years and 25 adults. Both creeping on hands and knees and walking on hands and feet modes were firstly VTR recorded (30 frames / sec.). The VTR analysis were then performed to obtain time sequence data of leaving and touching-ground of the four limbs. On the basis of these results the following three variables were obtained: (i) stance / cycle mean of four limbs (ii) fore limbs leaving follows hind limbs leaving on the same side / cycle mean left and right (iii) fore limbs touching follows hind limbs touching on the same side / cycle mean left and right. We made two leaving and touching-ground gait graphs according to one quadrupedal walking by using these three variables.

RESULTS

Figure 3. shows the modified Hildebrand's (1,2) gait graph of human quadrupedal walking. The gait graphs of creeping on hands and knees and walking on hands and feet are shown in the left and right respectively, and leaving and touching-ground gait graphs are shown upper and under respectively.

For creeping on hands and knees of infants showed LS gait both in leaving and touching-ground. Fore older ages, however, the gait of touching and leaving-ground became different. Until 3 year old leaving-ground changes to the area of DS gait, then to the area of LS gait with age, which is not absolutely all LS gait. In touching-ground creeping on hands and knees showed also a small portion in DS gait in the age of 4 or 5. There appeared no remarkable change as in leaving-ground, which maybe considered to be distributed in LS gait area in each age.

For walking on hands and feet both leaving and touching-ground lied in LS gait area regardless of ages. (Three cases of walking on hands and feet were observed for 0 year old infants.) The distribution after 4 year old became vertical, which, however, was not the LS gait area.

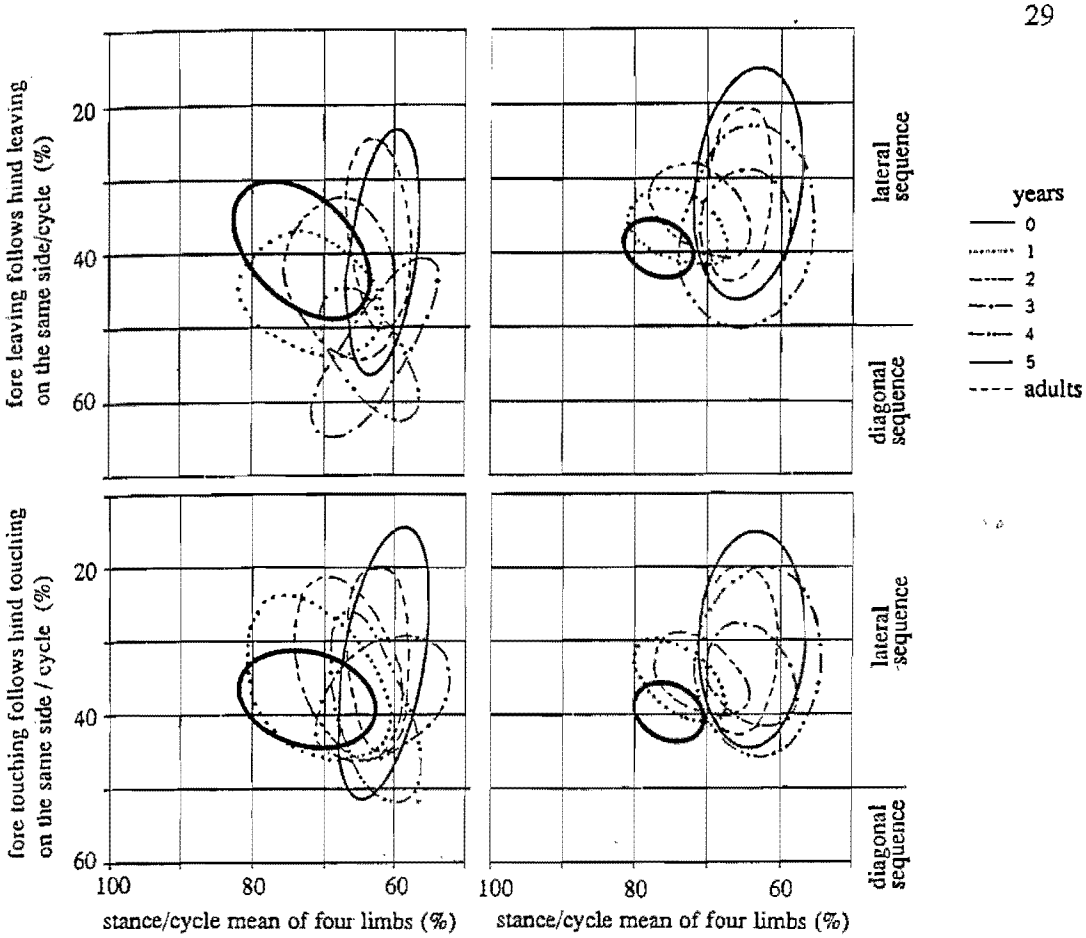

Figure 3. The gait graphs of human quadrupedal walking

DISCUSSION

The new results presented here are the gait graph of creeping on hands and knees and walking on hands and feet of children of aged 1 to 5 years and of creeping on hands and knees of adults. The confirmations are the gait graph of creeping on hands of infants were in good agreement in the scale with that of Hildebrand's (1) rather than that of Sparrow's (4), and the gait graph of walking on hands and feet of adults were in agreement with that of Sparrow's (4).

It is believed to be a appreciable result to apply the graphic method to the development of human quadrupedal walking gait as a first purpose of this study.

As for the second purpose of this study the phylogeny of quadrupedal locomotion must be then considered. The area of LS gait in creeping on hands and knees and walking on hands and feet of infants lied in quite near region of the area which Hildebrand (2) thought to be a source of quadrupedalism. Walking on hands and feet also showed the same LS gait as mammals in leaving and touching-ground. From these results above mentioned human has possibility of being quadrupedalism, which is even remarkable in walking on hands and feet mode, and human walking on hands and feet mode is thought to have evolution continuation with quadrupedalism of mammals. The creeping on hands and knees of infants seemed to be a by-product from a motion restriction of physical weakness and of being difficult to perform walking on hands and feet.

REFERENCES

1. Hildebrand, M. Am J Phys Anthrop 26:119-130, 1967
2. Hildebrand, Neural Control of Locomotion, Plenum, 203-236, 1976
3. Abe et al. Biomechanism 12 (ed. Society of Biomechanism,Tokyo) Univ. Tokyo Press,Tokyo, 125-135,1994 (in Japanese)
4. Sparrow, W. A. Am J Phys Anthrop 78:387-401, 1989

CONTRIBUTIONS MADE BY THE GASTROCNEMIUS AND PLANTARIS MUSCLES TO THE KNEE JOINT MOMENT IN CATS DURING JUMPING AND WALKING

Abelew, T.A. and R.J. Gregor, Department of Health and Performance Sciences, The Georgia Institute of Technology, Atlanta, Georgia. U.S.A.

INTRODUCTION

Considerable data exist quantifying the mechanical output of selected hindlimb extensors with respect to the ankle joint using implanted force transducers *(Gregor & Abelew, 1994)*. Recently, individual muscle moments were reported for the major ankle extensors in the cat (Fowler et al., 1993). However, the bi-articular nature of gastrocnemius and plantaris muscles anatomically and physiologically links the knee and ankle joints to the degree that understanding their function necessitates examining their contribution at both joints. The purpose of this investigation was to quantify the moment arms at the knee as well as the knee joint moments for the medial and lateral heads of the gastrocnemius and plantaris muscles in the freely moving cat.

METHODS

Three adult female cats (wt.=4.03±0.4kg) were trained to jump from within and walk within a Plexiglas enclosed walkway containing two force platforms capable of recording 3-D ground reaction forces (GRF). Under sterile conditions, tendon force transducers were implanted on the individual tendons of the medial gastrocnemius (MG), lateral gastrocnemius (LG) and plantaris (PLT) muscles (Fowler et al., 1993). Reflective markers were utilized to approximate segment endpoints on each hindlimb and high speed film (100fps) used to record marker displacement during movement. Marker data were subsequently digitized, smoothed and differentiated for input, with appropriate body segment parameters, to Newtonian equations of motion for calculation of generalized muscle moments (GMM). Film, muscle-tendon unit forces and GRF were synchronized using a DC pulse and a light in the camera field of view. Moment arms for each muscle at the knee joint were calculated for each trial using a computer algorithm that produced coefficients relating knee joint angle and muscle-tendon unit excursions obtained from film. For each trial muscle-tendon unit lengths were plotted as a function of knee joint angle for each muscle-tendon unit, fit with a 3rd order polynomial and differentiated to yield equations describing the instantaneous moment arms (An et al., 1983). Individual muscle moments were calculated using individual tendon force and moment arm records for each trial.

RESULTS

Exemplar data for muscle moment arms during jumping (0.67 m) and overground walking are shown in Figures 1a and 1b, respectively. Moment arm length changes during a trial ranged from 0.2 mm (walking) to 1.2 mm (jumping). Peak LG and PLT moment arms were consistently greater than those of the MG and were reached at knee angles of approximately 1.5 radians (walking) and 1.65 radians (jumping). Moment arms were similar in magnitude and timing between jumping trials with higher variability observed between walking trials. During jumping, moment arms reached their peak value just prior to take-off while during walking trials peak values occurred early in the stance phase. A second peak was observed near paw-off during late stance. Peak moment arms for all three muscles compared favorably with estimates of maximum values made during post-mortum dissections (LG/PLT = 7 mm, MG= 5 mm). Individual muscle moments are shown in Figures 2a and 2b for a jumping (0.67 m) and walking trial, respectively. Peak LG moments were the largest followed by the MG and PLT during jumping. The PLT peak moment exceeded peak LG moment during walking. Timing of peak moments were similar across muscles within each activity. During jumping the peak moment occurred between 75 and 90% of the contact phase while during walking the moments reached their peak value between 20 and 30% of the stance phase.

DISCUSSION

Results indicate that knee moment arms for the MG, LG and PLT muscles vary throughout jumping and walking in a cat and that maximum lengths are reached at knee angles within a physiological range of motion. This situation offers the potential for the moving cat to take advantage of the maximal moment capabilities of the muscles during natural movements. The significance of this capability lies in the potential for power transfer between knee and ankle via gastrocnemius and plantaris muscles. The high degree of variability in moment arm lengths between walking trials is attributed to the variation in knee position selected by the cat as part of overall body posture during a particular walking trial. In conclusion, recent data on the contribution of individual cat ankle extensors to the ankle joint kinetics (Fowler et al., 1993) and information on their contribution made at the knee joint presents a more comprehensive assessment of the overall role played by these muscles during natural movements.

Figure 1a

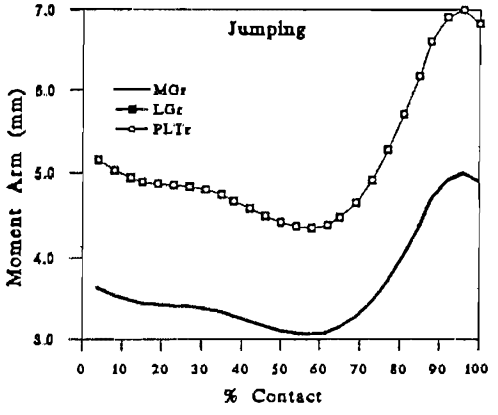

Figure 1b

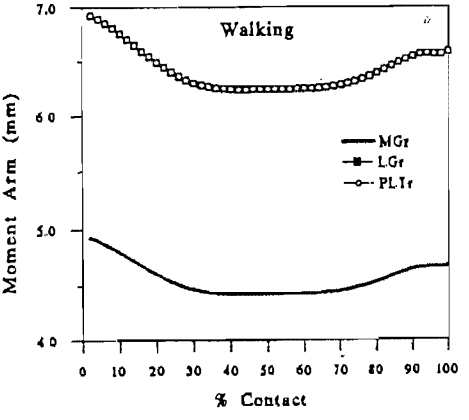

Figure 2a

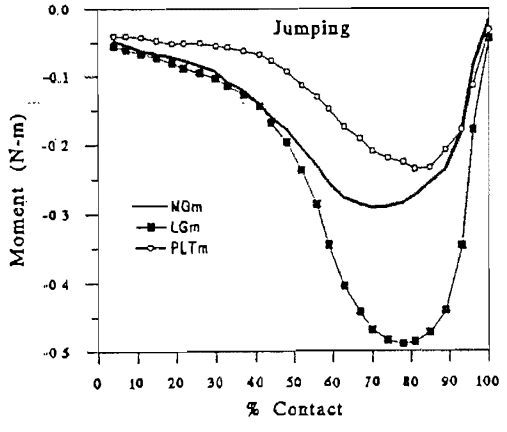

Figure 2b

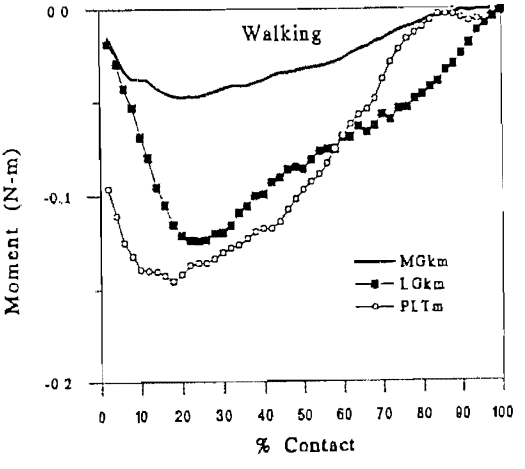

REFERENCES

1. An, K.N., Ueba, Chao, E.Y., Cooney, W.P. and R.L. Linscheid (1983) Tendon excursion and moment arms of index finger muscles. J. Biomech. 16: 419-425.
2. Fowler, E.G., R.J. Gregor, J.A. Hodgson and R.R. Roy. (1993) Relationship between ankle muscle and joint kinetics during the stance phase of locomotion in the cat. J. Biomech. 26: 465-483.
3. Gregor, R.J. and T. Abelew (1994) The use of directly measured tendon forces in musculoskeletal biomechanics and neural control: a review. Med. Sci. Sport Exerc. 26: 1359-1372.

ELECTROMYOGRAPHY AND BIOMECHANICS OF THE BLEDSOE PRO-SHIFTER BRACE FOR ANTERIOR CRUCIATE LIGAMENT DEFICIENCY

S.P. Acierno, R.V. Baratta, M. Solomonow, R. D'Ambrosia

Bioengineering Laboratory, Department of Orthopaedic Surgery, Louisiana State University Medical Center, New Orleans, Louisiana, USA

INTRODUCTION

Tears to the anterior cruciate ligament (ACL) often result in knee instability: th proximal tibia translates anteriorly with respect to the distal femur and causes a painfi subluxation episode. While ACL tears may be treated operatively or conservatively extensive rehabilitation is always a necessary component of the treatment process. T maintain stability during rehabilitation, orthotic knee braces are often prescribed (Cabor and Johnson 1993). However, the effectiveness of knee bracing has been questione (Vailas and Pink 1993) and tested by a number of authors through subjective, cadaveric functional and arthrometer studies. In these studies, the braces demonstrated varyin degrees of biomechanical effectiveness, but it is difficult to compare the result quantitatively, or to assess the effect of bracing on the recovering knee joint's neuromoto behavior (Ott and Clancy 1993, Cawley et al. 1985, Mishra et al. 1989).

Recently, braces have been developed which are intended not only to maintain genera stability, but to actually supplement the ACL by providing posteriorly directed force durin extension tasks. Therefore, it is the objective of this study to assess the effect of one suc advanced design--the Bledsoe Pro-Shifter (Medical Technology Inc.)--on the extensio force capabilities and knee muscle activity of ACL-deficient patients and thereby re evaluate the usefulness of functional knee bracing in the ACL rehabilitation process.

METHODS

First, the twelve subjects' ACL deficiencies were documented by an orthopaedi surgeon; none of the subjects had posterior cruciate ligament deficiency, and all of then had been released from their rehabilitation programs. Next, the subjects were groupe according to activity level: high-activity (N=5) or low-activity (N=7). Not surprisingly, th subjects' respective activity levels correlated well with their remaining symptoms. Eac subject was fitted by the same certified orthotist with a Bledsoe Pro-Shifter dynamic kne brace. Once Ag-AgCl surface electrodes were placed in a bipolar arrangement over th belly of the rectus femoris and biceps femoris muscles, EMG signals were recorded an amplified with a gain of 2200, a CMRR of 110 dB, and a bandwidth from 10 to 500 Hz The subjects were then placed on a Kinetic Communicator (KinCom) evaluation device se up for isokinetic extension exercises (25°/sec). After a warm-up and several familiarizatio trials, the patients were instructed and verbally encouraged to perform maximal-effor concentric extensions ranging from 90° of flexion to full extension. To prevent fatigue, a five-minute rest period was observed between each of the four trials. This protocol wa performed with and without bracing in random order. The knee angle and torque from th KinCom as well as the quadriceps and hamstrings EMG were collected by a PC-controlle A/D system at a rate of 1024 Hz. After linear envelopes of the EMG data were obtaine digitally (τ= 200 mSec), they were pooled according to corresponding muscle, activity group and bracing conditions. Finally, ANOVA with repeat measures was used to discer the knee angles at which extension force or EMG activity differed when the results unde braced and non-braced conditions were compared.

RESULTS

Figure 1 shows typical extension force results under braced and non-braced condition for patients from both the high-activity group (a) and the low-activity group (b); points with

asterisks indicate angles at which significant differences in mean extension force occurred. In general, high-activity, asymptomatic patients wearing the brace exhibited decreased extension force in the range of 60° to 15° of flexion, but showed no significant change in agonist or antagonist muscle activity throughout the range of motion compared to the non-braced condition. In contrast, low-activity, symptomatic subjects using the brace were able to increase extension force at 60° and 55° of flexion, with increased quadriceps activity occurring at 80° and in the 45° to 15° range. Also, hamstrings activity decreased within the 45° to 30° range for this group.

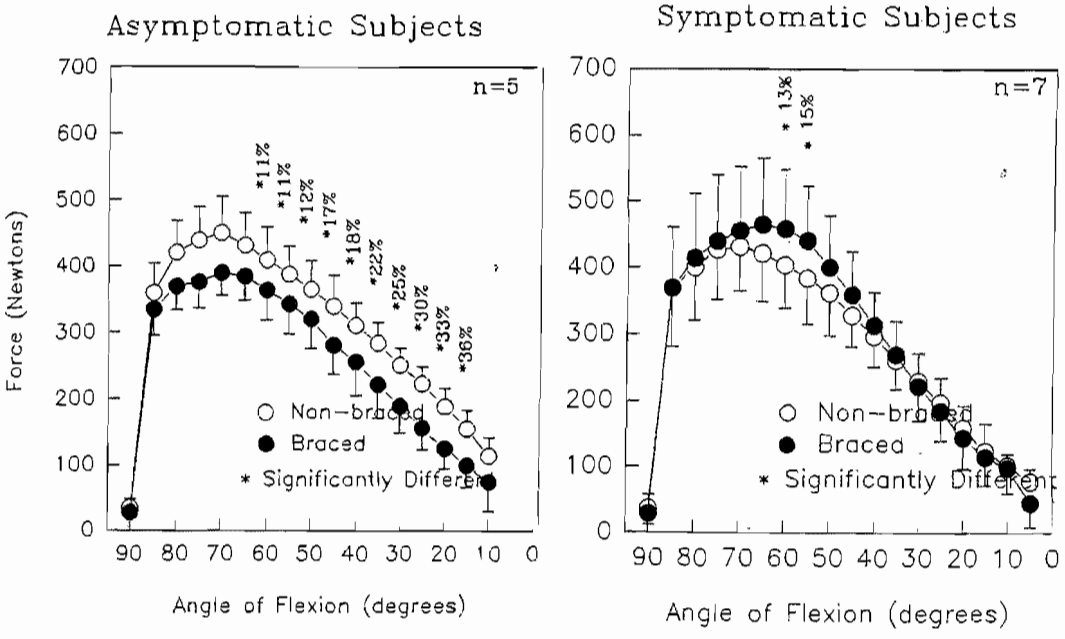

DISCUSSION

Based on the force results, our analysis concurs with Mishra et al. (1989): the functional effectiveness of dynamic knee bracing depends on the rehabilitation results and activity level of the individual patient. Furthermore, in our study, we confirmed this conclusion with EMG analysis of the knee musculature. In patients with persistent symptoms, the Pro-Shifter brace allowed increased extensor activity with decreased hamstrings action. This suggests that the brace can actively control knee stability in synergy with the antagonist, possibly resulting in lesser reflexive inhibition of the agonist. In contrast, the stable knees of asymptomatic patients did not benefit to the same extent, and were able to deliver less extension force because the brace exerted a posteriorly directed force on the proximal tibia. In other words, there was no change in muscle activity for these asymptomatic patients because no additional stabilizing forces were needed.

REFERENCES

Caborn, D. M., and Johnson, B. M. (1993) The natural history of the anterior cruciate ligament-deficient knee. *Clin. Sports Med.* **12**, 625-635.

Vailas, J., and Pink, M. (1993) Biomechanical effects of functional knee bracing. *Sports Medicine* **13**, 210-218.

Ott, J., and Clancy, W. (1993) Functional knee braces. *Orthopedics* **16**,171-176.

Cawley, P., France, E. P., and Paulos, L. (1989) Comparison of rehabilitative knee braces. *Am. J. Sports Med.* **17**,141-146.

Mishra, D.K., Daniel, D. M., and Stone, M. L.. (1989) The use of functional knee braces in the control of pathologic anterior knee laxity. *Clin. Orthop.* **241**, 213-220.

MOTOR UNIT FIRING BEHAVIOR IN THE FIRST DORSAL INTEROSSEOUS: EFFECTS OF PREFERENTIAL HAND USE

Alexander Adam*, Carlo J. De Luca*†

*NeuroMuscular Research Center and Departments of Biomedical Engineering and †Neurology, Boston University, Boston, MA USA

INTRODUCTION

Daily preferential use has been shown to alter physiological and mechanical properties of skeletal muscle. Using contralateral hand muscle pairs, a previous study showed lateral asymmetries in the surface electromyographic signal during constant force isometric contractions. In particular, the first dorsal interosseous (FDI) in the dominant hand exhibited a lesser decrease of the median frequency, suggesting higher fatigue resistance and possibly a higher percentage of Type I fibers (De Luca *et al.* 1986). Other researchers investigated the response of contralateral FDI muscle pairs to electrical stimulation. The dominant muscle was shown to possess a slower twitch and a greater ability to maintain tetanic force output during repeated stimuli, both of which are indicative of a shift in fiber type composition towards Type I fibers (Tanaka *et al.* 1984; Zijdewind *et al.* 1990). The present study was aimed at revealing differences in the control strategy of contralateral muscle pairs in humans who show a clear preference for one hand.

METHODS

We compared the motor unit (MU) recruitment and firing behavior in the FDI muscle of the dominant and non-dominant hand in eight male volunteers aged 21 to 39 (27.5 ± 7.5, mean ± std) whose hand preference was evaluated using a standard questionnaire. The protocol employed a test of the maximum voluntary contraction (MVC) force for the left and right hand followed by sustained isometric contractions at target force levels of 30% MVC. Subjects were instructed to increase the abduction force of their index finger to the target force level, hold the force constant for 20 sec, and decrease the force again while following a trapezoidal force trajectory displayed in front of them. Abduction force and myoelectric signals of the FDI were simultaneously recorded using a strain gauge and a quadrifilar needle electrode. The myoelectric signals were subsequently decomposed into individual MU firing time impulse trains using the Precision Decomposition technique.

RESULTS

Three of the subjects were right-handed (R), four left-handed (L), and one showed no hand dominance according to the questionnaire. No significant difference was found in mean MVC values with respect to hand dominance when measurements were pooled for all subjects. Individual lateral differences in MVC values ranged up to 40%, but were not correlated with handedness or MU firing behavior.

A total of 239 action potential trains was extracted for MUs that fired in a stable fashion during the constant force part of the contraction. For each of the MUs, the recruitment threshold, defined as the total muscle force at the time of the first firing of a MU; the initial firing rate, defined as the inverse of the mean of the first three interfiring intervals; and the average firing rate, calculated over a 5 sec interval at constant force, were analyzed. Every single R subject showed a lower recruitment threshold, lower initial firing rate, and lower average firing rate in the MUs of the dominant hand. In the L group, not all subjects exhibited similar trends for each of the parameters, making the lateral difference in MU firing behavior in this group less distinct. The one subject who lacked a clear hand preference did not exhibit any lateral asymmetry in the above parameters. For the R subjects, the lateral differences in mean values of recruitment threshold ($p<0.005$), initial firing rate ($p<0.01$), and average firing rate ($p<0.05$) were all significant, but not for the L subjects ($p>0.05$). When comparing only MUs recruited at low force levels (≤15% MVC), the differences in the average firing rates were more significant ($p<0.01$) in both the R and L subjects. Low threshold MUs in the L subjects were then also found to have significantly lower initial firing rates in the dominant hand ($p<0.05$).

The joint behavior of MUs within single contractions was assessed by cross-correlating mean firing rates signals (lowpass filtered firing time impulse trains) of MU pairs. Mean values and latencies of cross-correlation peaks were not significantly different across hands for both L and R subjects. To assess the effect of common fluctuations in MU firing rates on the force output of the muscle, mean firing rate signals were also cross-correlated with corresponding force records, revealing a significantly greater lead time of the firing rates over the force in the dominant hands ($p<0.005$).

DISCUSSION

The presence of lower MU firing rates in the FDI of the dominant hand is consistent with the notion of an increased percentage of slow twitch fibers, which allow twitch fusion and force build-up to occur at lower discharge rates. Direct evidence for an increased percentage of slow twitch fibers were the lower mean recruitment threshold and the greater delay between mean firing rate and force signals in the dominant hand of our subjects. No lateral difference was observed in the joint behavior of MUs as measured by the firing rate cross-correlation analysis, suggesting a similar central drive to the MU pools in dominant and non-dominant hand when producing equivalent contractions. We are led to believe that the different firing behavior of contralateral MUs is a result of peripheral adaptation to increased usage. Everyday activity can be viewed as a moderate training stimulus specific to the low threshold MUs in the preferred hand, since only low threshold units are recruited during low force contractions typical of everyday usage. In support of this hypothesis, we found a greater difference in firing rates for the low threshold MUs. Furthermore, mean MVC values did not differ between dominant and non-dominant hands, which has been reported in earlier studies (Tanaka *et al.* 1984; Rutherford and Jones 1988). The maximal strength is dominated by the force output of high threshold MUs, but these are rarely used in everyday activities and should not have adapted to preferred use of one hand.

REFERENCES

De Luca, C. J., M. A. Sabbahi, *et al.* (1986). "Median frequency of the myoelectric signal. Effects of hand dominance." European Journal of Applied Physiology **53**: 457-464.

Rutherford, O. M. and D. A. Jones (1988). "Contractile properties and fatiguability of the human adductor pollicis and first dorsal interosseous: a comparison of the effects of two chronic stimulation patterns." Journal of Neurological Science **85**: 319-331.

Tanaka, M., M. J. N. McDonagh, *et al.* (1984). "A Comparison of the Mechanical Properties of the First Dorsal Interosseous in the Dominant and Non-Dominant Hand." European Journal of Applied Physiology **53**: 17-20.

Zijdewind, C., W. Bosch, *et al.* (1990). "Electromyogram and force during stimulated fatigue tests of muscles in dominant and non-dominant hands." European Journal of Applied Physiology **60**: 127-132.

SUSTAINED LOADING GENERATES STRESS CONCENTRATIONS IN LUMBAR INTERVERTEBRAL DISCS.

M.A. Adams*, D.W. McMillan+, T.P. Green#, P.Dolan*.
* Comparative Orthopaedic Research Unit, University of Bristol, U.K. + School of Engineering and Advanced Technology, University of Sunderland, U.K.
# Department of Orthopaedic Surgery, University of Keele, U.K.

INTRODUCTION Intervertebral discs from young people distribute compressive stress evenly between adjacent vertebrae because the central region of the disc acts like a pressurised fluid in which the compressive stress does not vary with location o direction (1). The hydrostatic "cushion" effect depends upon the disc's high water content, and it is diminished in old age (1) when degenerative changes reduce the hydration of the nucleus by 15-20%. Disc dehydration also occurs when the spine is subjected to prolonged "creep" loading. MRI measurements on living people indicat that the volume (and by implication, the water content) of lumbar discs falls by abou 20% during the course of a day's activity (2). In our experiment, we test the hypothesis that creep loading reduces the size of the central hydrostatic region of the disc, and generates non-hydrostatic stress concentrations in the annulus. Stress concentrations may lead to pain, structural disruption, and alterations in chondrocyte metabolism.

METHODS 22 human lumbar spines were collected from subjects who had experienced no spinal injury, or prolonged bed-rest, prior to death. Spines were stored at -17^{o}C for up to three months, thawed overnight at 3^{o}C, and dissected into "motion segments" consisting of two vertebrae and the intervening disc and ligament 27 motion segments were used in the present experiments: they were divided at random into three similar-sized groups (A, B and C).

A preliminary creep test (300N for 15min) was performed on each specimen order to guard against the possibility of post-mortem "superhydration" of the discs. Each specimen was then positioned in 2^{o} of extension in order to simulate the lordot lumbar curvature typical of standing erect, and a constant compressive force was applied for a period of 20sec while a strain-gauged pressure transducer was pulled through the disc in the mid-sagittal plane, as described previously (1). The transduc sensing element was 0.8mm wide by 2mm long, and it was mounted in the side of a 1.3mm-diameter needle. Transducer output was sampled at 25Hz, A-D converted, and stored on a microcomputer. "Stress profiles" were obtained with the transducer pointing upwards, and then sideways, so that both the vertical and horizontal components of matrix compressive stress could be measured. The applied compressive force during stress profilometry was 1kN for Group A discs, and 2kN f Groups B and C.

Group A and B specimens were then creep-loaded with a compressive force o 1-2kN, depending on specimen size, for a period of 2-3 hours. Group C specimens were positioned in 4-8^{o} of flexion and creep loaded at 1-2kN for 6 hours. A graph c specimen height loss against time was plotted in "real time". Stress profiles were repeated immediately after the main creep test, using the same needle track. Finally, the discs were sectioned, and the pieces dried to constant weight so that their water content might be measured and compared with adjacent non-loaded discs from the same spine.

RESULTS Motion segment height loss was 1.2$\pm$0.3mm in Group A, 1.2$\pm$0.3mm Group B, and 1.7mm-2.2mm in Group C. No specimen reached a creep limit, even after 6 hours. At this time, the inferred water loss from the whole disc was 19% on average. The "before creep" stress profiles showed variations with age and posture similar to those described previously (1). Following creep, the hydrostatic pressure i the nucleus pulposus fell, and stress peaks appeared, or grew in size, in the annulus (Figure 1). Profiles were analysed digitally in order to calculate the mean and maximum horizontal and vertical stress in each region of the disc. The boundaries between these regions were specified using the following criterion: the "functional nucleus" was the central region of the disc in which the horizontal and vertical stress did not differ by more than 5% from each other, and did not vary by more than 5% with location. Regions of disc on either side of this were designated posterior and

anterior annulus. The size of a stress "peak" was defined as the maximum stress minus the pressure in the nucleus. Results are shown in Table 1.

Creep reduced the pressure in the nucleus by 13-36% Compressive stresses in the annulus were reduced slightly when the profiles were measured at 1kN (Group A) but at 2kN (Groups B and C) localised peaks of compressive stress appeared (or grew in size) in the posterior annulus following creep.

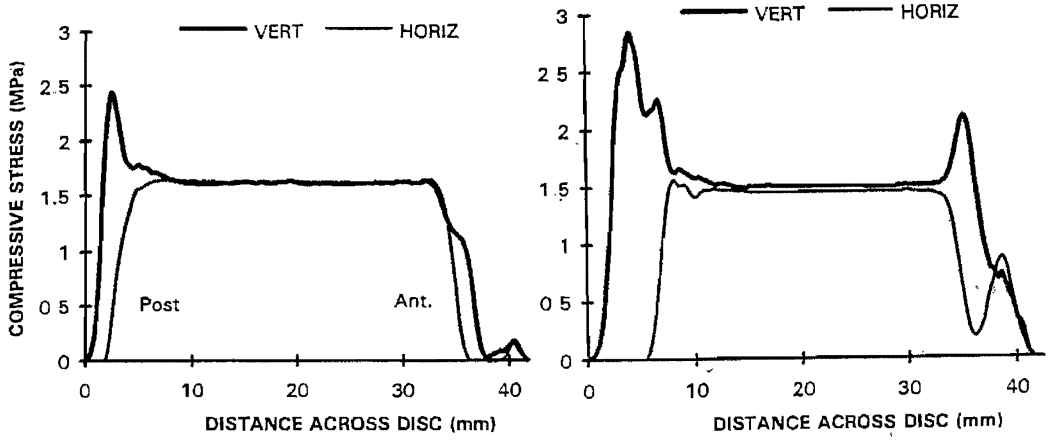

Figure 1. Stress profiles before (left) and after (right) creep for a Group B disc.

GROUP	n	AGE	% CHANGE FOLLOWING CREEP			
			IDP	Max(AA)	Max(PA)	PEAK(PA)
A	10	50	-15**	-17*	-16*	-14
B	8	43	-13**	-4	+2	+36*
C	9	56	-36**	-26	-8	+35

Table 1. Summary of average results. IDP=pressure in nucleus; Max(AA)= maximum stress in anterior annulus; PA=posterior annulus; *P<0.05; **P<0.001

DISCUSSION Any errors and artifacts in these experiments were minimised by treating each disc as its own control. The average water loss from each disc (19%) is consistent with the 20% diurnal variation in disc volume seen in-vivo (2).

The most pronounced change in intra-discal stress following creep was the 13-36% reduction in the hydrostatic pressure in the nucleus. This effect is partly attributable to increased loading of the apophyseal joints (1). However, the increase in stress peaks often observed in the posterior annulus requires another explanation. In effect, load is being transferred from the nucleus to the annulus, and this is probably because the nucleus can be likened to a sealed hydraulic system, in which a small loss of fluid leads to a large drop in pressure. Thus, water loss from the nucleus leads to more load being thrown on to the annulus, and the posterior annulus is affected most because it is the narrowest part of the disc. Evidently, disc mechanics depend on loading *history* as well as applied load.

The results are interesting for several reasons. High concentrations of compressive stress in the annulus would threaten the structural integrity of the lamellae, and might lead to fissure formation. Also, changes in matrix compressive stress would be expected to affect the metabolism of the chondrocytes (3). Finally, stress concentrations may possibly give rise to pain from the outer annulus (4) or from the adjacent vertebral bodies.

References.

1. **McNally DS, Adams MA (1992).** Internal intervertebral disc mechanics as revealed by stress profilometry. Spine 17 1 66-73.

2. **Botsford DJ, Esses SI, Ogilvie-Harris DJ (1994).** In-vivo diurnal variation in intervertebral disc volume and morphology. Spine 19 935-940.

3. **Hall AC, Urban JPG, Gehl KA (1991).** The effects of hydrostatic pressure on matrix synthesis in articular cartilage. J Orthop Res 9 1-10

4. **Kuslich SD, Ulstrom CL, Michael CJ (1991).** The tissue origin of low back pain and sciatica. Orthop Clin N Amer 22 2 181-7.

OPTIMAL TENSION OF ISOTONIC TOWING FOR SPRINT TRAINING

M. Ae*, N.Itoh**, Y Muraki*, and K.Miyashita*
* Institute of Health and Sport Sciences, University of Tsukuba, Tsukuba City, Japan
** Department of Education, Yokohama National University, Yokohama, Japan

Introduction

Supramaximal running velocity has been used to improve sprint speed, which is attained by various methods. Although some investigations(Mero and Komi,1985; Bosco et al.,1986) have been reported, in these investigations the towing tensions could not be controlled because of some restrictions of towing systems used. Therefore, optimum tension for sprint trainig is still unclear, and characteristics of supramaximal runs under various tensions are not examined throughtly. The purpose of this study was to find out optimal towing tension for sprint training, investigating the effects of different tensions on biomechanical parameters and subjective intensity.

Methods

Subjects were three excellent sprinters and five jumpers of varsity track team. They ran five different sprints as fast as possible, i.e. maximal run, three supramaximal runs under tension of 15N, 30N, and 45N(henceforth Tow15, Tow30, and Tow45), and post-maximal run. Subjects were videotaped over 10m interval following 40m accelaration phase with a panning high speed VTR camera(HSV-400, NAC Co.) operating at 200 Hz. Supramaximal runs were performed with an isotonic motor-driven towing system. Towing tension was controlled by a powder cratch system so as to keep the tension constant. Feeling of the subjects during supramaximal runs were collected by a questionnaire which asked the degrees of exertion and comfort/fear perceived. Coordinates data of the endpoints of the body segments were obtained by digitizing video images over at least one running cylcle and smoothed with a Butterworth digital filter cutting off at 10Hz. Running velocity, stride length, stride frequency, running kinematics, joint moments and powers were computed by Newtonian mechanics on a multi-link model.

Results

Table 1 shows performance descriptors of maximal and supramaximal runs.

Table 1 Performance descriptors of maximal and supramaximal runs

	Maximal	Tow15	Tow30	Tow45
Running velocity(m/s)	9.96±0.21	10.40±0.33**	10.63±0.38**	10.82±0.28**
(%)		4.44±1.88	6.69±1.96	8.70±1.72
Stride length(m)	2.13±0.05	2.20±0.07*	2.25±0.06**	2.31±0.06**
Support 1st half	0.46±0.05	0.51±0.06	0.49±0.04	0.50±0.03
2nd half	0.51±0.05	0.48±0.05	0.50±0.04	0.46±0.06
Nonsupport	1.16±0.07	1.21±0.04	1.26±0.07*	1.34±0.06**
Stride frequency(Hz)	4.67±0.13	4.74±0.17	4.72±0.19	4.70±0.15
Duration(ms)				
Support 1st half	46±6	49±5	47±4	48±3
2nd half	49±5	43±4	44±5*	41±5*
Nonsupport	122±6	120±6	120±9	125±8

Test of significance ** $p < 0.01$, * $P < 0.05$

Running velocity significantly increased with the increase in the towing tension. Stride length also significantly increased in supramaximal velocities, which was caused by the increase in the nonsupport distance Although stride frequency did not significantly change, the duration of the second half of support phase significantly decreased in Tow30 and Tow45. Although the degree of exertion for supramaximal runs was smaller than the maximal run, it increased with the towing tension(86.9% at Tow15 to 92.5% at Tow45). Subjects felt comfort at the Tow15, but fear at Tow45.

Figure 1 shows changes in joint moment powers of the hip and knee joints during the recovery phase of maximal and supramaximal runs for the excellent group. Patterns of the joint powers of supramaximal runs were similar to those of the maximal run. However, positive power of the hip extensors and negative power of the knee flexors were significantly larger in the late recovery phase of Tow30 and Tow45

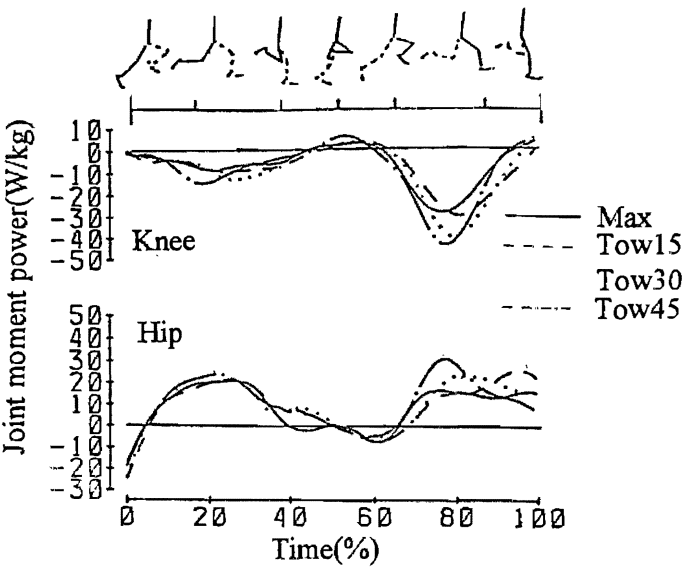

Figure 1 Joint powers of the knee and hip in sprint

Discussion

On the average, increase in stride length seems to be major factor of the increase in velocity observed at the surpamaximal runs. Remarkable difference between the excellent and poor groups was observed in the response of stride frequency. Excellent sprinters could increase stride frequency by 3 to 4 % at the supramaximal velocity while the poor group could not. This results suggested that skill level of sprinters should be considered in applying towing to the sprinters' training.

Increase in maximal joint moment powers of the hip extensors and knee flexors in the late recovery phase was observed in supramaximal runs. Therefore, supramaximal runs can be used as one of effective training means specific to sprint for the improvement of concentric power of the hip extensors and eccentric power of the knee flexors. Maximal power and negative work at the knee joint of the late recovery phase were significantly larger in Tow30 and Tow45 than the maximal run and Tow15. Although increase in running velocity in Tow45 was the largest, kinematics of the leg was different from the maximal and other supramaximal runs. The subjects felt fear and difficulty to control their own sprint motion at Tow45

It is concluded that towing tension of 30N will be optimal for ordinary and excellent sprinters and that tension of 45N should be used only for excellent sprinters because of excessive physical and mental loads

References

Bosco,C. and Vittori,C.(1986), Biomechanical characteristics of sprint running during maximal and supra-maximal speed. NAS 1, 39-45.

Mero,A. and Komi,P.V.(1985), Effects of supramaximal velocity on biomechanical variables in sprinting. Int J. Sport Biomech. 1(3), 240-252.

ASSISTED TRANSFERS IN QUADRIPLEGIA - TOWARDS A SOLUTION

GT Allison[1], RN Marshall[2] and KP Singer[1]. [1]The School of Physiotherapy, Curtin University, Shenton Park Western Australia. 2 Department of Human Movement, The University of Western Australia, Nedlands, Western Australia.

INTRODUCTION

The application of biomechanical analysis to human movement for both normal and abnormal conditions has led to the development of fundamental motion analysis paradigms that are the basis for many rehabilitation intervention regimens. Within the spinal cord injury (SCI) population, this is demonstrated by the development of orthotic and/or FES interventions which have been based on the motion analysis of normal human gait. The ability to transfer in individuals with quadriplegia represents a significant factor in overall functional mobility and independence. Approximately 30% of all SCI result in lesions at the C4 and C5 levels (1). The majority of individuals with these lesions are unable to transfer and the variance in the performance is related to factors other than neurological lesion level (2). This represents a major clinical rehabilitation goal, yet has received little biomechanical inspection.

This research group, has previously demonstrated that there are two movement strategies where individuals with weak triceps attempted to transfer with a rotatory pattern rather than a translatory pattern. Furthermore, the rotatory pattern had a more upright pre-transfer body position, with higher acromion processes and wrists placed closer to the body (3,4). Unpublished data from our laboratory also indicates that individuals with quadriplegia are less stable (higher mean frequency of movement) in the pre-transfer position when compared to paraplegics.The purpose of this research was to assess the reaching and transferring performance of a C5 quadriplegic with and without an orthosis which was designed from biomechanical models and associations established in our previous research.

METHODS

The research design was a case study interrupted time-series analysis (ITSA) and statistical significance was accepted at the 0.05 level of confidence (5). The case study involved a complete C5 (Frankel B) quadriplegic (age 26yrs, 56.6kg) who had previously received posterior deltoid muscle transfer surgery on his left arm. There were two conditions: with and without an orthosis. Two tasks were tested in long sitting: a maximal lateral and forward reach with one hand and, a lateral transfer. The reaching task was assessed by the maximal displacement of the trajectory of the wrists as viewed from an overhead camera relative to the knees and body mid-line. Stability assessments (amplitude and frequency) of the displacement of the centre of pressure (COP) for the maximal lateral reach position were recorded.

The transfers were performed on a force platform and video recordings were made from the lateral and posterior views of the spatial models from reflective landmarks. The pre-transfer postures and lateral displacement of the pelvis were determined for each trial. The force plate trigger was synchronised with the video by a frame marker. Movement analysis cross-correlations were used to identify movement strategies as previously reported (3).

A brace was developed to allow forward flexion of the trunk without upper extremity support and increased options of hand positioning for the transfer. It was rigid with adjustable hinges at the hip and a chest plate. The three point support system incorporated a lumbar and two thigh supports (distal anterior and proximal posterior).

RESULTS

The brace altered the longsitting posture of the subject (Figure 1). The subject demonstrated a rotatory movement strategy independent of the use of the orthosis since all trials had strong negative correlations (normal mean -0.976, SD 0.022 orthosis mean -0.842, SD 0.074). The mean distance the pelvis was transferred laterally without the brace was (16.0 ± 3.4 cm) and with the brace (19.6 ± 2.5 cm). This was not statistically significant using a ITSA.

Figure 2 illustrates the ITSA for the lateral displacement of pelvis during the transfer and the overall displacement of the COP during the maximal lateral reach

task.The area of reach past the line of the knees was significantly increased (F=9.55 df=2,12 p=0.003) from 285± 80 cm^2 to 1770± 308 cm^2.

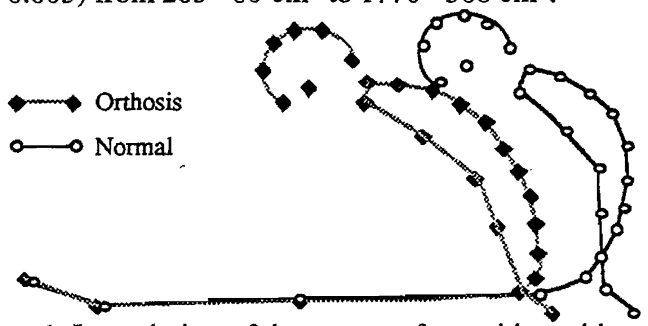

Figure 1. Lateral view of the pre-transfer position with and without an orthosis.

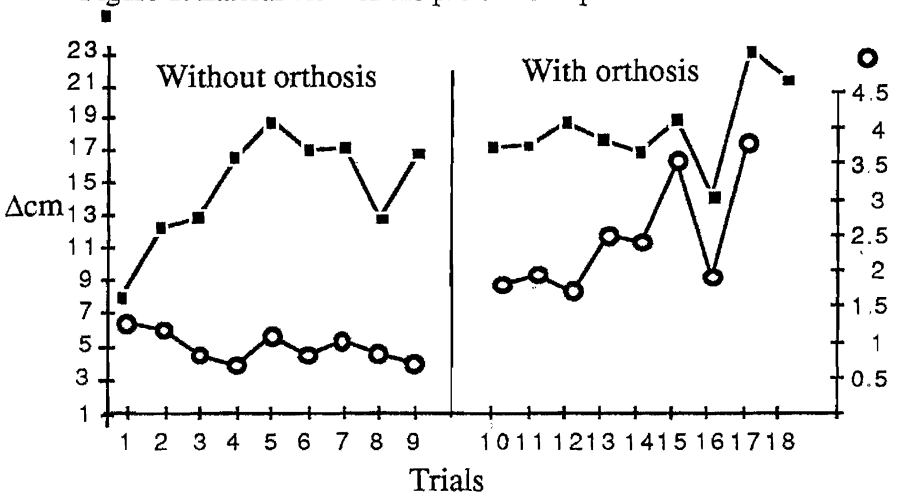

Figure 2. ITSA of pelvic lateral displacement during each transfer (■) and excursion of COP during the reach task (●). All measurements are in cm.

DISCUSSION

The ability to transfer in individuals with quadriplegia represents a significant factor in their overall mobility. Most research to date associated with SCI mobility has been directed towards gait and is based on fundamental biomechanical analysis of the gait cycle. However, the ability to transfer independently represents a greater functional improvement and is associated with the more dependent individuals than gait is in paraplegics. This study has utilised previous biomechanical research which has identified factors related to the ability to transfer, developed an orthosis on the basis of the biomechanical analysis and demonstrated that an individual has increased forward arm reach with greater safe excursion of the COP during the dynamic phase of the reach. The improved arm reach was a result of further forward flexion and a more extended lower trunk. There was no significant difference in the excursion of the COP in the static reach however, with the orthosis the excursion of the COP was significantly greater. This reflects the role of the orthosis on trunk stability. Using the orthosis the subject was on average able to displace the pelvis an additional 3.6cm. This was found not to be statistically significant and the clinical significance is yet to be elucidated.

It is clear that further development of the system is required, yet it represents a possible unique solution, based on motion analysis principles, of transferring in dependent individuals with quadriplegia. The possible user population, the overall functional benefits, the compliance of the users and possible modifications to the device using functional electrical stimulation are all possible directions for future research.

REFERENCES

1. De Vivo et al (1992) Arch Phys Med Rehab 73, 156-162
2. Yarkony GM, et al., (1988) Arch Phys Med Rehab 67 (2) 73-76.
3. Allison, GT, Singer KP and Marshall, RN (in press) Disability and Rehabilitation.
4. Allison, GT, Singer KP and Marshall, RN (submitted) Aust J Physio.
5. Crosbie J & Sharpley CF (1989). DMITSA (2.0) Victoria, Australia.

FACTORS ASSOCIATED WITH TRANSFERRING IN SPINAL CORD INJURY

GT Allison[1], KP Singer[1] and RN Marshall[2]. 1.The School of Physiotherapy, Curtin University, Shenton Park Western Australia. 2. Department of Human Movement, The University of Western Australia, Nedlands, Western Australia.

INTRODUCTION

The ability to transfer in individuals with spinal cord injury (SCI) represents a significant factor in overall functional mobility and independence. Approximately 55% c all indiviuals with SCI are quadriplegics. About half of all quadriplegics have weak triceps and the majority of these can not transfer. This represents a major rehabilitation problem. Many biomechanical factors have been associated with the ability to transfer, f example, functional arm length (arms relative to stem height), muscle strength and hand placement, however the majority of these reports are anecdotal. Bergstrom et al., (1) demonstrated a significant difference in body mass, % body fat and the placement of the leading hand when attempting to transfer between C6 quadriplegics who could and coul not transfer. There was no difference between the groups for functional arm length. Allison et al., (2) provided a preliminary report of two movement strategies adopted by individuals with SCI. It was found that some individuals performed the lateral transfer using a rotatory movement pattern, where the head moved in the opposite direction to th pelvis. Others performed a translational strategy where the head and pelvis moved in concert. The fact that there are at least two movement strategies may account for the variability in the literature of factors associated with the ability to transfer. The factors which determine outcome for each movement strategy are yet to be objectively elucidate

The purpose of this research was twofold: i) to identify difference between the movement strategy groups in anthropometric and biomechanical variables and, ii) to assess the factors which are associated with the ability to transfer.

METHODS

17 male volunteers with SCI (quadriplegics n=12, paraplegics n=5) performed series of lateral transfers while positioned on a force platform. During the transfers, vic recordings were made from the lateral and posterior views of the spatial models from reflective landmarks. Force plate centre of pressure (COP) data for pre-movement stability and displacement of the COP (ΔCOP) were determined for each trial. The ΔCC was used as an outcome measure for the ability to transfer. Event markers for the trans were established (2) and all data were synchronised and time normalised. Movement analysis techniques (3) were used to identify movement strategies as previously report (2). Dependent variables also recorded were: anthropometric data (upper extremity lengths, body mass), elbow extension strength and pre-transfer hand placements.

Individuals were classified into rotatory (n=4) or translatory (n=10) groups. Three individuals performed a mixed motor pattern. Three statistical analyses were performed: i) analysis of group differences (Mann-Whitney U), ii) stepwise logistic regression (translation = 1, rotation = 0) to determine the factor which predicted the selection of the movement strategy and, iii) correlations between ΔCOP and the depen variables.

RESULTS

Individuals who performed the translatory movement strategy when compared the rotatory group were able to displace the COP a greater distance, their wrists were further apart, and their acromion process heights were lower. They also had greater elbow extension strength relative to their body weight (see Table 1).

Elbow extension strength accounted for the greatest amount of variance when predicting the selection of the movement strategy ($R^2 = 0.76$). The next variables included in the equation were the length of the arm span (-ve) and biacromial width (+ Using a Jackknife technique (4) all subjects were correctly allocated to the appropriate groups. The associations between the ability to displace the COP and the dependent

variables for all subjects and the translatory subgroup are shown in Table 2. The rotatory group (n=4) sample was too small to calculate the associations.

Table 1. Means and SD and group differences of selected variables.

Variable	All SCI x (SD)	Translatory x (SD)	Rotatory x (SD)	Group p
Displacement of COP	28.3 (12.2)	32.5 (11.1)	15.2 (6.9)	$p < 0.01$
Arm Span	166.1 (4.8)	166.3 (5.0)	167.8 (2.7)	ns
Biacromial Width	40.1 (2.2)	40.8 (1.8)	38.1 (1.1)	$p < 0.05$
Body Mass	65.1 (8.7)	62.4 (9.7)	69.1 (3.6)	ns
Elbow extension strength (R)	24.2 (16.2)	31.6 (11.8)	6.9 (3.0)	$p < 0.05$
Functional Arm length (transfer)	125.4 (9.4)	127.6 (10.6)	121.9 (5.9)	ns
Acromion height (transfer side)	47.2 (4.4)	45.5 (4.2)	51.4 (0.7)	$p < 0.05$
Distance between wrists	73.3 (8.8)	76.7 (8.8)	63.6 (3.5)	$p < 0.05$

Table 2. Correlation with the ability to displace the COP

Variable	SCI N=17	Translatory (n=10)	Variable	SCI N=17	Translatory (n=10)
Elbow extension strength (R)	0.641	0.496	Arm Span	0.116	0.605
Fnl Arm length (transfer)	0.311	0.028	Biacromial	0.424	0.345
Acromion ht (transfer side)	-0.622	-0.303	Body Mass	-0.434	-0.346
Distance between wrists	0.618	0.479			

DISCUSSION

From the results of this study it is evident that there are fundamental differences between the two transfer movement strategies and that the strength of elbow extension determines the strategy adopted. The individuals who perform the rotatory movement strategy are weaker and are unable to displace the COP as far as the translatory group. It would seem that this movement strategy incorporates those individuals who are able to transfer without functional triceps (C6 and above). The differences between the groups also indicate that anthropometric and biomechanical factors such as hand placement may play an important role in the overall performance. It would seem that functional arm length does not differ between the groups. This may reflect the inability of individuals with a high lesion and short arms to flex forward and thereby increase their functional arm length (i.e. arm length relative to their stem height).

To date the factors associated with the ability to transfer in individuals with SCI have been based on subjective or anecdotal information. This is the first study to demonstrate associations between the ability to displace the COP and anthropometric and biomechanical variables. It would seem that the outcome of the lateral transfer is dependent on the interaction between the movement strategy and many biomechanical and anthropometric factors. These findings support the hypothesis that the inconsistencies in the literature may be related to the fact that there are at least two movement strategies being performed when individuals with SCI attempt to transfer. The group differences also infer that the biomechanical factors which determine successful performance may differ between the particular strategies. Further research may indicate the factors associated with the ability to transfer. This is particularly important in the rotatory pattern which has greater clinical importance since it identifies the most dependent group of individuals.

REFERENCES

1.Bergstrom et al., (1985) International Rehabilitation Medicine 7, 51-55.
2. Allison, GT, Singer KP and Marshall, RN (in press) Disability and Rehabilitation.
3. Whiting WC & Zernicke, RF (1982) Journal of Motor Behaviour 14(2), 135-142.
4. Stevens, J (1992) Applied multivariate statistics for social sciences.

THERMAL ANALYSIS OF THE TAPED ANKLE AFTER EXERCISE

Alt, W., H. Lohrer, C. Scheuffelen, A. Gollhofer

INTRODUCTION

Many authors found that adhesive strapping looses up to 50% of its original sup after as little as 10 Minutes of exercise. Beside numerous publications concern efficacy in terms of restricting motion of the ankle - this study addresses these is from a new perspective: The **thermal aspect** of **various taping techniques different types of tape**. Our purpose was to compare temperature swing beneath and thermal radiation of the surface with two taping techniques and two different ta materials.

MATERIAL AND METHODS

12 subjects underwent 5 trials in a randomized order:

- **A** - without tape
- **B** - right ankle taped conventional ("Fast Gips" *Montag*) with Tape 1 (Beiersdorf - Leukotape®)
- **C** - right ankle taped conventional ("Fast Gips" *Montag*) with Tape 2 (Lohmann - Porotape®)
- **D** - right ankle taped new (unpublished technique) Tape 1
- **E** - right ankle taped new (unpublished technique) Tape 2.

A series of exercises were used to stress the ankle:

5 Drop jumps,

10 minutes running (treadmill),

3 minutes of jumping using a special device with sloping surfaces.

The course was performed two times. Temperature beneath adhesive tape was recor Thermocouples were placed at skin and fixed by tape. Thermal radiation of the ankle measured by a special thermographic device. 4 positions were recorded during a no stance phase. **lateral, frontal, medial** and **dorsal** view. In addition to this we used v records to get a more detailed understanding of thermographical consideration respect to anatomical structures. 4 small metal landmarks gave orientation.

We defined the following **quantitative** parameters:

a) Value of highest temperature "hot spots"; **b)** Mean of temperature in special areas

	view	lateral	frontal	medial	dorsal
a	label	**VoHSL**	**VoHSF**	**VoHSM**	**VoHSD**
b	label	**MoTL**	**MoTF**	**MoTM**	**MoTD**

Qualitative parameters:

a) **Location** of "hot spot" **LoHS** and

b) **appearance** of dark (very cold) areas **AoDA.**

RESULTS

1. Skin temperature of taped ankle increases more compared to untaped ankle during exercise (Fig.1).

2. Temperature after all exercises increased up to 20%.

There were only small differences of the values of "hot spot" (**VoHS**) comparing the types of tape and the two techniques. The location of "hot spot" (**LoHS**) showed differences between conventional and new taping technique.

Figure 1:

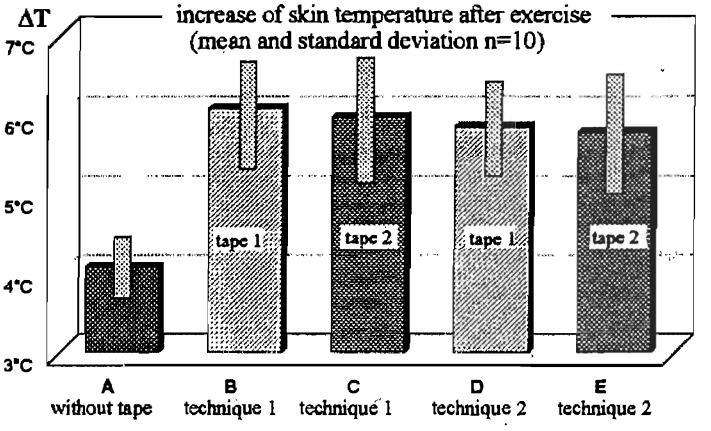

Ankles taped conventionally showed **LoHS** near the m. extensor dig. brev.; the new method showed this area more distal - **40% outside the tape** - compared to untaped ankles. **MoTD** generally showed the lowest level (tendo calcanearis).

AoDA was seen more often from dorsal position. Ankles in Tape 2 showed a tendency to a higher level of **AoDA**.

DISCUSSION

Thermographic images give a new perspective of evaluating ankle taping. Our findings support the assumption that moisture accumulates beneath tape, leading to lessened skin adherence. The finding of "hot spots" was separated into two categories: **a) anatomical** - located over vascular regions and **b) non anatomical**. This could be interpreted as a higher amount of tension within the various strips especially the "figure of eight" strip in the area of the retinaculum musculorum extensorum inferius.

Appearance of fully moistened areas could bee seen in two different ways: as "hot spots" or as "dark areas".

The second form consists possibly not only of sweat but also of an "air bag" resulting by lost skin adherence.

The remarkably higher value of **AoDA** and the lower level for **MoTD** (tendo calcanearis) is not only a result of folds of tape in this region due to dorsal/plantar flexion during running but must also bee seen as global cooling in this section and has to be considered in relation to achillodynia. Further studies have to be done to find out if more tension in different tape strips has an influence on thermal regulation in artery/veins circle and if there is a transfer between thermal and mechanical receptors which would leading to more effective proprioceptive control of the ankle joint.

KINEMATIC CHANGES WITH FATIGUE IN FRONT-CRAWL AND BACKSTROKE SWIMMING

Francisco Alves and Raquel Madeira

Faculty of Human Movement, Technical University of Lisbon, Lisbon, Portugal.

INTRODUCTION

Performance in swimming relies mainly on maximal energy output and the efficiency of the power transfer process to overcome drag. This last factor depends on technical ability. The impact of the reduction in skill level with progressive fatigue needs to be analysed and quantified for each sport activity. Clearly, the efficiency of power transfer changes as an athlete fatigues and technique deteriorates needs to be carefully considered.

The purpose of this study was to investigate the relationships between changes in swimming velocity, stroking characteristics and kinematics characteristics of the arm pull.

METHODS

Twelve well trained male swimmers participated in this study (age: 17.75±1.82 years, height: 178.46±6.07 cm, body mass: 67.63±6.59 kg, and %FAT: 7.63±2.02). Each subject performed a 400 m maximal swim Swimmers were free of equipment and were instructed to keep a constant pace in each swim, following a light tracer. Oxygen uptake measured after the maximal swim was considered to be the $\dot{V}O_2$ peak for each swimmer in that stroke. Arterialised blood samples were collected after the last bout, for the determination of the blood lactate concentration. The swimmers were filmed underwater (sagital plane) during the 400 swim with a video camera (25 Hz), fixed from the wall, 6 m from the swimmer, perpendicular to the direction of swimming and 20 cm underwater.

Pull kinematic characteristics and hip velocity were obtained by numerical treatment of data from hand displacement and hip horizontal displacement and evaluated by a video analysing system. The duration of the four phases in front crawl (entry/glide, downsweep, insweep, upsweep) and the five phases of backstroke (entry/glide, downsweep, upsweep, final downsweep, finish/exit) was calculated in milliseconds and expressed as a percentage of the duration of the total underwater armstroke.

Mean pulling length and mean pulling depth (cm), as defined by Schleihauf et al.[1], distance between point of entry in the water and point of exit of the hand from the water (cm), and absolute and relative duration of each phase of the underwater stroke were determined for each subject in the first and in the last 25 m laps and used for descrimination of possible differences in the pull pattern with increasing fatigue. In spite of the known differences between intracycle velocity measured at the center of gravity or at the hip, Maglischo et al. [2] have proposed that the horizontal velocity of the hip can be used as a tool for technical evaluation because the velocities of the hip and center of gravity follow similar patterns in the four competitive strokes. Every swimming effort was filmed from out of the water for the assessment of stroke rate and velocity. The effective velocity sustained at each stage was measured over 15 m within two points 5 m from each end of the pool, to eliminate the influence of the turn. Distance per stroke was then estimated by simple arithmetic calculations. The statistics consisted of means and standard deviations for description of measured variables and ANOVA for repeated measures to test the significance of statistical differences

RESULTS

Peak $\dot{V}O_2$ ($l.min^{-1}$) and lactate concentration ($mmol.l^{-1}$) attained were 4.13±0.4 and 11.94±1.51 in front-crawl and 3.91±0.39 and 9.68±2.23 in backstroke.

Swimming velocity was significantly lower at the last lap of 50 meters than at the firs one in both strokes. This difference was concomitant with a decrease in distance pe stroke and a maintenance of stroke rate, in agreement with previous studies [3].

In front crawl, the spacial characteristics of the arm pull showed significant change in the last lap, with a decrease in both the pulling length and the pulling depth. In backstroke, on the contrary, swimmers were able to maintain pulling length and depth stable through the entire swim. Distance between point of entry and point of exit of the hand did not change significantly in both strokes.

In front crawl, relative duration decrease of the entry-glide phase and of the upsweep occurred at the last lap of the swim. In backstroke a decrease of the relative duration of the final downsweep was the only significant change observed.

DISCUSSION

In front crawl, relative duration decrease of the entry-glide phase and of the upsweep denotes less body roll and incapacity of creating large amount of propulsive force in the finish of the pull as happens at the initial laps, due to local fatigue. In backstroke, decrease of the relative duration of the final downsweep is possibly the origin of the decrease in distance per stroke.

The absolute and relative durations of each phase showed strong interindividual differences, varying up to three times in some cases.

This results give evidence that individual strategies for obtaining even paced maximal swims should be studied in order to make possible an adequate technical advise and optimisation of competitive performance.

REFERENCES

1.Maglischo, E.W., Maglischo, C.M. and Santos, T.R. (1987) The relationship between the forward velocity of the center of gravity and the forward velocity of the hip in the four competitive strokes. *Journal of Swimming Research*, Vol.3, No.2, pp.11-17.

2. Schleihauf , R.E., Higgins, J.R., Hinrichs, R., Luedtke, D.L., Maglischo, E.W., Maglischo, C.W. and Thayer, A.L. (1988) Propulsive techniques: front crawl stroke, butterfly, backstroke, and breastsroke, in *International Series on Sport Sciences: Vol.18. Swimming Science V*, (eds. B.E. Ungerechts, K. Reischle and K. Wilke), Human Kinetics, Champaign, pp. 53-59.

3. Alves, F. (1994) Analysis of swimming races (abs). Journal of Biomechanics, Vol. 27, No. 6, p. 653.

ENERGETIC ASPECTS OF THE TRIPLE JUMP

A.C.Amadio[1], W.Baumann[2]
1- Universidade de Sao Paulo - EEF, Laboratorio de Biomecanica - Brasil
2- Deutsche Sporthochschule Köln - Institut für Biomechanik - Germany

INTRODUCTION

The study focuses on sports activity, considering the different types of energy a the interpretation of the process of energy transformation which occurs during movement analysed - the triple jump. The total mechanical energy of the body, or o body segment (E_{ti}), can be obtained by adding up the following types of mechani energy, potencial, E_{pot} ($m_i g h_i$) and kinetical, E_{kin} (translational, E_{trans} ($m_i v_i^2/2$) a rotational, E_{rot} ($I_i w_i^2/2$)).

$$E_{t_i} = m_i g h_i + \frac{m_i v_i^2}{2} + \frac{I_i w_i^2}{2}$$

Therefore, the quantification of the mechanical energy (defined as the sume of external and internal energy) was carried out in order to describe the triple jump. T external energy is related to velocity and vertical position of center of gravity (E_{kin} E_{pot}) and the internal energy is related to relative movements of the limbs with respect center of gravity ($E_{rot} + E_{trans}$). Inevitably all physical activities of the human bo involve changes in the type of energy.

This concept encompasses the transformation from one type of energy to anot following its basic forms: chemical, mechanical (potential, translational, rotatio elastic), thermal, etc., according to Winter (1979). Another important concept mechanics is that, in an isolated system, the total mechanical energy remains consta The energetic transformations can also be interpreted based on the work product needs of each body segment, required by the task to be performed.

METHODS

This research was undertaken using a kinemetric procedure, where a pan camera with external calibration and markers was used, according to Amadio (1985), a calculate the X,Y body coordinates. To conduct this analysis, we focused measurements that characterize an analysis of movement, synchronizing the follow procedures: Cinematographic (Locam high speed 16 mm Camera, 100 f/s) a Anthropometric (utilizing Hanavan, mathematical model to determine center of grav inertia and center of gravity of body segments). The anthropometric procedure w practised as a reference system to calculate the kinematic variables based on cinematographic data

The coordinates of marked body points were achieved through analysis of ea picture, receiving mathematical numerical treatment by using a 5 point parabo aproximation method. Considering the predomination of the movement in the sagit plane and mechanical shock during the support phase, which causes a enorm displacement of muscular mass, a great error in the determination of the rotational ene as well as a reduced contribution of this type energy to the movement analysed w observed. Hence the rotational energy was not utilized for the present investigation.

RESULTS AND DISCUSSION

The models of calculation enable quantification of the external mechanical ene for the center of gravity of the jumper in a real competition situation; therefore, it represented as shown in *Fig.1*, in view of the structure of movement in the axis of r execution time. In this figure it is evident the typical behavior of mechanical ene development in its diversified forms towards the jumper center of gravity.

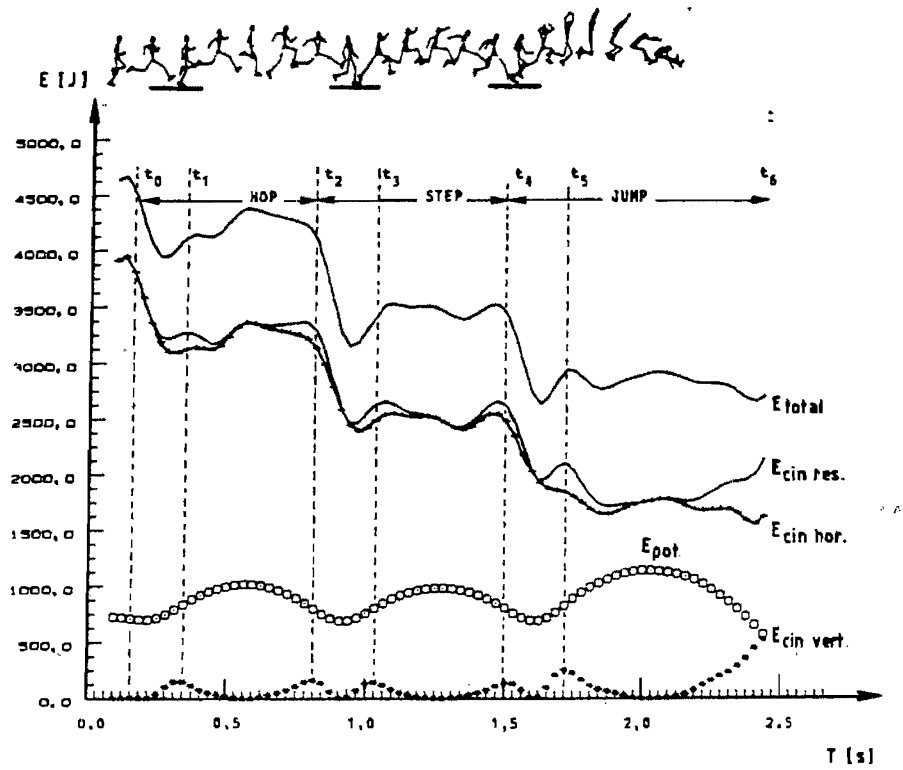

Fig.1: Interpretation of the modifications occured in the external mechanical energy during the 17.33 m triple jump performed by athlete PB, according to Amadio (1985).

This survey involved the analysis of 57 triple jumps, resulting in average performance of 15.57 m (14.38 - 17.33). The analyzed jumps refer to competition performance in German Athletic Championships. The value of the average error rate when quantifying mechanical energy is determined in relation to the control of value variance observed during the aerial phase of the movement, which is the largest variance phase, where maximum deviation reached 360 J, which means an average error rate of less than 8%. The potencial energy observed during the supporting phases show an alteration of the minor values for Step ± 50 J while for Hop and Jump these values are ± 150 J. Concerning kinetic energy horizontally, it is noted that loss in the supporting phase increases from support to support and that for the greater jump performance, the larger energy loss. Furthermore, regarding total mechanical energy alterations, it was revealed the lowest loss value for Hop, whilst the highest loss values were noted for Step during the supporting phase. A meaningful correlation ($p<0.001$) was found for the alteration of potencial energy between Hop and Step with triple jump performance, during both the supporting and the aerial phases. Another important correlation was detected ($p<0.001$) for the total mechanical energy loss in the triple jump support and performance, considering alterations occured between Hop and Step, as well as between Hop and Jump. This means that the loss ratio of total mechanical energy is increased from first to third jump in the supporting phases, i.e., the following loss proportional values were obtained: Hop ±5%, Step ±15%, Jump ±18% The maintenance of these values becomes more difficult for Step than for Hop and Jump.

REFERENCES

AMADIO, A.C. (1985): Biomechanische Analyse des Dreisprungs. Institut für Biomechanik - Deutsche Sporthochschule Köln, *Dissertation - Doktor Sport-wissenschaften*, Köln.

WINTER, D.A (1979): Biomechanics of human movement. John Wiley & Sons, New York, Chichester, Brisbane, Toronto.

FOOT PRESSURES DURING GOLF SWINGS BY PROFESSIONAL GOLFERS AS MEASURED BY A HIGH RESOLUTION SENSOR

[1]AMANO, K., [2]YANAGI, H., and [3]HIRAYAMA, M.

[1] Kanto Gakuen University, Ota-City, Japan; [2] Institute of Sport Medicine and Science Agui-town, Japan; [3] Human Dynamics & Design, Tokyo, Japan

INTRODUCTION

Previously we measured foot pressures during golf swings at various lies by Japanese professional golfer (Amano & Hibi, 1994). We found that foot pressures were observed to be influenced more by differences in right-left inclination than front -rear inclination. We concluded this is because the human body maintains high front-rear foot stability through action of the foot digits. Right-left balance, however, requires the use of both feet. This is due to the structure of the foot. On the other hand, the soles of the feet are the first parts of the body to absorb large reaction forces, before they are transmitted to other parts of the body. We consequently considered that foot pressure indicated the total capacity of the physical fitness (muscle power and flexibility etc.) and structure of the body. In other words, the total capacity is the net usefulness of physical resources, not maximum values. The purpose of this study is to find the relationship between the foot pressures measured during golf swings and total capacity, and performance.

METHOD

The subjects were 18 professional golf players involving three major title holder (shown in Table 1) and 18 amateur players handicapped 6 to 36. Foot pressures were measured by an F-scan system(Tekscan Co., USA) using a high resolution(maxim sensing points: 1240p), pressure-sensitive insole sensor. The sensor is flexible and can be easily trimmed so that it fits most any shoe size or shape. This system allows for the visualization of foot pressures as a function of time(100HZ). The subjects swung about 10 times at balls with driver . Foot pressures of the best shot of each were used for analysis.

RESULTS AND DISCUSSION

Foot pressures of the professionals were clearly different from those of the amateurs. In the right foot at the top of swing, the professionals' foot pressures were observed to maintain the address condition or to register higher foot pressure on the inside of the foot than on the outside. In the amateurs, the toe, the heel or the outside of the right foot registered higher foot pressures at the top of swing. Foot pressures of the left foot at the impact were similar to these at the top of swing for both the professionals and the amateurs. From the comparison of the professionals and the amateurs, we assessed that a wider pressure area of the right foot at the top of swing and the left foot at the impact was superior, because a wide pressure area can be stable. But the the total capacity of the body

is required. We considered the total capacity may be the dynamic flexibility of hip joints in the golf swing. The total capacity assessed from foot pressures is shown in Table 1. It could not necessarily be correlated with either money ranking or career wins.

Table 1. Money Ranking of the Japanese Professional Golf Tour in 1994 (NO.1 to 14) or main career(NO.15 to 18), and assessments from foot pressure during swing (at the top of swing and the impact) of 16 subjects are indicated in this table.

NO	Subj.	Nationality	Ranking* or Career	Assessment from FP**	
				Top	Impact
1	H.K.	JPN	13	A	A
2	T.N.	JPN	+	D	B
3	H.H.	JPN	81	B	B
4	S.K.	JPN	+	D	D
5	D.S.	JPN	48	C	D
6	M.K.	JPN	80	D	C
7	T.E.	JPN	94	B	C
8	H.U.	JPN	20	C	D
9	H.S.	JPN	8	B	D
10	N.U.	JPN	53	C	C
11	Y.M.	JPN	14	C	B
12	B.W.	USA	2	B	C
13	I.B.F	AUS	BO***(1991)	A	B
14	J.P.	SWED	-	D	D
15	J.S.	USA	USPGA(1988)	C	C
16	W.G.	AUS	USPGA(1990)	C	C

*: Money Ranking of Japanese Professional Golf Tour in 1994.

: Foot Pressure, BO*: British Open, +: over 100,

Assessments are indicated with 5 classes (from A to E)

REFERENCE

1. Amano, K. and Hibi, N.(1994) Foot Pressures during golf swings at various ball lies by a Japanese professional golfer as measured by a high resolution sensor. Abstract of Asian Sports Congress, Hiroshima, p.116.

ACTIVATION PATTERNS DURING MAXIMAL VOLUNTARY KNEE EXTENSION IN HIGH-SKILLED AND SEDENTARY INDIVIDUALS.

I.G. AMIRIDIS, A. MARTIN, B. MORLON, G. COMETTI, and J. VAN HOECKE
Groupe Analyse du Mouvement, UFR-STAPS BP 138, Université de Bourgogne, 21004 Dijon Cedex, France.

INTRODUCTION

The Torque/Angular Velocity (T/AV) relationship could be influenced by the individual level of strength. In fact, high-strength subjects present a more rising-pattern of T/AV curve than sedentary subjects (Hortobagyi and Katch 1990). Several factors, such as neural inhibition by Golgi-tendon organs and/or co-activation of antagonist muscles, could explain this phenomenon (Westing et al.1990, Osterning et al. 1986).

The aim of this study was to examine the shape of the T/AV curve in high-skilled and sedentary individuals with special attention to the myoelectrical activity of agonist and antagonist muscles during knee extension.

METHODS

Subjects: Eight high skilled-athletes (HS) of international level in athletics (x $\pm$SE : 22.8$\pm$0.1 years ; 183.4$\pm$1 cm ; 75.5$\pm$3 kg) and eigth sedentary (S) males (x $\pm$SE : 23.1$\pm$0.5 years ; 178.8$\pm$2.5 cm ; 74.4$\pm$3.2 kg) participated in this study. Subjects of group HS trained on average 6 times per week for the last five years.

Experimental conditions: Isokinetic tests were carried out using a Biodex (Biodex Corporation, Shirley, NY, USA) dynamometer. After a period of standardized warm-up and familiarization with the measurement apparatus, the subjects were asked to perform three maximal voluntary leg extensions (range of motion 90°, 0°: full extension) at different angular velocities (-120°, -90°, -60°, -30°, -15°, 15°, 30°, 60°, 90°, 120°, 180°, 240°, 300°.s^{-1},) and to hold three maximal isometric actions at 65° of the knee angle. A rest of 3-5 minutes was allowed between each trial. Constant Angular Torques (CAT) at 65° obtained directly by the Biodex software were used. All tests were performed at the same time of day.

Myoelectrical activities of vastus lateralis (VL), vastus medialis (VM) and semi-tendineous (ST) were detected by using three pairs of silver chloride surface electrodes placed over the belly of each muscle. The myoelectrical signal (EMG) was amplified with a bandwidth frequency ranging from 1.5Hz to 2kHz. Angular position, EMG signals and torque were digitazed on line at a sampling frequency of 1000 Hz. The myoelectrical amplitude activity as Root Mean Square (RMS) was calculated.

Statistical Analysis: Analysis of variance (ANOVA) was used to test the statistically significant differences in strength measurements and electrical activity. A probability level of significance was established at $p<0.05$ for all procedures.

RESULTS AND DISCUSSION

The shape of the T/AV relationship is different between the HS and S groups. The torques developed, at all angular velocities, by the group HS were significantly ($p<0.05$) higher than those developed by the group S (fig.1). Eccentric torques of group HS increased with increasing angular velocity, whereas no difference was observed for the group S. Similar results have been previously obtained (Hortobagyi and Katch 1990).

For both experimental groups, the RMS values obtained for the agonist muscles (VL and VM) increased with increasing angular velocity during concentric and eccentric action (fig 2). In addition, the co-activation of the antagonist muscle (ST) was not significantly affected by the angular velocity. However, the RMS values of the ST in HS group were significantly lower than in group S at all angular velocities. Thus, the participation of the antagonists to the resultant torque was more important in group S than in HS. This could partly explain the torque output differences between HS and S groups.

Moreover, at the same velocity, the RMS values obtained for the agonist muscles (VL and VM) during concentric action, were significantly higher than those obtained during eccentric action.

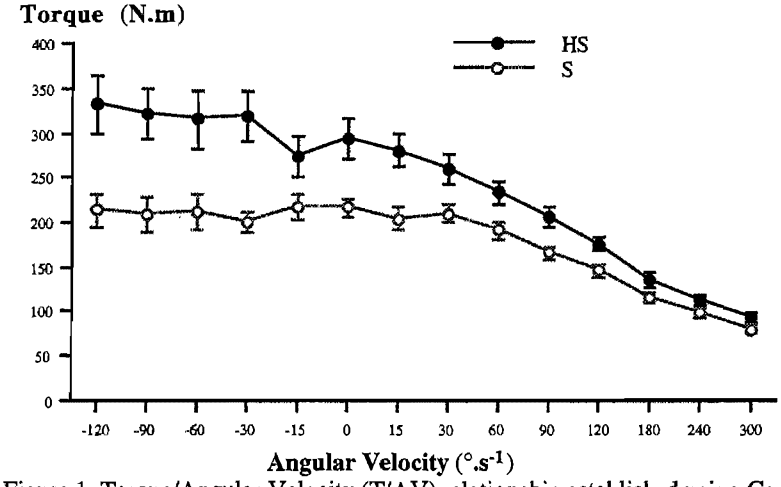

Figure 1. Torque/Angular Velocity (T/AV) relationship established using Constant Angular Torque at 65° (CAT) in High-Skilled athletes (black symbols) and sedentary individuals (open symbols) Values are mean (± SE).

This result could reflect a non-maximal activation under high-tension eccentric loading conditions as suggested previously (Westing et al. 1990). The difference between concentric and eccentric RMS values was more pronounced in S than in HS.

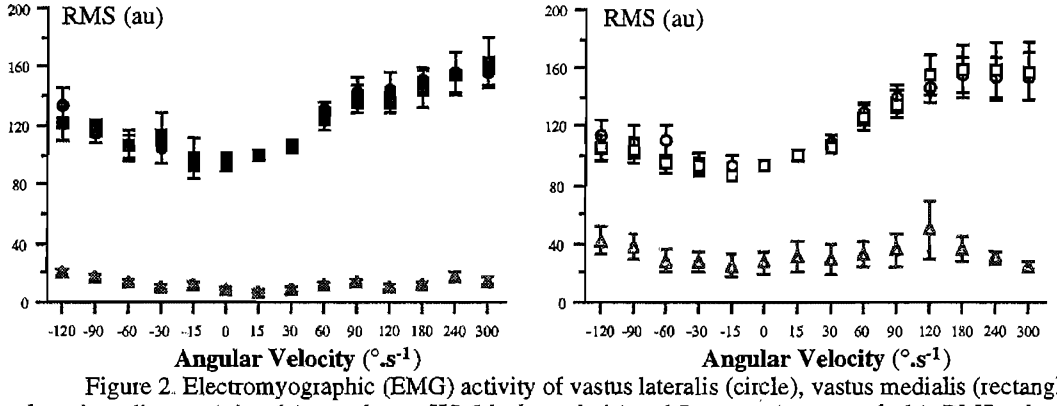

Figure 2. Electromyographic (EMG) activity of vastus lateralis (circle), vastus medialis (rectangle) and semi-tendineous (triangle) muscles on HS (black symbols) and S groups (open symbols). RMS values (± SE) were normalized by dividing all scores by the concentric 15°/s values.

The results of this study suggest that T/AV relationship could be dependent on the individual level of training. Myoelectrical activity of antagonist muscles during knee extension is significantly greater in untrained than in trained subjects. More important differences between concentric and eccentric RMS values in S than in HS group, confirm that the action of a tension-regulating mechanism may be a trainable phenomenon.

REFERENCES

Hortobagyi, T. and Katch, F.I. (1990). Eccentric and concentric torque-velocity relationships during arm flexion and extension. *EurJ Appl Physiol,* 60: 395-401.

Osterning, L.R., Hamill, J., Lander, J.E. and Robertson, R. (1986). Co-activation of sprinter and distance runner muscles in isokinetic exercise. *Med Sci Sports Exerc,* 18(4): 431-435.

Westing, S.H., Cresswell, A.G., Thorstensson, A. (1991). Muscle activation during maximal voluntary eccentric and concentric knee extension. *Eur J Appl Physiol,* 62: 104-108.

THE FLEXION-RELAXATION PHENOMENON REVISITED AND INTERACTIONS BETWEEN QUADRATUS LUMBORUM AND ERECTOR SPINAE FOR BACK STABILITY

E. A. Andersson, L. Oddsson, J. Nilsson, H. Grundström* and A. Thorstensson
Department of Neuroscience, Karolinska Institute,
University College of Physical Education and Sports
*Department of Radiology, Danderyd Hospital
Stockholm, Sweden

INTRODUCTION

It has become an accepted fact for healthy persons in standing, that the lumbar spine stability is only due to discs and ligaments, when the flexion-relaxation phenomenon occurs for the medial lumbar erector spinae, that is when its activity ceases in the latter half of the range of forward flexion of the trunk, held relaxed kyphotic (1). However, a contribution to the stability could be made by the quadratus lumborum, a muscle whose actual functions are relatively unknown (2). We have earlier reported on the roles played by the psoas and iliacus muscles for the stability and movements at the spine, pelvis and hip (3). The aim of this study was to investigate the activity patterns of quadratus lumborum and the lateral and medial lumbar erector spinae in various tasks, including a test of the flexion-relaxation phenomenon.

METHODOLOGY

Seven healthy subjects, four men and three women, aged 20-35 years, performed various standardized tasks. Electromyography, EMG, was recorded at the level of the third lumbar vertebrae, with fine-wire electrodes (0.22 mm in diameter). They were inserted with a needle, directed via guidance of ultra sound (3), into the midportion of quadratus lumborum (QL), and into the lateral deep erector spinae (l-ES), 0.5-1 cm behind the middle of the dorsal fascia of QL. The electrode site in the medial superficial erector spinae (m-ES), was 3 cm lateral to the midline and 1 cm into the muscle. Average EMG-amplitude was measured for two seconds at different static body positions from the amplified (1000-5000 times), filtered (10-1000Hz) and rectified EMG-signals, sampled at a frequency of 0.5kHz. The EMG values for each task and muscle were expressed as percentage values, normalized to the highest activity observed. The mean (±SE) of the normalized EMG values for all subjects was calculated. Goniometers were used bilaterally to record angular displacements at the hip joint.

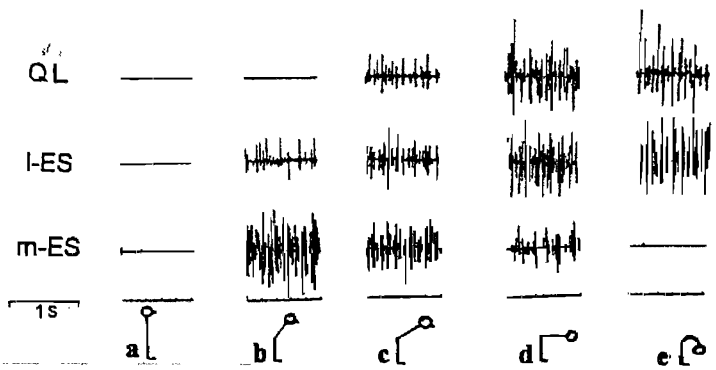

	a	b	c	d	e
QL	1	2	7	8	15
SE	1	1	2	3	2
l-ES	1	7	13	26	19
SE	0	2	5	11	7
m-ES	2	23	23	10	4
SE	1	4	4	6	4

Figure 1. Raw EMG recordings from quadratus lumborum (QL), lateral (l-ES) and medial erector spinae (m-ES) for one representative subject in a) normal standing, and standing with b) 30, c) 60 and d) 90 degrees of hip flexion with the whole trunk held straight, and e) with the trunk relaxed, kyphotic, at the 90 degrees hip angle. The means (±SE), of the normalized EMG levels for all subjects in the tasks a-e are given to the right.

RESULTS AND DISCUSSION

A new finding was that quadratus lumborum (QL) and lateral deep lumbar erector spinae (l-ES) were activated when the well known flexion-relaxation phenomenon, i.e. cessation of activity, occurred for its medial portion (m-ES) during full forward flexion of the whole relaxed and kyphotic trunk (Fig. 1). Activity was absent in m-ES in this position for all, except one subject. Consequently, the lumbar spine stability is not only due to ligaments and discs as has been proposed earlier (1).

The highest activity for QL and l-ES was seen in maximal ipsilateral flexion of the trunk in a side-lying position (100±0 and 78±16%, respectively), while m-ES was activated to a lower extent (43±13%) in this position, showing its highest value instead in maximal bilateral leg lift in a prone position (94±4%).

Marked involvement of both QL and l-ES was observed during contralateral leg flexion both in standing (36±8 and 31±10%, respectively, at 90 degrees) and in a supine position (15±3 and 16±8%, respectively, at 60 degrees). This is probably to maintain stability of the lumbar spine in the frontal plane, since psoas on the opposite side is highly engaged (3). In these tasks m-ES showed no or low activation. There were several other situations where QL and l-ES appeared to have an important stability function of the trunk sideways. When holding a weight of 34 kg in an upright standing position, QL was only involved in contralateral one hand lifts (39±12%), and not at all with two hands in front of the body. The values for contralateral l-ES and m-ES were 68±14% and 31±9%, respectively, in the former task, and 27±12% and 41±8%, respectively in the latter. All three muscle portions were generally quiet when holding the weight in the ipsilateral hand.

During the normal postures, the majority of the subjects showed no or only minor activity in the three muscle portions in standing at ease and in sitting with a relaxed kyphotic or with a straight back. In the latter task psoas has been shown to be involved (3). QL was generally not substantially activated during forward pelvic tilt and in hyperlordosis of the lumbar spine in upright standing, and during a combination of these tasks in sitting (4±2, 2±1 and 2±1%, respectively), while m-ES and l-ES were more involved, the former to higher relative levels (39±11, 24±9 and 19±5% vs 13±5, 13±4 and 8±6%, respectively). Earlier it has been demonstrated that psoas and iliacus markedly contribute in these tasks only in sitting, which is true also in lateral flexion of the trunk to the contralateral side (3). In this situation, moderate activity was seen for QL and l-ES both in sitting (21±4 and 28±12%, respectively) and in standing (17±3 and 34±14%, respectively) whereas the activation of m-ES was low or absent. In ipsilateral flexion of the trunk all three muscles showed negligible activity in both standing and sitting. QL as well as l-ES and m-ES were engaged when elevating the pelvis maximally at the ipsilateral side, both in standing (33±7, 44±11 and 28±8%, respectively) and in sitting (30±9, 33±10 and 16±4%, respectively), and also in maximal abduction of the ipsilateral leg in standing (32±5, 59±13 and 40±16%, respectively). All these exercises performed on the contralateral side resulted in no or low activity in all three muscles.

REFERENCES

1. Allen, C. E. L. (1948) Muscle action potentials used in the study of dynamic anatomy. *British J. Actinotherapy and Physiotherapy* **11**, 66-73.
2. Waters, R. L. and Morris, J. M. (1972) Electrical activity of muscles of the trunk during walking. *J. Anat.* **111**, 191-199.
3. Andersson, E., Oddsson, L., Grundström, H. and Thorstensson, A. (1995). The role of psoas and iliacus muscles for stability and movement for the spine, pelvis and hip. *Scand. J. Med. Sci. Sports.* **1**, 000-000.

A MODEL FOR CANCELLOUS BONE OF THE FEMORAL HEAD

Anderson, I.A.* and Carman, J.B.**
*Industrial Research Ltd., Auckland, New Zealand
**Department of Anatomy, University of Auckland, Auckland, New Zealand

INTRODUCTION

The mechanical behaviour of cancellous bone depends upon numerous factors, including the material properties of the bony tissue and the architecture of the trabecular plates; the complex interrelations of these factors are not completely understood [1]. As part of a cellular solid the trabecular plates must to a greater or lesser degree bend and compress as they take up load. For a cellular solid the modulus E and apparent density ρ are related by the equation $E = C\rho^n$ (1) [see ref. 2] where C is a constant. Gibson and Ashby [2] have suggested several mechanical models for cancellous bone. Experimental determination of modulus, of the index **n** in equation (1), and observations of bone structure can help to elucidate which model is most appropriate. This can then be used as a starting point for a more elaborate three dimensional representation of the bone. We have obtained estimates of modulus and **n** in principal directions on cubes cut from the heads of five human femurs and sectioned some of this bone to study local cancellous architecture. These observations have been drawn together using three dimensional finite element models representing the principal features of a subset of the cubes.

MATERIAL AND METHODS

The femoral heads (four embalmed, one dry) were each cut and lapped into 90-100 test cubes, 5mm on a side. The principal plane of sectioning was normal to the 16° infero-laterally directed load line in walking, designated supero-inferior (SI). Secondary directions orthogonal to SI were medio-lateral (ML) and antero-posterior (AP). The cubes were loaded in compression at a rate of 3.5 to 6 N/s to a maximum strain of 0.6%. A linear regression analysis performed on the upper third of each load/displacement curve gave a stiffness from which a modulus could be calculated. Cubes were weighed after cleaning of soft tissue by blowing through with high pressure air, soaking under vacuum in a collagenase solution, and further blowing. Up to 45 cross-sections were prepared from each of 23 cubes by a serial ablation process; blocks were mounted in a jig and one face sanded off 100μm at a time, the exposed surface highlighted, photographed and digitized. Structural features were studied on computer reconstructed models of the sampled bone. Statistics of bone plate length and angle of orientation were compiled from the digitised data using a computer aided design drawing package on two dimensional 'skeletonised' images of the bone. Mean trabecular wall thickness t was calculated as $t = A\rho'/T'$, where A is the image area, ρ' is the apparent density taken as the area fraction of bone and T' is the total length of plates in the picture. Finite element models representing the principal features of the cancellous bone architecture were developed. These models, consisting of over 1900 first order shell elements, were based on the extended side by side array of prismatic tubes described by Gibson and Ashby [2]. Representative values for material modulus of 10 GPa and Poisson's ratio 0.3 were chosen. Two model types were used. Type 1 was a 5mm×5mm regular hexagonal honeycomb 5 cells across in plane with walls 5mm high; type 2 was based on type 1 but with the middle 2mm portion of the tubes staggered sideways in the in-plane direction by half a cell diameter. The middle portion was joined to undisplaced 1mm thick top and bottom portions using intermediate layers 0.5mm thick of nearly longitudinally oriented bridging plates so that the structure was continuous. This model represents an extended foam with partially interdigitating layers of side by side "ellipsoidal" cavities 3mm long. Three versions of each model type with plate

thicknesses of 0.04, 0.08 and 0.16mm were subjected to simulated compression tests. A fixed displacement of 0.05mm in compression was applied to nodes at one end. Nodes at the opposing end were constrained from movement in the load direction but all nodes were otherwise unconstrained to simulate friction-free end conditions. The effective modulus was calculated using the nodal reaction force, the area and the applied strain (1%).

RESULTS

1. In all femurs there was a column of bone with intermediate to high SI modulus stretching from the center of the contact area to the cortical bone at the medial edge of the neck diametrically opposite.

2. The cancellous bone consisted of perforated plates and cavities oriented in the SI direction, principal orientation being within 10° of SI. The SI modulus was generally 3-4 times the modulus in the other two directions. Typical average plate thicknesses fell within the range 0.16mm to 0.22 mm wide.

3. The values for 62 cubes from these columns were: **average relative density** 0.28, range 0.12 to 0.48; **modulus — SI** 0.5 to 3.2 GPa, **ML** 0.1 to 1.6 GPa, **AP** 0.1 to 2.3 GPa, **n — SI** 1.14 (r^2=0.46), **ML** 1.8 (r^2=0.56) and **AP** 2.18 (r^2=0.82)(see fig. 1).

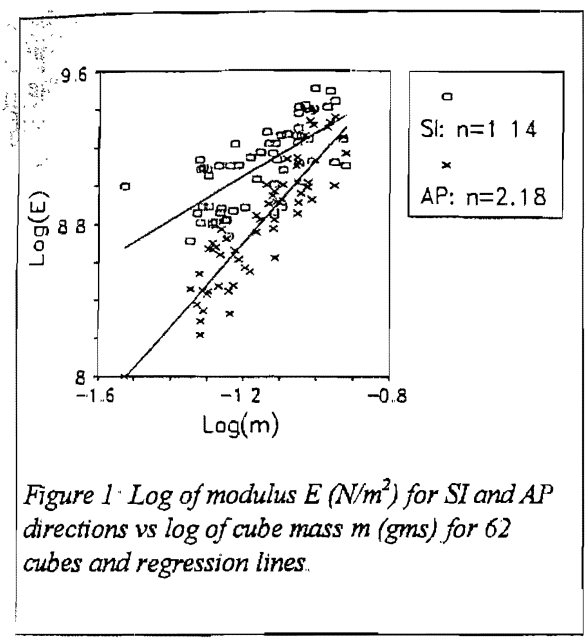

Figure 1: Log of modulus E (N/m^2) for SI and AP directions vs log of cube mass m (gms) for 62 cubes and regression lines.

4. The relative densities for the three versions of each model type were 0.08, 0.15 and 0.30. The effective moduli for type 1 with 0.16mm wall (relative density 0.3) in the out-of-plane and in-plane directions were 3.4GPa and 0.4 GPa respectively giving an anisotropy ratio of (approx.) 9:1. The corresponding results for type 2 were 3.3GPa and 0.8GPa for out-of-plane and in-plane directions respectively giving an anisotropy ratio of 4:1. The values for **n** for type 1 were 1.0 and 2.8 for out-of-plane and in-plane directions respectively and for type 2 were 1.1 and 1.4 for out-of-plane and in-plane directions respectively.

DISCUSSION

The experimental results show that the bone of the central core of the femoral head is moderately anisotropic. The experimentally determined values for **n** indicate a different functional relationship between modulus and density in different directions. A value for **n** close to 1 as obtained for SI suggests that cell walls compress longitudinally (instead of bend) under load in this direction. The finite element models provide modulus results approximating those of the experimental findings. In contrast, the anisotropy ratio for type 1 was quite high. The effect of staggering cells in type 2 results in a structure which is much stiffer in the in-plane direction with a very small addition of mass, and produces an anisotropy ratio within the range determined experimentally.

REFERENCES 1. Keaveny T.M. and Hayes W.C. J.Biomech. Eng. 115, 534-542,1993

2. Gibson, L.J. and Ashby M.F. Cellular Solids. Pergamon Press, 1988

ACKNOWLEDGEMENTS The authors are grateful for the modelling advice provided by Peter J. Hunter (Univ. of Auckland). This work was supported by a grant from the New Zealand Foundation for Research Science and Technology.

ANALYSIS OF HEMORHEOLOGICAL DATA, DETERMINED BY COUETTE VISCOMETER

Nadja Antonova
Institute of Mechanics and Biomechanics, Bulgarian Academy of Sciences
Sofia, Bulgaria

INTRODUCTION

The complex rheological properties of blood and their great variability between different state and conditions of the person, its health, physico-chemical composition of blood components and mechanical properties of the flow make difficult the interpretation and comparison of hemorheological data. These problems can be overcomed by approximation the experimental data in a given area of shear rates by a some constitutive equation. The obtained parameters of the equations can be an useful tool, if can be shown that at some diseases the parameters of the equation are changed in comparison with those in norm. The aim of the study is to analyze rheological properties of blood by different constitutive equations on the basis of the obtained parameters of these equations, applied for normal blood and blood from patients, suffering from erythraemia.

METHODS

Eight different constitutive equations, describing the rheological properties of blood were considered - functions of the kind :

$$\tau = \tau (\gamma, H, \{ \alpha_i \}_{i=1,k})$$

τ are shear stress, γ - shear rates, H - hematocrit, α_i - row of parameters, defining specific form of the equations and allowing their approximation to the experimental data.

Table 1. Considered constitutive equations

1.Ostwald-de-Waele	$\tau = \kappa.\gamma^n$
2. Herschel-Bulkley	$\tau = \tau_o + a.\gamma^m$
3.Walburn-Schneck	$\tau = a.e^{bH} [e^{d/H^2}]^{(1-cH)}\gamma$
4.Phillips-Deutsch (A)	$\tau = a\{(1+ b\gamma^2)/(1+ c\gamma^2)\}\gamma_{dH}$
5.Phillips-Deutsch (B)	$\tau = a\{(1+ b\gamma^2)/(1+ c\gamma^2)\}e^{\gamma}$
6.Quemada (A)	$\tau = \eta_p \{1/(1-kH)\}\gamma$
7.Quemada (B)	$\tau = \eta_p \{1-(\kappa_0+\kappa_\infty \gamma_r^{1/2})H / (1+\gamma_r^{1/2})\}\gamma$
8.Riha-Charova	$\tau = [(\eta_\infty - 1) + 10^{A.\exp(-B.\log\gamma)}]\gamma$

The problem for parameter estimation was solved. The approximation of every one of the considered equations to the experimental data was done by determination of the parameters, minimising the square functional D: $D = \sum (\tau_I - \tau_E)^2$,where τ_I - theoretically defined shear stresses by the equations, τ_E - experimentally determined shear stresses. The non-linear problem for parameter estimation was solved by the gradient method . The differences of the normal blood and of the patients, suffering from erythraemia was sought on the basis of the determined parameters of each constitutive equation by two-group t-test.

25 blood samples of patients, suffering from erytraemia and 32 blood samples from healthy persons were investigated. The shear stress-shear rates relationship was determined at 25° C and 37° C. The flow curves were determined by Couette viscometer under steady flow in the newtonian range of shear rates from 144 s^{-1} to 1312 s^{-1}.

RESULTS

The groups of patients suffering from erythraemia were compared with those of the healthy subjects on the basis of the parameters of each of the considered constitutive

equation by means of two-group t-test. The results at 37° C show (Table2) that significant differences can be found by the parameters **k** with $p \leq 0,05$ for equation 1; for equation 2 - this is the parameter **m** with $p \leq 0,01$; for equation 3 - by the parameters **a**, **b** and **d** with $p \leq 0,008$; for equation 4 - by the parameters **a** and **c** correspondingly; for equation 5 - these are the parameters **b** and **d** with $p \leq 0,09$ and $p \leq 0,06$; for equation 6 - by **k** with $p \leq 0,1$; for equation 7 - by $\mathbf{k_\infty}$ with $p \leq 0,2$. The parameters **A** and **B** of equation 8 allow the groups to be divided correspondingly with $p \leq 0,07$ and $p \leq 0,1$.

Table 2. The values of the function t and the probability p, obtained by t-test (* - separate variances, ** pooled variances)

Eq. No	Parameters	t	p - value	t	p-value
		T=37° C		T = 25° C	
1a	**k**	-7,84*	0,0000		
3	**a**	3,54*	0,0125	3,17*	0,0186
		4,75**	0,0001	4,11**	0,0006
	d	3,23*	0,0078		
		2,97**	0,0079		
4	**b**			-4,62*	0,0003
	c	- 2,67*	0,0370		
		3,54**	0,0022		
6	**k**			2,32*	0,0408
				2,23**	0,0399
8	**A**	- 5,32*	0,0013	-1,82*	0,0898

Similar are the results at 25° C: for power law 1 the parameter **k** allows the groups to be divided correspondingly by $p \leq 0,2$ and $p \leq 0,1$; for equation 2 - this is the parameter **m** with $p \leq 0,05$; for equation 3 - parameters **a**, **b**, **c** and **d** with p between 0,00 and 0,2; for equations 4 and 5 - parameter **b** with $p \leq 0,1$; for equation 6 - parameter **k** by $p \leq 0,09$. The differences of the investigated groups can be found on the parameters $\mathbf{k_0}$ and $\mathbf{k_\infty}$ with $p \leq 0,2$ and $p \leq 0,09$ correspondingly for equation 7 and for equation 8 on the parameter **A** with $p \leq 0,01$.

CONCLUSION

Analysis of hemorheological data can be done on the basis of the parameters, describing rheological properties of blood. 1. For each of the considered equations there exist at least one parameter, by means of which the experimental hemorheological data can be divided in the two groups. 2. The power law describes the shear stress-shear rate relationship for blood in the investigated newtonian range with the highest accuracy (standard deviation $s = 0,6884 \pm 0,5349$).

REFERENCES

1. Phillips,W.H. and Deutsch, S. (1975) Toward a constitutive equation for blood. Biorheol. 12: 383 - 389.
2. Quemada,D. (1977) Rheology of concentrated disperse systems and minimum energy dissipation principle. I. Viscosity - concentrated relationship. Rheol. Acta 16 (1): 82-94.
3. Quemada,D. (1978) Rheology of concentrated disperse systems and minimum energy dissipation principle. I. Viscosity - concentrated relationship. Rheol. Acta, 16 (6): 632-642.

An Analysis of the Contribution of Each Body Segment to the Long Jump during Take-off

[1] K.Aoyama [2] A.Hamamatsu [3] K.Ogiso [1] H.Sawamura
[1] Nihon University,Tokyo,Japan [2] Hosei Women's High School Kanagawa,Japan
[3] Toba National college of Marintime technology,Mie,Japan

Introduction

Much reserch has already been completed concerning the take-off for the long jump. However,most of this research focussed on investigating the relationship between performance and kinematics or kinetics during take-off. There are very few studies of the role or contribution of each body segment to the long jump during take-off.

The porpose of this study was to investigate the segmental role or contribution to the take-off in the long jump.

Methods

Five male long jumpers performed the long jump. Their take-off were filmed at 200 frames/second with a Nac high speed-camera. From the resulting video tape, two dimensional coordinates of twenty-three points on the various body parts were obtained by digitizing with a sampling frequecy of 100Hz. This data was filtered with a Butterworth digital filter at 10Hz(Winter 1979). Body parameters were used following Chandler et al.(1975). This data was used to calculate the generated monentaof the arms,head and trunk,free leg, using the method of Ae and Shibukawa(1980).

Segnmental generated impulses(holizontal and vertical) in each frame were also computed by subtracting generated momenta at tuchdown of the take-off foot from those each frame, and then the mean percent contribution of the segments were obtained by dividing total impluse of each segment over the take-off phase by the whole body impulse. To determine the average patterns of the monenta generated, theywere divied by body mass(BM) and they were normalized to take-off contact time set at 100%.

Results and Discution

1. The mean percent contribution(Fig.1)

With regard to the horizontal direction, the highest contribution was made by the trunk, and the smallest(negative) by the take-off leg. The percentage of contribution were small for both the arms and the free leg.

As for the vertical direction, all of the bogy segments showed positive contribution. The take-off leg showed the highest percentage contribution.

2. Patterns of the momenta generated by the body segments

The upper part of Fig.2 shows the momentaum generated in the horizontal direction during take-off. The trunk shows negative generated momenta from the take-off point to about 30%, and then shows positive generated momentum. The take-off leg shows highly positive generated momentaum in all phases of the take-off. From this data it was concluded that the trunk and the take-off leg have a mutually supportive relationship.

The lower part of Fig.2 shows changes in generated momenta in the vertical direction.The trunk shows positive generated momentum until about 55%, and then shows negative generated momentaum. Also,the arms and the free leg show positive generatedmomenta throughout the take-off.

References

1.AE,M. and Shibukawa,K.(1980) A biomechanical method for the analysis of the contribution of the body segments. Japanese Journal of Physical Education,25,233-243.

2.Chandler et al.(1975) Investigation of Inertia Properties of Human Body.Aerospace Medical Reserch Laboratory,USA.

3.Winter,D.A.(1979) Biomechanics of Human Movement. John Wiley and Sons.

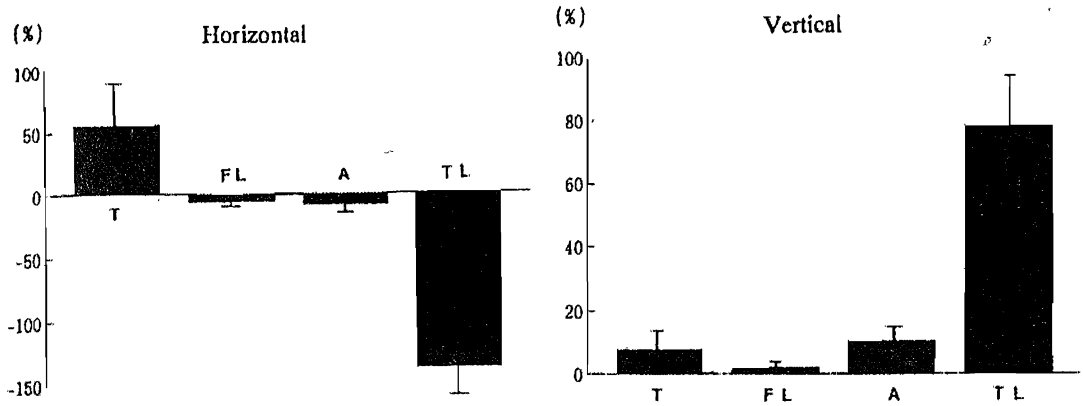

Figure 1-Mean percent contribution of the body segments

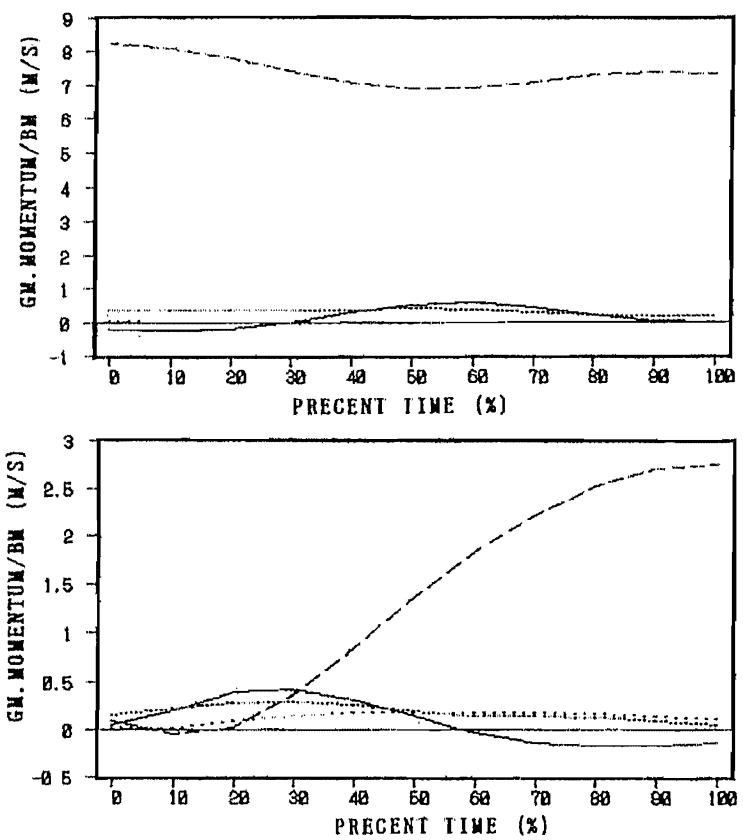

* T:trunk FL:free leg

A;arms TL:take-off leg

Figure 2- Patterns of the Momenta Generated by the Body Segments

MATHEMATICAL MODEL OF THE HIGH BAR IN GYMNASTICS - OPTIMIZATION OF THE GIANT SWING PRIOR TO RELEASE

D. Arampatzis, G.-P. Brüggemann
Institute for Athletics and Gymnastics, German Sport University Cologne, Germany

INTRODUCTION

In the first part of the descending phase of the giant swing the total energy of the body decreases. Energy is at the same time transferred to the system through the muscles, absorbed by friction and transferred to the high bar. The difference between the energy transferred to the bar and the total energy decrease of the body can be used as a criterium for the utilization of the elasticity of the high bar.
In the remaining giant swing the total energy of the body increases. Furthermore the energy transferred to the bar is returned to the body. The difference between the increase in the total energy of the body and the energy returned from the bar can be used as an index indicating the utilization of the muscular capacity. This index can also be regarded as a criterium for a successful execution of the movement.

METHODS

A model was designed representing the human body connected to the high bar (RMK model). The human body was comprised of a 15 segment system. The 15 segments were connected by 14 hinge joints and four sliding joints. The joint-beam method (superelement) was applied to the bar. A superelement is comprised of four rigid bodies which are connected by joints (two Cardan joints and one hinge-sliding joint) and springs (seven rotatory springs and one extension-compression spring). The high bar was modelled by three such superelements.
The input data necessary for the RMK model were obtained by video kinematographics (50 Hz) and dynamometry (500 Hz). The mass and moment of inertia data of the 15 segments were calculated with a) the information provided in the model of HANAVAN (1964) and b) the information provided by ZATSIORSKY et al. (1984). The giant swings preceding dismounts and aerial manoeuvres of three first division gymnasts were analyzed. The parameters investigated were the total energy of the human body and the individual segments, the propulsive forces and moments, the mechanical power and propulsive work and the energy flow (high bar - human body and within the body segments) arising from the gravitational and inertial forces. The validities of the high bar model and of the RMK model were controlled by comparing the measured and calculated bending of the bar. The maximum discrepancies were less than 10%.

RESULTS AND DISCUSSION

In the first phase of the downswing (up to a position angle of 230°) the gymnasts attempted to supply energy to the high bar / human body system through the musculature and then to store this energy in the bar. This phase was primarily responsible for the utilization of the elasticity of the high bar. The difference between the energy transferred to the bar and the decrease in the total energy of the body can be used as a criterium for this utilization of the elasticity of the bar (fig. 1). The larger the difference, the better the utilization of the elasticity.
In the remaining giant swing (from an angle of approx. 230° until the completion of the giant swing) the energy supplied to the bar was returned to the body. An advantageous increase in the total energy of the body towards the end of the movement could only be achieved through energy supplied by the muscles. If the muscles were used efficiently

and the movement was well executed, then the increase in the total energy of the body should be greater than the energy returned from the bar. An index can be formed by the difference between the increase in the total energy of the body and the energy returned from the bar, which describes the utilization of the muscular capacity and can be regarded as a criterium for a successfully executed movement (fig. 2). A greater difference is an indicator for a more successful execution. The choice of anthropometric model did not influence the results of either criterium.

A temporally delayed and initially slower, but even reduction of the hip and shoulder angles provided advantageous release conditions. Increases of the body's total energy of up to 15%, of the vertical release velocity of the centre of mass of up to 10% and of the angular momentum of up to 35% were possible.

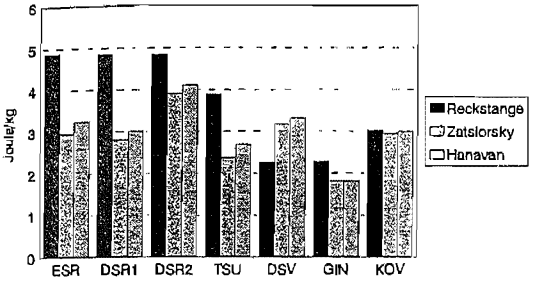

ESR :single backward somersault
DSR1 :double backward somersault 1
DSR2 :double backward somersault 2
DSV :double forward somersault
GIN :Gienger somersault
KOV :Kovacs somersault

Fig. 1: Energy transferred to the high bar and decrease in the total energy of the body

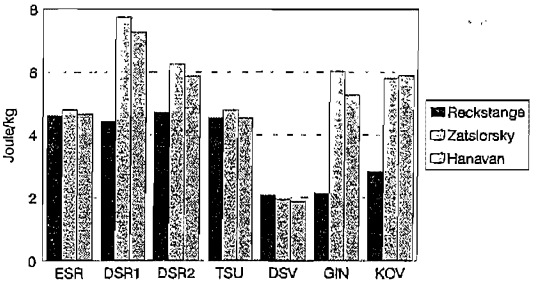

ESR :single backward somersault
DSR1 :double backward somersault 1
DSR2 :double backward somersault 2
DSV :double forward somersault
GIN :Gienger somersault
KOV :Kovacs somersault

Fig. 2: Energy returned from the high bar and increase in the total energy of the body.

REFERENCES

1. Brüggemann, G.-P., Cheetham, P., Alp, Y., Arampatzis, D. (1994): Approach to a biomechanical profile of dismounts and release-regrasp skills of the high bar. J. Appl. Biomechanics 10, 291-312.
2. Hanavan, E.P. (1964): A Mathematical Model of the Human Body. WADC Technical Report AMRL-TR-64-102. Wright-Patterson Air Force Base, Ohio.
3. Rauh, J. (1987): Ein Beitrag zur Modellierung elastischer Balkensysteme. Reihe 18: Mechanik/Bruchmechanik Nr. 37. Düsseldorf.
4. Zatsiorsky (Saziorski), V.M., Aruin, A.S., Selujanov, V.N. (1984): Biomechanik des menschlichen Bewegungsapparates. Berlin.

EVALUATION OF INCREASE IN FORCE AND EMG ACTIVITY'S CURVES.

R. C. ARAUJO, M. DUARTE, A. C AMADIO
Biomechanics Laboratory - School of Physical Education
University of São Paulo - São Paulo - Brazil

INTRODUCTION

In a previous study [1], we have studied a correlation between maximal isometric voluntary force and surface electromyography (SEMG), in order to evaluate the correlation among them in dependence of a training with Neuromuscular Electrical Stimulation (NMES). That study did not show a reliable correlation to explain an interpretation of muscle torque from SEMG signal. Besides, such training has produced a significant change in this correlation, it was different for each muscle: *m.Interosseus dorsalis I* (FDI), *m. Biceps braquii* (BB) and *m. Quadriceps femoris* (QF) and it was different for men and women.

As it is well known, the interference pattern in SEMG signal represents a sum of superimposed motor unit potentials (MUPs) [2]. For that, it is a hard work to preview how force will behavior from SEMG signal. The determinant force factors are the recruitment of the motor units and the firing rate of motor-neurons. While force signal is still increasing, SEMG signal stays in a steady state because there is a limit of measurable MUPs. For this reason we performed this study with the purpose of determine the MVC percentile related to SEMG steady state.

MATERIALS AND METHODS

There were realized 10 synchronized acquisitions of force and SEMG of 4 individuals in BB under MVC training for a 8 sessions. Signals sampling rate was 100 Hz to both signals that were analyzed by computer using an A/D convertor. For the SEMG analysis we used a ETK90 X/4K-d60 amplifier with a gain of 1000 times. The figure 1 shows the curves of force (upper) and rectified SEMG (lower). We fit sigmoidal curves to each one to eliminate the spikes and fluctuations or artifacts and to permit the evaluation of the exponential growth in the curves. Thus, it was possible to determine the point in the SEMG curve at 90 % of the maximum and the correspondent level of force in this moment (represented in straigth line in figure 1).

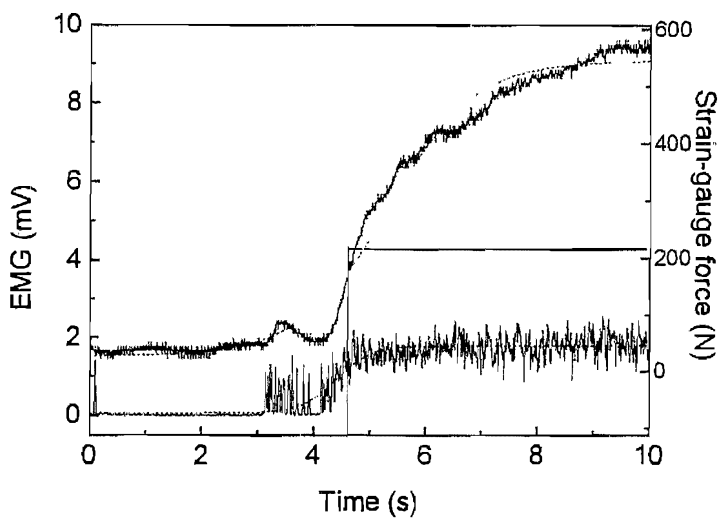

Figure 1 - The curves of force and rectified SEMG and their sigmoidals made to determine the exponential growth and the level of force where the SEMG in *m. Biceps braquii* reaches 90 % of the maximum value

RESULTS AND DISCUSSION

The figure 2 shows the values of force where the SEMG signals are 90% of MVC. As contraction speed was not controlled, in some acquisitions was not able to calculate the sigmoidal curve representing the signal increasing stables the beginning of steady state of both force and SEMG. Our results suggest that such steady state is 46 % (SD 13%) of MVC for this muscle

These results can reflect questions discussed by DELUCA [3] that shows the difference between the area of a muscle and the area of the SEMG electrodes for each person. On the other hand, these acquisitions were made in isometric condition without their control of increasing time. Then, the pattern of recruitment in slow or fast contractions can be reflected in different saturations levels.

The results obtained in this work show that there is not a direct correlation between the growth of SEMG and force curves

We are looking for the possibility about to acquire the SEMG signal with highest frequency to confirm if this values where the SEMG saturates can reflect the changes in firing rate, since this study was performed with a fixed frequency. Besides, other studies with the control of velocity in isotonic conditions possibly can explain better this variations

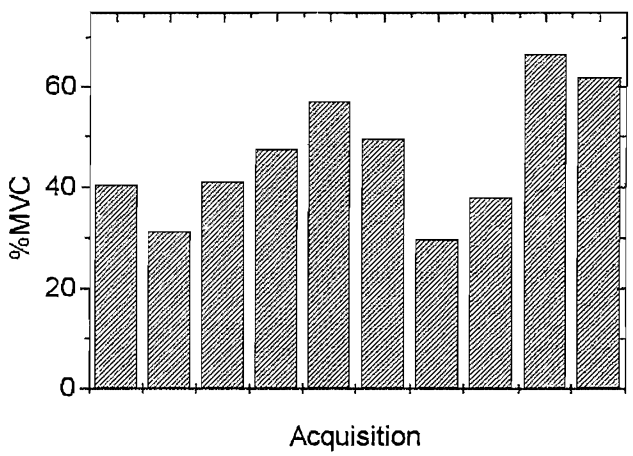

Figure 2 - The level of force where the SEMG signal saturates represented for each acquisition for *m.biceps braquii*.

REFERENCES

1 ARAUJO, R.C., AMADIO, A.C., MOCHIZUKI, L., FURLANI, J (1994) Correlation Between Force and SEMG Activity in Subjects Under A Neuromuscular Electrical Stimulation Training. *Physical Therapy* In press.

2 BASMAJIAN, J V , DE LUCA, C.J (1985) *Muscle Alive.* Baltimore, Williams & Wilkins.

3 DE LUCA, C. J (1990) *Surface electromyography: what is new?* Torino, Dipartamento di Elettronica/Politecnico di Torino

BIOMECHANICAL APPLICATIONS IN CYBERSPACE

Gideon B. Ariel and M. Ann Penny

University of California, Irvine

Trabuco Canyon, California USA

INTRODUCTION: The Internet provides access to a worldwide collection of information resources and services as a window on the ever-expanding world of on-line information. The new communication links afforded by rapid satellite/computer exchanges will enable the field of Biomechanics to advance into a new age of technology, resources, research, data base development, as well as interaction among scientists. Utilizing the tools available in Cyberspace, the Biomechanist can retrieve and display data as well as documents from virtually anywhere on the planet. Studies can be conducted at multiple locations and data rapidly exchanged among these sites. Application of multiple media sources within Cyberspace is referred to as "hypermedia". Thus, with the Internet's hypermedia-based interface, documents can include color images, text, sounds, and animation. As a hypermedia technology designed for searching and retrieving, Internet provides a unified interface to the diverse protocols, data formats, and information archives appropriate for biomechanical endeavors. Most of the documents are "hypertext" which are papers containing links to other texts, media, and/or locations. Using electronic links, known as Hyperlinks, specified information can be incorporate within a document by embedding full-color images, sounds, graphs, bibliographies, supplementary resources, data bases, etc. located within that text or at some distant site. This interface allows information located around the world to be interconnected in an environment that permits users to access the information super-highway by clicking on "hyperlinks". Similarly, complex biomechanical research segments at different research sites can be "tethered" through these "hyperlink" phases. Biomechanical research and subsequent reports become virtually three-dimensional with this multiple level access.

METHODS: The present study was designed to test the efficacy of acquiring data at a "host" site with simultaneous on-line interaction with a second location. The following Internet tools were selected as appropriate for the study: (1) FTP (File Transfer Protocol) - to transfer large video and document files from site to site; (2) Gopher - To retrieve and post research finding and progress documents; (3) WWW (World Wide Web) - To hyperlink documents with video images and sound; (4) HTML (Hyper Text Mark-up Language) - To create the Hyper-link documents.

The study's purpose was to test the capabilities of the Internet in conducting a Biomechanical study. The subjects performed an arm flexion-extension exercise in two minute bouts on a specialized device which controlled and recorded the force for each repetition. At the completion of each bout, the Subjects performed a five second isometric contraction during which both the force exerted and the EMG signals from the biceps and triceps brachii were recorded. A simple movement task, pointing to a target, was performed and captured by two video cameras. There was a one minute rest following the isometric test and then the next flexion-extension exercise bout was begun. Modem connections for the computers which controlled and recorded data for the exercise, EMG, and the isometric contraction were established prior to the initiation of each subject's first bout of exercise. Baseline and test measurements were secured for the maximum voluntary isometric contraction and EMG signals and immediately transmitted via Internet to the remote site for quantification. Transmission of the video from each camera view followed for subsequent quantification. The goal was for the scientist at the remote site to receive and quantify the force and EMG data using the fatigue formula presented by Basmajian and De Luca (1) for determining the point of fatigue. Following this fatigue-induced failure point determination, decisions regarding the continuation or cessation of exercise could be made.

The study was conducted between two locations within the United States. A computerized exercise device was employed for the arm flexion-extension task with the subject's arm stabilized in an effort to restrict extraneous bodily movements. The exercise conformed to a predetermined iso-acceleration pattern throughout the entire exercise. Software

regulated the iso-acceleration pattern regardless of the level of fatigue in a manner which was transparent to the exercising subject. The investigator was situated in an appropriate position to monitor the subject's performance and to regulate the timing sequences. EMG data was collected simultaneously with force data immediately before and at the end of each exercise bout.

Exercise data, isometric force values, and the EMG signals were transferred from the Host site to the recipient site immediately following the data recordings. EMG and force quantifications were transferred from the recipient site back to the Host as soon as the results had been calculated. Figures 1 and 2 illustrate one of the video picture transmitted and the associated digitized data, respectively. Figure 3 illustrates part of a raw and processed EMG signal.

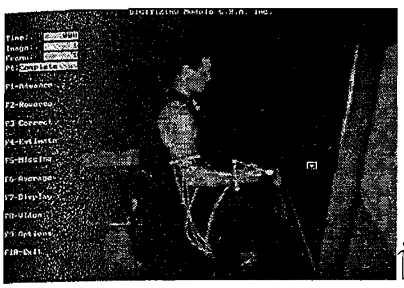

Figure 1 -Transmitted Video Picture

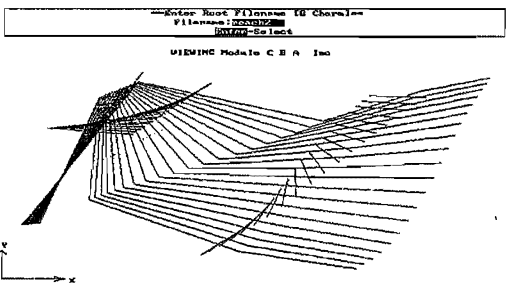

Figure 2 - Digitized data

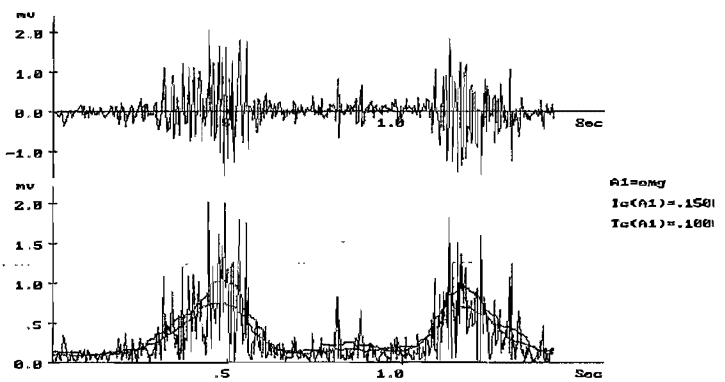

Figure 3 - Example of raw and processed EMG signal.

RESULTS: Following repeated bouts of fatiguing exercise, the results demonstrated remarkable similarity for the time required to reach the failure point. This was an unexpected finding despite the effort to find subjects who represented a homogeneous population, in this case, weight lifters. Following the data collection and Internet calculations between sites, subsequent kinematics, force, EMG, and fatigue level determinations were calculated and reported in documents at each site. Hyperlinks were embedded in the graphic documents to link the video images with the associated kinematics parameters such as position, velocity and acceleration. In addition, the EMG data was hyperlinked with the kinematic parameters from the video analysis and kinetic data from the computerized exercise device.

DISCUSSION: Although the Internet electronic linking capabilities allow more elaborate and exotic research protocol, the efficacy of a simple two site participation with nearly real time data transference and quantification was deemed sufficient for this study. This study successfully demonstrated that biomechanical research can utilize the power of the Internet when conducting and sharing research globally.

BIBLIOGRAPHY: 1. Basmajian, John V. and De Luca, Carlo J. Muscles Alive. 5th Edition. Baltimore: Williams & Wilkins, 1985.

THE BIOMECHANICS OF THE TRANSITION FROM TAKE-OFF TO EARLY FLIGHT IN SKI-JUMPING

Arndt, A.*, Brüggemann, G.-P.*, Virmavirta, M.° and Komi, P.°

* -Institute for Athletics and Gymnastics, German Sport University, Cologne
° -Department of Biology of Physical Activity, University of Jyväskylä, Finland

INTRODUCTION

There is abundant biomechanical research concerning the take-off phase of ski-jumping and some two-dimensional analyses of the flight phase. There is however, a lack of information describing optimal technique in the transition stage between these two phases and also of three-dimensional data of the early flight phase. This is of especial relevance to performance since the development of the V-technique (Schwameder, 1993). In order to identify important contributing factors to the total distance jumped by elite level ski-jumpers, the K90 event at the 1994 Winter Olympic Games in Lillehammer was analysed.

METHODS

Two video cameras (50Hz) were used for data collection of the early flight phase. An algorithm employing the DLT technique with panned and tilted cameras was applied (Drenk, 1988). The take-off was regarded as a two-dimensional motion and was filmed by one high speed video camera (100Hz) with its optical axis perpendicular to the take-off edge. Both jumps of the ten best placegetters and ten randomly selected poorer performers were analysed. The data were manually digitised on a Peak Performance Analysis System. A 3D model defined the following angles for the early flight phase: lower body angle to X axis (horizontal; in the direction of the jump), torso position to X axis, ski "V" angle, ski position to X axis and leg abduction. The 2D model for the take-off defined the lower body angle to X axis, torso position to X axis, knee angle and somersault angle (angle formed between the X axis and a line joining the knee and shoulder joint centres).The somersault angle was introduced as a means of quantifying forward angular momentum at take-off. All results were normalised over distance: $xi = f(d)$, as an analytical method of standardising the data and comparing jumps. A second set of parameters analysed were centre of mass (CM) characteristics, as these have often been stated in the literature as correlating highly to the final distance jumped. The statistical analysis was comprised of an ANOVA to identify differences between groups and a linear correlation analysis between the measured variables and the total distance jumped.

RESULTS

In order to identify the most important characteristics of the analysed phases on the total performance, the CM characteristics and the body configuration at the furthest distance analysed (17m from the edge of the take-off table) were determined. The body configuration at 17m, defined by the five angles mentioned above provided an R^2 value of 0.84 to the dependent variable: distance. Surprisingly, a similar combination of CM parameters (vertical and horizontal velocities, height) proved insignificant ($R^2 = 0.20$, $p \leq 0.05$). As this result indicated the importance of obtaining an optimal body position for the flight phase, the jumps were traced back through the early flight and take-off to determine how these positions had been achieved (figure 1). These angles showed that the most successful ski-jumpers had achieved a relatively steady flight position by 10m - 12m after the take-off edge. Prior to this the most important contributors to the flight configuration were a rapid extension motion of the torso combined with a decreasing lower body angle approximately three metres prior to take-off. After a slight decrease from approx. 30° to approx. 20° in the three meters after take-off, the continued reduction in the lower body angle to the X axis was the major contributor to the eventual flight position in which the body and the skis formed an angle of approx. 20° to the horizontal. An ANOVA comparing the better and poorer performers showed significant differences ($p \leq 0.05$) in the patterns of the leg abduction angles. The better performers had

smaller abduction angles in the first five metres after take-off however, between five and seven metres the pattern was reversed and from approximately 10m the better jumpers had greater values in this parameter. A similar comparison of the ski "V" angle showed no significant differences. Significant differences were also found in the somersault and knee angular velocities at take-off.

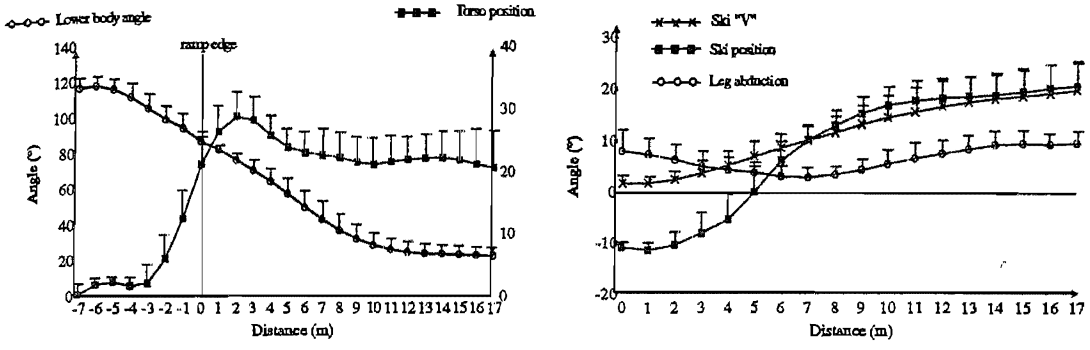

Figure 1. Means and standard deviations of five angles through take-off and early flight of the 10 best placegetters

DISCUSSION

Contrary to results cited in previous studies (eg. Schwameder, 1993), CM parameters at take-off provided no significant correlation to the distance jumped in this study; it was found that angular parameters related to the configuration of the ski-jumper system were better determinants of performance either in correlations to final distance or in differences between better and poorer placegetters. The high angular velocities of both knee extension and somersault angle of the better ski-jumpers indicated the importance of rapidly assuming an extended position at an optimal angle to the flight path (torso and lower body at approx. 20°). The combination of ski "V" angle, leg abduction angle and body position to the X axis illustrated various movement sequences which resulted in a compact configuration in the early metres of flight after which the better performers began to increase their lifting surface area to obtain the greatest advantage from the remaining flight phase. An example of such a sequence was a small leg abduction angle in the first few metres of flight while the feet were being externally rotated to increase the "V" angle, followed by an increasing abduction once the lower leg angle (and thus the potential frontal area) had been reduced to below 40°. At the furthest distance analysed (17m) the greatest individually contributing angle to the final distance jumped was the torso position ($R^2 = 0.77$). When compared to the insignificant CM parameters, this result reinforced the necessity of coordinating the body in such a manner as to obtain a position which provided the optimum aerodynamic prerequisites for the remaining flight. This study therefore, showed the importance in ski-jumping of combining complex sequences of movements in a very short time (17m was reached in less than one second). This could be determined by providing a thourough profile of the transition phases involved. It was the execution of these movements which proved vital to the final placings rather than the CM parameters involved during the movements.

REFERENCES

Drenk, V. (1988). Erarbeitung photogrammetrischen Auswerteverfahren für den Einsatz schwenkbarer Kameras in der Leistungssportforschung. Doctoral Thesis, Forschungsinstitut für Körperkultur und Sport, Leipzig.

Schwameder, H. (1993). Dreidimensionale biokinematische Bewegungsanalyse der Absprung- und ersten Flugphase im Skispringen. In Kornexl. E. and Nachbauer, W. (Eds.): **Bewegung, Sport, Forschung,** Inst. f. Sportwissenschaft der Universität Innsbruck, 379 - 401.

EFFECT OF SPRINT TRAINING ON A CYCLE ERGOMETER ON THE MUSCLE POWER-VELOCITY MEASURED DURING CYCLING

L.M. Arsac, C.A. Hautier, J.-R. Lacour, A. Belli.
laboratoire de Physiologie-GIP Exercice, Faculté Lyon-sud, Univ. Lyon 1, France.

INTRODUCTION

In vivo mechanical properties of muscles could be described by the power-velocity relationship established from cycling measurements (Sargeant et al. 1981). The parabolic relation previously obtained made it possible to confirm that active muscles operate at an optimal velocity (Vopt) to produce their maximal power output (MPO). Both Vopt and MPO have been supposed to be in relation with muscle fibre composition (Gregor et al. 1979, Sargeant et al. 1984) and training specificity (Komi et al. 1977). Furthermore training effects have been reported to have significant effect on muscular properties that can be measured through force, velocity and power outputs (Duchateau et al. 1984).

This study was undertaken to examine the effects of short-term and long term training on the power-velocity relationship observed during cycling. The results obtained would then be discussed in relation with muscle properties.

METHODS

A Monark 818E friction loaded cycle ergometer was transformed so that (i) the force necessary to balance the resistance imposed by the friction belt (F_{fric}) was measured by a calibrated strain gauge with an accuracy of 0.05 N, (ii) the velocity was obtained by a first order digital derivation of the flywheel displacement measured by an optical encoder with an accuracy of 11815 points per pedal revolution, (iii) the force necessary to accelerate the flywheel was obtained from the second order digital derivation of the flywheel displacement providing the flywheel acceleration and the calculation of the inertial force (F_{inert}) (Lakomy 1986). The analog signal from the gauge was digitally converted by a 12 bits converter and sampled concomitantly with the digital displacement signal at 200 Hz on PC computer. The instantaneous power values were calculated according to: power = (F_{inert} + F_{fric}) · velocity . The instantaneous force, velocity and power were averaged per each pedal downstroke period identified between two minimum values of instantaneous power since they corresponded to top and bottom dead centres in the pedal rotation. This procedure respects the complete contraction cycle of the involved muscle groups (Williams et al. 1988).

Two groups of subjects volunteered for this study. They were 10 recreational students (age mean ± SD 20.2 ± 0.8 years, height 175.6 ± 7.2 cm, body mass 65.7 ± 8.5 kg) tested before (BT) and after (AT) short-term training and 16 elite sprint (SP) runners (age 22.2 ± 2.1, height 174.8 ± 6.9, body mass 72.5 ± 8.3) competing at the international level after a long term training. The short-term training consisted in 4 series of ten 5-s sprint repetitions performed on the cycle ergometer, 4 days a week during 9 weeks. The testing procedure consisted in three (SP) to six (BT and AT) 8-s sprint bouts completed against different friction loads ranging from 0 to 75 $g.kg^{-1}$. Sprint bouts were separated by at least 10 min of rest. Twelve to thirty pedal downstrokes were necessary to perform each sprint and the power-velocity relationship of each subject was built from all the downstrokes of all the sprints he performed. Indeed, it was already demonstrated that the chosen load has no influence on the power-velocity relationship (Arsac, submitted).

RESULTS

Typical power-velocity data obtained for two subjects are presented in Figure 1. Individual strong correlations were obtained ($0.94 < r < 0.99$) when the data were fitted with third order polynomial curves. Significant positive correlations between Vopt and MPO were obtained in BT ($r = 0.64$, $P < 0.05$) and AT ($r = 0.87$, $P < 0.001$) conditions and in the SP group ($r = 0.65$, $P < 0.01$, Fig. 2). MPO values of the students group were increased by short-term training (11.7 ± 1.7 $W.kg^{-1}$ BT vs. AT 15.0 ± 2.5 $W.kg^{-1}$, $P < 0.01$). Nevertheless, MPO in the short-term trained students remained significantly lower that MPO in long-term trained sprinters (17.5 ± 1.6 $W.kg^{-1}$). On the other hand, Vopt values were not increased by short-term training (BT 123.2 ± 7.1 rpm, and AT 122.2 ± 11.8, ns.) although Vopt values in long-term trained sprinters were significantly higher than students values in both BT ($P < 0.001$) and AT ($P < 0.001$) conditions.

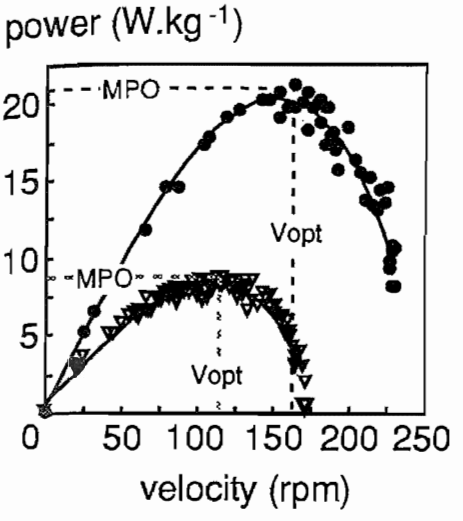

Figure 1. Typical power-velocity relations in two subjects.

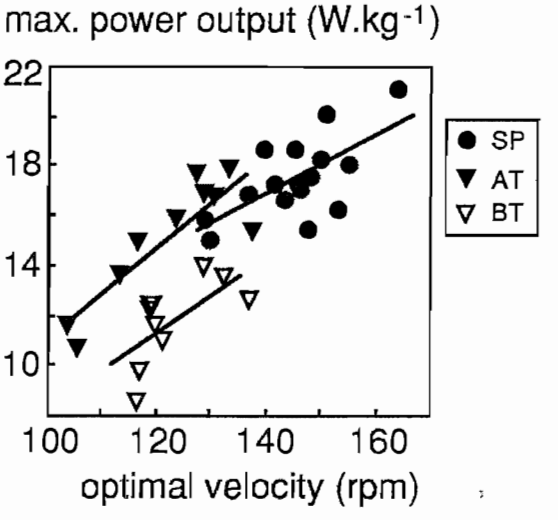

Figure 2. Effect of training on MPO and Vopt

DISCUSSION

The present study observed a significant correlation between individual Vopt and MPO in each subjects group whatever the training status (Fig. 2). Such results could suggest that both MPO and Vopt could be in relation with the same functional property of muscles.

However the main result of the present study is that short-term training increased significantly MPO but not Vopt. In fact, an enhancement of MPO could be due to an increase of cross sectional area of muscles and/or to an increase of the percentage of fast twitch fibres (%FT). Since Vopt remained the same after short-term training, it could be hypothesised that this type of training had no effect on %FT. Accordingly, several studies have failed to demonstrate any changes in muscle fibre composition, thus suggesting the genetic determination of muscle composition (Komi et al. 1977). Thus it seems that the enhancement of MPO is rather due to an increase in force production associated to hypertrophy in the literature (Häkkinen et al. 1981). Alternately the significantly higher Vopt observed in the sprint group lead to suggest that in this group, the MPO improvement is also due to an high %FT. Rather than a long-term training effect, it could be proposed that high level sprinters are genetically characterised by high %FT. This hypothesis is supported by the overlap observed in Vopt values between student and sprinter groups. In order to validate this hypothesis, precise measurements of %FT should be associated with both MPO and Vopt changes through training. In conclusion, the power-velocity features obtained during cycling could provide insights on the mechanical properties of muscle contraction and their adaptation through training.

REFERENCES

Arsac L.M., Lacour J.-R., Belli A.*J. Applied Physiol.* submitted.
Duchateau, J. and Hainaut, K. *J. Applied Physiol.* 56: 296-301, 1984.
Gregor, R. J., Edgerton, V. R., Perrine, J. J., Campion, D. S. and Debus, C. *J. Applied Physiol.* 47: 388-392, 1979.
Häkkinen, K., Komi, P. V. and Tesch, P. *Scand. J. Sports Sci.* 3: 50-58, 1981.
Komi, P. V., Rusko, H., Vos, J. and Vihko, V. *Acta Physiol. Scand.* 100: 107-114, 1977.
Lakomy, H. K. A. *Ergonomics* 29: 509-517, 1986.
Sargeant, A. J., Dolan, P. and Young, A. *Int. J. Sports Med.* 5: 124-125, 1984.
Sargeant, A. J., Hoinville, E. and Young, A. *J. Applied Physiol.* 51: 1175-1182, 1981.
Williams, J. H., Barnes, W. S. and Signorile, J. F. *J. Applied Physiol.* 65: 2343-2348, 1988.

COMPUTER MODELLING OF COMPLEXLY COORDINATED HUMAN MOTIONS WITH PRE-SET CHARACTERISTICS

D G Arsenjev , A A Ivanov, V V Konovalenko, V A Sholuha, A V Zinkovsky
State Technical University of St Petersburg, St Petersburg, Russia

INTRODUCTION.

Computer modelling of human skeletal-muscular apparatus (SMA) allows to assess energy-force characteristics of motions, synthesize motions with pre-set characteristics, develop integrated man-machine systems. As a basis for complex computer modelling of SMA motions serve systems of differential-algebraic equations, describing the dynamics of a system of bodies with constraints. A most full review of programmes for modelling of such systems can be found in the book editored by Schiehlen (1990). The up-to-date state of the problems to be solved and their complexity are quite fully reflected in abstract books of biomechanics congresses. As an example of the most resourse requiring problem (from the calculation point of view) we should cite here the work by Pandy et al (1994) which presents results of solution of an anthropomorphic model motion optimization problem. There is also a large number of models, aimed at investigation of concrete simple human motions. In this report we consider the principles of creation of a computer system for analysis and modelling of complexly coordinated SMA motions, realized on IBM compatible personal computers. Programme blocks of the system allow to carry out analysis and choice of an adequate model, synthesis of new motions with pre-set characteristics, adequacy criteria analysis on the basis of interaction of analysis and synthesis problems results. Partial results of usage of the modelling system can be found in previous author's works (Sholuha, Zinkovsky, 1994a; 1994b).

METHODS.

Computer model of SMA is actually a complex of interacting programmes of traditional structure, including user interface; modules realizing mathematical model equations solution; employing numerical methods for solution of main modelling problems, experimental data processing. The choice of model stucture, mass-inertia characteristics of elements and properties of joints is carried out on the basis of adequacy criterion, previously formulated for the given class of motions. The adequacy criterion form is chosen from results of preliminary investigation of coincedence of anthropomorphic model motion synthesis and analysis problems solution and their sensitivity to parameters change. The synthesized motion (with pre-set characteristics) is used as a basis for analysis problem. Solution of the synthesis problem for motion with pre-set kinematics and dynamic properties is realized by means of a system of parametrically defined equations of nonstationary constraints and restrictions on forces. In the computer model there were used vector-scalar kinematic constraints equation systems with parameters allowing to realize a wide diapason of model motions. Along with the equations setting the goal of the motion one should solve additional constraint equations, defining the possibilities of its perfomance by the anthropomorphic model (i.e. that this motion can be fulfiled as a result of action of only "internal" control functions and reactions of external constraints).

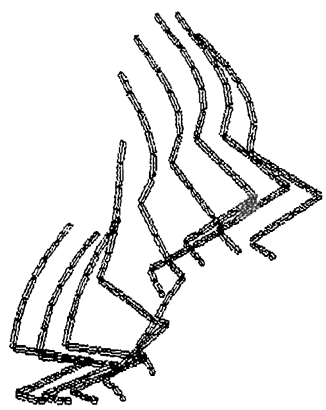

Fig 1 Upward jump during horizontal motion (15-elements model)

As an example of such additional equations there are used motion equations of system of bodies comprising SMA (two main laws of dynamics) External with respect to SMA forces and moments can be obtained as functions of time from experiment (e g for supportless phase of motion external forces and moments are equal to zero, in support-phase ground reaction can be observed as function of time) Analogously there can be restricted kinematics of any group of SMA elements which are exposed to a given generalized force In particular, one can satisfy in this way natural restrictions on power of generalized forces which cause given motion. Let us note that suggested approach to motion synthesis either realizes motion goal or brings the system to a kinematic or force constraint which means that given motion goal can not be realized under given initial conditions

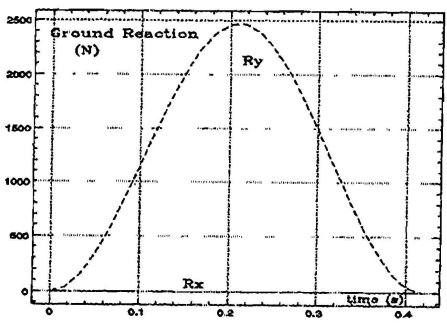

Fig. 2 Ground reaction (R_x=0) in push-off phase.

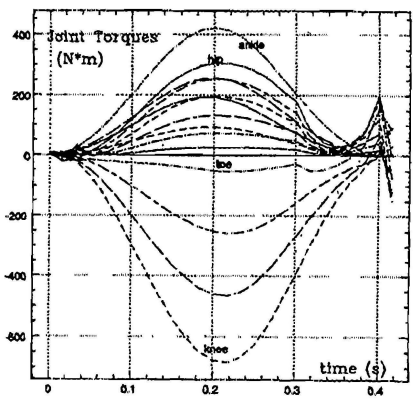

Fig 3 Joint and bending moments

RESULTS AND DISCUSSION.

Synthesis of motion with required properties was considered for modelling of walking, jumping, object throwing and gymnast excercises. Let us demonstrate described in previous section constraints formation method on example of upward jump performed by a model with non-ramified kinematic chain (Fig 1 - 3-element foot, shank, thigh and 6-element trunk). Ground reaction amplitude and form is considered to be preset (Fig.2) Natural kinematic constraint follows from the fact that reaction impulse should be completely formed before model elements straighten out into a straight line. Motion control in support phase was performed through imposition of five constraint equations. Position of foot fingers was fixed - 2 equations; theorems of center of mass motion and moment of momentum increment give 3 more equations. This allows to determine ground reaction behaviour (Fig.2) and external moment (equal to zero). Resulting motion was considered then as initial for analysis problem. Calculations yielded inter-element moments which cause the synthesized motion (Fig 3). In the considered example along with constraints equations for correction of inter-element moments there were used located spring and visco-elastic elements which also allow to model distributed elasticity of SMA elements.

REFERENCES

Pandy, M.G , Anderson, F.C. and Ziegler, J.M. (1994) Optimization algorithms appropriate for sports perfomance. In Proceedings of the Second World Congress of Biomechanics. Amsterdam, the Netherlands, II-139b.

Schiehlen, W. (1990) Multibody Systems Handbook, Springer-Verlag Berlin Heidelberg.

Sholuha, V.A., Zinkovsky, A.V. (1994a) Investigation of adequacy criteria of computer models of human motions. In Proceedings of the Second World Congress of Biomechanics. Amsterdam, the Netherlands, I-179b.

Zinkovsky, A.V , Sholuha, V.A (1994b) Technology of imitational dynamic modeling of biomechanical systems. In Proceedings of the Second World Congress of Biomechanics Amsterdam, the Netherlands, I-180a.

IMPACT PROCESS OF KICKING IN FOOTBALL

Takeshi Asai*, Takao Akatsuka**, and Masaru Kaga***

* Faculty of Education, Yamagata University, Kosirakawa, Yamagata-city, Yamagata 990, Japan

** Faculty of Engineering, Yamagata University, Jyounan, Yonezawa-city, Yamagata 990, Japan

***Faculty of Education, Okayama University, Tsusimanaka, Okayama-city, Okayama 700, Japan

Introduction

Techniques of hitting a ball with a body or with a tool in ball games are known abundantly. However, only a few studies of the impact process itself have been done before. The purpose of this article is to clarify the impact process of instep-kick in football by using a high- speed video camera (4,500fps).

Methods

Six university football players were chosen as the subjects. The players kicked a ball with the instep toward a mini football goal 4m ahead. The high-speed camera was set up 1.5m apart in the side direction. The ball used in this experiment was an official ball of FIFA (434.6g,700m/cm^2). This experiment was photographed by using the high-speed camera (FASTCAM-ultima), which can take 4,500 frames per second with 256×256 pixel, and then it was recorded on VTR.

Nine markers for digitizing were attached on the kicking leg of the subjects (tibia, lateral malleolus,calcaneus,tubersity of base of fifth metatarsal,head of fifth metatarsal, toe, etc.). The coordinate values were input in a computer by a video-position-analyzer. In order to analyze the degree of plantar flexion of the foot joint in the impact process, three angles A, B and C were measured from the graphic data.The angle A is made up by the markers No.2-3-6, the angle B by the markers No.3-6-8, and the angle C by the markers No. 3-7-9. The contact time of the instep with ball was obtained from the number of the frames in which the contact between them was observed.

Results

An example of stick-picture of the foot joint in the impact process is shown in figure 1. The degree of plantar flexion on the side of the phalanges of the toe is shown to be a little greater than that on the side of talsal bones, and also that in the latter half is a little greater than that in the first half. In the case of this trial, the contact time of the foot with the ball is 9.3msec., the horizontal contact distance is 144mm, and the horizontal velocity of the ball after the impact process is 25.2m/sec..

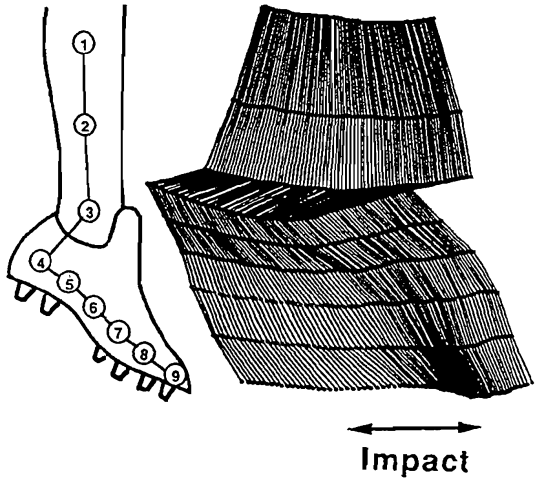

Fig.1 An example of stick-picture of a foot joint in impact process

The horizontal velocities of the markers No.3, 5, 7 and 8 of the foot in the impact process is shown in figure 2. The velocity of the tubersity of base of the fifth metatarsal (No.8) is a little greater than that of the lateral malleolus (No.3) just before the impact, and the velocity of the tubersity of base of the fifth metatarsal (No.8) is a little smaller than that of the lateral malleolus (No.3) after the impact.

There is a tendency that the angles A, B and C of the foot joints increased during the impact process.

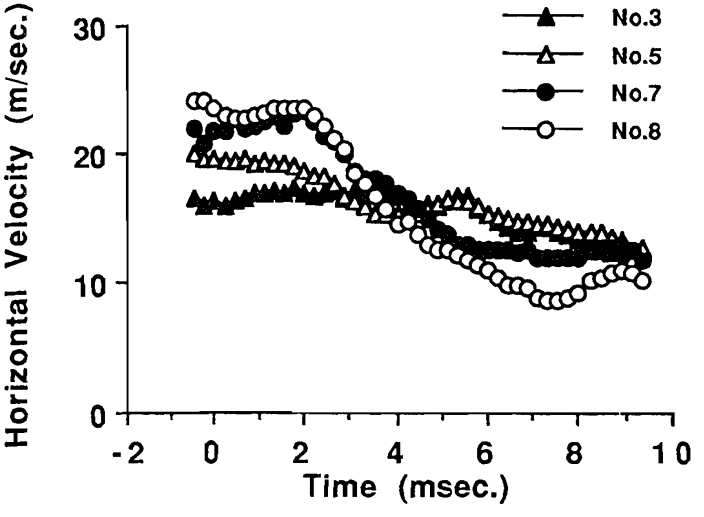

Fig. 2 The horizontal velocities of the markers No.3,5,7 and 8 of the foot in the impact process

Discussion

The average value of the contact time of the instep with the ball is 9.12msec. This result is a little shorter than the value 12.0msec. given by Asami and Nolt(1982), who used a 500fps high-speed camera. The discrepancy of the two results may be explained by the differences of the dynamical characteristic of the balls used in the experiments, the contact points and the collision velocities. The detailed analysis will be a subject for a future study.

The average value of the horizontal contact distance is 147mm. It becomes clear that the contact of the foot with the ball ends before the instep of the foot moves by the diameter(223mm) of the ball.

As mentioned above, the angles A, B and C of the foot joints are increased during the impact process. Especially the degree of the angle A is a little greater than the others. The correlation is found between the impulse at the impact and the range of the angle A ($R=0.886, p<0.05$),and between the impulse at the impact and the range of the angle C ($R=0.76, p<0.1$). Asami and Nolt (1982) found a negative high correlation between the degree of plantar flexion of the forefoot and the ball velocity, which is an opposite conclusion to our experiment. This may be due to the fact that the contact points of the instep with the ball are dispersed from the ankle joint to the toe in the experiment of Asami and Nolt (1982), while the contact points in our experiment are centered around the instep from the tarsal bones to the metatarsal bones.

From the above results, it will be concluded that the angles of the ankle, the tarsal and the metatalsal joint, i.e., the degree of plantar flexion increases as the impulse at the impact increases with a narrow range of contact points.

Reference

Asami,T.,Nolt,V.(1982) Analysis of Powerful Kicking. In,H.Matsui,K.Kobayashi,(Eds),Biomechanics VIII-B,Nagoya 1983,695-700.

THE VISCOELASTIC FUNCTION OF THE POSTERIOR LUMBAR SPINE DURING LIFTING

Aubert M-P., Yahia L.H., Mitnitski, A., Ecole Polytechnique de Montréal, Newman N., Université de Montréal/ Hôtel Dieu, Gracovetsky S., Concordia University, Asselin S., Diagnospine Research Inc., Montreal, Québec, Canada.

INTRODUCTION

The function of the lumbar spine during lifting is the subject of controversy with regard to the generation of extensor moment. Paralumbar muscle contraction is considered by some (McGill and Norman 1986) to be the major contributor whereas anatomic studies (Bogduk et al. 1992) and theoretical studies (Gracovetsky 1988) suggest that the dorsolumbar fascia and other passive mechanisms may be predominant.

METHOD

Ten healthy men (mean age - 26.9 yrs., height - 1.77 m, weight - 82.15 kg) underwent a preemployment weightlifting examination consisting of bar lifting from ground level according to tolerance (0 to maximum permitted - 68 kg) without external constraint or instruction. Light-emitting diodes were placed over the cervico-dorsal, lumbar and sacral spine, and skin surface motion was measured by 2 cameras allowing three-dimensional reconstruction. Lifting speed **v**, global trunk flexion α and lumbar lordosis Ψ were estimated. Skin surface EMG over multifidus was recorded simultaneously. Torque **Tm** at L5 was calculated from anatomical data, contour measurements and moment equilibrium equations (Fig. 1).

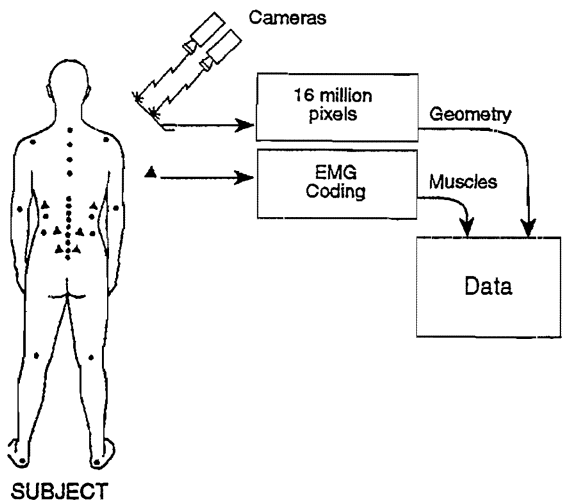

Figure 1: Schematic of data acquisition. A set of cameras collects information on the kinematics of skin markers placed according to a standardized procedure. From the data collected, the three dimensional coordinates of the specific marker being fired are calculated. In addition, EMG of multifidus is monitored bilaterally at the L5 level.

RESULTS

All subjects began the weightlifting with the lumbar spine flexed to within 5° of the subject's maximum lumbar flexion, considered to be the degree of lumbar flexion associated with the muscle relaxation phenomenon. Maximum torque at L5 occurred with the lumbar spine at, or close to, maximum flexion (within 5°). Vertical speed of weightlifting was variable for 0 kg external loads. With loads of 11 to 68 kg, subjects showed a clear trend to maintain or increase speed of lifting with increasing load, in spite of the increase in torque due to acceleration that this implied (Fig. 2). Maximum surface EMG occurred during the second half of the weightlifting rather than during the resistance to maximum torque.

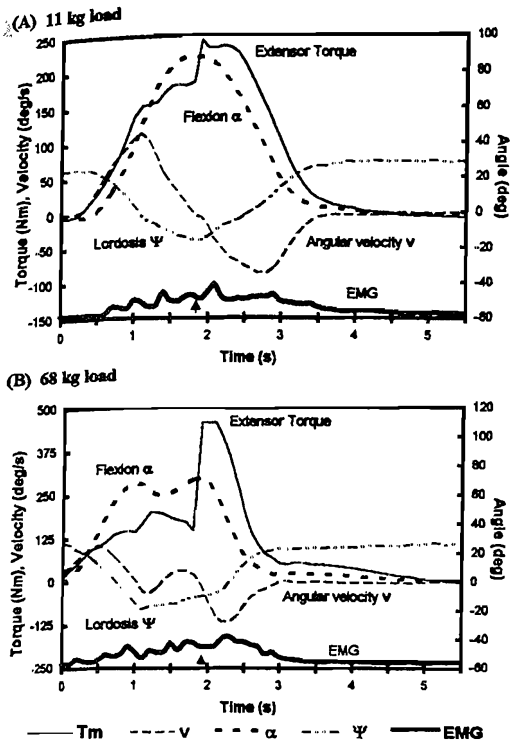

Figure 2: Extensor torque (moving torque **Tm**) at L5, sagittal angular velocity **v**, sagittal flexion angle α from vertical, estimated lumbosacral angle (lordosis Ψ) and multifidus EMG activity in arbitrary units plotted against time for two different loads, **(A)** 11 kg and **(B)** 68 kg. The arrow indicates starting point of weightlifting movement. Duration of lift is shorter for the heavier load. Trunk flexion varies in phase with lordosis during both movements. Note that the value of maximum speed of lifting is greater with the heavier load and that the EMG activity peaks during trunk mid-extension.

DISCUSSION

The rapidity of weightlifting, in spite of the increased torque caused by acceleration, is consistent with a viscoelastic function rather than a purely muscular contraction phenomenon. The degree of lumbar flexion during resistance to maximum torque suggests that posterior ligamentous stretching, including passive muscle stretching, are very important. A recent study (Yahia et al. 1993) has shown that higher ultimate tensile strengths and lower strains are recorded at increasing strain rates in the dorsolumbar fascia, confirming its viscoelastic properties and the need for speed of loading. Considering that the lumbodorsal fascia is larger than all the other posterior ligaments put together (McGill and Kippers 1994), and has the largest lever arm (9 cm) (Dolan et al. 1994), we propose that this structure is of predominant importance in resisting lumbar torque during lifting. The lumbodorsal fascia is put into tension by lumbar flexion (equivalent to posterior pelvic rotation) and to some extent by intra-abdominal pressure and paralumbar muscle contraction and latissimus dorsi contraction. The energy of lifting comes from the glutei and hamstring muscles and is transmitted via the pelvis to the lumbodorsal fascia by passive stretching of the lumbar spine in flexion.

REFERENCES

Bogduk N, MacIntosh JE, and Pearcy MJ (1992) A universal model of the lumbar back muscles in the upright position. Spine 17:897-913.

Dolan P, Mannion AF and Adams MA (1994) Passive tissues help the back muscles to generate extensor moments during lifting. J Biomech 27(8):1077-1085.

Gracovetsky S (1988) The Spinal Engine. New York/Wein, Springer-Verlag.

McGill SM and Kippers V (1994) Transfer of loads between lumbar tissues during the flexion-relaxation phenomenon. Spine 19(19):2190-2196.

McGill SM and Norman RW (1986) Partitioning of the L4-L5 dynamic moment into disc, ligamentous, and muscular components during lifting. Spine 11(7):666-678.

Yahia LH, Pigeon P and DesRosiers EA (1993) Viscoelastic properties of the human lumbodorsal fascia. J Biomed Eng 15: 425-429.

JOINT MOTION OF THE LOWER LIMB AND GROUND REACTION FORCES IN VERTICAL LANDING

M. Ayalon, A. Ayalon and D. Ben Sira

The Zinman College of Physical Education at the Wingate Institute, Israel

INTRODUCTION

Vertical landing is a common skill which characterizes a variety of sport activities The magnitude of the Vertical Ground Reaction Force (VGRF)and the vertical acceleration of the center of mass of the body as well as the acceleration of each of the segments are highly related. The timing of the sequential acceleration of the segments and it's relationship with the total force curve is of great importance to the understanding of the common and unique aspects of landing performance (Lees, 1981).

The purpose of this study was to characterize the coordination chain of the angular movements of the joints of lower limb during landing and to examine its relationships with major phases of the VGRF curve.

METHODS

Ten physical education students (age 23-27) were the subjects in this study. Each subject performed ten vertical landings from a specially designed platform set at a height of 0.60 m. This platform ensured verticality of the landings by folding underneath the subject immediately after he voluntarily activated a push-button. The ground reaction forces were measured with a Kistler force plate (model 9281b). The joints angles were measured by Mie electrogoniometers set at the ankle, the knee and the hip. All data were transferred through a Metro-Byte A-D converter , into an IBM computer at a sampling rate of 2.5 KHz for analysis. The following parameters were derived from the recorded data. a. The time from touchdown to local peaks in the VGRF curve b The magnitude of the local peaks c The time of local trough of the VGRF curve d The timing of the onset of the rotation phases at the ankle, knee and hip joints f The timing of the end of the rotation phases at the ankle, knee and hip joints

RESULTS

Force-time curves differed in amplitude and timing between and within individuals Nevertheless, in all 100 trials certain common characteristics were evident Accordingly, a typical landing VGRF curve (fig. 1-a) can be divided into four phases. a Ground contact to the first peak of the VGRF(P1). b From P1 to the local minimum (M1) c. From M1 to the second peak (P2) d From P2 until the force stabilizes at approximately body weight. TP1, TM1 and TP2 are the times from touch down to P1, M1 and P2 respectively

In typical curves of angular movements at the hip, knee and ankle (fig. 1-b) the onset of rotation can be determined from the change in the slope of the curve SH, SK and SA are the respective onsets of flexion. The time of the end of the movement of ankle was labeled EA. The end of the rotation phase of the knee and the hip was later than TP2. The reliability coefficients for all the variables were 0.9 or higher

Two way ANOVAs indicate that the differences in timing between SA and TP1, SK and TM1 and between SH and TP2 were not significant. The trials main effect was found to be statistically significant in all three analyses. Interaction effect were minor In an inter-individual multiple correlation model for the ten trials the dependent variable was P2 and the independent variables were SA, SK, EA, SH The range of Rs for the 10 trials was 0 70-0 92. In a similar intra-individual model for each of the 10 subjects 9 of

the Rs were in the range of 0 81 to 0 99 while one was 0 66 In all models, EA was the dominant dependent variable

DISCUSSION

The intersegmental timing occurs in a very short time period. Lees (1981) suggested that the duration of the absorption phase is 150-200 ms The present work focuses on the time between the initial contact with the ground and the development of the second peak This time lasts 40-70 ms In this very short period the joints exhibited a precise timed coordination to decelerate the velocity of the center of gravity in order to minimizie the forces which act on the body The time to TP1, was 6 5-15 3 ms During this time the angular movement at the joints was negligible supporting other observations (Nigg, 1981) of an initial passive phase

In the second part various phases of the VGRF curve were found to be related to the movements at the lower limb joints In this part, which is the active absorption phase, the attenuation of forces is achieved by specific intersegmental timing. The descent from P1 coincides with the beginning of movement at the ankle, the rise from M1 is timed with the beginning of movement at the knee and the descent from P2 coincides with the movement at the hip joint From P1 to P2 there is angular movement at the ankle followed by angular movement at the knee Therefore, it is evident that the attenuation of P2 is associated with the coordination of angular motion at these two joints Furthermore, the ankle was the only joint which terminated it's active phase before P2 The dominance of the ankle joint is supported by the multiple regression models, indicating that the longer the ankle dorsiflexes the lower is P2

The higher correlation coefficients in the intra-individual modes supports the conclusion that each individual has a unique landing strategy Thus, it is necessary to analyze performance on the individual level then trying to define an universal timing pattern

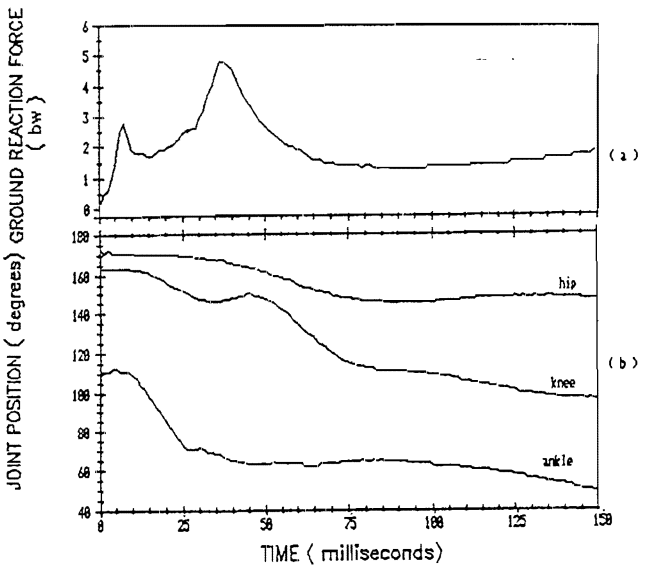

Figure 1: A typical landing VGRF curve (a) and typical curves of angular movements at the hip, knee and ankle joints (b)

REFERENCES

Lees, A. (1981), Engng Med **10**, 207-211

Nigg, B.M., Denoth, J & Neukomm, P A. (1981), Biomechanic VII-B , pp. 88-99 University Park Press. Baltimore

CHARACTERISATION OF HUMAN GAIT IN DEXTRAL AND NONDEXTRAL SUBJECTS

MB AYRES[1] MJ PEARCY[2] RA FRICK[3] and MH SHARPE[1]
[1]School of Physiotherapy and [2]School of Mathematics, University of South Australia,
[3]School of Engineering, Flinders University of South Australia, Adelaide, Australia

INTRODUCTION

The motor control of limbs by the brain is organised such that each cerebral hemisphere acts predominantly on the contralateral limbs One hemisphere usually is considered dominant as indicated by any individual showing marked preference and skill for the use of one hand over the other. The definition of leg dominance, however, is complicated due to the varied functions of the leg, thus it may refer to either the leg that an individual prefers to stand on, or the leg used for such activities as kicking. The task of walking may be considered superficially as an activity without side preference, if there is Biomechanical symmetry within the individual If there is cerebral lateralisation with dominance on one side then it might be expected that gait would not be symmetrical. If asymmetry can be measured then injury and disease that affect one hemisphere of the brain should be identifiable by changes in gait and this should lead to greater understanding of cerebral control on motor activity

The aim of this study was to measure three-dimensional rotations of both legs during walking and to determine if the measurements could differentiate groups identified as having different cerebral lateralisation

METHOD

The 3SPACE Tracker (Polhemus, Vermont USA) was used to measure simultaneously, the three dimensional rotations of both thighs of subjects walking at their preferred pace and at a slower pace of 40 steps per minute, both controlled using a metronome. The source module was secured over the sacrum of each individual and the sensors were attached to the leg 7cm above the lateral femoral condyle and aligned with the greater trochanter Hence the measurements were of the rotations of each leg relative to the pelvis defined as Flexion/Extension, Ad/Abduction and Ex/Internal Rotation The vertical foot force was measured using pressure sensitive insoles, Krusen limb load monitors, to enable stance and swing phase to be identified. Measurements were made while subjects walked along a 5 5m walkway starting from a standardised position (Ayres et al 1993)

An initial study looked at the repeatability of the equipment application by repeating measurements after removal and reapplication of the equipment four times on one subject. Reproducibility of the subjects' movements was assessed by measuring twelve subjects on two different days. The main study measured 80 normal subjects (40 male, 40 female), aged between 18 and 65 years with an equal representation of left and right handed dominance Leg dominance was determined as the preferred standing leg using a modified Annett's questionnaire (Annett 1970)

DATA ANALYSIS

The data were analysed in two ways. During gait, the phase of Ad/Abduction and Ex/Internal rotations compared with Flexion/Extension were assessed by determining the lag at peak cross-correlation within a leg and comparing like rotations between legs In addition, angular excursions during stance phase were analysed for each rotation. Intraclass correlations were conducted on the data from the equipment and procedural repeatability studies and repeated measures analyses were applied to the main data

RESULTS

The 3SPACE Tracker gave high repeatability within a session, less high repeatability between sessions, and there was consistency between equipment applications, (r=0.89 and r=0 96 for peak lags and excursion angles respectively) There was a highly specific subject effect between sessions. The general subject data revealed that preferred standing leg was contralateral to the preferred hand in the majority of subjects (72.6% males and 87 5% females).

Results for the within-leg phase relationships identified peak coupling of External rotation to Flexion, on the left leg, as significant for cerebral dominance ($p<0.05$) This measure was not affected by pace or gender There were significant differences between left and right leg measurements within the right handers, but no similar differences were evident in the right-handers

For the excursion angles, Adduction on the loaded leg revealed a significant handedness by measured leg interaction. For males, excursions on the left leg were larger in right-handers, conversely, excursions on the right leg were larger in left-handers This indicated that for the majority of subjects in each handedness group, angular excursions were larger for the preferred standing leg

DISCUSSION

The general subject data revealed leg dominance opposite to hand dominance These results were in agreement with other studies when leg definition was clarified

The External Rotation lag compared with Flexion/Extension within left sided femoro-pelvic movement was significant for cerebral lateralisation One cerebral hemisphere controls motor output to the contralateral side of the body, therefore left leg differences may be due to alteration in the right cerebral hemisphere, known to specialise in temporo-spatial processing (Kertesz et al 1985) The significant lack of leg differentiation, within the left-handed group, suggests less cerebral lateralisation in this group, in agreement with other studies(e g. Corballis 1989)

Difference in temporal couplings during gait within left-sided femoral rotation measured by cross-correlations between transverse plane and sagittal plane movement was observed in dextral and non-dextral subjects The difference may be related, either directly or indirectly, to an alteration in the temporo-spatial ability of the right cerebral hemisphere Of the few gait experiments that have studied laterality, differentiation between dextrals and nondextrals has been observed in gait analysis by footprints (Chodera 1974) Standing leg preference was not related to handedness on observations throughout gait, but during the specific single-stance phase, larger leg angular adduction excursions, whilst the leg was weightbearing, were associated with standing leg preference.

CONCLUSION

This study has developed a technique that is able to discriminate the effects of cerebral lateralisation in a basic motor function of the lower limb and may be of assistance in the future in further examination of this phenomenon

REFERENCES

Annett M (1970) A classification of hand preference by association analysis. Br J Psychol 61 303-321.

Ayres MB, Pearcy MJ, Frick RA, Sharpe MH (1993) Bilateral femoral rotations measured during walking using the 3SPACE Tracker system Proc XIV Congress on Biomechanics, p 126-127

Chodera JD (1974) Analysis of gait from footprints Physiotherapy 60.179-181

Corballis MC (1983) Laterality and human evolution Psych Rev 96 492-505

Kertesz A, Nicholson I, Canalliere A, Kassa K, Black SE (1985) Motor impersistence a right hemisphere syndrome. Neurology 35.662-666

IMPROVING THE PERFORMANCE OF A TOP ATP TENNIS PLAYER WITH A KINEMATICAL APPROACH, AND A 3-D INTERACTIVE VISUALIZATION OF THE SERVE.

Xavier Balius, Carles Turró, Jordi Carles, Javier Jáuregui, Josep Escoda, Joan A. Prat
Biomechanics Department, Olympic Training Center (CAR)
Sant Cugat del Vallès, Catalunya, Spain

INTRODUCTION

As a result of the interest expressed by the coach of a top ATP tennis player, the Biomechanics Department of the Olympic Training Center (CAR) at Sant Cugat, have developed a program with the aim of improving the performance of the professional tennis player with the help of kinematical data.

We have found relevant literature concerning different aspects of biomechanics, and its description and explanation of the technique studied: the serve. However, although studies by Eliott, et al., give biomechanical information from a 3D approach (1) of the tennis serve, we have not found literature containing kinematical data in relation to the improvement of a high level tennis player's performance throughout the tennis season.

METHODS

The serve of a top ATP professional tennis player was recorded twice: once during a training session (fast court), and secondly during a championship (fast court), the weight of the subject was 89 kilos and his height 1.88 meters.

Two fixed cameras (Panasonic WV-F70E) for the training session, and four fixed cameras (2 JVC TK-1280E and 2 Panasonic WV-F70E) for the championship were used for data collection. The optical axes were oblique to the right hand side of the player during the training session, and oblique to the right and the left hand side of the player during the championship, obtaining in both cases an angle of approximately 90°. The cameras were genlocked and time code synchronized, and inserted. The space was calibrated using an object of known coordinates and a volume of 3x3x3m. and, a known position of 5 points in the field helped us to rotate and translate the general coordinates of both studies.

We used the Direct Linear Transformation technique with 11 paramenters (DLT-11) to calculate three-dimensional position coordinates of 25 system body-racket landmarks. A quintic spline function was used for smoothing. The average mean errors for the estimation of 3D points were RMS x = 0.006 m, RMS y = 0.004 m, RMS z = 0.002 m, and RMS total = 0.008 m, for the training project, and RMS x = 0.003 m, RMS y = 0.006 m, RMS z = 0.004 m, and RMS total = 0.007 m, for the championship project.

Data collection was done at 50 Hz, and 25 landmarks (23 body, 2 raquet) were manually digitized in each frame for both cameras. The digitized and analyzed serves were choosen by the coach. A Panasonic AG-450 and a Loewe High 8 were used to calculate the ball velocities for each recording, and additionally a Panasonic NV-S7E was also used to record the result of the play, training and competing.

RESULTS

Kinematical data for the serve includes: kinematic chain of the system, which is the Resultant Velocity of the raquet arm Shoulder (RVS), Resultant Velocity of the raquet arm Elbow (RVE), Resultant Velocity of the raquet arm Wrist (RVW), Resultant Velocity of the Raquet (RVR). Also components of the kinematical chain, and Height of Impact (HI), Depth of Impact into court (DI), Ball Flight Time (BFT), the Height of the Ball Touch (HBT), Horizontal Distance into court Touch (HDT) of the ball, and first Step DeptH (SDH).

From the results record during the training session the coach was able to decide the gestures to be analysed. The decision was initially made upon two well performed serves with the only apparent difference being the spot where the ball bounced in the opponents reception rectangle. From the kinematical data, one can obtain the differences between the better serve in respect to the not so good serve: (the first value is always of the serve that bounced closer to the net, and considered not as good as the one that bounced farther from it) HBT = 2.86 m vs 2.89 m, HDT = 0.74 m vs 0.55 m, SDH = 0.41m vs 0.50 m, the kinematic chain was better for the second serve as the sequence of achievent of the maximum Resultant Velocities had a better rythm: RVS = 0.1 s before contact (bf), RVE

= 0.08 s (bf), RVW = 0.04 s (bf), and RVR = 0.02 s (bf). The first serve did not show a good coordination between shoulder and elbow: RVS = 0.08 s (bf), and RVE = 0.1 s (bf).

DISCUSSION

It is important to mention the limitations in obtaining qualitative data. This is due to the fact that the data collection does not allow us to obtain all the necessary information for the study of a high velocity motion. However, the differences between the two well performed serves has allowed us to obtain biomechanical data which provides the coach with concrete information about the serve that he wants the player to obtain, thus backing up his own intuition of how the serve should be played.

This is an ongoing program that is already giving a good advice to the coach, and that also offers a control of the good technique that the player has to adapt in order to improve his performance.

In the near future we expect to obtain biomechanical information from other top ATP professional players, above all players that have anthropometrical characteristics similar to that of our subject, and players with a good good 1st serve. The comparisson of his own technique through out the season, suported with 3D interactive visualizatiuon of all the actions analysed (Figure 1), and that of other good servers can provide us with valuable data to improve the performance of our player.

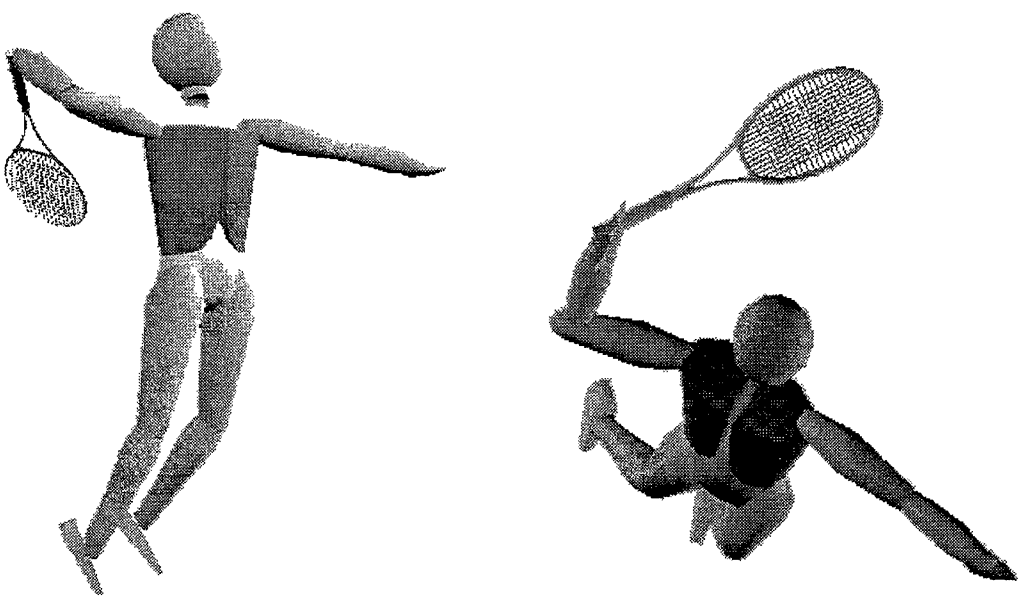

Figure 1 - 3D interactive visualization of one of the serves analysed.

REFERENCES

1 - Elliott, B.; Marsh, T.; Blanksby, B.; A three-dimensional cinematographic analysis of the tennis serve. International-Journal-of-Sport-Biomechanics.; 2(4), 1986, 260-271.

KNEE JOINT FORCES DURING ISOKINETIC ECCENTRIC EXERCISE

V. Baltzopoulos and G. Keddie

Department of Movement Science, Faculty of Medicine,
University of Liverpool, Liverpool, U.K.

INTRODUCTION

The main feature of isolated joint isokinetic movements is a resistive dynamometer moment that is variable and equivalent to the resultant joint moment. This provides constant joint angular velocity and optimal muscular loading. The maximal joint and resistive moments throughout the range of movement (ROM) result in considerable joint loading. However, only a limited number of studies examined the joint forces developed during isokinetic concentric movements (Baltzopoulos, 1995a; Kaufman *et al.*, 1991; Nisell *et al.*, 1989). The moments developed during eccentric isokinetic movements are significantly increased but there are no studies examining muscular and tibiofemoral contact forces during eccentric isokinetic movements. The widespread applications of isokinetics in the assessment of dynamic muscle function both in normal and pathological conditions require the examination of the dynamic joint forces in order to prevent possible rehabilitation or training induced injuries, caused by excessive joint forces. The purpose of this study therefore was the examination of muscular and tibiofemoral forces during eccentric isokinetic knee exercise at angular velocities ranging from 0.52-2.62 $rad \cdot s^{-1}$, using a biomechanical model of the knee joint.

METHODS

A Biodex II isokinetic system (Biodex Medical Systems Inc, Shirley, N. York) was used in the present study for the assessment of eccentric isokinetic knee flexion. Moment and angular position data were collected at a sampling rate of 100 Hz. Six males without knee joint injury history signed informed consent and volunteered to participate in this study. The mean (s.d.) age was 22.8 (3.4) years, height 1.80 (0.05) m and mass 79.85 (2.91) kg. The mean femoral condyle width measured using a Holtain anthropometer was 0.099 (0.022) m. The mean length between the medial tibia border and the superior aspect of the medial malleolus was 0.452 (0.035) m. The subjects were seated on the Biodex Chair with the back rest at an angle of 1.8 rad. Stabilising straps were placed across the anterior aspect of the distal end of the right thigh, the pelvis and the trunk of the subject. The axis of rotation of the dynamometer was aligned with the most prominent point of the lateral femoral condyle. The dynamometer arm was secured on the leg proximal to malleoli.

Eccentric knee flexion was examined at angular velocities of 0.52, 1.52 and 2.62 $rad \cdot s^{-1}$. The testing protocol consisted of five maximal reciprocal eccentric repetitions of the knee extensors. The ROM was adjusted on the dynamometer from approximately 0.17 to 1.57 rad of knee flexion. The tests were completely randomised and rest periods of 5 min were given between the tests. A familiarisation and warm-up period was given before the test. The dynamometer moment was displayed on the computer monitor in real-time for feedback-motivation purposes. All subjects were given written, standardised instructions to work as hard and as fast as possible against the resistance of the dynamometer. Dynamic muscular and tibiofemoral compressive and shear forces were determined using a previously developed two-dimensional biomechanical model of the knee joint. This model is based on X-ray video of knee extension-flexion (Baltzopoulos, 1995b). The resultant joint moment ($\mathbf{M_m}$) was calculated from the moment recorded by the isokinetic dynamometer ($\mathbf{M_d}$) using:

$$\mathbf{M_m = M_d + M_{wd} + M_{ws}}$$

with M_{wd} and M_{ws} the gravitational moments of the dynamometer arm and segment respectively. Inertial moments are not included because only constant angular velocity data were considered. The muscular (Fm) and tibiofemoral compressive (Fc) and shear (Fs) forces were calculated using the model described in Figure 1.

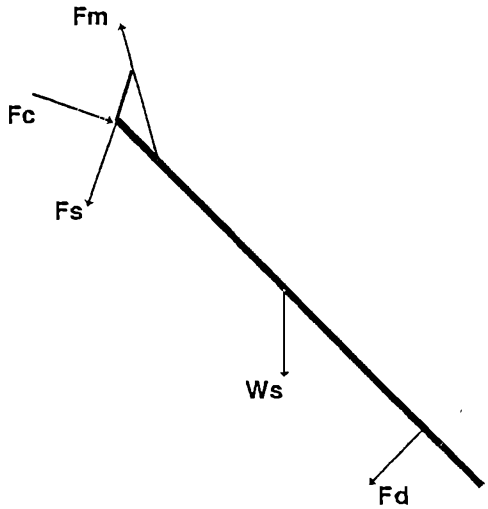

Figure 1. Biomechanical model of the knee joint for the calculation of joint forces (Fm: Muscular Force, Fc: Compressive force, Fs: Shear force, Fd: Resistive dynamometer force).

RESULTS AND DISCUSSION

The mean maximum resultant moment ranged from 334 (48) Nm at 0.52 rad·s^{-1} to 311 (34) at 2.62 rad·s^{-1} and was recorded at approximately 1.05 rad of knee flexion. The maximum muscular force ranged from 11.48 (1.41) times body weight (BW) at 0.52 rad·s^{-1} to 10.68 (1.07) BW at 2.62 rad·s^{-1}. The compressive tibiofemoral force ranged from 11.41 (1.41) at 0.52 rad·s^{-1} to 10.64 (1.11) BW at 2.62 rad·s^{-1}. The maximum shear tibiofemoral force was in the anterior direction and ranged from 1.16 (0.21) BW at 0.52 rad·s^{-1} to 1.17 (0.16) BW at 2.62 rad·s^{-1}. Repeated measures one-way ANOVA tests indicated that there was no significant difference between the mean maximum moments, forces and knee flexion angles of maximum forces at the different angular velocities. These results indicate that the forces developed during maximal isokinetic eccentric knee flexion are lower compared to other powerful dynamic activities involving eccentric activations but are higher than joint forces during simple walking and cycling activities and isokinetic concentric movements. Appropriate precautions and adjustment of the isokinetic protocol are required, so that eccentric movements are performed only in the final phases of joint injury rehabilitation. Reduction of joint loading during exercise, especially when a large number of eccentric repetitions is performed, can be achieved by adjusting the joint range of movement and performing submaximal repetitions.

REFERENCES

Baltzopoulos, V. (1995a). Muscular and tibiofemoral joint forces during isokinetic knee extension. *Clin. Biomech.*, **In Press**.

Baltzopoulos, V. (1995b). A videofluoroscopy method for measurement of knee joint kinematics. *Clin. Biomech.*, **In Press**.

Kaufman, K., Kai-Nan, A., Litchy, W., Morrey, B. and Chao, E. (1991). Dynamic joint forces during knee isokinetic exercise. *Am. J. Sports Med.*, **19**, 305-316.

Nisell, R., Ericson, M., Nemeth, G. and Ekholm, J. (1989). Tibiofemoral joint forces during isokinetic knee extension. *Am. J. Sports Med.*, **17**, 49-54.

NON-INVASIVE MEASUREMENT OF THREE DIMENSIONAL SCAPULOHUMERAL KINEMATICS

N D Barnett, R D D Duncan, G R Johnson, Centre for Rehabilitation and Engineering Studies, University of Newcastle upon Tyne, UK

INTRODUCTION

Codman (1934) used the term *scapulohumeral rhythm* to the rotation of the scapula during motion of the arm Measurement of this phenomena however has proven rather difficult as the motion of the scapula occurs beneath the skin, inhibiting the fixation of any externally applied measurement system Many measurement techniques have been presented, including radiography (Inman *et al*, 1944) and goniometry (Doody *et al*) It is only recently that three dimensional techniques have been employed in this measurement (Pronk, 1991) This technique, involving palpation of anatomical landmarks, was further developed by Johnson *et al* (1993) Developing further his work, this study reveals all six degrees of freedom of scapula motion over a range of arm abduction in the coronal plane The data collected from five subjects, by two observers has been compared to prove inter-observer repeatability

METHODS

Measurement of the position of a rigid body in three dimensional space requires knowledge of the coordinates of three non-collinear points on or within that body For measurement of scapular position, three palpable landmarks may be identified, the posterior angle of the acromion, the root of the scapula spine and the inferior angle Johnson's palpation fixture had three adjustable legs, the ends of which located over these points Its position was recorded relative to a sternal sensor using an Isotrak™ electromagnetic measurement system In order to improve both rotational and, primarily translational accuracy, a new palpation fixture (Locator) has been designed to enable more repeatable positioning over the landmarks This has been achieved by designing the ends of each leg on the Locator to be specific to the landmark over which they locate, enabling the fixture to locate snugly over the scapula

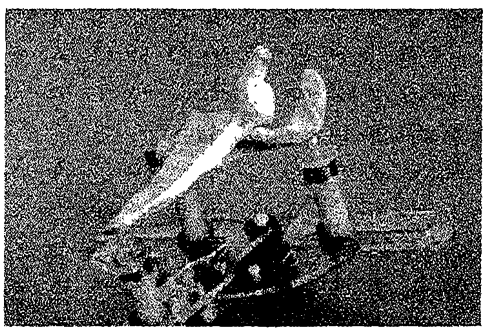

Figure 1: *Illustration of the Locator*

For collection of the data, a standard test was defined for the subjects This involved abduction of the arm in the coronal plane from 0° to 90° in 10° increments, measured with a fluid filled goniometer During this motion, all subjects were instructed to keep their elbow flexed at 90° with their forearm pointing directly forwards at all times This position was adopted to discourage rotation of the humerus about its long axis which will alter the rotations of the scapula At each increment, the Locator was applied and a record of scapular position taken

The left shoulder of each subject was tested five times by each of the two observers over a period of approximately four weeks Five subjects were tested in all

The Euler angle rotations of the scapula, together with the translations of the posterior acromial angle were determined in the trunk coordinate frame, where the axes are defined as follows +x (motion vertically upwards), +y (lateral motion) and +z (motion backwards) The Euler angle rotations were defined in the following sequence alpha about y (forward/backward tip), gamma about z' (lateral rotation) and beta about x'' (protraction/retraction) The Euler angle rotations were also determined in the initial scapula frame, with the rotation sequence as used by Pronk for direct comparison

RESULTS

Inter-observer repeatability is illustrated below, showing the data recorded by each observer from the same subject.

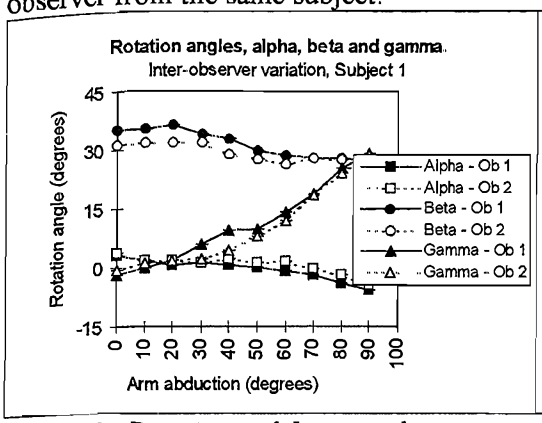

Figure 2: *Rotations of the scapula.*

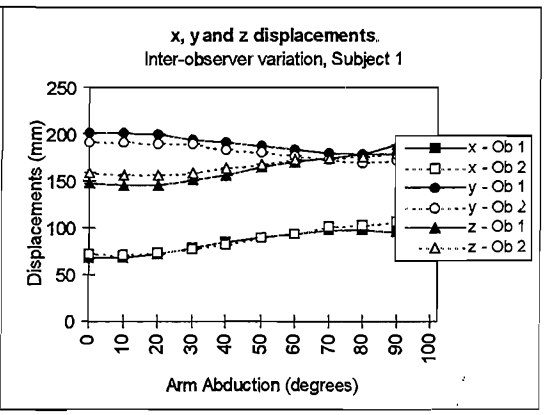

Figure 3: *Translations of the acromion.*

Comparison of the rotation angle gamma (lateral rotation) between both observers and Pronk may be seen in Figure 4

Figure 4: *Comparison with Pronks' data*

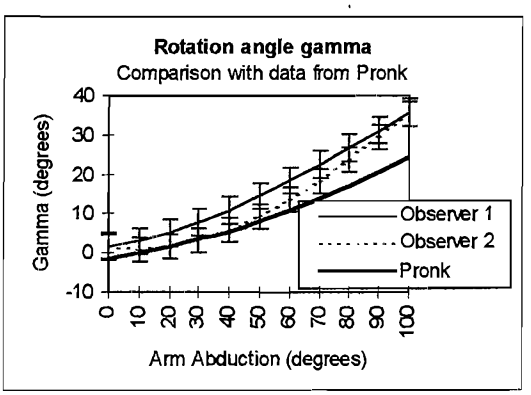

Statistical analysis of inter-observer variation (ANOVA across each incremental position for each of the six variables, over all subjects), shows that in 78% of all measures over the five subjects, there were no significant differences between observers ($p<0\ 05$)

DISCUSSION

A non-invasive method of measuring all six degrees of freedom associated with the kinematics of scapulohumeral rhythm over a range of arm motion has been demonstrated It has been shown that the two observers have each measured the same scapulae motion on each of the five subjects (78% of all measures) Repeatability was affected by errors in the measurement of arm abduction, and the gaining of experience in using the Locator (learning effects)

The in plane rotations (gamma) agree well with other data (Pronk), but the out of plane rotations (alpha and beta) exhibit differences This is probably because Pronk's data was collected relative to a point independent of the subject

It has been shown that it is possible to reliably measure both rotations and translations, and it is planned to continue this work with an investigation into the use of finite helical axes to describe the three dimensional kinematics of the scapula

REFERENCES

Codman, E A (1984). Rupture of the Supraspinatus Tendon and other Lesions in or about the Subacromial Bursa. In Anonymous, *The Shoulder* (pp. 1-31) Malabar, Florida: Robert E. Kreiger Publishing Company

Doody, S G., Freedman, L., & Waterland, J.C. (1970). Shoulder Movements during Abduction in the Scapular Plane. *Archives of Physical Medicine and Rehabilitation,* 595-604.

Inman, V.T , Saunders, M , & Abbott, L C (1944) Observations on the Function of the Shoulder Joint *Journal of Bone & Joint Surgery, XXVI(1),* pp1-30.

Johnson, G.R., Stuart, P.R , & Mitchell, S (1993) A Method for the Measurement of Three-Dimensional Scapular Movement. *Clinical Biomechanics, 8,* pp269-273

Pronk, G.M (1988) Three-Dimensional Determination of the Position of the Shoulder Girdle during Humerus Elevation In Anonymous, *International Series on Biomechanics* (pp. 1070-1076) Amsterdam: Free Univ. Press

SOFTWARE METHODS FOR THE IMPROVEMENT OF MARKER DISPOSITION MODELS ON LOWER LIMBS

Baroni, G , Glitsch, U , Baumann, W
Institute of Biomechanics, German Sport University Cologne, Germany

INTRODUCTION

The quantitative assessment of kinematics and kinetics of body segments and joints requires the reconstruction of position and attitude of relevant bones during the execution of physical exercises For this aim, automatic motion analyzers are used in order to compute with a high frequency the three dimensional co-ordinates of a set of external landmarks, identified by light reflecting or light emitting markers Relative marker movements with respect to the underlying bone, caused by interposed passive and active tissues, are considered the main source of inaccuracies in the three dimensional photogrammetric marker identification Due to the fact that the so called skin movement artifacts are caused by the movement performance, no filtering procedure can be useful in order to quantify and reduce their entity, which can be generally considered one order of amplitude major than the commonly estimated photogrammeteric errors (Angeloni et al 1992)

METHODS

The necessary trade off between the reliability of the analysis and the swiftness and repeatability of the procedures has induced to implement a rigid body algorithm, in order to obtain a proper reference for the evaluation of relative marker displacements during the execution of the movement The set of rigid body co-ordinates has been obtained through an unweighted least-square method, which estimates frame per frame an approximation r of the position vector of the center of the marker distribution and an approximation H of the exact rotation matrix R The least-square function $F(r,H)$ represents the difference between the measured markers position in a frame and the fitted markers position at that time (Veldpaus et al 1988) A previously acquired standing reference frame provides the rigid body algorithm with an initial marker configuration and allows to carry out the anatomical calibration, necessary for the reconstruction of anatomical points of interest, such as joint centers (Baumann et al 1993)

An experimental marker disposition model has been identified on shank (figure)

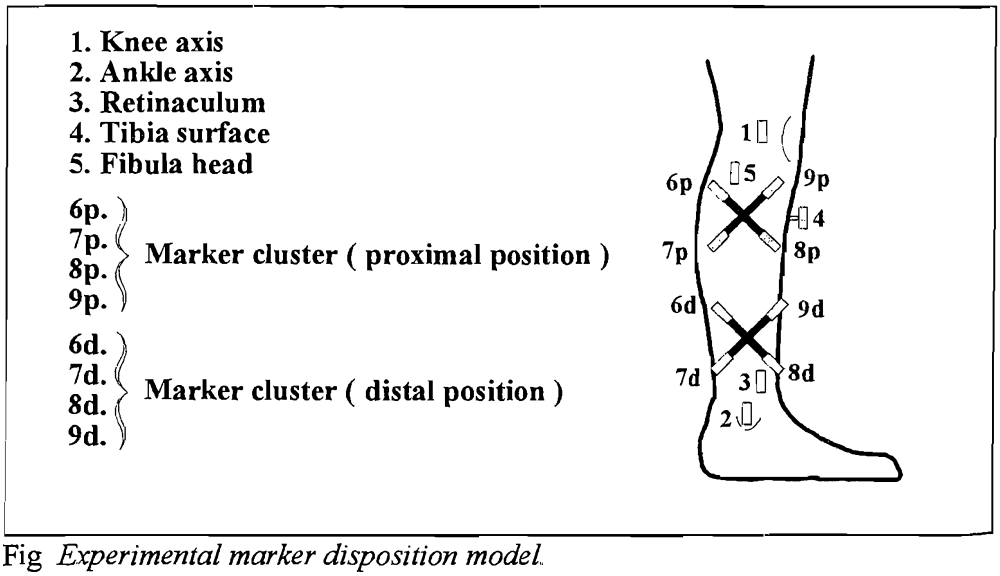

Fig *Experimental marker disposition model.*

It consisted on nine diodes, five apposed on traditional anatomical landmarks and four on a marker cluster The cluster was a cross-shaped form, made of light darkened PVC The experimental acquisitions have been carried out exploiting a SELSPOT movement analysis system, with a frequency of 312 5 Hz Two sets of five movements of gait and run have been acquired, placing the cluster respectively on a medial and a distal position on shank The successive kinematics data analysis has been articled on two fundamental topics

- estimation and quantification of relative marker displacements with respect to the rigid reference configuration
- evaluation of different marker disposition models as technical reference system, in terms of affordable accuracy in the three dimensional reconstruction of joint centers in knee and ankle

RESULTS

Considering, as initial reference configuration for the rigid body algorithm, the five skin-mounted diodes and no more than one plate-mounted diode, systematical marker displacements have been pointed out, particularly concerning the diodes on ankle and knee axis On the contrary, *retinaculum* and *fibula head* have turned out to be more reliable anatomical landmarks No significant differences have been noticed in the behavior of the marker cluster in the two considered positions In both cases, the plate-mounted diodes have not shown significant relative displacements with respect to the extracted rigid configuration

On the basis of these preliminary results, different technical reference systems for knee and ankle joint center reconstruction have been identified and evaluated In order to improve the reconstruction accuracy, two fundamental aspects have been pointed out Beside the obvious identification of the markers which undergo as less as possible to relative displacements, the configuration of the reference system and its geometrical relationships, with respect to the joint centers, should be considered The propagation of inevitable acquisition inaccuracies, through the mathematical reconstruction procedures, has been limited, individuating an orthogonal technical reference system with the origin proximal to the anatomical point to be reconstructed

DISCUSSION

The development of software methods for the evaluation of the accuracy in kinematics acquisitions, has meant to introduce more flexibility with respect to other investigations, restricted to particular cases A previous improvement process of the quality of the marker disposition model could be systematically carried out, considering the specific anatomical peculiarities of the subject and the characteristics of the movement to be analyzed

REFERENCES

Angeloni,C , Cappozzo,A , Catani,F , Leardini,A (1992) Quantification of relative displacement between bones and skin- and plate-mounted markers In Proceedings of the Eight Meeting of the European Society of Biomechanics p 279, Rome, June 21-24

Baumann,W ,Glitsch,U ,Siebertz, K (1993) Intersegmental loads during locomotion In Joint Dynamics, CAMARC (A2002)/AIM/DG XIII-F/CEC, Deliverable 6(Public Report) 100-110

Veldpaus,F E , Woltring,H J , Dortmans,L J M G (1988) A least-squares alghoritm for the equiform transformation from spatial marker co-ordinates J Biomechanics 21,45-54

OPTO-ELECTRONIC TECHNIQUES FOR PATIENTS REPOSITIONING IN RADIOTHERAPY

Baroni, G.[1], Ferrigno, G.[1], Pedotti, A [1], Milani, F [2]
1. Centro di Bioingegneria, Fnd Pro Juventute Don Gnocchi, Politecnico di Milano, Milan, Italy.
2 "C" Radiotherapy Division, Istituto dei Tumori di Milano, Milan, Italy

INTRODUCTION

A crucial aspect in the modern radiotherapy practice is to fill the accuracy gap between treatment planning and treatment realization. Dedicated computerized systems allow to elaborate a precise and personalized treatment strategy, on the contrary, no quantitative objective methods are available, in order to transfer in the reality of the irradiation, the accurate therapy modalities evaluated in treatment planning Patient mispositionings at therapy units are considered one of the major source of an incorrect definition of the geometrical relationships between radiation beam and target volume, necessary premise to the most efficacious disease treatment and to the best preservation of surrounding healthy tissues and organs (Glasgow et al ,1992)

METHOD

A computerized dedicated system for the control and the automatic correction of patient position, has been developed It has been based on the movement analysis system ELITE (Ferrigno et al ,1990) exploiting its high precision and flexibility ELITE calculates with a high frequency the tridimensional co-ordinates of a set of body surface points identified by light reflecting markers, when individuated by at least two CCD cameras The core of the method consists on the analytical comparison between the 3D co-ordinates of a reference marker configuration and the current 3D co-ordinates acquired at each patient repositioning The reference ELITE acquisition is carried out during the preliminary traditional centering procedure, in which all the centering and immobilization means are usually decided and prepared In this phase, depending on the required accuracy of the specific marker spatial re-localization, a geometrical tolerance value is established as the diameter of the sphere with center in the reference position and containing the correspondent current marker In order to limit the inaccuracies introduced by breathing movements, reference and current co-ordinates sets are obtained as a co-ordinates average of three frames cluster, in correspondence of the instants of patient FRC (Functional Residual Capacity) identified in the acquisition. The FRC frames identification has been carried out evaluating a quantity F defined as.

$$F = \sqrt{(y_2\sqrt{(x_1-x_2)^2+(y_1-y_2)^2+(z_1-z_2)^2})^2+(y_3\sqrt{(x_1-x_3)^2+(y_1-y_3)^2+(z_1-z_3)^2})^2}$$

with marker 1 on jugular lacuna and marker 2 and 3 on transversal umbilical line Even if F does not represent any physiological breathing parameter, its reliability as breathing phases indicator has been proved The analytical calculation of marker displacements with respect to the reference localization, has allowed to implement an automatic correction procedure based on an unweighted least-square method The function to be minimized is expressed in vectorial terms as

$$\sum_{i=1}^{i=n^{\circ}marker} (\mathbf{P}_i - \mathbf{M} - \mathbf{P}_{0i})^2$$

where $\mathbf{P}_i$ represents the position vector of the i_{th} current marker, $\mathbf{P}_{0i}$ the corresponding reference position vector and $\mathbf{M}$ the correcting translation The

coincidence between the three numerically controlled treatment couch translations with the axis of the ELITE reference system, is the necessary premise in order to exploit the three couch translations for the correction procedure.

RESULTS

A set of experimental repositionings has been carried out, exploiting as traditional centering system a laser projector For the supine position, a 10 marker disposition model has been evaluated as follows.

1. jugular lacuna **2.** right transversal umbilical line **3.** left transversal umbilical line **4.** clavicle right emiclavear line **5.** clavicle left emiclavear line **6.** Louis angle **7.** xiphoid process **8.** inferior umbilical ring **9.** anterior superior right iliac spine **10.** anterior superior left iliac spine

For every marker a localization tolerance value of 10 mm has been established .The acquisition time has been set to 15 seconds with a frequency of 25 Hz Table I shows the current marker displacements in millimeter, with respect to the correspondent reference marker, before the correction procedure Table II reports the situation after the correction procedure

	3D offset	Frontal plane offset	Sagittal plane offset	Transversal plane offset
Marker 1	**11,428**	8,595	7,600	**11,378**
Marker 2	**12,534**	**12,457**	7,597	**10,068**
Marker 3	5,700	5,061	3,659	5,188
Marker 4	6,068	4,087	4,786	5,834
Marker 5	9,761	7,146	6,722	9,711
Marker 6	7,916	6,698	4.298	7,874
Marker 7	5,329	4 662	3,479	4,896
Marker 8	8,233	8,233	5,173	6,404
Marker 9	**14,417**	**14,407**	**10,281**	**10,120**
Marker 10	5,936	5,924	3,302	4,947

Tab I Marker offsets before correction procedure The underlined bold values report unacceptable displacements with respect to the prefixed tolerance value (10 mm).

	3D offset	Frontal plane offset	Sagittal plane offset	Transversal plane offset
Marker 1	6,494	3,407	6,311	5,736
Marker 2	7,087	6,223	6,436	4,509
Marker 3	5,293	2,579	4,640	5,278
Marker 4	5,508	4,915	4,433	4,107
Marker 5	4,760	1,020	4,759	4,650
Marker 6	3,603	2,839	3,586	2,247
Marker 7	6,956	5,062	6,293	5,616
Marker 8	3,805	3,229	3,768	2,100
Marker 9	9,186	8,832	8,645	4,002
Marker 10	3,401	2,431	2,701	3,151

Tab II Marker offsets after correction procedure

DISCUSSION

The development of a dedicated repositioning system implemented on opt-electronic techniques, allows an automatic quantitative control on patient position, completely independent from the irradiation physical and geometrical set-up In this way, a more reliable control can be carried out, with respect to the traditional quality control methods based on therapy images detection, because the low quality of high energy films rarely permits an effective evaluation of patient mispositioning.

REFERENCES

Ferrigno G, Borghese NA, Pedotti A Patterns recognition in 3-D automatic human motion analysis ISPRS Journal of Photogrammetry Remote Sensing 45.227, 1990.

Glasgow GP, Purdy JA External Beam Dosimetry and Treatment Planning In Perez CA, Brady LW Principle and Practise of Radiation Oncology 2° ed Philadelphia, J B Lippincot, 1992.

THE FEASIBILITY OF A NEURAL NETWORK APPROACH FOR ASSESSING INSOLE MATERIALS A PRELIMINARY STUDY

J G Barton and A Lees
Centre for Sport and Exercise Sciences, School of Human Sciences, Liverpool John Moores University, Liverpool, UK

INTRODUCTION

Several studies have tried to differentiate insole materials based on objective measures combined with statistical evaluation, however some of them have failed (Sanfilippo *et al.*, 1992). As an alternative approach, objective pressure measurement can be combined with Neural Networks (NN), which are a relatively new method of non-linear multivariate analysis NNs can be taught to recognise patterns by examples instead of defining the underlying rules (Zurada, 1992).

The MICRO-EMED system is a particularly useful tool for insole material evaluation because it enables in-shoe pressure measurement However, the pressure transducer matrix built into a thin insole is vulnerable The pressure insole may get damaged, and the output changes substantially

The aim of this preliminary study was to find answers to three questions Firstly, are NNs able to differentiate pressure distributions in the shoe with different insoles, secondly, are NNs robust enough in case of a mechanical failure to the data acquisition equipment, and thirdly, are NNs robust against random noise?

METHOD

Extensively pre-processed pressure data from the MICRO-EMED system were used to train a backpropagation NN (972-20-4 structure) to distinguish four different insole materials of the same thickness Seven male subjects of the same shoe size (42, UK 8) and without a history of locomotor disorder walked at a controlled speed of 1 11 m/s at 1 73/s cadence on a treadmill wearing the same pair of shoes The MICRO-EMED system recorded the maximum pressure print below the dominant foot of ten consecutive steps of each subject while wearing four different insoles and without an insole (5 conditions in total) The mean of the ten steps was taken resulting in five average pressure patterns (one each for the 5 conditions) for all seven subjects. The differences between the no-insole condition and wearing one of the four insoles were calculated to get purely the effect of the insoles on the pressure distribution The values of the difference patterns were scaled into the range 0-1 which is the input range of the NN

With regard to aim 1 The four difference patterns were linked with the code of the corresponding insole material and the NN was trained to map the maximum pressure prints to the corresponding four digit codes Testing of the NN was performed by presenting the same patterns

With regard to aim 2 Subsequent to training the effects of damaging the pressure patterns (simulation of mechanical failure to the pressure measuring insole) were examined The pressure values of the difference pattern under the midfoot were set equal to 0 which would happen if the middle of the pressure insole got damaged. This location of the mechanical error is quite likely, because this part of the pressure insole is exposed to bending forces when pulling out the insole from the shoe The incomplete difference patterns were presented to the NN

With regard to aim 3 The effect of noise were considered A more general way of testing the robustness of the NN was performed by adding random noise in three levels to the difference patterns The noisy difference patterns were presented to the NN

RESULTS

1 The NN learned to map the 28 difference patterns to their corresponding insole-codes in 173 runs During testing the NN classified all 28 patterns to the right class (100% correct recognition)

2 In case of presenting the incomplete difference patterns to the same trained NN, 4 patterns were classified wrongly out of 28 (85% correct recognition)

3 Presenting the noisy difference pattern to the same trained NN yielded the following results dependent on noise level

noise level	test results
0.1	28/28 (100%)
0.3	27/28 (96%)
0.5	22/28 (78%)

DISCUSSION

1 A backpropagation NN could successfully learn to map pre-processed below foot pressure prints of four different insole conditions, into the code of the insoles This proves that a NN can find a set of coefficients in a multivariate, non-linear equation, which describes the complicated relationship among the difference-patterns and the codes of the insoles

2 Even in case of a mechanical failure to the pressure insole the remaining pressure patterns can be used in the evaluation of insole materials Because of their unique structure and function NNs are tolerant to incomplete patterns The responses of the NN remained reasonable even if a part of the pattern was harmed.

Apart from proving the robustness of a NN, this experiment suggested that the pressure distribution below the midfoot had a small contribution in the decision making process

3 The insensitivity to random noise confirmed that NNs are robust against noise, therefore NNs can cope with the small errors associated with pressure measurements below the foot

In this study the same or modified patterns were used in testing the NNs, which proved to be successful Utilising the generalisation capabilities of NNs (Zurada, 1992), previously unknown pressure patterns (obtained by wearing unknown insoles) could be classified, which would reinforce the feasibility of NNs for the assessment of insole materials

REFERENCES

Sanfilippo, P B et al (1992) Dynamic plantar pressure analysis, comparing common insole materials Journal of the American Podiatric Medical Association 82, 10, 507-513

Zurada, J M (1992) Introduction to artificial neural systems St Paul: West Publishing Company

A PHYSICAL MODEL OF CAT TWIST

W.L. Bauer, and M.R. Yeadon*
Sensomotorik-Laboratory, University of Bremen, Bremen, Germany
*Department of Sports Science, Loughborough University, United Kingdom

INTRODUCTION

The design of a physical model of a twisting cat is presented The model comprises a pair of cylinders which together make a hula hoop motion by means of two control strings. In order that the total angular momentum remains zero, the whole system rotates in the opposite direction Typically one cycle of hula movement produces a half twist (Yeadon, 1993)

METHODS

The design of the physical model was done according to the methods described by Bauer (1987)

RESULTS

Description of the design

The cat twist model consists of a rectangular frame mounted on a table or a base plate (Fig 1). Two cylinders (5, 18) of identical construction, whose axes form an angle of 120 degrees, are suspended within the frame with two forks (4, 19) Each fork is fixed to the frame with ball-bearings (34), which permit an almost frictionless rotation about the vertical main axis of the model. Each cylinder is mounted within a slide bearing (6, 17) which allows the cylinders to be rotated about their main axis The outer ring of each slide bearing is pivoted (22, 31) in one fork of the suspension system The two cylinders touch each other at their bases (11,12) in the centre of the drawing

The two cylinders are connected with a ball-and-socket joint (28). Four strings (10, 25, 26, 27) representing four muscles have been mounted in such a way that they can be shortened and lengthened successively by applying forces to control strings (1, 21) coming out on top and bottom of the frame, causing the two cylinders to make a hula movement

Two of the four strings (25, 26) are connected to prestretched springs fixed within the cylinders Each of the remaining two strings (10, 27) can be shortened and lengthened with control string (1 or 21) via a special sliding mechanism Each control string is led through the pipe of each fork (2) from above or below Upon coming out of the pipe each control string is divided into two strings (23, 24 and 32, 33) which are fixed symmetrically to the outer rings of the sliding mechanisms after passing around the shafts (22, 31) of the slide bearings (6, 17) The forces of the control strings are transferred from the outer rings (7, 16) across a ball-bearing (15) to the inner rings (8, 14) of the sliding mechanism. From there on a string (10, 13) transfers the respective control force to the opposite cylinder base after passing through a hole in its own base

The innner rings (8,14) of the sliding mechanisms turn with the rotating cylinders due to a bolt (9) which slides up and down in a slot (30) of each cylinder during a hula movement. The outer rings (7, 16), however, turn only when the forks of the suspension mechanism rotate

Control mechanism

In the constellation which is shown in the drawing (Figure 1) control force (1) has its maximal value Thus string (10) pulls the cylinder bases against each other The force of the opposite string (26) which is attached to spring (3) is approximately of the same magnitude as string (10). The forces of the remaining strings (25) and (27) are equal although each of them has only one half of the magnitude of string force (26) Once

control string force (1) and control string force (21) are lowered simultaneously - (string forces 10 and 27 also become lower) - the point of contact moves towards string (25) Once both control string forces are zero the point of contact of the cylinder bases lies between strings (25) and (26) which are extended by springs (3) and (20) Increasing control string force (21) again - (which causes string force (27) to increases as well) - moves the point of contact in the same direction ahead towards string (26) and (27), creating a hula movement of the two cylinders The opposite direction of motion will be obtained, when control string force (21) is increased instead of lowered whilst control string force (1) is lowered as of the drawn starting position

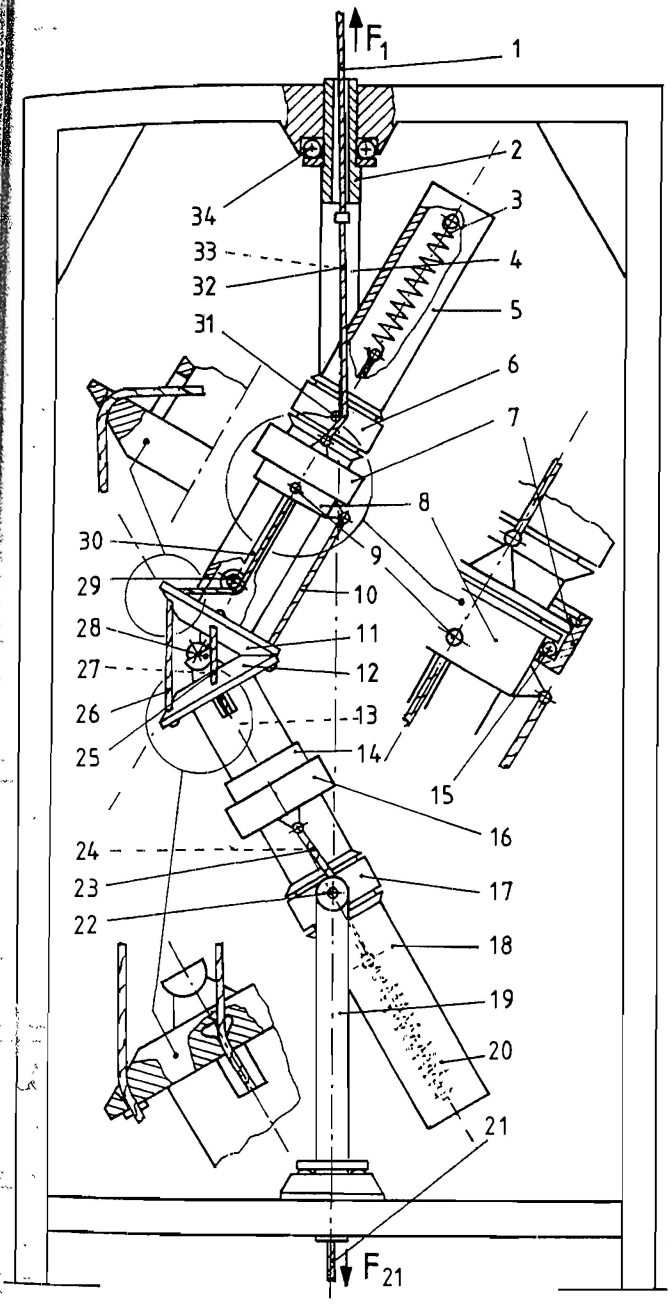

Figure 1 Cat twist model

Doing the hula movement in the above described manner causes the two cylinders to rotate about the vertical axis of the model according to the law of conservation of angular momentum Thereby the friction of the ball-bearing (34) and its counterpart have to be made very small in order to get optimal observable results

When the sliding mechanism is positioned halfway of its sliding path, the centre of gravity of each cylinder coincides with the positions of the shafts (22) and (31) Moving the sliding mechanics to and fro, shifts the centres of gravity accordingly Since the cylinders have been arranged vertically this shift has no negative effect on the overall performance of the model Due to the selected design, the two cylinders cannot be moved away from the vertical and out of the piked position

In order to apply no torque to the cylinders from outside the model during operation, the control forces must be inserted across swivels to the control strings

REFERENCES

Bauer, W L (1987) Physical models in sports biomechanics In Current Research in Sports Biomechanics, 107-141, Karger, Basel

Yeadon, M R (1993) The biomechanics of twisting somersaults Part III. Aerial twist Journal of Sports Sciences 11, 209-218

COMPARISON OF 3D JOINT MARKER SETS FOR THE STUDY OF HUMAN MOTION

M.D. Bauman[1], A. Plamondon[1], D. Gagnon[2]

[1]École de l'activité physique, Université Laurentienne, Sudbury, Canada
[2]Laboratoire de biomécanique occupationnelle, Université de Sherbrooke, Canada

INTRODUCTION

Cinematography has limitations to its accuracy due in large part to the lack of consistent locating of joint centres-of-rotation. There exists a need for an adequate method of locating these joint centres with external markers. Rab (1991) suggested that a flexible approach to marker placement is necessary to account for age, neuromuscular disease, the use of walking aids, and the particular aims of the study. Some common marker sets use stickers or spherical balls to mark superficial landmarks, but these markers are susceptible to being hidden from the view of the camera during filming of a movement. Another marker set uses wide fluorescent elastic bands to mark the ankles, knees, elbows, and wrists, which are less likely to be blocked from the view of the camera. It is, therefore, important to quantify the differences encountered between existing marker sets. The purpose of this study was to compare the kinematic data of three different marker sets, two using balls to mark joints and one using elastic bands. It was also the purpose of this study to present the elastic band marker set as an alternative to some commonly used marker sets.

METHODS

Three healthy male subjects participated in the study. The subjects were each filmed statically in anatomical position and performing a simulated lift at normal and fast speeds. A PEAK motion measurement system with four video cameras (Panasonic WV-CL700) was used to collect the 2D positions of the anatomical markers. The 3D loci of the anatomical landmarks were obtained with a DLT (Direct Linear Transformation) algorithm. Eight body joints were marked (the right and left ankles, knees, elbows, and wrists) with three marker sets. The first set consisted of of wide fluorescent elastic bands which encircle the joint (band method). A second set consisted of two fluorescent spheres placed on the either side of the joint (ball method) and a third set which defined the position of a local coordinate system using three spheres placed on the segment near the joint (coordinate system). Joint centres-of-rotation were estimated for the band method by assuming that the centre of the visible arc of the band approximated the position of the joint centre in each of the 2D views. For the ball method the centres-of-rotation were estimated by calculating the midpoint on a line between the two balls that mark the joint. For the coordinate system the joint centres-of-rotation were located in the static condition and then assumed to remain the same throughout the dynamic movements. The three marker sets were compared by calculating the difference between their joint centre positions. Comparisons were done between the band method and ball method, between the band method and the coordinate system, and between the ball method and the coordinate system. Average differences (AD) were calculated and the results were combined for the three subjects and left and right joints.

RESULTS

Table 1 summarizes the results for the raw data of the simulated lift.

Table 1 Raw Data (non filtered) : Normal Speed

		AD (mm)	SD (mm)	Max (mm)
Wrist	Band & Ball	17	9	75
	Band & Coordinate	8	5	30
	Ball & Coordinate	18	10	86
Elbow	Band & Ball	23	11	62
	Band & Coordinate	12	8	37
	Ball & Coordinate	31	11	65
Knee	Band & Ball	26	7	45
	Band & Coordinate	14	8	41
	Ball & Coordinate	25	8	52
Ankle	Band & Ball	17	6	32
	Band & Coordinate	11	6	34
	Ball & Coordinate	19	7	45

DISCUSSION

The results support the assumption that the band method can be used as an alternative method to other commonly used marker sets. The range of reported average difference (AD) values are acceptable when it is considered that Cappozzo et al. (1993) reported errors in the order of 10-20 mm due to skin movement artefacts alone. In general, when comparing the three methods, the band method and the coordinate system had the smallest AD values or were the most similar (7-15mm). The ball method and the coordinate system were the least similar and had the largest AD values (18-32mm), except for the knee where the band and ball methods were the least similar. However, the ball and band methods generally showed intermediate AD values (16-26mm). In conclusion, the band method is a valuable alternative marker set because of its low incidence of missing points, especially when complex movements are being studied.

REFERENCES

Cappozzo, A., Catani, F. and Leardini, A. (1993) Skin movement artefacts in human movement photogrammetry. In *Abstracts. International Society of Biomechanics XIVth Congress, Vol.I* (pp. 238-239). Paris: Societe de Biomecanique.

Rab, G.T. (1991) Flexible marker set for human gait analysis. *Journal of Electromyography and Kinesiology,* **1**(2), 139-145.

A CYCLE-ERGOMETER MOUNTED ON A STANDARD FORCE PLATE FOR MEASUREMENT OF PEDAL FORCES

ALAIN BELLI and JEAN-RENE LACOUR
Laboratoire de Physiologie - GIP Exercice, Université Lyon 1, France.

INTRODUCTION

Cycle ergometers are usually found in laboratories for training and testing purposes. External resisting force could be measured accuratly allowing research on metabolic, fatigue and efficiency problems. However, they are limited in precise three-dimensional biomechanical analysis of forces exerted on the pedals. These forces are used in research when ones want to study the cycling effectiveness as well as joints, muscles and bones forces of the lower limb. In order to measure precisely these forces a number of researchers have developed specific pedal force plates (e.g. Newmiller et al 1988, Ericson and Nisell 1988, Brocker and Gregor 1990). However their specificity and their dimensions make them expensive and/or difficult to handle and limited in applying their principle in standard situation.

The objective of this presentation is to report a new method to measure the pedal forces during cycling by means of general purpose force plateform and cycle ergometer. The principle of this new method and the preliminary results obtained are presented.

METHODS

Mechanical device and measurements. In order to obtain an isolated mechanical system, the pedal and the gear mechanism were separated from the bicycle frame and tightly fixed on a force platform (Kistler type 9281B). The bicycle frame, including flywheel and friction system was fixed aside from the force platform (see figure 1) in such way that the original dimensions of the whole bicycle were maintained. The following parameters could then be measured and calculated:

- Forces and torques exerted on the force platform. They were calculated, according to the manufacturer, from the data obtained from height elementary force channels.
- Force exerted by the chain. It could be calculated from the measurement of the friction force exerted by the friction belt on the flywheel and from the calculation of the inertial force due to the flywheel accelerations (Lakomy 1986). The friction force was measured by means of a strain gauge (200 N, Interface MFG, USA) mounted on the friction belt while the displacement of the flywheel was monitired by an incremental encoder (600 points/turn, Hengsler, Germany).
- Coordinates of the application points of chain force and of pedal forces (assumed to be located at the middle of the upper surface of each pedals (Newmiller et al. 1988)). They were determined by precise measurement of the dimensions of the pedals and gear system. It was also necessary to calculate the instantaneous position of the pedals from the displacement signal given by the incremental encoder and by a magnetic transducer detecting the rear horizontal position of the left pedal.

Signal from strain gauge, displacement encoder, position transducer and 8 channels force platform were sampled (200 Hz) and stored on a PC computer (386 type) via a 12 bit A/D converter. The instantaneous force and displacement data were low pass filtered (Butterworth 4th order with no phase lag) with a cut-off frequency of 25 Hz.

Computations of pedal forces. Assuming that dynamic effects due to pedal rotation are neglectible, static mechanics ($\sum \vec{F} = 0$, $\sum \vec{M} = 0$) applied to the isolated pedal and gear system give a system of six equations. At a given instant of time, this system of equations can be written in matrix form and posed as the standard linear algebra problem: [A].[x] = [b], where the [A] matrix contains the moment arms for the pedal forces, the [x] vector is constituted of unknown pedal forces and the [b] vector is constituted of the measured forces and moments exerted by the chain and by the force platform (moments acting on the pedals are assumed to be neglectible). The numerical solution can then be found using standard algebra techniques such as lower triangular-upper triangular decomposition of the A matrix followed by back substitution of the b vector.

The dynamic effects were mesured and modelised during free deceleration of the pedal and gear system. They were then taken into account in the [b] vector.

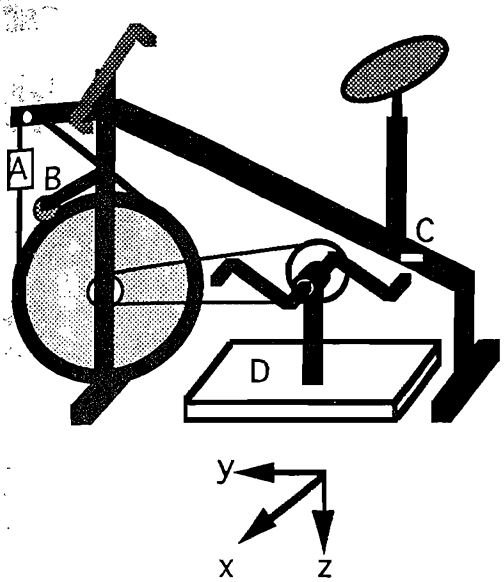

Figure 1: Schematic view of the device (A: strain gauge, B: encoder, C: position transducer, D: Force plate).

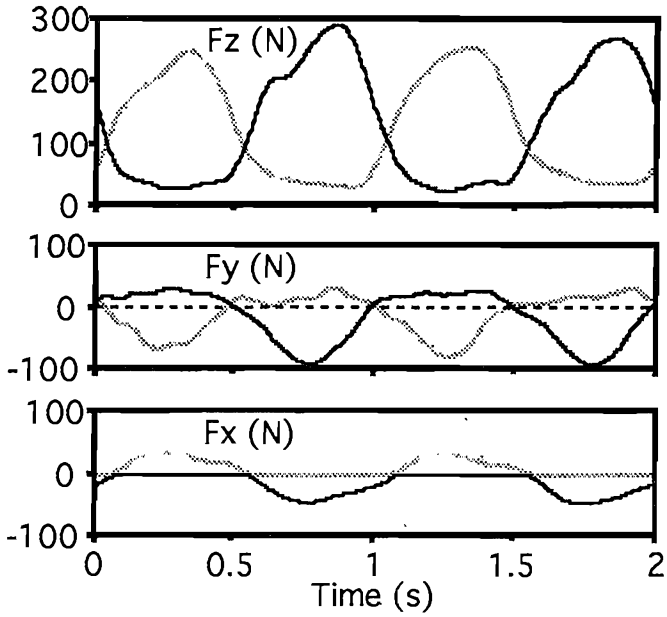

Figure 2: Typical results (Left foot: solid line; Right foot: grey line).

RESULTS

Typical measurements obtained during two complete rotations (starting from top position of the right foot) at a velocity of 60 rotation per minute (rpm), with a friction load of 2 kg and without toe clips are presented in figure 2. During downstroke peak values of Fz, Fy and Fx were respectively about 300 N, -100 N and ±40 N, they were oriented respectively downward, backward and laterally. During upward movement of the legs Fz and Fy were respectively about 40 N and 20 N and it was assumed that Fx forces were negligible. An asymmetry between left and right foot could also be noticed. The forces due to dynamic effects, measured during free pedal deceleration, were found to be negligible (less than 2%) when compared to the forces exerted by the feet at 60 rpm and with a friction load of 2 kg.

DISCUSSION

The magnitudes and directions of the measured forces were in agreement with measurements obtained in current literature (e.g. Newmiller et al 1988, Ericson and Nisell 1988, Brocker and Gregor 1990). However, the influence of moments acting on the pedals (Brocker and Gregor 1990) is not yet taken into consideration and further experiments and analysis are in progress in order to determine precisely the accuracy of the measurements. Nevertheless, the preliminary results obtained showed that it is possible to perform a complete biomechanical 3D analysis of pedalling with force platforms and ergometers usually found in laboratories. Furthermore this design does not modify the mechanical properties (weight, dimensions, inertia) of the pedals and dimensions of the bicycle, allowing same mechanical conditions during training and testing.

REFERENCES

Broker, J.P. and Gregor, R.J. (1990) A dual piezoelectric element force pedal for kinetic analysis of cycling. *Int. J. Sports Biomech.* **6,** 394-403.

Ericson, M.O. and Nisell R. (1988) Efficiency of pedal forces during ergometer cycling. *Int. J. Sports Med.* **9,** 118-122.

Lakomy, H.K.A. (1986) Measurement of work and power output using friction-loaded cycle ergometers. *Ergonomics* **29,** 509-517.

Newmiller, J., Hull, M. and Zajac, F.E. (1988) A mechanically decoupled two-force component pedal dynamometer. *J Biomechanics* **21,** 375-386.

A TREADMILL FOR MEASUREMENT OF GROUND REACTION FORCES DURING WALKING

ALAIN BELLI, PHONG BUI, ANTOINE BERGER and JEAN-RENE LACOUR
Laboratoire de Physiologie - GIP Exercice, Université Lyon 1, France.

INTRODUCTION

Ground reaction force measurements during locomotion are necessary to study mechanical properties of the lower limbs during contact phase. In field conditions ground mounted force platforms are generally used for that specific purpose, but they are limited in the number of successive ground contacts they can measure. In laboratory conditions, treadmills are usually found for training and testing purposes. Although they allow easy metabolic measurements, they are limited in precise three-dimensional biomechanical analysis of ground reaction forces. Kram and Powell (1989) proposed to incorporate a force platform under the moving belt of the treadmill. However, this technical solution allowed accurate measurements of the vertical force only.

The objective of this presentation is to report a new method to measure both the vertical and the horizontal ground reaction forces during treadmill walking by means of specially designed treadmill frame mounted on crystal transducers. The principle of this new method and the preliminary results obtained are presented.

METHODS

For measurement of forces produced only by the subject's feet it was chosen to mechanically isolate the entire treadmill. In that case forces due to treadmill movements or to belt friction could be considered as internal forces. With this aim in view, all the treadmill components including the motor (Leroy Somer, 1.5 kW, asynchronous type) were tightly mounted on a single metal frame. This frame was calculated to be as rigid as possible and was tightly fixed to the ground through two crystal transducers (Kistler type KI 9067). The associated amplifiers (Kistler type KI 5038A3) allowed the measurement of the 3 dimensional (3D) forces. Only cables providing power supply to the motors were linked to the isolated frame. Electrical circuits were designed in order to minimise electromagnetic noise. Furthermore, the treadmill was constituted of two symmetrical parts (figure 1) separated by a 7 mm gap, allowing measurement of left and right leg during the double support phase of walking.

Static calibration of vertical and horizontal forces were first performed with a set of known mass ranging from 0 to 80 kg. Dynamic response and natural frequency were then measured after sudden impacts produced by a hammer. Finally, typical force measurements were performed on a subject walking at velocities ranging from 2.0 to 10 km.h^{-1}.

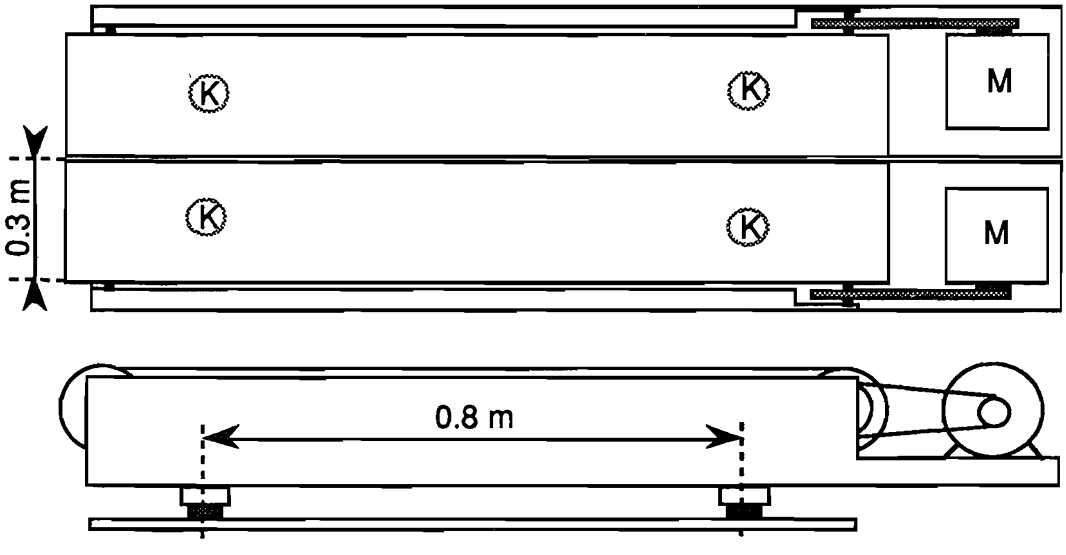

Figure 1: Schematic top view (upper part) and side view (bottom part) of the treadmill (K: location of force transducers; M: motors).

Signals from crystal force transducers were sampled (1000 Hz) and stored on a PC computer (386 type) via a 12 bit A/D converter. Force data obtained during walking were also low pass filtered (Butterworth 4th order with no phase lag) with a cut-off frequency of 20 Hz.

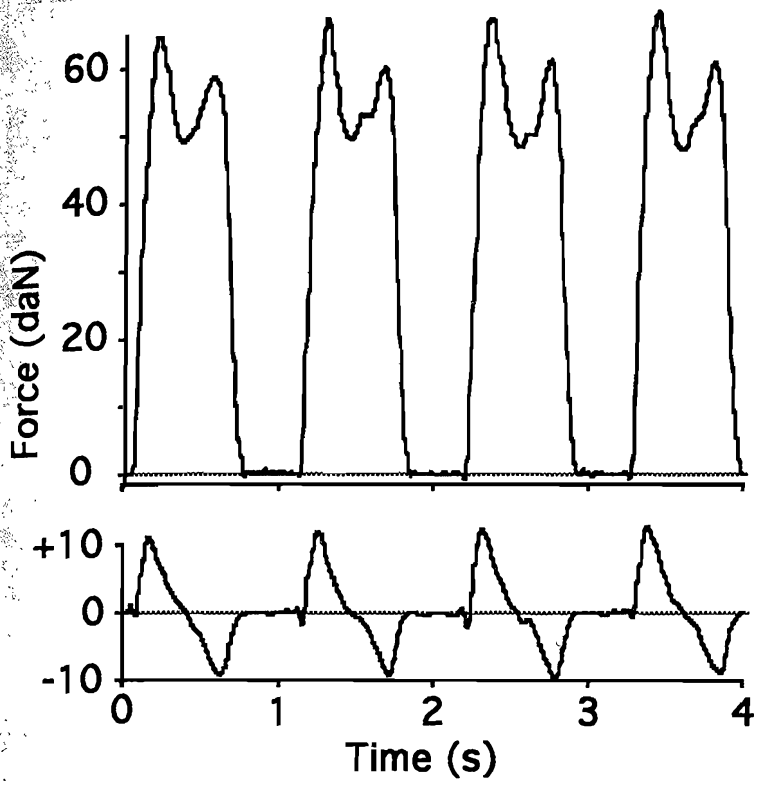

Figure 2: Typical measurements of vertical (upper part) and horizontal (bottom part) force.

RESULTS

The calibration showed that linearity of vertical and horizontal force was better than 0.1% and 0.5%, respectively and that natural frequencies were over 45Hz and 33Hz respectively.

Typical data (left foot) obtained on a 65 kg healthy subject walking at a velocity of 5.5 $km.h^{-1}$ (1.52 $m.s^{-1}$) are presented in figure 2. The stride frequency and the stride length were respectively 0.9Hz and 1.38m. During the support phase the vertical force presented two peaks (Z1, Z2), separated with an interjacent trough. The anteroposterior force had a small initial impact peak, followed first by a breaking peak (X1) and second by a propulsive peak (X2). The values of Z1, Z2, X1, and X2 peak were approximately equal to respectively 1.05 body weight (bw), 0.95 bw, 0.2 bw and 0.15 bw. The mediolateral forces (not shown) presented two opposite peaks of about ±0.05 bw.

DISCUSSION

Static measurement showed the very good linearity which was expected from crystal transducers. Natural frequencies were acceptable in walking conditions and could be easily filtered without significant modifications of original force signal. (Winter et al. 1974). Therefore, the magnitudes and directions of the forces measured during walking were in agreement with previous measurements obtained in current literature (e.g. Nilsson and Thorstensson 1989) when using ground mounted force platforms.

However, natural frequency could be improved and further analysis and trials are in progress in order to obtain stiffer and lighter treadmill frames. Nevertheless, the preliminary results already showed that it is now possible to get, in normal laboratory conditions, 3D "ground" (treadmill) reaction forces with a high number of steps.

REFERENCES

Kram R. and Powell A.J. (1989) A treadmill mounted force platform. *J. Appl. Physiol.* **67**, 1692-1698.

Nilsson J. and Thorstensson A. (1989) Ground reaction forces at different speeds of human walking and running. *Acta Physiol Scand* **136**, 217-227.

Winter D.A., Sidwall H.G. and Hobson D.A. (1974) Measurement and reduction of noise in kinematics of locomotion. J Biomechanics 7, 157-169.

CONTRIBUTION OF LIFT FORCE TO PROPULSION IN FRONT CRAWL SWIMMING

Monique A.M. Berger, A. Peter Hollander and Gert de Groot
Faculty of Human Movement Sciences, Vrije Universiteit, Amsterdam, the Netherlands.

INTRODUCTION

Propulsive force in human swimming consists of two components: the drag force, opposite to the line of motion of the hand, and a component perpendicular to the line of motion: the lift force. From a theoretical point of view it has been shown that propulsive forces in human swimming can be more efficiently derived from lift forces than from drag forces (de Groot and van Ingen Schenau, 1988). Propulsive forces can be calculated from a three dimensional kinematic analysis procedure, combined with hydrodynamical characteristics of hand and forearm derived from fluid laboratory studies (Berger et al., 1995). In the present study the contribution of the lift force to the propulsive force is calculated.

METHODS

Six subjects, three male and three female swimmers of national and international level participated in the experiments. The swimmers were asked to swim front crawl at steady velocity during 25 meter.

Three-dimensional (3D) underwater videography was used to record the path followed by the hand and arm during a full stroke of one arm. The underwater pulling patterns of the right arm were filmed from the front, the right (2x) and the bottom side using four gen-locked Panasonic video cameras. Two periscope systems (Hay and Gerot, 1991) and an underwater housing were positioned to collect these views of the arm strokes. Calibration took place with a reference frame of 2.0 * 1.0 * 1.0 meter. Registration of motions and orientation of the hand were analysed with help of black markers drawn with kohl pencil on anatomical landmarks on the hand and forearm of the swimmer. Image co-ordinates were obtained manually at a sampling frequency of 50 Hz, and transformed to three-dimensional co-ordinates using the direct linear transformation (DLT) method.

The magnitude of drag and lift forces were calculated according to the following equations:

$$F_d = 0.5\rho\, v^2\, A_w C_d \qquad (1)$$

$$F_l = 0.5\rho\, v^2\, A_w C_l \qquad (2)$$

where F_d = drag force (N), F_l = lift force (N), ρ = density of water, v = velocity of the hand ($m.s^{-1}$), A_w = wet surface area (m^2), C_d = drag coefficient and C_l lift coefficient, obtained in a previous study (Berger et al., 1995).

The propulsive force (F_p), defined as the component of the resultant force in swimming direction, was calculated at each video frame according to:

$$F_p = F_{dx} + F_{lx} \qquad (3)$$

In order to define the relative contribution of the lift force to the propulsive force, a lift to propulsive force ratio ($F_{l\text{-}p}$) was computed:

$$\overline{F_{l\text{-}p}} = \frac{\overline{F_{lx}}}{\overline{F_p}} \qquad (4)$$

where $\overline{F_{lx}}$ is the mean lift force in swimming direction and $\overline{F_p}$ is the mean propulsive force. The mean F_p and mean F_{lx} values were calculated over the frames of one full stroke, where F_p was positive.

RESULTS AND DISCUSSION

Figure 1 shows the calculated forces, in forward direction, at each video frame for two subjects during one stroke. This figures demonstrates that at different phases in the stroke the contribution of lift and drag to the propulsive force are different. During the first

phase of the stroke a positive value of F_p can be observed although the drag force is negative. The contribution of the lift force in this phase of the stroke causes a positive propulsive force. At the last phase of the stroke the propulsive force is the highest due to the high velocities of the hand. It can also be observed that the shape of the force curves is different for the two subjects. For subject F3 in figure 1 (left part) the lift force is much higher than the drag force. For subject M2 in figure 1 (right part) the differences between lift and drag force is less.

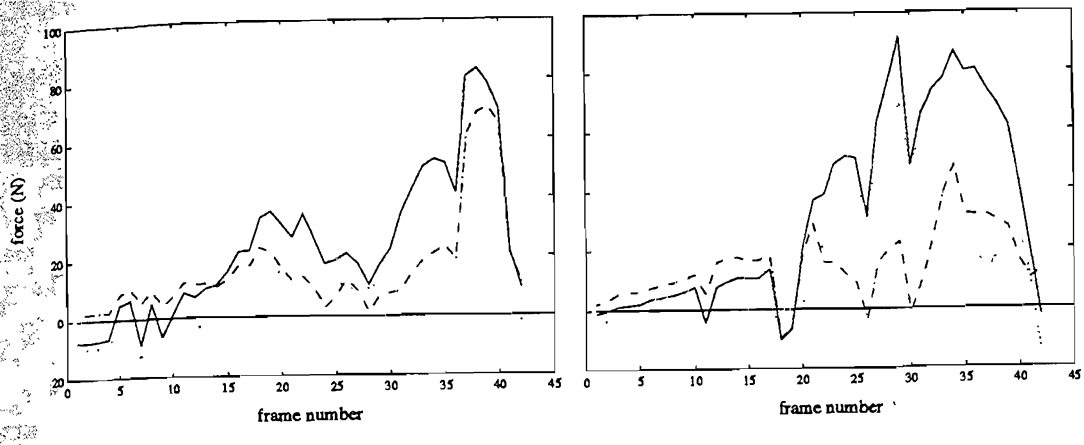

Figure 1. Propulsive forces of two subjects: left : subject F3, right: subject M2
(- = propulsive force, ·· = drag force, -· = lift force)

The differences in contribution of lift and drag to the propulsive force are also obvious when calculating the $F_{l\text{-}p}$ ratio. The $F_{l\text{-}p}$ ratio for the stroke plotted in the left part of figure 1 was 0.64, so 64 % of the propulsive force is due to the lift component. The calculated $F_{l\text{-}p}$ ratio for the stroke plotted in the right part was 0.45.
The $F_{l\text{-}p}$ ratio calculated for all subjects is given in table 1.

subject		mean $F_{p\text{-}l}$	std
F1	(n=7)	0.53	0.03
F2	(n=8)	0.54	0.05
F3	(n=8)	0.65	0.06
M1	(n=6)	0.61	0.06
M2	(n=8)	0.48	0.05
M3	(n=8)	0.50	0.05

Table 1. $F_{l\text{-}p}$ ratio for all subjects, three females (F1-F3) and three males (M1-M3).

The contribution of the lift force to the propulsive force is about 50% and for some subjects even higher. As stated earlier propulsive force is much more efficiently derived from lift forces than from drag forces. Therefor, swimmers with a technique which leads to a high $F_{l\text{-}p}$ ratio will have a higher propelling efficiency. For the future, it is interesting to see if there is a correlation between the contribution of the lift force to propulsion and swimming performance.

References

Berger, M.A.M, Groot, de G., Hollander, A.P., (1995) Hydrodynamic lift and drag forces on human hand/arm models. *J. Biomechanics*, 28, 125-133.

Groot, G. de and van Ingen Schenau, G.J. (1988) Fundamental mechanics applied to swimming: technique and propelling efficiency. In: *Swimming Science V* (Edited by Ungerechts, B.E., Wilke, K. and Reischle, K.), pp. 39-43. University Park Press, Baltimore, MD.

Hay, J.G. & Gerot, J.T. (1991) Periscope systems for recording the underwater motions of a swimmer. *Int. J. Sports Biomech.*, 7, 392-399.

ON A BODY STABILITY CONTROL

Alexander Bilenko, Galina Ivanova
Academy of Physical Culture, St.Petersburg, RUSSIA

INTRODUCTION. Human ability to the retention of orthograde posture belongs to one of the adaptive features of the human activities responsive to the changes of mechanical stability conditions, human functional conditions, training susceptibility, fatigue, pharmacology effect, etc. [1-2]. Among all methods of balance improvement the training at a movable support is considered as the most efficient one. In this case the degree of support mobility still remains unresolved issue since parameters of the support tilt with respect to the base influence considerably on the training effect of the exercise on the human body.

METHOD. New training unit for balance improvement was developed and tested. The construction of the movable support was extremely simple (see Fig.1). The upper plate is swinging on a hinged support at a certain angle with respect to the lower base while contacts at the edge of the platform are closed at the moment of balance disruption as evidenced by light indicators Constructional feature of the device consists in the availability to match platform parameters with the degree of physical development and proprioceptive sensitivity of a trainee aimed at the improved adaptation of a human being to the "body-platform" system. The device provides for the rigidity tuning of springs connecting the movable platform with the immovable one as well as for changes of the distance between them. The latter limits the critical deflection angle and thus sets the magnitude of oscillation amplitude. The degree of a human body stability was measured from the conventional factor of the balance confinement time at the movable support. It was determined that "stability time" of a human body depends on a certain number of parameters among which the governing ones are the stabilizing moment (M_{st}) and conditions of sensor correction of a body posture The stabilizing moment is defined by the spring rigidity (C) and the gap (Δl) depending on the diameter of the hinged support: $M_{st} = 2C\,\Delta l$.

RESULTS. Stability tests were carried out with the platform of the following parameters (see Table 1.). In order to determine the role of visual feedback in the balance confinement the experiments were performed both with and without visual control (see Fig.2).

N	Diameter of hinged support, mm	Deflection angle, deg.	Δl, mm	M_{st}, Nm		
				C=1N/mm	C=2N/mm	C=4N/mm
1	9,5	0,27	1,0	0,43	0,86	1,72
2	11,0	0,67	2,5	1,08	2,17	4,32
3	12,6	1,10	4,1	1,76	3,52	7,04
4	15,0	1,73	6,5	2,80	5,60	11,20

Table 1. Mechanical parameters of the training unit.

DISCUSSION. The experimental results (Fig.2) can be approximated within certain accuracy by analytical expression of the stability time versus the stabilizing moment: $t \approx 10[M_{st}^{1/2}] - 6$. At the range of small moments (up to 3Nm) the approximation curve displays noticeably greater slope. One can suppose that the given relation provides real "stimulus-reaction" function. The sensitivity of joint receptors of

the posture is higher at the beginning of elongation at small deflections in the joint. The function is non-linear; the sensitivity drops with the increase of M_{st} emphasizing the importance of the vertical posture analysis. In case of very small muscle stretchings (up to 0,1% of l), which occur at the platform oscillations within 0,3°, the analysis of muscle contraction presents a problem and the posture control is presumably governed by the elastic force of crossings between mesofibre filaments creating "short-range stiffness" [3-5] in the joint.

The training unit found many applications among professional sportsmen (gymnasts, spring-board divers, synchronized swimmers) for the improvement of peripheral mechanisms of muscle activity and joint reception. The training device was successfully used in ergonomics for the evaluation of functional conditions of patients.

LITERATURE.

[1]. V.S.Gurfinkel, Ja.M.Kotz, M.P Shik. Control of the human posture. (Moscow, 1965).

[2]. A.G.Bilenko, G.P.Ivanova "On a problem of Biomechanical Stability of a Human Body" in the Proceedings of the VIII-th International Symposium of the Society of Biomechanics in Sports, p.373.

[3]. V.S.Gurfinkel, Yu.S.Levin. Skeleton muscle: its structure and function. (Moscow, 1985).

[4]. P.M.Rack, D.R.Westbury. The short-range stiffness of active mammalian muscle and its effect on mechanical properties. J.Physiol. (Gr.Brit.), v 240, p.331-350 (1974).

[5]. A.K.Tsaturyan. Biomechanics of muscles and structure of motions (Nizhni Novgorod, 1992).

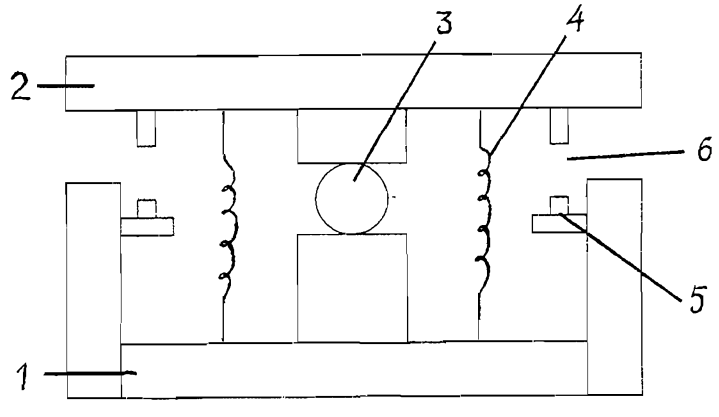

Fig 1 Mechanical scheme of movable stabilograph. 1- lower plate, 2 - upper plate, 3- hinged support, 4- adjustment spring, 5 - limit switch, 6 - gap.

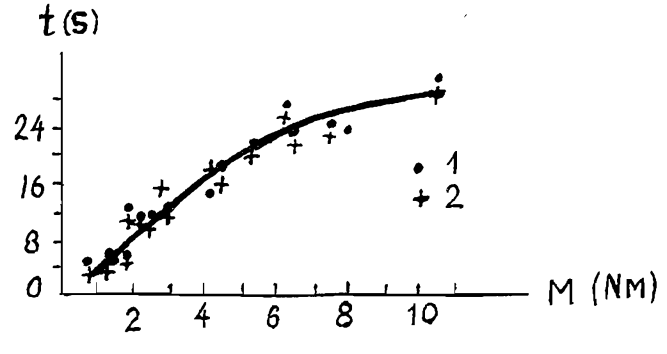

Fig.2. Stability time t versus M_{st}: 1 - with visual control, 2 - without visual control.

ELBOW JOINT STIFFNESS DYNAMICS DURING LEARNING OF POSTURE MAINTENANCE IN THE PROCESS OF ARM UNLOADING

E.V.Biryukova[1], V.Y.Roschin[1], A.A.Frolov[1], M.E.Ioffe[1], J.Massion[2], M.Dufosse[2]

[1] Institute of Higher Nervous Activity and Neurophysiology of Russian Academy of Sciences, Moscow, Russia
[2] Laboratory of Movement Neurobiology, CNRS, Marseille, France

INTRODUCTION

The acquisition of bimanual coordination when one forearm is triggering the unloading of the postural forearm has been investigated by several authors (Paulignan et al., 1989; Ioffe et al., 1994). The kinematic parameters of the movement such as amplitude and maximal velocity were analyzed to assess the role of central and spinal control in postural adjustment. In the present study we use the equilibrium point hypothesis of muscle torque generation (Feldman, 1979) in order to evaluate changes in central control parameters in the process of learning of posture maintenance using recordings of movement dynamics.

METHODS

In the frames of the equilibrium point hypothesis the muscle torque is described by linear spring equation with modifiable stiffness, viscosity and equilibrium angle:

$$T = -k(S - Seq) - v\dot{S}, \qquad (1)$$

where S is the joint angle, $\dot{S}$ is the angular velocity, Seq is the equilibrium angle, k is the stiffness and v is the viscosity. The stiffness can be considered as the central command for a coactivation of antagonist muscles, and the equilibrium angle as the reciprocal command for a shift of invariant characteristics of the joint (Feldman, 1980).

During experiment when a load initially applied to the forearm was released subjects were instructed to maintain the forearm horizontally. 3 sessions of 20 trials each were carried out for eight subjects. The elbow joint angle, angular acceleration and external load of postural forearm were recorded. The muscle torque T has been calculated using the recorded data and forearm inertial and geometrical parameters. The multiple linear regression analysis was applied to the equation (1) in order to determine the stiffness, viscosity and equilibrium angle. The array of muscle torque values at every instant of each particular movement was considered to be dependent variable, while the joint angle and angular velocity arrays were considered to be independent ones.

RESULTS

Torque time course was simulated according to linear spring model (1) with obtained values of stiffness, equilibrium angle and viscosity. For the whole time of movement except of the first 50 ms a good agreement between simulated and experimental torque time courses was obtained for all analyzed trajectories (Fig.1).

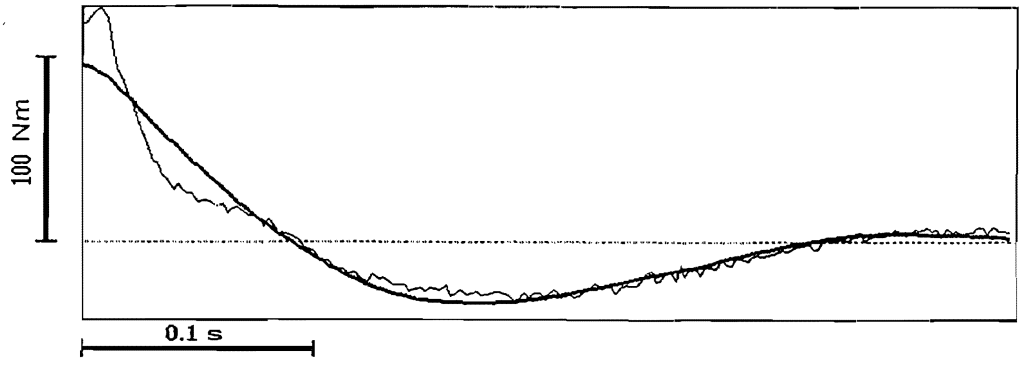

Fig.1 Simulated (thick line) and experimental (thin line) joint torques for a particular trajectory.

In the process of learning the joint stiffness increases during movement execution (Fig.2). It allows to assume that a subject increases the coactivation of muscles antagonists in order to minimize posture disturbance. It is in agreement with the decreasing of the amplitude during learning (Ioffe et al., 1994). The obtained values of stiffness and viscosity correspond to the data cited in the literature (Mussa-Ivaldi et al., 1985). Differences between calculated equilibrium angle and initial joint angles decrease during learning what corresponds to minimization of deviation of final forearm position from the initial one.

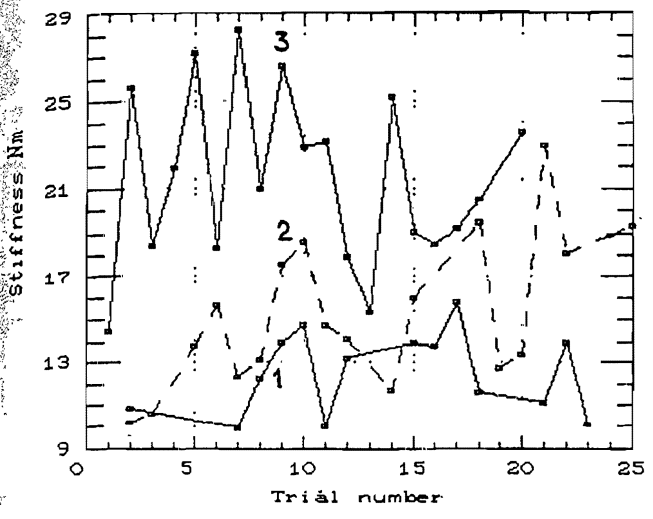

Fig.2 Joint stiffness vs trial's number. Curves 1, 2 and 3 correspond to three consequent learning sessions.

DISCUSSION

We suppose that proposed model can be applied only to the time period when delayed stretch-reflex feedback reflects the unloading. Good agreement between simulated and experimental joint torques after 50 ms from the unloading allows to use the equilibrium angle and joint stiffness as the estimation of central commands during posture maintenance after unloading.

In spite of many arguments in favor of nonlinearity of the process of joint torque generation (e.g., Flanagan et al., 1993) the movement caused by the unloading can be adequately described by simple linear model (1). The good agreement between experimental and simulated joint torque time courses (illustrated in Fig.1) argues for the fact that the movement is performed under the constant values of central commands controlling joint stiffness and equilibrium angle. Hence for the unloading motor task the multiple linear regression procedure applied to the whole trajectory seems to be rather reliable and simple method of estimation of elbow joint stiffness and viscosity.

REFERENCE

Feldman A.G. (1979) Central and reflex mechanisms of motor control. Moscow, Nauka (in Russian).

Feldman A.G. (1980) Superposition of motor programs. I. Rhythmic forearm movements in man. Neurosc., 5, 81-90.

Ioffe M.E., Massion J., Ganchev N., Dufosse M. (1994) Coordination between posture and movement in a bimanual unloading task: is there a transfer? (submitted to Exp. Brain Res.).

Paulignan Y., Dufosse M., Hugon M., Massion J. (1989) Acquisition of co-ordination between posture and movement in a bimanual task. Exp. Brain Res., 77, 337-348.

Mussa-Ivaldi F.A., Hogan N., Bizzi E. (1985) Neural, mechanical and geometric factors subserving arm posture in humans. J.Neurosc., 5, 2732-2743.

Flanagan J.R., Ostry D.J., Feldman A.G. (1993) Control of trajectory modifications in target-directed reaching. J. Motor Behav., 25, 140-152.

The work is supported by Russian Foundation of Fundamental Research, projects NN 93-04-6267, 94-04-11318 and by EEC contract ERB-CHRX-CT93-0266.

INFLUENCE OF SPEED, STIFFNESS, AND ANGLE OF ATTACK ON JUMPING DISTANCE

R.Blickhan[1], A.Friedrichs[1], F.Rebhan[1], T Schmalz[2], V Wank[1]

[1] Institut für Sportwissenschaft, Friedrich-Schiller-Universität Jena, Germany
[2] Otto Bock - Orthopädische Industrie Duderstadt, Germany

INTRODUCTION

The athletes objective in a long jump is to obtain a maximum distance for given anatomical and physiological parameters. At present the influence of various parameters on jumping distance is estimated by statistical methods requiring a large number of trials (Hay 1993, Lees 1993). We use a dynamical model to predict jumping distance and the influence of initial conditions and global system properties

METHODS AND MODEL

In a training's competition in Jena (1994) 10 sport students were filmed for later analysis (50 halfframes/s). The vertical and horizontal reaction forces were registrated with a 3D- forceplate (IAT, Leipzig) Kinematic input parameters for the dynamic model were obtained by digitising the video sequences (APAS, ARIEL) A spring-mass system (Blickhan, 1989) was selected as a model of the jumping athlete during ground contact The simulation was improved by allowing the unloaded length of the spring to increase with the angle of rotation The model was described by a system of two nonlinear differential equations.

$$\ddot{x} = x\omega^2(l(\alpha)/(x^2+y^2)^{1/2} - 1)$$
$$\ddot{y} = y\omega^2(l(\alpha)/(x^2+y^2)^{1/2} - 1) - g$$

x, y= horizontal and vertical components of centre of mass, $\omega = (k / m)^{1/2}$= natural frequent of centre of mass, k= mean spring stiffness, m= mass, $l(\alpha)$= initial spring-length, α= angle of rotation.

The input parameters of the system are the horizontal and vertical velocity, the angle of attack, the mean spring stiffness and the observed initial length of the spring. Because of the properties of the system and the lack of distal masses only the sinusoidal impact is modelled (Fig 3) The explicit consideration of the impact for the examined long jumps led to a reduction of the jumping distance of about 10cm. The differential equations were integrated using a Runge-Kutta algorithm (6th order) with a numerical simulation tool (ALASKA, Mechatronik)

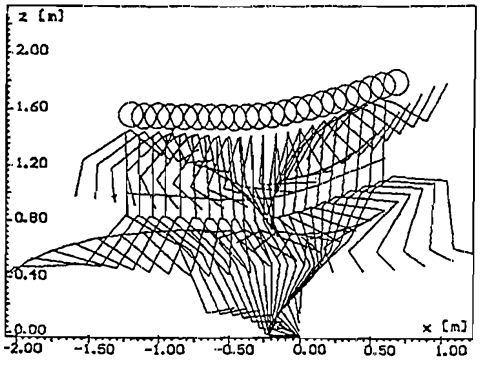

Fig 1: a) Pictogram of take-off

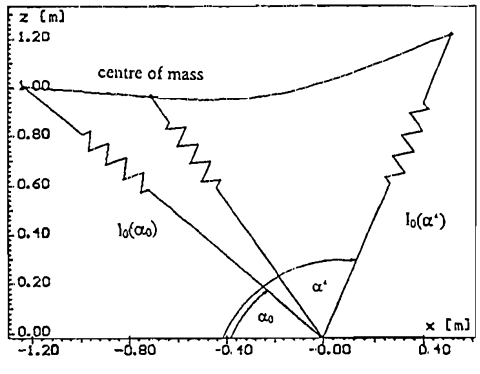

b) Dynamic model and path of the measured centre of mass, l_0: initial length of the spring, α_0: angle of attack, α': angle of take-off

RESULTS

The experimental jumping distances of the longjumpers reached from 4,55m up to 6,90m. Our simple model lacking muscle properties yields quite realistic jumping distances and contact times (Tab.1). Differences between the calculated and measured jumping distance were about 7 % ± 5 % SD

experiment		simulation	
jumping distance w_E [m]	contact time t_E [s]	jumping distance w_S [m]	contact time t_S [s]
5,20	0,13	5,26	0,144
6,55	0,14	6,99	0,122
4,55	0,17	4,73	0,154
6,55	0,14	6,62	0,143
5,87	0,13	5,83	0,125
6,20	0,15	6,25	0,144
6,90	0,12	6,69	0,136
6,70	0,14	6,54	0,146
6,35	0,14	6,64	0,148
6,50	0,13	6,67	0,144
6,48	0,12	6,60	0,126

Tab 1: Comparison of experiment and simulation

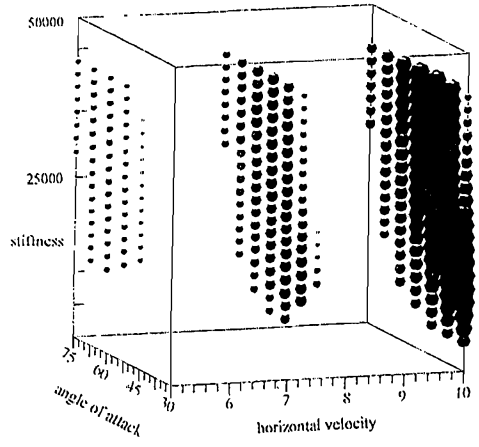

Fig.2: Jumping distance (thickness and darkness of markers) in depence of mean spring stiffness (k), velocity (v), and angle of attack (α) (spring length l_0= 1m, v_y= 0)

Clearly, jumping distance can be improved by increasing running speed (v_x, Fig 2) For a given speed and given stiffness a maximum jumping distance can be achieved at a certain angle of attack (Fig.2) By using a smaller angle of attack a jumper with a more compliant leg can achieve the same distance as a jumper with a stiffer leg The influence of the vertical velocity (v_y) on jumping distance is small (not shown)

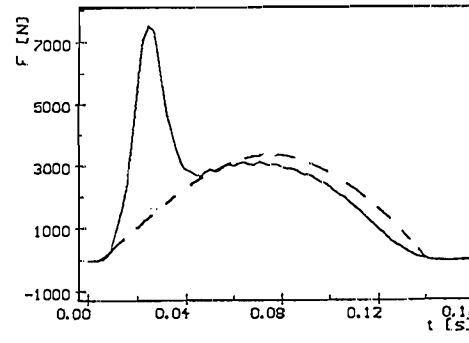

Fig.3: Measured (——) and simulated (----) vertical force

DISCUSSION

The proposed model should support athletes during training by providing information about promising parameter changes The predictions for the influence of the horizontal velocity (v_x) are consistent with literature (Alexander 1990, Hay 1993)

The maximal jumping distances can not be reached as a generation of leg stiffness is limited by the properties of the muscle skeletal system We will investigate the influence of anatomical and physiological parameters by stepwise enhancing model complexity

REFERENCES

Alexander, R McN , (1990) Optimum take-off techniques for high and long jumps Phil. Trans. R. Soc. Lond B 329, 3-10

Blickhan, R , (1989) The spring-mass model for running and hopping. J Biomechanics 22, 1217-1227.

Hay, J G , (1993) The biomechanics of jumping for distance J Biomechanics 26, S1, 7-21

Lees, A., (1994) A biomechanical analysis of the last stride, touchdown, and takeoff charakteristics of the men's long jump J Appl Biomechanics 10, 61-78

EXPLANATION OF DIFFERENCES IN JUMP HEIGHT BETWEEN COUNTERMOVEMENT AND SQUAT JUMPS

M.F. Bobbert, K.G.M. Gerritsen, M.C.A. Litjens and A.J. van Soest

Department of Functional Anatomy, Faculty of Human Movement Sciences, Vrije Universiteit, Amsterdam, The Netherlands

INTRODUCTION

There is ample evidence that performance in explosive movements is increased by a countermovement, a preparatory movement in a direction opposite to the goal direction. For instance, it has been shown that subjects achieve a greater jump height in a countermovement jump (CMJ), where they start from an erect position and make a downward movement before starting to push-off, than in a so-called squat jump (SJ), where they to start from a semi-squatted position and are not allowed to make a countermovement. In the literature, several mechanisms have been proposed to explain the positive effect of a countermovement on performance in the subsequent concentric action: (1) it allows for storage of elastic energy that can subsequently be re-utilized, (2) it enhances the properties of the contractile machinery, (3) it triggers neural responses, and (4) it provides the opportunity to build up muscle active state and muscle force. If we are to explain the greater jump height in CMJ compared to SJ, we should additionally take into account: (5) the position of the body at the start of the concentric phase, and (6) muscle co-ordination during the push-off. The purpose of the present study was to identify the factors responsible for differences in mechanical output between CMJ and SJ.

METHODS

Six male volleyball players participated in this study. Each subject performed, with arms akimbo, maximum height countermovement jumps (CMJ), as well as squat jumps (SJ) starting from a posture adjusted to the posture in CMJ at the start of upward movement. During each jump, positional data of anatomical landmarks were monitored, ground reaction forces were measured, and electromyograms were recorded from six muscles of the lower extremity. The highest jump of each type was selected for further analysis. Net joint moments and work were obtained by combining kinematic and ground reaction force information. Electromyograms were rectified, smoothed, and normalized to the maximum level attained by a given muscle, to yield *NSREMG*-time curves.

To assess the contribution of the factors mentioned above to differences in performance between CMJ and SJ, a model of the musculoskeletal system was used. The model comprises interconnected segments representing feet, lower legs, upper legs and upper body, as well as six major muscle groups of the lower extremity, each represented by a Hill-type unit. Independent input of the model were individual time-histories of joint angles obtained from the experimental study and muscle stimulation *STIM*, a one-dimensional representation of the effects of recruitment and firing frequency of α-motoneurons. In this study, *STIM*-time histories were assumed to correspond to measured *NSREMG*-time histories, scaled by a fraction f_i representing the relative activation of each individual muscle. As proposed by Hatze (1981), *STIM* was coupled via first-order dynamics to free calcium concentration, which in turn was related to active state by an algebraic saturation curve. Since the purpose was not to predict the mechanical output about joints during CMJ or SJ but to explain *differences* in this output among jumps, the f_i-values were optimized for each subject, using as criterion the time-integral of squared differences between

calculated and measured net joint moments, summed over CMJ and SJ.

RESULTS AND DISCUSSION

In spite of the fact that the body position was the same at the start of the push-off, jump height was found to be 3.4 ± 0.09 cm greater in CMJ than in SJ. The possibility that non-optimal coordination in SJ explained the difference in jump height could be ruled out: there were no signs of movement disintegration in SJ, and take-off position was the same in SJ as in CMJ. There was also no indication that muscle stimulation in CMJ was enhanced by neural responses triggered by pre-stretch: the average *NSREMG*-level during the upward movement was not higher in CMJ than in SJ in any of the muscles. The greater jump height in CMJ seemed to be due primarily to the fact that the countermovement allowed the subjects to attain greater joint moments at the start of upward movement, especially at the hip joints. As a consequence, muscle moments were greater over the first part of the range of joint extension in CMJ so that more work could be produced than in SJ. This is illustrated in figure 1a, which shows average moment-angle curves for the hip joints. Figure 1b shows the corresponding relationships calculated using the model. Although the amount of work produced (the area under the moment-angle curves) is lower in the model, the key difference between CMJ en SJ in measured joint moment histories is replicated: over the first part of the range of joint extension, joint moments are higher in CMJ than in SJ. In the search for an explanation of this finding, two manipulations of model input were carried out. First, the *NSREMG*-time history of the preparatory phase in CMJ was replaced by that in SJ (CMJm1). As illustrated in figure 1c for the hip joints, this effectively changed the calculated moment-angle curves of CMJ into those of SJ. The second manipulation was to eliminate the pre-stretch in CMJ (CMJm2). As illustrated in figure 1c, this had little effect. Apparently, the crucial contribution of the countermovement is that it allows the muscles to build up a high level of active state and force before shortening begins, so that they are able to produce more work over the first part of their shortening distance. Other mechanisms, such as potentiation of the contractile machinery by pre-stretch or storage and re-utilization of energy, seem to play at best a secondary role in the enhancement of performance in CMJ over that in SJ.

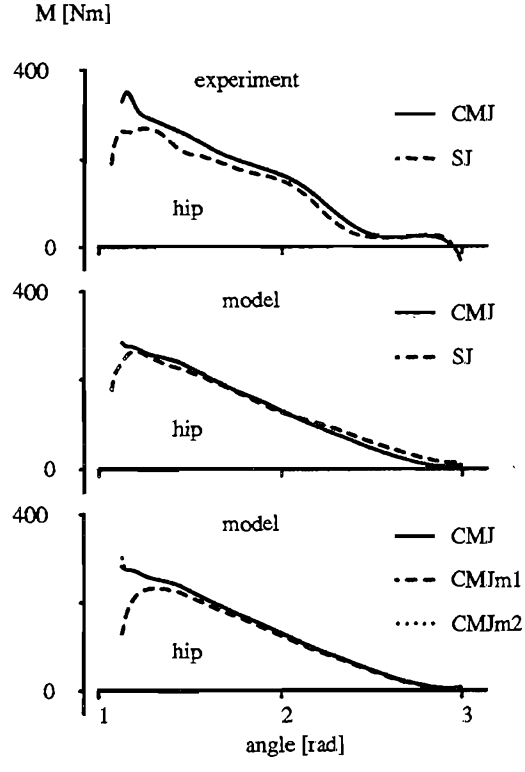

Figure 1. Average moment-angle curves for the hip joint in CMJ and SJ. a) experimental data, b) model calculations, c) model calculations for CMJ with manipulated input. For further explanation, see text.

REFERENCE

Hatze, H. *Myocybernetic Control Models of Skeletal Muscle.* University of South Africa, Pretoria, 1981.

TRUNK STIFFNESS IN AXIAL ROTATION OF TRACTOR DRIVERS AND OFFICE WORKERS.

Anna Bodén & Kurt Öberg

Swedish University of Agricultural Sciences, Department of Agricultural Engineering

Uppsala, Sweden

INTRODUCTION

Static and awkward working postures in combination are likely to cause musculoskeletal disorders. One such posture is the twisted trunk posture required during tractor driving in the field with a pulled implement. This posture exceeds the normal range of rotating motion (Öberg, 1993) and may cause, for example, lumbar back problems and hip joint arthrosis (Thelin, 1990). In order to define the load on the back when sitting twisted backwards, and to find out more about the magnitudes and mechanisms of torques exerted on the spinal column as a result of these sitting conditions, a biomechanical model of trunk rotation at the lumbar level has been defined (Öberg, 1993). One part in the work with the model concerns measuring the torque from passive tissues when the trunk is twisted.

When sitting twisted backwards, the only counteracting torque is the torque from the passive tissues, i.e, trunk stiffness. Trunk stiffness in axial rotation has been measured during standing (McGill et al, 1994). The purpose of this paper is to describe the measurement method and to present some preliminary results of the experiments when measuring torque from passive tissues at different twisting angles in a sitting position.

METHODS

The measurements were made on ten male tractor drivers and ten male office workers. Selection criterias were length 170 - 190 cm, age 20 - 40 years old and weight 70 - 90 kg. The tractor drivers should have had tractor driving as their major work task and the office workers should never have driven a tractor and should have a work task mainly requiring a sitting work posture. The subjects were matched according to length and age, one tractor driver and one office worker in each block. During the experiment the two persons in each block alternated between being twisted and pausing.

During the measurements the subjects were sitting in a conventional tractor chair without backrest. The torque needed to twist the subject was measured by using a shoulder frame mounted on a vertical bar with a strain gauge transducer for torque measurements. On the shoulder frame a device with a manually operated crank was mounted which allowed slow twisting at relatively constant speed (approximately 1.5 degree/second).

The subjects were instructed to sit with a straight back and relaxed. They were instructed to stop the operator turning the crank as soon as they started to feel uncomfortable.

The twisting angle was measured by using a three-dimensional optoelectronic position measurement system which measures the three-dimensional position of reflecting markers. Two reflecting markers were mounted on the shoulder frame and on a frame attatched to the pelvis, respectively. The twisting angle was calculated from the x-, y- and z-positions of the markers. This means that the twisting angle is defined as the angle between the shoulder frame and the pelvis frame, i.e, the spine at the T7-level and the pelvis.

Surface-EMG was used as a control of the relaxation of the subject. The EMG-electrodes were mounted on left and right rectus abdominis, left and right obliquus externus and left and right erector spinae. All electrodes were mounted around the circumference of the L1-level.

RESULTS

The statistical analysis of the whole material is still being processed and only preliminary results can be presented.

Figure 1 shows raw data of trunk stiffness in relation to twisting angle. The curves represent three trials made on one subject. The twisting is done to the left.

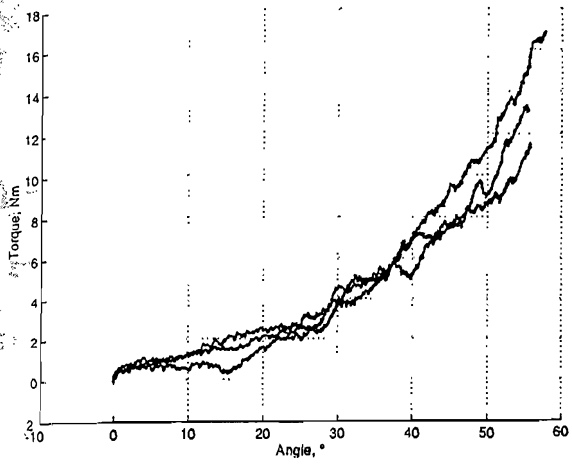

Figure 1. Raw data from one subject of trunk stiffness due to twisting angle. Twisting to the left.

The characteristics of the trunk twisting curve seem to be uniformly progressive. Up to 20 ° rotation the trunk twisting stiffness is approximately 0.1 Nm/degree. After 40 ° rotation the corresponding value is 0.4 Nm/degree.

DISCUSSION

The initial step on the curves in Figure 1 is probably a result of initial resistance as the subject is to be twisted at constant speed. The subjects might have difficulty in relaxing during the initial part of the twisting phase. The possibility to measure trunk stiffness at different preset angles was also tested. As the purpose of the measurements was to find the relation between torque and twisting angle, an experiment with preset angles was found to be too big, and too difficult to achieve within the accuracy limits.

According to the literature, the possible maximum angle from T7 to pelvis (with maximum rotation in the sacroiliac joint) varies between 29 ° and 52 ° with a representative angle of 38 °(White and Panjabi, 1978). The experiments shown in Figure 1 exceed the maximum possible angle, even though the experiment was done within the individual tolerance of the subjects, as they set the limits of the twisting range themselves. There are several explanations of this. First, because of the design of the shoulder frame, the possible deformation of the ribs at the T7-level is included in the twisting angle. Second, there is also deformation in the tissues of the chest because of the attatchment to the shoulders. Evaluation of these errors will be carried out.

This far, the measurement method seems to be a good tool in conducting experiments of this kind. The results given by the method are considered to be promising and the method will be used in further experiments.

REFERENCES

McGill, S., Seguin, J. & Bennett, G. 1994. Trunk stiffness of the lumbar torso in flexion, extension, lateral bending, and axial rotation. Effect of belt wearing and breath holding. *Spine* **19(6)**, 696-704.

Öberg, K. E. T. 1993. A model of lumbar spine load due to twisted trunk postures during tractor driving. In *Proceedings of the XIVth congress of the International Society of Biomechanics. Paris, France.*

Thelin, A. 1990. Hip joint arthrosis: an occupational disorder among farmers. *Am. J. Ind. Med.* **18**, 339-343.

White, A. A. & Panjabi, M. M. 1990. *Clinical biomechanics of the spine*. Second edition. J. B. Lippincott Company, Philadelphia.

THE EFFECT OF DECREASING STIMULATION CURRENT ON THE LENGTH FORCE CHARACTERISTICS OF RAT GASTROCNEMIUS MUSCLE

Peter Bosch and Peter A. Huijing
Faculteit Bewegingswetenschappen, Vrije Universiteit, Amsterdam
The Netherlands.

INTRODUCTION

There is evidence that the mechanical properties of partially activated muscles may differ substantially from those of fully activated muscles (e.g. Huijing, 1992). During 'in situ' experiments the easiest way to achieve partial activation of a muscle is the reduction of stimulation current.
If stimulation current is reduced to a submaximal level, it is expected that the smaller units will not be excited anymore because of higher excitation thresholds (Kernell, 1966). The object of this study was to examine the effects of decreasing stimulation current on the mechanical properties of rat gastrocnemius muscle.

METHODS

Under sodium pentobarbitone anaesthesia the medial gastrocnemius of 6 young adult male wistar rats was exposed. The distal end of the severed sciatic nerve was placed in a tripolar cuff electrode (electrode separation 3mm). A tripolar electrode was used in order to avoid leakage of current and virtual cathode excitation. Tetanic contractions were induced by stimulating the sciatic nerve using rectangular pulses (100Hz, 100μs). During the plateau phase of the tetanus photographs were taken in order to determine muscle geometry. Length force characteristics were obtained at one supramaximal and two submaximal currents.

RESULTS

At the original optimum length (lmao) mean force decreases were 74% and 34% respectively for the two submaximal conditions. The length force data show a shift of muscle optimum to lower muscle lengths for 3 muscles, and a shift to higher muscle lengths for the remaining 3 muscles. Figure 1 shows typical raw and fitted length force data for shifts of muscle optimum to lower and higher muscle lengths. Shifts to lower muscle lengths had a magnitude of maximally 1.79 mm and for shifts to higher muscle lengths the magnitude was maximally 1.93mm. Twitch tetanus ratios were determined (twitch force/ tetanic force) at lmao. Relating twitch tetanus ratio to decrease of force revealed a significant correlation ($r=-0.80$, $p<0.01$) for the muscles in which a shift to lower muscle length was observed. Such a result would be expected if the faster motor units remain active after current reduction because these units have higher twitch-tetanus ratios compared to slower units (Fitts et al, 1991). For the muscles in which a shift to higher muscle lengths was observed, relating relative twitch force to normalized tetanic force did not yield a significant correlation.

DISCUSSION

Shifts of optimum muscle length cause the amplitude of force decreases at submaximal recruitment levels to be quite length dependent. Based on results

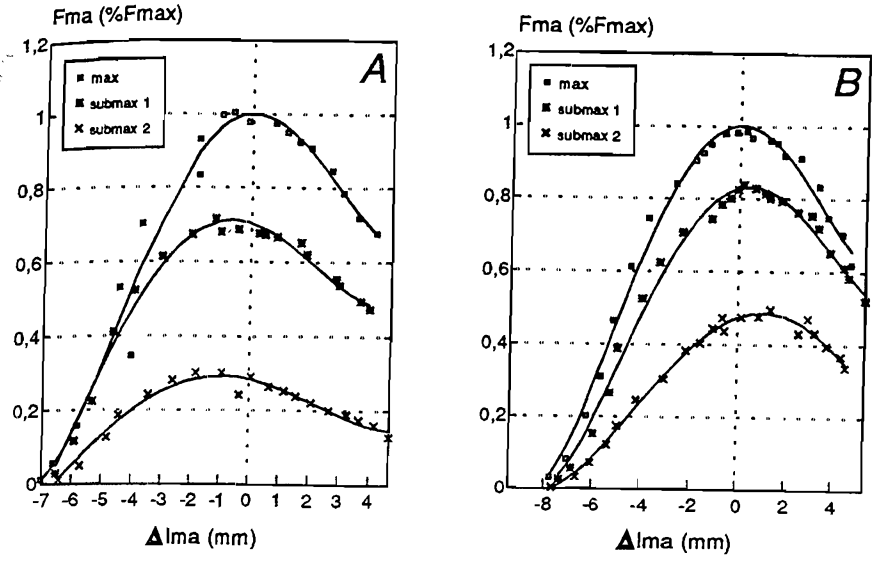

Fig 1. Typical examples of raw and fitted length force data for shifts to lower (A) ans higher (B) muscle lengths.

of previous studies it can be hypothesized that the smaller, fatigue resistant units have their optimum length at higher muscle lengths. It was therefore expected that stimulation current reduction would shift muscle optimum to lower lengths. The results of this study, however, show contradicting results. In three muscles lowering stimulation current was accompanied by a shift of optimum length towards lower muscle lengths, in three muscles the opposite was found. Two alternative explanations can be given for the results. First it is possible that motor unit optimum length is not systematically distributed with respect to motor unit size. However, twitch tetanus ratios increase with increasing magnitude of shift towards lower muscle lengths. This is an indication that in these cases the remaining motor units after current reduction were the faster units. Another explanation for the results may be that differences in neuron-electrode distances have biased the results. The excitability of an neuron for a stimulus is not only determined by its excitation threshold, but also by its position within the nerve with respect to the electrodes (Durfee and MacLean, 1989). Because the location of the axons with respect to the electrodes could not be controlled over experiments it is conceivable that in experiments in which a shift to higher muscle lengths was observed also larger units were derecruited because their axons were situated further from the electrodes.

REFERENCES

Durfee KW & MacLean KE:Methods for estimating isometric recruitment curves of electrically stimulated muscles, *IEEE transactions on biomedical engineering*, 36(7): 654-667, 1989.

Fitts RH, McDonald KS and Schluter JM: The determinants of skeletal muscle force and power: their adaptability with changes in activity pattern. *J. Biomechanics*, 24: suppl. 1, 111-122, 1991.

Huijing PA: Properties of submaximally stimulated muscle and some functional consequences of gradation of muscle force. In: *Neural aspects of Human movement: implications for control and coordination*, Bakker CMC, Berger MAM, Doorenbosch CAM, Peper CE, Willems MET and Zaal FTJM (eds), Swets Zeitlinger pp 23-29, 1992

Kernell D: Input resistance, electrical excitability, and size of ventral horn cells in cat spinal cord. *Science*, 152:11637-1640, 1966.

EFFECTS OF TRAINING ON VERTICAL JUMP PERFORMANCE AND FORCE-VELOCITY CHARACTERISTICS

Kostas BOUDOLOS
Department of Physical Education and Sport Science, University of Athens, Greece

In this study we try to analyse the results of the force-training of the Volleyball athletes: (a) with relation to the improvement of the vertical jump and (b) with relation to the force-velocity characteristics.

Method:
Twelve (12) athletes of the Greek National Volleyball Team, who also took part in the World Championship in October 1994, participated in this study. The characteristics (in mean values) of the ahletes were as follows: Chronological age - 25.23 ± 3.57 years, Training Age - 10.21 ± 3.38 years, Body Height - 196.45 ± 6.82 cm and Body Weight - 91.50 ± 6.27 Kg. The subjects undergoing the test, performed vertical jumps on a Kistler Force Platform. Some of the tests were carried out under different load conditions, (with the 0%, 25%, 75% and 100% of their body weights on the shoulders). These tests were the following:
1. Test ABALAKOV
2. Squat jump (SJ)
3. Counter Movement Jump (CMJ)
4. Counter Movement Jump with a load of 25% (CMJ 25%)
5. Counter Movement Jump with a load of 50% (CMJ 50%)
6. Counter Movement Jump with a load of 75% (CMJ 75%)
7. Counter Movement Jump with a load of 100% (CMJ 100%)
8. Repeated Vertical Squat Jumps for 60".

The Greek Volleyball players, in order to prepare themselves for the World Championship, are trained under the supervision of the coach G. Herrera. The training, in the course of the three months (May, June, July) included strength exercises for the leg muscles. The force-training comprised also exercises with loads as well as jumps with concentric and eccentric characteristics.The data collection for this tests took two sessions. The first one took place on 29-4-1994 and the second on 1-8-1994.

Results:
At each of the above sessions, the changes in the characteristics of the vertical jump and the force-velocity curve, were examined by statistical analysis. The coefficient of variation was used for each condition of load and the various kinds of jumps, while the t-test analysis was used for dependent samples.
The Coefficients of Variation calculated throughout the first session, fluctuate between 13.1 and 26.7% for the CMJ tests with and without loads (table 1).

Table 1. Mean, Standard Deviation and Coefficient of Variation of ABAL, SJ, CMJ 0%, CMJ 25%, CMJ 50%, CMJ 75% και CMJ 100% tests, before the first session

	ABAL [cm]	SJ [cm]	CMJ [cm]	CMJ 25%	CMJ 50%	CMJ 75%	CMJ 100%
X	53.5	36.3	41.8	25.7	19.8	14.3	10.1
SD	4.62	5.48	5.48	4.97	3.55	3.73	2.68
CV%	8.63	15.1	13.1	19.3	17.9	26.1	26.7

The Coefficients of Variation calculated throughout the second session, fluctuate between 10.3 and 28.9% for the CMJ tests with and without loads (table 2).

Table 2. Mean, Standard Deviation and Coefficient of Variation of ABAL, SJ, CMJ 0%, CMJ 25%, CMJ 50%, CMJ 75% και CMJ 100% tests, before the second session.

	ABAL [cm]	SJ [cm]	CMJ [cm]	CMJ 25%	CMJ 50%	CMJ 75%	CMJ 100%
X	53.2	39.1	43.3	31.3	22.9	16.0	10.9
SD	4.67	4.27	4.46	4.77	3.44	3.10	3.15
CV%	8.78	10.9	10.3	15.3	15.0	19.4	28.9

From the statistical analysis it can be seen that there is an important difference between the data collected throughout the first and the second session. These differences are as follows: CMJ ($t=2.38$, $p< .05$), CMJ 25% ($t=4.65$, $p< .01$), CMJ 50% ($t=5.83$, $p< .01$) and CMJ 75% ($t=2.17$, $p< .05$). Considerable difference is also noticed in the force-velocity index. F-V(50%) ($t=3.76$, $p<.05$).

The 60″repeated jumps between the first and second sessions remained invariable. The effects of the force-velocity characteristics were negligible.The results indicate that the training as far as the strength of the legs is concerned is not effective.

Conclusion:

The athletes were positively influenced from the force-training in the course of the three month period and the performance of their vertical jump was considerably improved. The vertical jumps with loads of 25% and 50% of their body wheight on their shoulders showed the most improvement. The results reflected in the athletes performance throughout the World Volleyball Championship.

3D MULTILINK HUMAN BODY MODEL : VALIDATION AND APPLICATION TO CHRONIC LOW BACK PAIN REHABILITATION.

S. BOUILLAND - F.X LEPOUTRE* - J.L VANHEE***

** Laboratoire d'Automatique et de Mécanique Industrielle et Humaine - CNRS URA 1775*
Université de Valenciennes - France

*** Centre L'Espoir - 25 Pavé du Moulin - 59260 Lille Hellemmes - France*

1. INTRODUCTION

Two lifting modes are currently used in Functional Restoration for chronic low back pain : isoinertial lifting and isokinetic lifting /MAYER 89/. In isokinetic mode, constant speed imposed to the virtual load can be seen as a constraint on learned natural way of lift, generating a new movement with new articular efforts. Our purpose is to compare natural and isokinetic lifting from a biomechanical point of view. Complementarity or potential opposition between the both lifting modes applied to low back pain rehabilitation will be examined. For different constraint levels (i.e. different speeds), the effects on articular efforts and on movement will be evaluated. Movement is recorded with a motion analysis system and a 3D multilink model is used to evaluate articular efforts. First results are presented for natural lifting and compared with existing studies in order to validate the whole method.

2. METHODOLOGY

In both isokinetic an natural lifting, each subject has to perform a lift from floor to hips in sagittal plane. Three isokinetic lifts are performed on the CYBEX LIFTASK at slow, middle and rapid speed (15.24, 45.72, 91.44 cm/s). Isokinetic lifting normally requires maximal effort. In order to compare both lifting modes, isoinertial lift has also to be performed with maximal effort. Then, by few increasing adjustments, subject determines the maximum weight he thinks he can lift without injury himself and the isoinertial lift is performed with this weight.

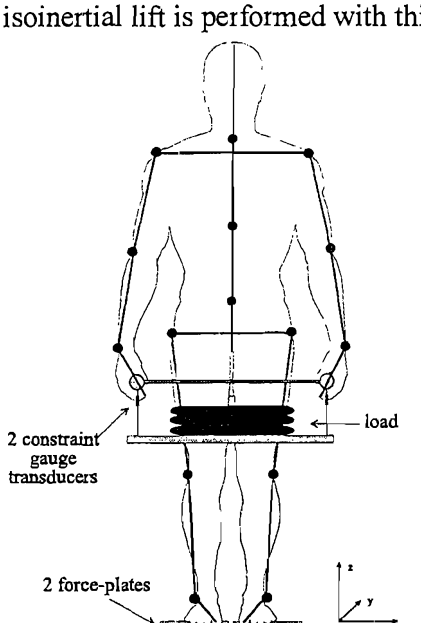

Fig 1 : Experimental procedure for free style lifting; in solid lines geometric model

Each lift is repeated four times to prevent from learning effects and to eliminate intra-individual variations. A warming up of five mn on ergometer is imposed to the subject before the test starts. Thirty-five reflective markers are used to record subject's movements at 50Hz with the motion analysis system SAGA3 /CLOUP 89/. Ground reaction forces are recorded under each foot with two force-plates (fig 1). Two constraint gauge transducers record force on each hand . The number of subjects is fixed to 10 for material reasons. Subjects will be chosen male, healthy, without history of low back pain, 20-30 years old in order to constitute a normative data-base for non LBP people. A 3D model of human body constituted of 16 rigid segments is used to evaluate articular forces and couples. Inertial characteristics are calculated from /ZATSIORSKY 90/. A 3D software has been developed to build the set of dynamic equations in a matricial form and to solve this system by full pivoting Gaussian elimination.

3. RESULTS

First results are presented for a natural lifting (one upward movement) with a 15kg load performed by one subject.

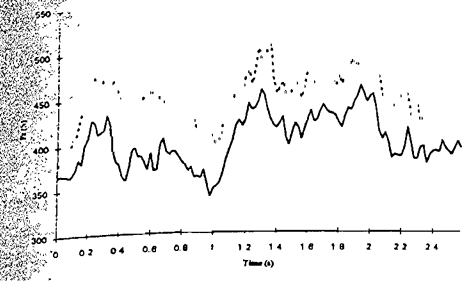

fig 2 : Recorded (dotted line) and predicted (solid line) vertical ground reaction under right foot.

Figure 2 presents the recorded vertical ground reaction force and the predicted one. The two curves have similar evolution and static error is probably due to a difference of 2.1kg between the model's mass and the real subject's mass.

/DE LOOZE 92/ reports peak torques about 250 Nm at L5/S1 and 40-50 Nm at shoulders for a 18.8kg lift calculated on a 2D model. Results presented in figures 3-4 are of same order. Torques on each shoulder must be added to get the 2D model's results. Moreover /LESKINEN 85/ reports average peak hip torques from 263 to 346 Nm for a 15kg lift which is of the same order as the 266 Nm hip peak predicted in this study.

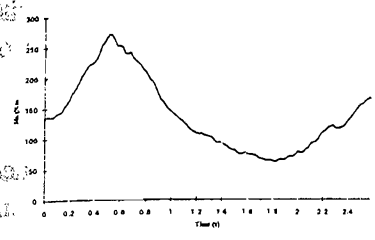

fig 3 : Predicted Mx torque at L5/S1

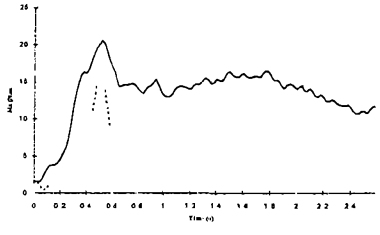

fig 4 : Predicted Mx torques on right (dotted line) and left (solid line) shoulder

4. DISCUSSION AND CONCLUSIONS

Above results seem to validate the global method used to collect data and evaluate articular efforts although segment's masses have to be corrected. They also point out the necessity to work with 3D model due to the non symmetric efforts applied by the subject to his environment (fig 5-6), even for healthy persons. This should be reinforced for subject suffering from deficient articulations and justify the choice of 3D modelling although the experimental and computational processes are heavier than for 2D analysis.

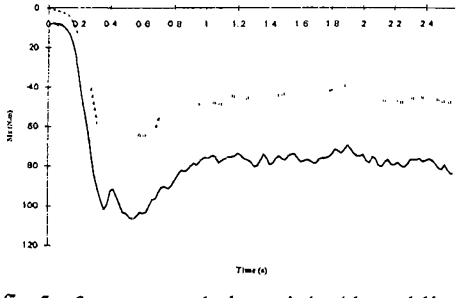

fig 5 : force recorded on right (dotted line) hand and on left (solid line) hand

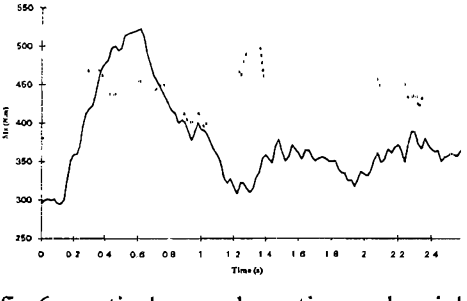

fig 6 : vertical ground reaction under right (dotted line) foot and left (solid line) foot.

5. REFERENCES

Cloup P. "Etude et réalisation d'un système d'analyse gestuelle en trois dimensions par traitement d'images en temps réel."Thèse de Doctorat. Université de Valenciennes; 1989.

De Looze M.P."Validation of a dynamic linked segment model to calculate joint moment in lifting"Clin. Biomechanics, 7,161-169,1992

Leskinen T.P.J."Hip torque, lumbosacral compression and intra-abdominal pressure in lifting and lowering tasks" Biomechanics IX-B pp 55-59, 1985

Zatsiorsky V"In vivo body segment inertial parameters determination using a gamma scanner method"Biomechanics of human movement pp196-202, 1990

Mayer G. "Functional Restoration for chronic low back pain Part "Pain Manag 2(2) : 67-73, 1989

ORIGIN AND INTERPRETATION OF ERROR IN ARTICULAR EFFORTS EVALUTION

S. BOUILLAND - F BARBIER - P.DRAZETIC
Laboratoire d'Automatique et de Mécanique Industrielle et Humaine - CNRS URA 1775
BP 311- Université de Valenciennes - 59304 Valenciennes Cedex - France

1. INTRODUCTION

Inverse dynamics is used by biomechanicians to evaluate articular efforts needed to realise a movement. A 2D or 3D linked rigid segment model of the whole body (or part of) is used and instantaneous application of Newtonian mechanics is made on each segment. Errors occur in model's definition and in data recording. These errors lead to incoherence between recorded forces and segments' positions applied to the model during articular efforts calculation. Due to errors, the whole model with its applied movement, its applied forces and its mass distribution is not in dynamic equilibrium. Our purpose is to remember what are main sources of error when calculating articular efforts and to present how dynamic equilibrium is restored in a mechanical point of view.

2. METHODOLOGY AND RESULTS

First source of error concerns the model definition. Each rigid segment is defined by parameters such as mass, moment of inertia and center of gravity relative position. /ZATSIORSKY 90/ reports 3-10% errors in individual segment mass estimates and 3-30% error in the moment inertia estimates. Precision on total body mass is usually about 2%. Second source of error concerns constraints applied to the model. Applied forces are recorded with the constraint gauge transducers or force-plate precision. So does the application point of ground reaction force. Recorded markers'positions are noisy and generate fictitious acceleration peaks. This can be partially corrected using tools as filters or quintic splines /WOLTRING 86/ for smoothing noisy data. Due to the skin sliding, relationship between external markers' positions and squeletton is not well known. Nevertheless methods are now proposed to take this into account /CHEZE 93/

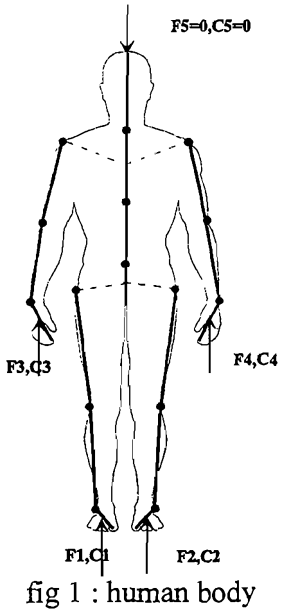

fig 1 : human body model

To calculate articular efforts, human body is seen as a 3D open chain system (fig 1) with n segments and (n-1) articulations. Each effort applied at each extremity of this system can be measured or is supposed to be null.

Set of dynamic equations for the system can be written with the following form :

$$_{6n}\overbrace{[\mathbf{D}]}^{6.(n-1)} \bullet {}_{6(n-1)}\overbrace{[\mathbf{F}]}^{1} = {}_{6n}\overbrace{[\mathbf{I}]}^{1}$$

with :

D : (6.n)*6.(n-1) Matrix containing the directions of unknown efforts

F : 6.(n-1) Vector of unknown articular efforts

I : (6.n) Vector of (inertial efforts - applied efforts).

In this set of 6*n equations and 6*(n-1) unknowns, 6 equations are linear combination of the others. To solve it, these 6 redundant equations must be eliminated. For a perfect model those equations should be also verified with the vector F, solution of the 6.(n-1)*6.(n-1) set of equations. This is false in our case, as our model contains errors. In fact, at the end of the calculation, the segment whose equation have

been removed won't be in dynamic equilibrium. This is equivalent to work on two subsystems. The error will cumulate from the beginning to the end of each subsystem.

Another way to proceed is to add 6 unknown to get a (6.n)*(6.n) set of equations. This means remove a measured applied effort on one extremity and replace it by a unknown force F_u and a unknown torque C_u. As the model contains errors and as the constraints applied to the model also contain errors, (F_u,C_u) will be used to restore the dynamic equilibrium. This impose the calculation end point and the direction where error will cumulate. In order to illustrate the cumulation of errors, a 3D model of human body constituted of 16 rigid segments was used to evaluate articular efforts during a 15kg lift. Ground reaction forces were recorded under each foot with two force-plates. Two constraint gauge transducers recorded force on each hand. Fig 2-3 present vertical force and torque in sagittal plane on right ankle for F1,C1 replaced by unknown (F_u,C_u) and for F3,C3 replaced by unknown (F_u,C_u).

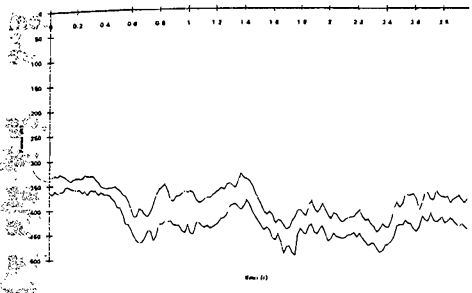

fig 2 : Compression force on right ankle with (F_u,C_u) applied on right foot (dotted line) and (F_u,C_u) applied on right hand (solid line).

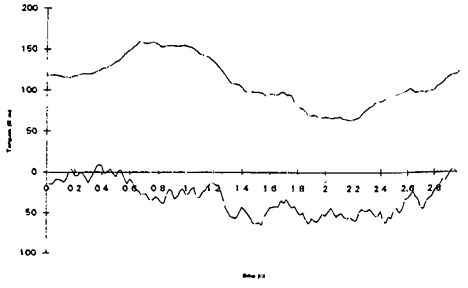

fig 3 : Torque on right ankle with (F_u,C_u) applied on right foot (dotted line) and (F_u,C_u) applied on right hand (solid line).

3. DISCUSSION

When adding unknowns, best results for each articulation, are obtained when measured efforts are applied near the articulation and worst results are obtained when the nearest measured effort is replaced by (F_u,C_u). Comparison of torques provides the worst result which is explained by the fact they include error on forces multiplied by error on lever arm and by the fact that rotations are less precise than translations; forces present a better agreement.

In dynamic equations, segment's mass is multiplied by linear accelerations and moments of inertia are multiplied by angular speeds and accelerations. Those quantities are the ones which include the biggest error. Error is then multiplied and the greater the mass or the acceleration the greater the error. When eliminating redundant equations, this permits to choose which ones to eliminate. As error is cumulated from one segment to the one following, calculation have to be done from the lightest segment to the heaviest and subsystems must have nearly the same numbers of segments. However, L5/S1 articulation is always near the end of each subsystem. This is a problem due to the particular role of this articulation in low back pain studies for example.

This work was supported by CENTRE L'ESPOIR, 59260 Lille-Hellemmes, France; MEDIMEX, 69410 Champagne au Mont d'Or, France; and Région Nord Pas de Calais.

4. REFERENCES

Zatsiorsky V.M., Seluyanov V.M."Methods of determining mass-inertial characteristics of human body segments"Contemporary problems of biomechanics, Boca Raton, MA : CRC press, 1990

Woltring H.J. "A FORTRAN package for generalized, cross-validatory spline smoothing and differentiation."Advances in Engineering Software 8(2):104-113 (U.K.) (1986)

Cheze L."Contribution a l'étude cinématique et dynamique in vivo de structures osseuses humaines" Thèse de doctorat, Université Claude Bernard, Lyon 1- 1993

SQUAT JUMP OPTIMIZATION FOR VARIOUS OBJECTIVE FONCTIONS

Paul Bourassa, University of Sherbrooke, Sherbrooke, Québec, Canada

The squat jump investigated in this paper is the result of the simulation of a dynamic system of differential equations, with a control vector, representing the motion of an articulated set of four rigid segments in the saggital plane actuated by three joint muscles groups.

These muscles have been modelized, using a Hill type contractile element, taking into account the force-length-velocity relationship and an activation factor. More specifically, a model described by Van Soest [1] has been programmed directly into the symbolic Autolev code which generates the complete set of second order differential equations with controls for this system. The activation factors are set as the ratio of actual joint angle to their final desired values and serve in this way as a control feedback loop over the system in the search of an optimum jump. Ligaments in the form of non-linear spring elements are incorporated into the model. Their role may be important and will be discussed.

The jumper is assumed to adopt initially a static posture over an elastic mat at starting time. Thus the system starts with zero initial generalized velocities and a given set of mat deflexion and body joint angles. The trunk initial joint angle is corrected in order to bring the initial center of mass directly above the contacting tip point of the foot body. The symbolic set of differential equations is then integrated using a Runge-Kutta-Myerson integrator of 4th order with a controlled convergence criterion and when the conditions for take-off are satisfied, the state variables are be used to predict exactly the jump height for the mass center.

Simulations may be performed back and forth over a range of parameters. In this study,the jump heigth was evaluated for various values of the isometric forces po1,po2,po3 for each muscle set. These values determine somehow the extent of the muscle work that will ensue afterwards.It takes a fairly long time to execute all the simulations that will cover the full range of this three-dimensional domain over the field of the isometric forces. It is usefull to do it at least once, in order to explore and validate any further optimum automatic search. For some particular set of physical constants and initial conditions it has been found that a fairly constant jump height occurs along a line of constant sum of two muscle isometric values po1 and po2 in the plane of these parameters for any fixed value of po3.This is shown on figure 1. This therefore suggests the following approach. Simulations can be carried for successive parameter increments in the direction of the jump height gradient which will lie somewhat close to the direction of constant differences in the isometric force components. The gradient may later be found through excursion in two orthogonal directions. Once a maximum jump height has been detected, the search direction may be carried in the orthogonal direction, that is, in a direction close to the constant sum of isometric forces.

The general pattern also shows that the jump height increases monotonically from low isometric values until it reaches a maximum, afterwhich a sudden drop occurs. Simulations performed in that region shows through animations that instability occurs immediately beyong the optimal region. It manifests itself in the form of joint angle increasing beyong maximum desired values. The ligament may then be seen as a safeguard element that will keep segment configurations whitin a stable domain.

Different optimum jumps can also be found such as those for which, for example, the highest coordinate of the tip of the trunk segment is the desired objective. This is a more difficult problem since the simulation must be carried over two different time domain, first when the body is still in contact with the mat and secondly, when the body is in its aerial phase with mat elastic forces set to zero.

CONCLUSION

Optimum jump height may be found through simulations using a gradient an a parrallel path approach over the field of isometric forces for three muscle groups. An animation programme becomes most usefull if not essential in assessing types of jumps belonging to various parameter domains, such as unstable jump pattern produced for parameters exceeding optimal values.

REFERENCES.

1. Bourassa P.,Masden B., Marshall B.,Ackland T., Modeling Ideas and Software for the Simulation of a Squat Jump. Proceedings, Eighth Biennial Conference, Canadian Society of Biomechanics, Calgary, Aug 18-20, 1994
2. Van Soest A.J.,Jumping from Structure to Control., PhD. Thesis, Vrije Universiteit, 1992.
3. Pandy M.G., Zajac F., An Optimal Control Model for maximum height Human Jumping, J. Biomechanics, Vol 23 no 12 pp 1185-1198, 1990

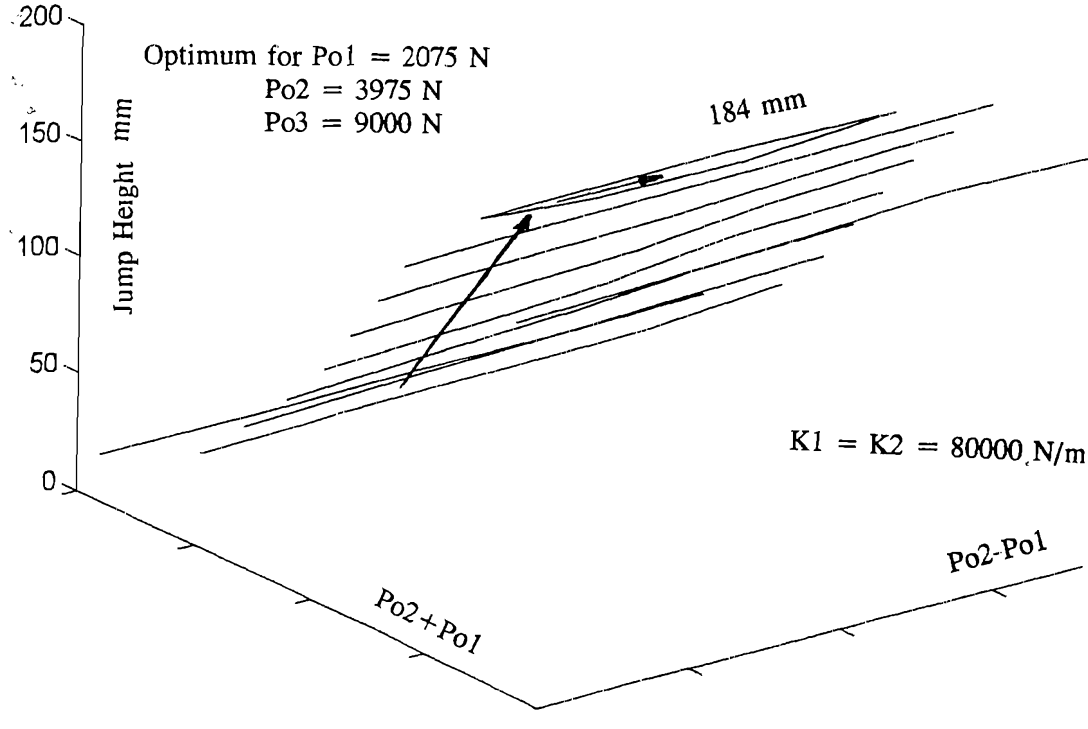

Figure 1. Jump Height for center of mass over the isometric domain.

EFFECT OF VELOCITY ON MECHANICS AND ENERGY COST OF RUNNING

M. BOURDIN, A. BELLI, L.M. ARSAC, C. BOSCO and J.R. LACOUR
Laboratoire de physiologie de l'exercice, GIP exercice, Univ. Lyon I, France

INTRODUCTION

It has been often observed that the energy cost of running (C_r: $J.kg^{-1}.m^{-1}$) is independent of the running velocity (Margaria et al., 1963; Di Prampero et al., 1986 and 1993). Cavagna et al (1964) have also showed that the total work (W_{tot}, defined as the sum of external and internal works) related to distance covered is independent of the running velocity. Both these results would indicate that the net running efficiency is constant for velocities ranging between 10 and 20 $km.h^{-1}$. However, Daniels et al. (1977) and Kearney and Van Handel (1989) observed that the slope of the relationship between oxygen consumption and running velocity can vary for a group of subjects depending upon the velocities chosen for the analysis. The purpose of this study was to re-examine the possible concomitant variations in C_r and in mechanical parameters associated with an increase in running velocity.

METHODS

Ten trained male subjects performed two 4 min running bouts on a motor-driven treadmill at 3.61 $m.s^{-1}$ and 5 $m.s^{-1}$. Expired gas and kinematic data were collected during the last 30 seconds of each bout.

Collection and analysis of expired gas: The Douglas bag method was used for the measurement of oxygen uptake. The ventilatory volume was determined with a Tissot spirometer and O_2 and CO_2 concentration in the expired gas were determined using respectively Beckman model OM11 and LB2 analysers. C_r was calculated as follow: net oxygen uptake (ml $O_2.kg^{-1}.s^{-1}$) divided by velocity ($m.s^{-1}$). In accordance with the value of respiratory quotient, C_r is expressed in Joules using the oxygen equivalent.

Kinematic parameters: a kinematic arm measured the displacements of body center of mass (CM) (Belli et al., 1993). Pressure transducers, put in both shoes of the runners, made it possible to determine the step frequency. Data were 200 Hz sampled on a PC computer via an A/D converter (12 bits).

The total mechanical work (W_{tot}) done per kg and per m is the sum of the mechanical work done to move the center of mass (W_{ext}) and the work done to move the limbs relative to the center of mass (W_{int}). W_{ext} was defined within each step as the sum of the CM potential energy changes (E_p) and CM kinetic energy changes (E_k) and was expressed in J per kg per m. W_{int} was obtained with the empirical equation used by Cavagna et al. (1991): $W_{int,norm}$ ($J.kg^{-1}.m^{-2}.s^2$) = $0.1451 \times 10^{-0.2091L}$ where L is the step length expressed as metre.

RESULTS

C_r measured at 3.61 $m.s^{-1}$ was significantly lower than the C_r measured at 5 $m.s^{-1}$ (3.41±0.21 *vs* 3.81±0.17 $J.kg^{-1}.m^{-1}$ respectively, $P < 0.01$; figure 1). On the other hand W_{tot} remained unaltered (3.74±0.35 *vs* 3.85±0.31 $J.kg^{-1}.m^{-1}$ respectively, NS; figure 1). As a consequence, the ratio W_{tot}/C_r was significantly higher at 3.61 $m.s^{-1}$ (1.09±0.05 *vs* 1.01±0.06; $P < 0.05$). The stability of W_{tot} when comparing the two velocities was a consequence of opposite changes of W_{ext} and W_{int}: W_{ext} tended to decrease (2.92±0.36 *vs* 2.87±0,29 $J.kg^{-1}.m^{-1}$ for 3.61 and 5 $m.s^{-1}$ respectively, NS) and W_{int} increased significantly (0.82±0.09 *vs* 0.98±0.12 $J.kg^{-1}.m^{-1}$ for 3.61 and 5 $m.s^{-1}$ respectively, $P < 0.01$).

Furthermore, C_r and W_{tot} were interrelated at 3.61 and 5 $m.s^{-1}$ ($r=0.92$, $P < 0.001$ and $r=0.67$, $P < 0.05$ respectively) (figure 2).

DISCUSSION

The significantly lower (9%) W_{tot}/C_r ratio observed at 5 $m.s^{-1}$ suggests that, in the studied group, net running efficiency was better at 3.61 $m.s^{-1}$. This lower ratio was not due to a decrease in W_{tot}, but to an increase of C_r. The stability of W_{tot} with increasing velocity is in agreement with the previous literature (e.g. Cavagna et al., 1964). On the other hand the significantly lower C_r observed at 3.61 $m.s^{-1}$ was not in line with previous studies of Margaria et al. (1963) and Di Prampero et al. (1986, 1993). In fact the apparent stability of C_r seems to be valid only within a specific velocity range or

limited subject groups. For instance, Di Prampero et al. (1986) were interested by low running velocity (3.45±0.42 and 3.76±039 $m.s^{-1}$ for the two compared groups) and by higher ones in their study of 1993 (4.68±0.58 $m.s^{-1}$) and Margaria et al. (1963) have studied only two subjects. It seems then that the variation of C_r due to velocity and measured for subjects running at the same absolute velocity had never been extensively studied. Therefore, in specific velocity conditions and for a homogeneous group of trained runners like in the present study or in the previous study of Daniels et al. (1977) and Kearney and Van Handel (1989), the C_r stability paradigm could not be confirmed.

Although the significant relationship observed between W_{tot} and C_r at both 3.61 $m.s^{-1}$ and 5 $m.s^{-1}$ (figure 2) underline the importance of W_{tot} in intra-individual C_r differences, the changes of C_r and W_{tot}/C_r ratio observed between 3.61 $m.s^{-1}$ and 5 $m.s^{-1}$ could not be attributed to modifications in W_{tot}. A possible explanation of C_r and W_{tot}/C_r changes could be found in recent work of Cavagna et al. (1991). These authors observed that at 13 $km.h^{-1}$ (3.61 $m.s^{-1}$) the free chosen step frequency correspond to the step frequency at which the step-average power is minimised. It could be thus hypothesized that at about 3.61 $m.s^{-1}$ the net running efficiency was the highest because the energy cost of running is optimized by the step frequency. Elastic energy recoil due to stretch-shortening cycle is an other factor which could influence efficiency (Cavagna et al., 1964). Further analysis of EMG signals during the eccentric and the concentric phases are in progress in order to also determine possible changes in the contribution of stretch shortening cycle.

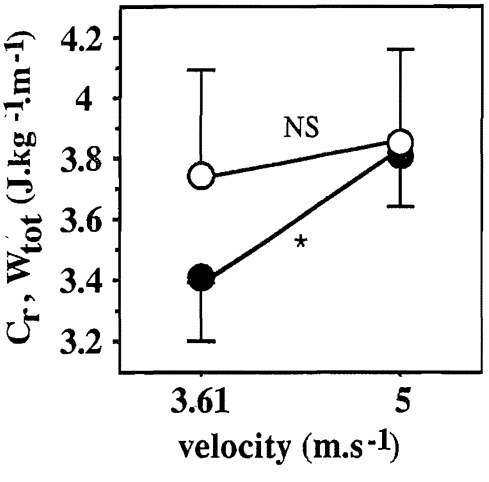

figure 1- evolution of C_r (●) and W_{tot} (○) with velocity.*: $P < 0.01$.

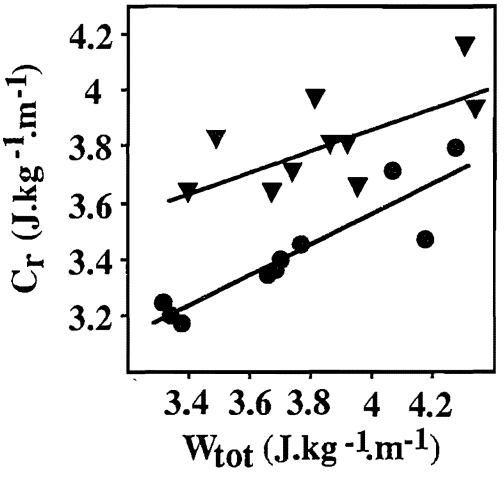

figure 2- relationship between C_r and W_{tot} at 3.61 $m.s^{-1}$(●) and at 5 $m.s^{-1}$(▼).

REFERENCES

Belli A., J. Avela and Komi P.V. (1993) Mechanical energy assessment with different methods during running. *Int. J. Sports Med.* **14**, 252-256.

Cavagna G.A., Saibene F.P. and Margaria R. (1964) Mechanical work in running. *J. Appl. Physiol.* **19**, 249-256.

Cavagna G.A., Willems P.A., Franzetti P. and Detrembleur C. (1991) The two power limits conditioning step frequency in human running. *J. Physiol.* **437**, 95-108.

Daniels J., Krahenbuhl G., Foster C., Gilbert J. and Daniels S. (1977) Aerobic responses of female distance runners to submaximal exercice. In : P. Hilvy (ed) : the marathon: physiological, medical and psychological studies. New-York: Annals N-Y academy sciences, 726-733.

Di Prampero P.E., Atchou G., brückner J.-C. and Moia C. (1986) The energetics of endurance running. *Eur.J. Appl. Physiol.* **55**, 259-266.

Di Prampero P.E., Capelli C., Pagliaro P., Antonutto G., Girardis M., Zamparo P. and Soule R.G. (1993) Energetics of best performances in middle distance running. *J. Appl. Physiol.* **74**, 2318-2324.

Kearney J. and Van Handel P. (1989) Economy: a physiologic perspective. *Adv. Sports Med. Fitness* **2**, 57-90.

Margaria R., Cerretelli P. Aghemo P. and Sassi G. (1963) Energy cost of running. *J. Appl. Physiol.* **18**, 367-370.

GROUND REACTION FORCE AND LOAD RATE HISTORIES DURING DAILY ACTIVITY IN HUMANS

Gregory A. Breit and Robert T. Whalen

Life Science Division, NASA Ames Research Center, Moffett Field, CA, USA

INTRODUCTION

Theoretical models and experimental studies of bone remodeling have identified peak cyclic force levels (or cyclic strain energy density), number of daily loading cycles, and loading (stress or strain) rate as possible determinants of bone density and structure [3]. Estimation of long-term loading histories in humans is usually achieved by assessment of physical activity level by questionnaires, logbooks, and step counters, since the majority of lower limb cyclic loading occurs during walking and running. These methods provide some indication of the mechanical loading history, but fail to consider the true magnitude of the lower limb skeletal forces generated by various daily activities. These techniques cannot account for individual gait characteristics, gait speed, and unpredictable high loading events that may influence bone mass significantly.

The present study describes portable instrumentation to measure and record the vertical component of the ground reaction force (GRF_Z) during normal daily activity. This equipment allows long-term quantitative monitoring of musculoskeletal loads, which in conjunction with bone mineral density assessments, promises to elucidate the relationship between skeletal stresses and bone remodeling.

METHODS

The GRF_Z monitoring system consists of a single capacitance insole force sensor and signal conditioner (EQ; Plymouth Meeting, PA) coupled with a battery-powered data logging system (Tattletale; Onset Computer; North Falmouth, MA) interfaced to a 2-megabyte RAM card and LCD display. GRF_Z data are sampled continuously at a rate of 100 Hz. For short-term high-resolution studies, force data are stored directly to RAM for off-line analysis, allowing for a maximum of 3 hours of data collection. For long-term studies, a real-time algorithm stores only significant force extrema to RAM, increasing the data capacity to approximately two weeks duration. A record of peak loading rate during each significant cycle and a histogram of time at force are also retained in real time. The conditioner and data logging system are packaged together in a single unit, 4.5cm x 6.5cm x 13cm, which is worn on a belt around the waist.

A rainflow sorting algorithm [2] is used to categorize each significant GRF_Z cycle in terms of its magnitude (range) and offset from zero. These data are presented as histograms which summarize the number of cycles counted at a particular range and offset. The peak loading and unloading rate occurring during each significant (range $\geq$0.1 body weights; bwt) force cycle is also summarized in a histogram. These plots are effective tools to visualize cyclic loading histories associated with various activities.

Ground reaction force data were collected from a single subject during three distinct types of activity: 1) 40 minutes of outdoor walking and running; 2) 40 hours of sedentary laboratory work; and 3) 40 minutes of recreational (6 m/s) bicycling.

RESULTS

Figures 1, 2, and 3 show range/offset and load rate histograms summarizing cyclic loading histories for the three types of activity. The vertical axis indicates the total number of cycles which occurred at a particular force range and offset. Cycles which occur at an offset of zero and possess a range $\geq$1.0 bwt are associated with impact loads during gait, with those cycles in excess of 1.8 bwt attributed to running. An electronic step counter worn during data collection for Figure 1 indicated that 2390 steps were taken, which differs by 1% from the total of 2366 found by counting cycles. Cycles offset from zero with ranges <1 bwt usually occur midstance during walking and running. Disparate sub-distributions for walking and running are evident in the load rate histograms as well.

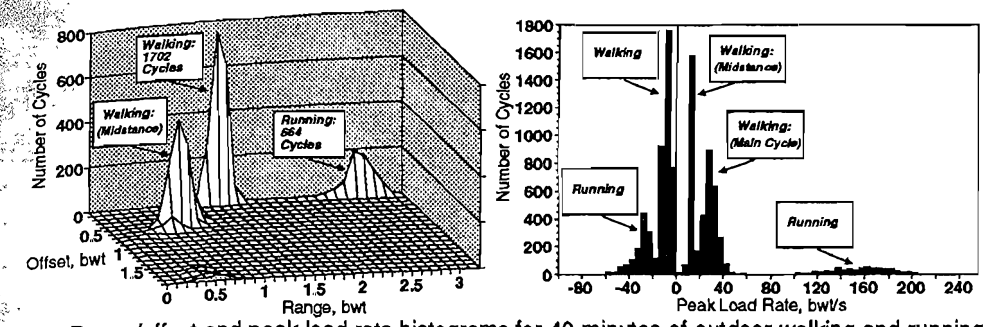

Figure 1: Range/offset and peak load rate histograms for 40 minutes of outdoor walking and running. These two activities are readily distinguishable by their characteristic force and load rate magnitudes.

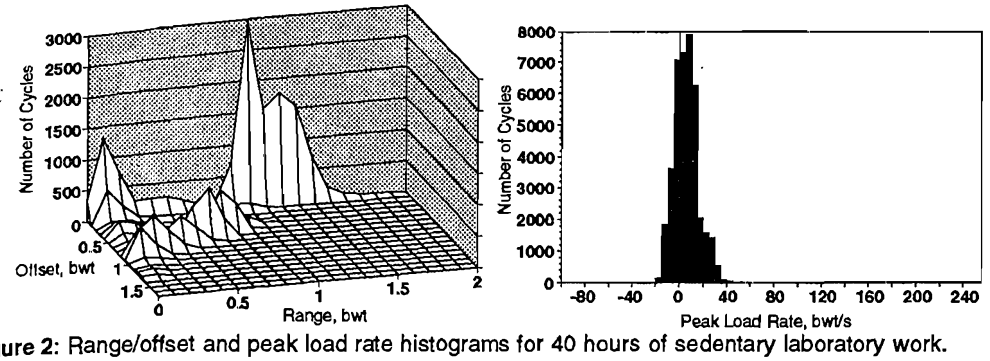

Figure 2: Range/offset and peak load rate histograms for 40 hours of sedentary laboratory work.

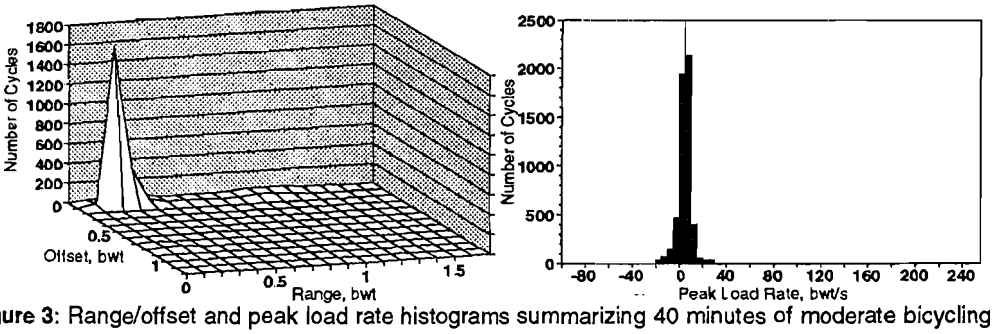

Figure 3: Range/offset and peak load rate histograms summarizing 40 minutes of moderate bicycling.

DISCUSSION

These results show that quantitative short- and long-term histories of physical activity can be collected using a portable, lightweight GRF_Z logger. These histories provide important distinctions between activity types in terms of their lower limb musculoskeletal loading characteristics. For example, the data in Figure 3 suggest that recreational cycling does not generate higher ground (pedal) reaction forces and load rates than sedentary office work. However, differences in limb geometry, kinematics, and energetics of cycling compared to upright gait must be considered before drawing any conclusions about the overall musculoskeletal value of cycling.

Current models of bone remodeling identify cyclic loading as a crucial determinant in skeletal adaptation. Because musculoskeletal forces and load (stress/strain) rates in the lower limbs are determined primarily by the ground reaction force [1,3], the techniques described here give a far more quantitative description of these skeletal loading histories than the traditional descriptive survey-based approach. Accurate determination of long-term GRF_Z histories may be essential to our understanding of the relationship between mechanical loads and bone remodeling and may be a useful approach to examine activity decline with age and its influence on bone density [3].

REFERENCES

1. Biewiener, AA. J. Biomech. 24 (Suppl. 1): 19-30, 1991.
2. Nelson DV and Fuchs HO. Fatigue Under Complex Loading: Analyses And Experiments, (pp. 163-187), SAE, Warrendale, PA, 1977.
3. Whalen RT *et al.* J. Biomech. 21:825-838, 1988.

STATIC BALANCE AND MOTOR COORDINATION IN ELDERLY

Bretz, K. & C.P. Lee
Hungarian University of Physical Education, Budapest

INTRODUCTION

This research is done to collect data on aged adults to lay the foundations of mass investigation and if so to recommend exercises to increase the balance and the motor coordination.
In this study, the displacement of centre of mass, the vertical projection of centre of mass, time function on anteroposterior and mediolateral directions and Fourier Spectra have been recorded with opened and closed eyes. /Bretz K. & R. J Kaske 1994 /

SUBJECTS AND METHODS

For preliminary investigations, 12 volunteer subjects with a mean age of 77 years were tested in the Social Home for the Aged under calm environment without psychological stress. Traditional Romberg test were performed on 2 subjects and the other 10 were tested in a standing position with both arms by the side of the body and feet approximately 10 cm apart. Subjects have no medical history of major musculoskeletal diseases that would impair their ability to stand without assistance.
The equipment we used includes self-constructed "Adam-Type" force platform, Psycho 8 differential measurement device, ADDON microcomputer and a personal computer.

Programme 1
1.1 Static balance test measured by a force plate on-line to a computer system.
1.2 Movement coordination test in connection with the voluntary displacement of centre of mass including an audiovisual biofeedback which consist of 4 motor coordination test.

Programme 2
2.1 Dispersion display of sampled data during the movement of centre of pressure projected on the covering plate of platform completed with time displacement diagrams and Fourier spectra.

The test batteries includes the following protocols.

a) Standing on the platform, looking ahead with both arms by the side of the body with opened eyes and feet width of approximately 10 cm.
b) As in **'a'** but with closed eyes.
c) Traditional Romberg Test
d) As described in 1.2, subjects using the visual feedback from the computer monitor endeavours to fill up a pre-determined area in a definite time span of 20 seconds by voluntarily manoeuvring their centre of mass "Adam" type platform and special electronic system have been used for the investigation.

RESULTS AND DISCUSSION

Table 1 demonstrates the summary of results and Fig. 1 shows the stabilometry dispersion diagram, the displacement-time functions and their Fourier analysis

PARAMETERS	MEAN VALUES AND STANDARD DEVIATIONS
MEAN AGE (years)	77 (10.3)
MEAN MASS (kg)	57.2 (10.7)
HEIGHT (cm)	158.5 (4.7)
BODY SWAY (R1) mm, OPENED EYES	6.3 (1.5)
BODY SWAY (R2) mm, CLOSED EYES	8.3 (2.9)
R2/R1 (%)	138 (64.7)
COORDINATION PERFORMANCE (%)	38.5 (12.5)
TIME PERFORMANCE (%)	79.4 (16.9)

Table 1 (n = 11)

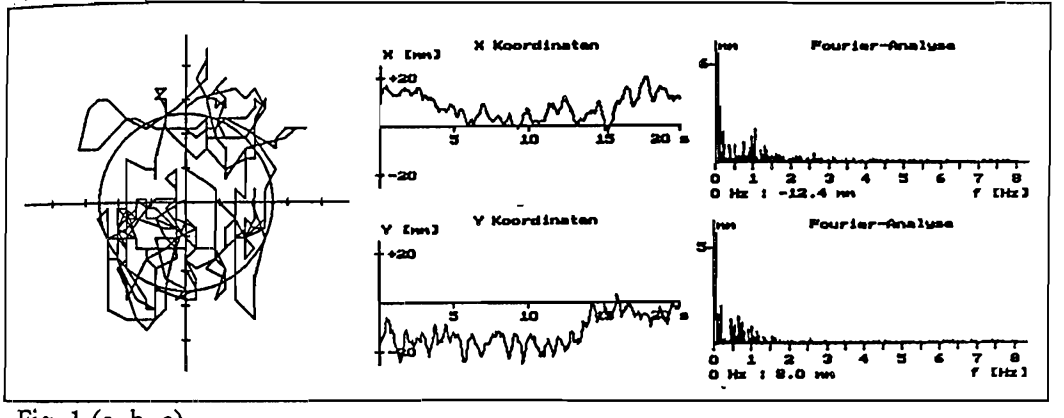

Fig 1 (a, b, c)

Difficulties were prevalent in the biofeedback test batteries with the subjects Test numbers a-c in this protocol were somewhat considered as a motor learning prior to the last test where results were recorded as mentioned in 1.2.

We can conclude that the mean value abstracted in this test of 39% substantiates that motor coordination were significantly impaired. As also shown by other investigators, G.N. Gantchev states that the decreased in muscular force due to fatigue influences the patterns of adaptive postural processes and Bretz, K. et.al.(1994), demonstrated that an increased in muscle tonus after a brief warm up by simple mild running around increases coordination performances in his experimental subjects.

Our findings here suggest that in view of the aspect of possible musculoskeletal deficiencies in relation to the decline of postural balance and motor coordination in the aged, we recommend a specially constructed exercise regiment for the elderly to develop and improve these capabilities.

REFERENCES

- Boloban V.N. /1988/ Sport Acrobatics. Izd. Ob. "Busha Shkola" Kiev. /in Russian/
- Bretz, K & R.J. Kaske, (1994), Some Parameters of Multi-Loop Biofeedback, Control of Posture, World Congress of Sports Biomechanics, Budapest-Siofok Gantchev G.N., (1990) Adaptive Postural Processes During Changes in the Functioning Capacity of Muscular System,, Disorder of Posture and Gait, Edited by Thomas Brandt, et.al., Georg Thiome Verl. Stuttgart, pp.269-276.

AERIAL AND AQUATIC TRAJECTORIES DURING A STROKE IN THE WILD WATER KAYAK.

[1]Brossat L., [1]Rouard A.H., [1]Masset J.B., [1]Monteil K.M., [2]Masson Y.
[1]Centre de Recherche et d'Innovation sur le Sport, University of Lyon I (France).
[2]Fédération Française de Canoë-Kayak, Paris (France).

INTRODUCTION

In 1979, Plagenhoef studied world's best paddlers using slow motion pictures, to describe the optimal stroke pattern. In 1980, Mann & Kearney analysed the speed of the upper limb joints and of the center of gravity during a kayak stroke. Kendal & Sanders (1992) filmed kayak paddlers with hight speed cinematographic camera. They described the upper limb patterns with the new wing paddle. Although these authors agreed with the importance of aquatic events, all kinematics in kayak, concerned mainly the aerial part of the stroke. Only Issurin (1989), investigated the aquatic part of the stroke, with stereostrobophotography to show the displacement of the blade under the water.

In regard to these previous researches, the aim of this study was to observe the trajectories of the hands, and blades during a stroke, in order to examin if the trajectory of the aerial points reflected what occured in the water.

METHODS

Subjects: 11 males wildwater paddlers, international and national level, participated in this study (table n°1).

Table n°1 : Characteristic of subjects

Characteristics	Size (m)	Weight (kg)	Age (year)
Paddlers (n =11)	1.79 (0.086)	67.5. (7.612)	22.41 (4.399)

Test : The test took place in a swimming pool (50m). All subjects realized two passages at race's speed. Every body used the same boat but keep his own paddle. White marks were placed on the tip of each blade and on the two hands.

Data collection : Two blockes of two camcorders (Sony Evo Hi 8, 30 fps) were used. For each block, on the same vertical axis, one camcorder was 35 cm under water and the other, 15 cm upon.The two bloc were fixed with a right angle. To synchronize the views Emetting Diodes lighted simultaneousely in the corner of each lense of each camecorder. A kinematic analysis 3D software (R.E. Schleihauf 1983), was used to digitize frame by frame each trial. The tips of aerial and aquatic blades, the left and right hands were digitized.

Data analyses : Displacements of the tips blades (aerial and aquatic), the right hand (aquatic) and the left hand (aerial) were studied for the stroke (i.e. Pull Time (P.T.): from blade entry to blade exit on the right side). The mean displacement of the 11 paddlers were calculed on each axis, x, z, y, for normalised time (P.T. = 100% for each subject).

RESULTS

Along the antero posterior axis, x, (fig 1): The aerial hand and tip of blade, and the aquatic hand were moving continuousely forward during pull time. The amplitudes of reach was more important for the more external points : the aerial blade and the hand, and less for the aquatic hand. The aquatic tip of blade presented a flat trajectory on this axis and as a result appeared to be fix. The low standard deviations indicated a great homogeneity of the population for all the studied points.

Along the lateral axis, y, (fig 1): The aerial hand and tip of blade, moved on the side during all the pull time. The displacement of the aquatic hand and tip of blade was also on the side in the first time (70%). At the end of the stroke the aquatic blade stayed fix, when the aquatic hand glided ligthly inside. The standard deviations of the aquatic hand and blade were smaller than the aerial one's.

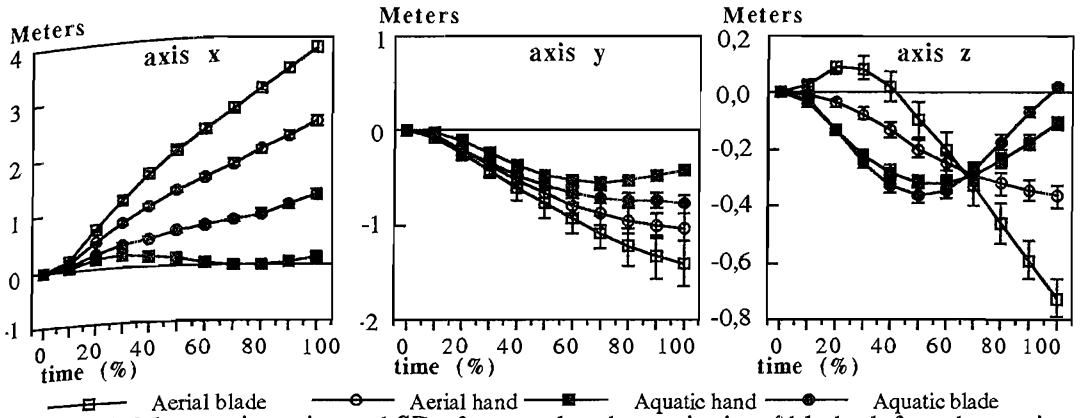

Figure 1. Mean trajectories and SD of external and aquatic tip of blade, left and aquatic hand during pull time on x,y,z, axis. (n=11).

Along the vertical axis, z, (fig 1): The aquatic hand and tip of blade, presented a similar path. They moved down during the first half part of the stroke, and pushed up until the end of the stroke. At the opposite the external tip of blade moved up at the begining of the pull time (25% of PT), and then down until the end of the stroke. In the same time the aerial hand moved down progressively during all the pulling time. The standard deviations were more important for the aerial hand and blade. They increased continuousely during the stroke. The population was more homogeneous for the aquatic hand and blade.

DISCUSSION :

The aerial trajectories observed, confirmed all previous studies as well for the horizontal and vertical axis, (Plagenhoef, 1979), as for the lateral axis, (Kendal & Sanders, 1992). Concerning the aquatic blade a slighty displacement forward was observed. Contrary of Issurin (1989), and Kendal & Sanders (1992), we never found a backward slip behind the entry point during the stroke. As mentionned by these last authors, this non slip movement of the blade reflected the hight level of the population studied. This aquatic blade would be a fixed point to alow the forward projection of the other points and the boat.

On the vertical axis the two blades presented an inversely trajectory around a rotation axis constitued by the aerial hand. This rotation point was previously observed by Plagenhoef (1979), and Mann & Kearney (1980).

As mentionned by Kendal and Sanders (1992), we observed a lateral movement of the aquatic blade wich was stabilised at the end of the stroke. Contrary to the other axis we observed a similar lateral translation for all the studied points.

Only on lateral and vertical axis a similar path for the aquatic hand and the aquatic tip of blade was observed.

The great variation between the subject appeared only for the aerial hand and blade on the lateral and vertical axis. This result could traduce the heterogenity of the subject's expertise level, and the importance of the aerial trajectories in the performance.

In conclusion, the lateral and vertical aerial trajectories seem to be more determinant in the level of performance than the other one. The propulsion in kayak appeared to be organized around different rotation axis : the aquatic blade for the horizontal axis, the aerial hand for the vertical axis.

REFERENCES

1. Plagenhoef, S. (1979). Biomecanical analysis of Olympic flatwater kayaking and canoëing. The Research Quartely, vol. 50, n°3 pp.443-459.
2. Mann, R.Y., Kearney, J.T. (1980). A biomecanical analysis of the Olympic-style flatwater kayak stroke. Medicine and Science in Sports and Exercice, 12(3), 183-188.
3. Kendal, S.J., Sanders, R.H. (1992). The technique of elite flatwater kayak paddlers using the wing paddle. International Journal of Sport Biomecanics, pp233-250.
4. Issurin, V. (1989). Biomechanical aspects of kayak related to strengh. In J Vrijens, J. Verstnyft, and D. de Clercq (Eds.), International Seminar on Kayak-Canoe Coaching and Sciences (pp. 83-91). Budapest, Hungary : International Canoe Federation.

INFLUENCE OF FATIGUE ON IMPACT FORCE AND REARFOOT MOTION DURING RUNNING

Brüggemann, G.-P , Arndt, A., Kersting,U G and Knicker, A.J
Institute for Athletics and Gymnastics, German Sport University, Cologne

INTRODUCTION

Impact force cushioning at touchdown, rearfoot motion control and guidance of the foot during pushoff have been treated as major requirements of technically functional shoes. All studies executed to approach the absolute and relative motion of the rearfoot during diverse sport activities, the loading ground reaction forces or the insole pressure distribution originate with the assumption of constant metabolic circumstances and stable neuromuscular control Studies dealing with the leg-shoe-surface interface did not take into account the muscular and neuromuscular control system of the human being in different metabolic and neural stages.

Therefore the purpose of our approach was to investigate the influence of different stages of peripheral or muscular and central fatigue on micro-control mechanisms and lower extremity function during running.

METHODS

A series of experiments was designed to determine the influence of muscular and central fatigue on lower extremity function during running The first study analysed the influence of local muscular fatigue of the shank muscles on lower extremity function during running. In a second experiment fatigue was induced by running and lower extremity function was examined.Thus in both studies running speed and mechanical properties of the shoes remained constant, whereas the different stages of fatigue were used as experimental variables.

Study no.1: After 5 minutes of adaptation to treadmill running at 3 5 m/s kinematic and kinetic variables and EMG signals of ten subjects were measured Then the shank muscles were locally loaded using a specially designed training device Immediately after the treatment the subjects entered the treadmill again and were examined for a second time. Before and after the treatment kinematic, kinetic and EMG measurements were taken during running on the instrumented treadmill

Study no.2: Ten subjects ran 45 minutes on the instrumented treadmill with a speed of 3 0 m/s. As not every completed the 45 minutes run complete data sets for 35 minutes running were available for further analysis The first data collection was executed after initial adaptation to treadmil running. Further data were collected every five minutes of running.

Data acquisition: Vertical ground reaction forces were measured using an instrumented treadmill (GaitKinetics) which allowed to register the ground reaction forces for both feet seperately An inshoe goniometer registered the rearfoot angle in relation to the shank.The measured rearfoot angle (β) incorporates movements of both the talo-crural and the talo-calcaneal joints. It defines the absolute position angle of the calcaneus relative to the shank. EMG signals from the m. triceps surae, the m. tib. ant., the m. peroneus longus, the m. vastus lat. and the m biceps femoris were preamplified and registered simulaneously with the force and angle data Data collection included 20 footfalls, which were averaged for further analysis. Ground reaction force data reduction included the impact peak force and matching instants in time.

RESULTS AND DISCUSSION

Study no 1: The matching time intervalls indicated a longer contact phase and a trend to a later occurrence of impact peak force induced by fatigue. The ß angles at touchdown increased for all subject with only one exception. The same result came true for the change of the angle ß from touchdown to its maximum. Fatiguing m. tib. ant. and

m peroneus longus seems to be related to a reduction of stiffness of the muscles supporting the ankle joint and thus to a decrease of impact peak force. In addition the ß values at touchdown indicated a lack in muscular control prior to heelstrike after the treatment resulting in an increase of range of motion

The EMG recordings reported a time shift of muscle activation for all analysed muscles to the right. The local fatigue treatment seemed to influence the dorsiflexor muscles as well as the knee extensor muscles. Mean power frequency of the m. vastus lateralis showed the expected decrease, although this specific muscle group was not specially fatigued by the treatment. The five minutes treadmil running combined with 3 minutes of local fatiguing seemed to produce this MPF decrease. The mean power frequency of the locally fatigued m. tibialis anterior increased significantly compared to the data before the treatment. It seems that during the treatment with the used training device the slow twitched fibers of the tibialis anterior muscle have been fatigued and fast twitch fibers of the tib. ant. muscle were recruited in the running after the treatment.

Study no. 2: For the comparison of subjects and different stages of running maximum impact peak of the ground reaction force was normalized to the mean of the second data collection executed 7 minutes after the start.The data indicated an increase of peak force in the first phase of running. This was combined with a small decrease of the time to peak. After this first adaptation the peak forces increased in relation to running or loading time. All mean values were significantly different from the second measurement. The decrease in the maximum impact peak was combined with an increase of time to peak but only the means of the sixth measurement were significantly different from the second measurement.

The rearfoot angle ß at touchdown and the time to maximum of ß showed thorough changes after aproximately 15 minutes of running. The rapid increase in the touchdown ß angle indicate a significant disturbance in the planting action of the foot. The increased time to maximum angle may be interpreted as a fatigue induced effect of the ankle stabilising medio-lateral structures. Both changes could be observed simultaneously.

The mean power frequency of the m triceps surae decreased significantly after the second data collection This indicates the fatigue of this muscle which might be correlated to the above discussed drecrease of the pushoff force.

In the 150 ms intervall prior to touchdown the mean power frequency of the m vastus lateralis decreased after approximately 7 minutes of running. Minimum values occured when data collection was performed for the third time, i e. after approximately 12 minutes of running This coinsided with the above discussed changes of the patterns of the rearfoot angle ß.

The changes of the mean power frequency of the m. vastus lateralis during the stance phase showed a very similar pattern as during preactivation This indicated a substantial fatigue of the knee extensor muscle after approximately 12 to 15 minutes of running in our subjects, which represent normal joggers .

CONCLUSION

Muscular fatigue was induced in both experiments and detected by a decrease of MPF. Muscular fatigue is related to a decrease of impact peak forces and to changes in rearfoot kinematics Therefore stiffness regulation is effected by fatigue. From the results it can be concluded that impact peak force and rearfoot motion is stongly correlated to stiffness control of the neuromuscular system.

LITERATURE

Nicol, C., Komi, P V. and Marconnet, P (1991). Fatigue effects of marathon running on neuromuscular performance Scand J. Med Sci. Sports, 1, 10-17

Nigg, B.M and Segesser, B (1992) Biomechanical and orthopedic concepts in sport shoe construction. Med Sci. Sport and Exercise, Vol.24, 5, 595-602

A NOVEL TECHNIQUE TO DETERMINE INTERFRAGMENTARY MOTIONS IN INTERNALLY FIXED FEMORAL FRACTURES

Brunner P, Bekic J, Lustenberger A, Nolte LP

M.E. Müller Institute for Biomechanics, University of Bern, Switzerland

INTRODUCTION

Postoperative stability of fracture fixation devices has previously been evaluated by performing *in vitro* stiffness measurements of the bone-implant construct. Despite increased recognition of the role of interfragmentary motions in the understanding of fracture healing, detailed description of the complex multidirectional movement in fracture fragments is not available [1]. The purpose of this study was to develop an *in vitro* technique for direct measurement of the six independent components of motion of fracture fragments and fixation devices in femoral fractures under quasi-physiologic loading conditions. The system was applied to measure and record clinically relevant motions in proximal femoral fractures stabilized with two different fracture treatment methods.

METHODS

Specimens: Five single and twenty paired fresh human cadaveric femora (Mean age: 70.2±13) were examined radiographically and by DEXA densitometry for grouping. Donor bodyweight was used to calculate experimental testing loads. *Fracture Models:* The fractures were modeled according to the AO/ASIF-Classification of Fractures: a) Three-part intertrochanteric fracture (5 pairs), b) Four-part intertrochanteric fracture (5 pairs), and c) Subtrochanteric fracture (5 bones). *Fixation Devices:* For the treatment of intertrochanteric fractures one side of a femur pair was fixed with a sliding hip screw DHS (Synthes, Paoli, USA), which is currently in clinical use. The contralateral side was fixed with a prototype intramedullary implant (IM) of the Gamma nail type. Unstable subtrochanteric fractures were treated with the medullary implant design (IM). *Femoral Loading*: A custom loading jig was mounted in a biaxial servohydraulic material testing machine. Quasi-physiologic axial and torsional loads were applied simultaneously [2]. Specimens were cyclically loaded using a sinusoidal waveform at 0.5Hz for the cranio-caudal force and at 0.25Hz for the antero-posterior force. Cranio-caudal peakloads were chosen at levels of 50%, 100%, 150% and 300% bodyweight (BW) with 3000 cycles in each increment. Antero-posterior force was 10% of the cranio-caudal force. *Motion Measurement*: Previous studies validated the reliability of an optoelectronic system for the measurement of joint kinematics [3]. In the present study the LED (light-emitting diode) based 3-D motion analysis system Optotrak (Northern Digital, Waterloo, Canada) was used. Its high spatial resolution allows the measurement of motions with an accuracy of 0.1mm in translation and 0.1° in rotation. Assuming rigid body motion, proximal and distal fracture fragments and fixation devices were instrumented with marker carriers, each with three noncollinear LEDs. Rotations and translations of clinical interest were: Varus deformity, rotational deformity in femoral shaft and neck axis, rotational instability of the implant in the femoral head or proximal fragment impaction. Local coordinate systems given by the anatomy were identified. A space digitizer was used to detect coordinates from anatomical landmarks in the frontal and sagittal plane of the femur, from which body fixed local coordinate systems, lying in the femoral shaft and neck axis, could be computed. During testing all marker positions were collected at a frame rate of 20Hz.

Data analysis: To uniquely describe the relative motion of the rigid bodies, the use of Euler angles was most convenient. A custom computer program, including Optotrak data analysis routines, was written to perform local coordinate transformations to anatomical local coordinate systems and to calculate motions of interest from collected marker position data. Two-tailed paired t-test was used to evaluate differences in the stability of the fracture treatment concepts.

RESULTS

The test series showed successful determination of the movements occurring at the fracture gap. In general, deformations remained approximately constant at each loading level and increased with higher loads (Fig.1). The data were reduced to show the envelope curves of mean data and high/low levels during cyclic loading.

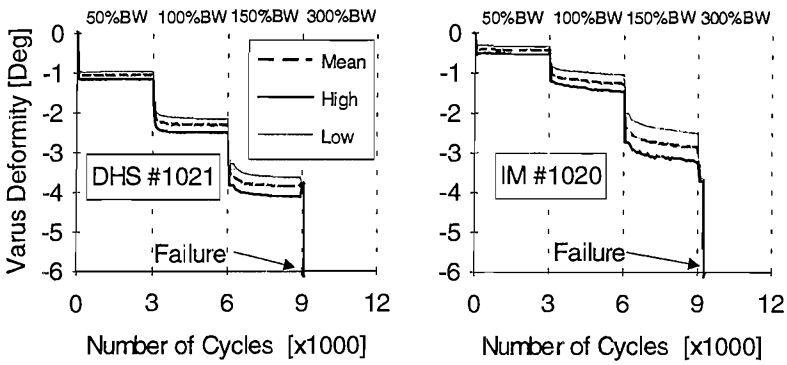

Fig.1: Typical varus deformity data for a 3-part fracture test

Fracture implant inherent mechanical characteristics could be detected: Rotational instability and/or lateral gliding nail were measured. Nevertheless, overall results of the two implant systems for the trochanteric fractures were not significantly different ($p>0.05$).

DISCUSSION

Previous investigators have used highly sensitive measurement systems to monitor motions of fracture fragments [4]. However, the instrumentation used has typically been limited to one or two selected degrees of freedom. In any type of motion analysis systems the accurate definition of the embedded local coordinate systems is essential for reliable and comparable estimation of relative motion between fragments. The use of an optoelectronic motion tracking system in combination with space digitization of anatomical axes and local rigid body concepts provides a convenient and accurate means for the measurement of interfragmentary motion in femoral fractures in three dimensions.

REFERENCES

[1] McKellop H et al., *J Bone Joint Surg* 75A, 1019-25 (1993)
[2] Bergmann G et al., *J Biomech* 26(8), 969-90 (1993)
[3] DeLuzio KJ et al., *J Biomech* 26(6), 753-9 (1993)
[4] Wainer RA et al., *J Orthop Trauma* 4, 58-63 (1990)

ACKNOWLEDGMENTS

This work was supported by the AO/ASIF-Foundation

A NEW FREEZING TECHNIQUE FOR THE FIXATION OF SOFT CONNECTIVE TISSUES IN *IN VITRO* BIOMECHANICAL TESTING

Brunner P[1], Schatzmann L[1], Rincón L[1], Stäubli HU[2], Nolte LP[1]

[1]M.E. Müller Institute for Biomechanics, University of Bern, Switzerland
[2]Orthopaedics and Traumatology, Surgical Clinic Tiefenauspital, Bern, Switzerland

INTRODUCTION

Fixation of soft connective tissue for biomechanical testing is difficult without tissue damaging. The quality of the fixation is essential for *in vitro* testing of structural and mechanical properties of the tendon. Different concepts of soft tissue fixation by a variety of suturing techniques, clamping devices are in use but fail in high load testing when slippage of specimen or premature failure at the fixation site occur [1, 2]. The fixation of frozen specimen ends has shown the potential for use in such testing [3, 4]. It was the aim of this study to develop a new freezing technique for soft connective tissue testing and to validate its applicability in failure testing of two autogenous ACL substitutes.

MATERIALS AND METHODS

The new device, called 'Cryofix', consists of an aluminum block (80x80x50mm) with a cylindrical (∅ 25mm) central hole. Before testing this block was cooled down by submerging it in liquid nitrogen (-196°C). The end of the specimen to be tested was looped around a 3mm transverse bar of a cylindrical central piece which tightly fits into the hole in the aluminum block. After insertion of the central piece in the block the resulting cavity around the specimen was filled with water. Immediately the formation of an ice block around the specimen end started, resulting in a secure fixation after approximately one minute.

16 pairs of quadriceps tendons (QT) and patellar ligaments (PL) from human cadavers were prepared as for the use in ACL repair. The patella was cut in half resulting in a remaining bony end for each of the specimens. The proximal end of the QT and the distal end of the PL were fixed with the new Cryofix. Mechanical failure testing was performed in a uniaxial tensile test in a servohydraulic materials testing machine. The deformation rate was chosen 1 mm per second. Displacement and load data were recorded from which ultimate load could be derived.

To study the potential of the Cryofix for long term testing the development of the temperature over time was measured with a PT100 temperature sensor placed in the aluminum block cavity where the ice was formed. An additional specimen was used for this test.

RESULTS

The mean ultimate loads and the failure modes of the quadriceps tendons and the patellar ligaments are shown in Table 1. Most of the failures occurred at the mid-substance, 10 mm above the Cryofix site, with no slippage or rupture observed in the fixation zone. Three specimens had an avulsion failure at the patella and data from three specimen were missing due to data recording problems. Mean ultimate load for all tested transplants was 2220 ± 445 N (Mean ± SD). One measurement showed the ultimate load of 2551 N for the quadriceps tendon and one resulted in 3401 N for a patellar ligament specimen.

Specimen	Failure Modes			Ultimate Load [N]
	Mid-Substance	Avulsion	Missing	
QT	13	2	1	2269 ± 543
PL	13	1	2	2168 ± 322

Table 1: Overview of failure modes and ultimate loads (Mean ± SD) in tensile testing

The temperature measurement shows the data for the ice block which has been formed after filling the water into the cavity of the supercooled aluminum block (Figure 1). The ice reaches its lowest temperature of -115 °C after 3 minutes and gradually increases towards 0 °C within the next 60 minutes.

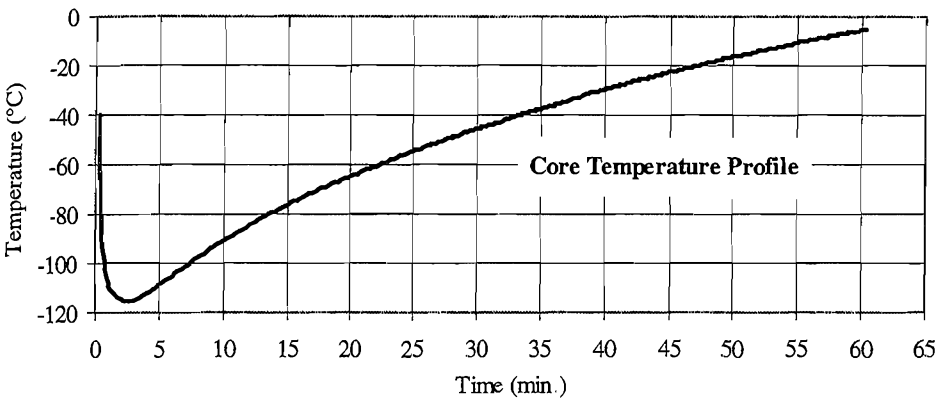

Fig. 1: Measurement of the core temperature in the ice block of the Cryofix

DISCUSSION

The new technique was found to be suitable to perform failure testing of ligaments and tendons in loading ranges of more than 3000 N Due to the high heat capacity and the size of the aluminum block it was possible to keep the temperature at the fixation site low. No thawing occurred during more than one hour. This might also make the Cryofix applicable in long-term studies, where preconditioning effects or cyclic loading should be studied. However due to the very low temperatures at the fixation site and the growth of the frozen zone towards the center of the specimen, detrimental effects on the biomechanical properties may result from longer testing duration.

REFERENCES

[1] Haut RC et al., *J Biomech Eng* 105, 296-299 (1983)
[2] Bonutti PM et al., *Clin Orthop* 229, 241-246 (1988)
[3] Riemersma DJ et al., *J Biomech* 15(8), 619-620 (1982)
[4] Liggins AB et al., *J Biomed Eng* 14, 440-441 (1992)

ACKNOWLEDGMENTS

This study was supported by the Swiss National Science Foundation.

MOMENT ARMS OF MUSCLES AT THE KNEE

W.L. Buford, Jr., F.M. Ivey, R.M. Patterson, G. L. Peare, D. K. Nguyen
Orthopaedic Biomechanics Lab, University of Texas Medical Branch,
Galveston, TX, USA

INTRODUCTION

To date the emphasis in prosthetic joint replacement has been in the development of compatible materials and geometries for the bone prosthesis interface. Very little attention has been paid to implant design based upon kinematic reconstruction or the expected forces and moments generated on the structures of the joints during daily activities. This report represents efforts to develop a uniform description of effective knee joint kinematics with a determination of muscle tendon moment arms for the normal knee, the ACL-minus knee, and two knee-prosthesis combinations. The results will improve our understanding of normal knee mechanics, help to describe specifications for improved prosthesis design, and define the effects of knee prostheses on muscle mechanics.

MATERIALS AND METHODS

A monitoring jig was designed for movement of the lower leg about the femur, monitoring of angular position, and measurement of muscle tendon displacement throughout the range-of-motion. Angular position was measured using single turn precision potentiometers about a flexion-extension (FE) axis and longitudinal rotation (LR) axis as described in [1]. Muscle/tendon excursions for all Knee muscles were measured using similar potentiometers connected to pulleys with weights providing tension. Effective muscle moment arms about both axes were calculated from this data using the tendon and joint displacement method described in [2].

Normal, adult, fresh, intact, lower extremities were utilized. Wire leaders through plastic tubing were sutured to the tendon insertions of the following muscles: sartorius, rectus femoris, vastus lateralis, vastus intermedius, vastus medialis oblique, patellar ligament, short and long head of biceps femoris, semitendinosus, semimembranosus, gracilis, popliteus, and medial and lateral gastrocnemius.

An O Ethibond running suture was then used to secure the cable sheath along the muscle belly. In certain muscles it was necessary to pass the leaders through drill holes in the pelvis to ensure a direct path with each muscle. The hemipelvis and thigh were secured in the support jig with 5mm threaded half pins. The hip and ankle were both fixed at neutral.

The excursion and angle measurements were determined for the normal knee by passively flexing the knee to maximal flexion, then gradually extending the knee to full extension and repeating this cycle several times per sample period. A real time data acquisition system (National Instruments, AT-MIO-16X A/D board, using LABView software) was used to measure potentiometer voltages of 16 channels during movement - one channel each for flexion/extension, longitudinal rotation, and excursion of 14 muscle/tendon units.

The anterior cruciate ligament (ACL) was then sectioned. The same testing sequence performed on the normal knee was repeated so that the moment arms could be calculated. Posterior cruciate sparing total knee arthroplasties were then performed according to standard protocol. The leaders were reattached and the knee tested using the same procedures as in the normal and ACL deficient knee.

Finally, the prostheses were revised to posterior stabilized total knee

arthroplasties and the moment arms were again determined according to the previously outlined sequence.

RESULTS

Data treatment included conversion of voltages to angles and excursions and smoothing with a five point running average. The moment arms were calculated using a polynomial least squares smoothed derivative applied to excursion and angle versus time ($dr/d\theta = dr/dt \div d\theta/dt$). The muscle excursion and moment arm for the normal knee, ACL deficient knee, uncemented PCL sparing knee, and cemented PCL sacrificing knee was then plotted for each muscle. Average moment arms for six sweeps through flexion-extension of the Vastus Medialis in each of these conditions are plotted in the Figure.

SUMMARY AND DISCUSSION

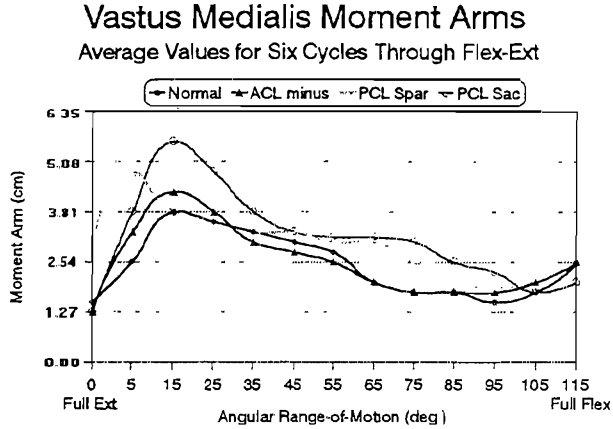

- There was no significant difference in range-of-motion for the Normal, ACL minus, or prosthetic knees.
- Total muscle excursion increased in the arthroplasties (5.7% PCL sparing, and 5.0%, PCL sacrificing).
- Concommitant with increased excursion is an increase in most muscles moment arms.
- There was a shift in moment arm balance; for example, most notably favoring extension over flexion for the arthroplasties.
- With continuous acquisition of data during multiple sweeping knee motions this study confirms the stochastic nature of muscle-tendon-skeletal motion.

The general shape of each muscles excursion and moment arm curve (for the normal knee) agrees somewhat with earlier reported data in the literature [3]. However, no reports to date have studied these parameters using fresh, hemipelvis (ankle and hip intact) specimens, with measurement during leg motion, following arthroplasty. Hopefully, these results more closely simulate physiologic motion and the information gleaned from determining the moment arms can be used to predict the forces acting upon a normal or prosthetic joint and thus influence future prosthesis designs. Also, these results provide a clearer understanding of the effects prostheses have on muscle balance.

REFERENCES

1. An, K.N., et al (1984), *Trans of the ASME*, **106**, 280-282.
2. Hollister, A.M., et al (1993), *Clin Ortho and Related Res*, **290**, 259-268.
3. Spoor, C.W., and J.L. van Leeuwen (1992), *J. Biomechanics*, **25:2**, 201-206.

ACKNOWLEDGEMENTS

This work is funded by Intermedics, Inc., of Austin, TX, and research gifts from Zimmer-Jones and Associates, and Biomet-Omni Medical, both of Houston, TX.

THREE-DIMENSIONAL MOTIONS OF FEMORAL PROSTHETIC STEMS: AN *IN VITRO* EVALUATION OF A NOVEL MEASURING CONCEPT

Bühler DW, Brunner P, Berlemann U, Nolte LP

M.E. Müller Institute for Biomechanics, University of Bern, Switzerland

INTRODUCTION

Primary stability of uncemented total hip replacements is regarded a major factor for the quality of bony ongrowth to the femoral stem and therefore for the long-term outcome [1, 2]. Micromovements as well as eventual subsidence of the prosthesis have to be considered under cyclic loading conditions. Most of the existing measurement strategies, e.g. based on micrometers, extensiometers, LVDTs, and/or strain gauges provide only information about one component of the three-dimensional (3D) motion at the bone-implant interface [3, 4]. Furthermore, fixation of sensors away from the point of interface motion measurement, as seen in various studies, may result in registration of superimposed motion due to elastic deformation of the femoral or prosthetic shaft. The objective of this study was to develop, validate, and apply a new technique which allows the precision measurement of the pure 3D interface motion at three different points along the femoral shaft.

MATERIALS AND METHODS

The measuring technique is based on a sensor combining optoelectronic with precision mechanical components. Spherical measuring tips of three sensors are placed on the prosthesis at predefined locations: tip of the prosthesis, middle third, and upper third of shaft. The measuring positions are relocated using components of a computer-assisted surgery system recently developed by our group. The sensors are mounted on a custom micro-positioning table which is anchored using a transverse 9 mm hole drilled in the cortex exactly centered over the measuring location. Precision ball bearing mechanics allow transition of the detected motion to a laser diode on the opposite end of the sensor. Photons emitted by this LED are registered by a silicon position sensitive detector (PSD). 3D motion analysis is made possible by considering output data of the PSD (x/y-axis) as well as the registered light intensity (z-axis). Thermistors are also integrated to exclude thermodrifts during long-term testing of the prostheses. Custom software based on LabView (National Instruments, Austin, USA) allowed for real-time graphical display of the applied forces and the detected movements. Static and dynamic validation indicated a maximal system error of ±4µm within a measuring range of ±750µm in each spatial orientation. Seven paired fresh cadaveric femora were used for testing of two different types of uncemented femoral stems: CLS stem (Spotorno) and Cone Prosthesis (Wagner; both Protek AG, Switzerland). Following implantation of the prosthesis the femora were subjected to sinusoidal cyclic loading in a two-axial materials testing machine. A cranio-caudally directed force F_{cc} with the frequency of 1 Hz was combined with an anterior-posteriorly directed force of 0.5 Hz measuring 10% of F_{cc}. Loading steps of 1-, 2-, 3- and 4-fold bodyweight were applied.

RESULTS

The micromovements of the Cone prosthesis showed a significantly smaller amplitude in all three spatial orientations indicating larger "micro-stability" compared to the CLS prosthesis (Fig. 1a, b).

Using the maximum, minimum, and mean Z-data value of each loading cycle the resulting graph indicates the subsidence during testing (Fig. 2). Both prostheses showed relative stability under the 1- to 3-fold body weight loadings. However, the 4-fold body weight caused a considerably increased subsidence mainly for the Cone prosthesis indicating less "macro-stability". In some cases with low bone mineral density the femur finally fractured under the maximum load at the tip of the prosthesis.

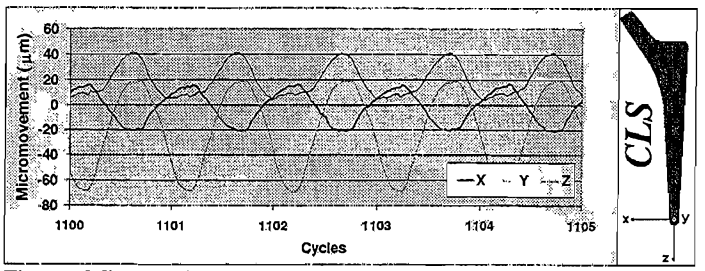

Fig 1a: Micromotion at prostheses tip / CLS

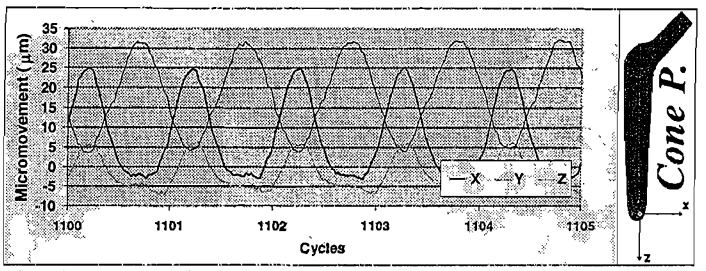

Fig. 1b: Micromotion at prostheses tip / Cone Prosthesis

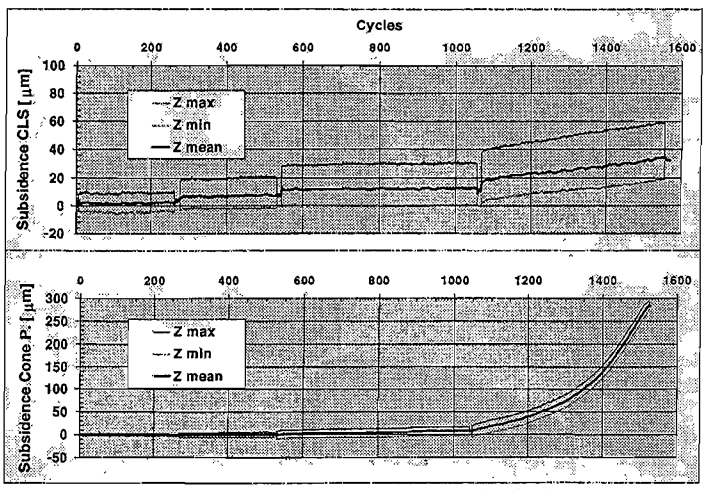

Fig. 2: Subsidence of CLS (top) and Cone prosthesis (bottom)

DISCUSSION

Our novel technique provided reliable and accurate data illustrating the pure 3D interface motion of uncemented femoral stems. Considerable differences in the "micro- and macro-stability" of two prosthesis types could be detected. For statistical evaluation the quasi-physiological 1- to 3-fold body weight loadings should be considered primarily, whereas the 4-fold body weight seems to represent an unphysiological and destructive loading. Analysis of different concepts of femoral stems with the presented standardized approach may further elucidate the role of primary stability for the long-term clinical outcome.

REFERENCES

[1] Whiteside LA, *Clin Orthop* 247, 138-147 (1989)
[2] Pilliar RM et al., *Clin Orthop* 208, 108-113 (1986)
[3] Whiteside LA et al., *J Arthroplasty* 8, 147-155 (1993)
[4] Nunn D et al., *J Bone Joint Surg* 71B, 452-455 (1989)

ACKNOWLEDGEMENTS

This study was supported in part by Protek AG, Münsingen, Switzerland.

3-D KINEMATIC STUDY OF THE CRUCIATE-DEFICIENT KNEE

Bull A.M.J, Targett J, Andersen H.N, Amis A.A.

Imperial College, London, England

INTRODUCTION

In clinical practice the pivot shift sign is a reliable indication of anterior cruciate ligament (ACL) deficiency and correlates with symptomatic instability. The pivot shift involves a forward subluxation of the lateral tibial plateau on the lateral femoral condyle near full extension and under a valgus load, followed by an abrupt reduction of the subluxation at 30° knee flexion. In vitro studies of the motion of ACL deficient knees under various loads have shown this tibial subluxation with a shift of the axis of rotation from the centre of the tibia towards an intact medial collateral ligament (Matsumoto, JBJS 1990; 72-B: 816-821).

The purpose of this study was to reproduce the clinical pivot shift in cadaver knees and to vary the applied loads in order to measure the relative contribution of valgus torque and iliotibial tract tension on the resulting motion. We measured 3-D motion as a dynamic analysis of actual pivot shift motion, because the pivot shift instability arises as a result of patient motion. Our review of the literature shows that this analysis has only been done statically before.

METHOD

Nine freshly frozen knees were prepared. The femur and tibia were cut to 180mm and potted using PMMA with a 600mm rod fixed in the tibia. The femur was clamped with the flexion plane of the knee horizontal and the lateral aspect facing down. The iliotibial tract was loaded via a pulley and weights were hung on the tibial rod to vary the valgus torque up to 13Nm. Varus torque up to 10Nm was applied via a pulley held above the tibial rod. Potentiometers measured tibial rotation and knee flexion. For each varus/valgus load the iliotibial tract was loaded at 10, 20, 30 and 40N and the knee was flexed from extension to full flexion. Data was collected on a personal computer. Every test was repeated five times and mean curves of tibial rotation against flexion angle were produced. The ACL was excised and the tests repeated. Knees with gross rotational instability had the ACL reconstructed using an APEX ligament routed over the top of the lateral femoral condyle. Implant tension of 5N was fixed at 45° flexion. After reconstruction the tests were repeated. For each condition the stability of the knee was assessed by an anterior-posterior (a-p) drawer test of ±150N at 20 and 90° flexion in a 4 d.o.f. fixture in an Instron tensile testing machine.

RESULTS

Following ACL section four of the nine knees displayed the pivot shift, two showed an increase in internal rotation and three had no significant change in rotation. Reconstruction abolished the pivot in all those knees in which it occurred, but did not reduce the increased internal rotation at flexion angles greater than 45° in three knees. The reconstruction restored normality in the a-p drawer test at 20° (Fig. 2): at 90° the knees still displayed some increased a-p laxity (Fig. 3). Three knees were not reconstructed due to their inconsistent rotational behaviour .

From our results we describe the pivot shift as a sudden external rotation of 34 (21-40)° over a flexion range of 8 (2-10)°. The pivot shift was seen between 30-65° flexion. The balance between applied valgus and iliotibial tract loads was critical and variable for each knee in producing the pivot shift and the angle at which the pivot shift

occurred; it could be abolished by changing either the valgus or the iliotibial tract or both loads by one increment. In those knees where a pivot was not obtained following ACL section the anterior draw displacements were less than those which did pivot, although with the small numbers this did not reach significance.

Examples of results in three knees:

(i): External rotation throughout knee flexion;
(ii): The lateral pivot shift;
(iii): Lateral tibial subluxation throughout flexion.

These results are shown in Fig. 1.

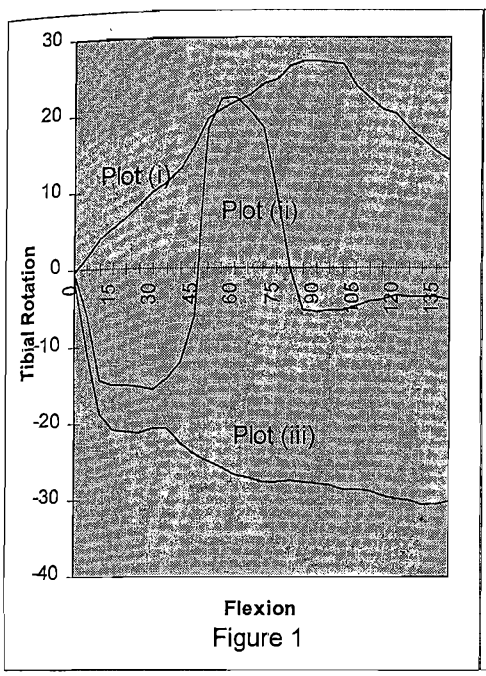

Figure 1

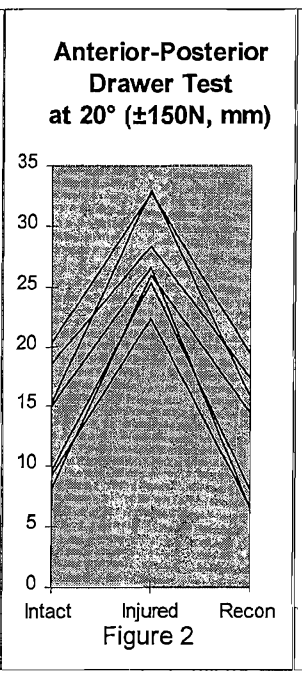

Figure 2

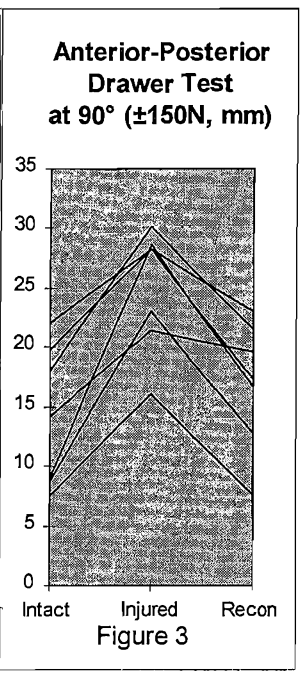

Figure 3

DISCUSSION

We have successfully produced and described the pivot shift in terms of tibial rotation against flexion angle in this cadaveric study. The magnitude of iliotibial tract and valgus loading has been shown to be critical in producing a pivot and these values vary between individual knees. Of those knees which did not exhibit a pivot shift following ACL section one feature of note was the relatively greater resistance to anterior draw displacement. Other factors which may contribute to this rotational instability include the convexity of the lateral tibial plateau, the contribution of the lateral meniscus and the effect of the secondary restraints to internal tibial rotation.

The ACL reconstruction successfully restored normality to the knee, except at the expected higher flexion angles as the routing was over the top of the lateral femoral condyle.

Whilst this study has produced an in vitro pivot shift, this instability in the laboratory cannot be easily compared with the clinical pivot shift sign, because it is the authors' belief that the clinical loading conditions are variable and not as consistent as is possible in the laboratory.

FOOT PROFILE OF COMPETITIVE ADOLESCENT FEMALE BASKETBALL PLAYERS AND RELATED FOOTWEAR CONSIDERATIONS

M J Burgess-Milliron and J A Healy

Biomechanics Laboratory, Converse Inc , N Reading, MA U S A

INTRODUCTION

The foot structures of athlete populations have been studied by a limited number of investigators (Robinson, et al , 1984, Bednarski, et al , 1987, and Milliron & Betty, 1993) These studies have focused primarily on college and adult age groups, with Bednarski providing the only investigation specific to the foot structure of female athletes Information on foot dimensions of particular athlete groups assists in the determination of proper fit and functional design of athletic footwear The fit of the shoe is dependent on the shape of the last, the three-dimensional form representing the foot in the shoe making process

The purposes of this study were (1) to provide normative foot dimensions of competitive adolescent female basketball players, (2) evaluate the change in foot parameters across a range of foot lengths, and (3) determine the level of predictability of foot dimensions based on foot length The first purpose provides information to compare to other groups in distinguishing foot dimension patterns Evaluation of the changes in foot dimensions and predictability of measures based on a given length can be applied to the development of improved last dimensions and grading schemes specific to the needs of this athlete group to improve fit and performance

METHODS

One hundred and three female competitive basketball players at an invitational basketball camp agreed to participate in this investigation Each subject provided self-reported age, height, mass, and lower extremity injury history Direct anthropometric measures were taken of the right and left feet Direct measures included (1) ball girth (BG) girth across the maximal prominences of the first and fifth metatarsophalangeal (MTP) joints, (2) short heel girth (SH) girth around the posterior - inferior aspect of the heel and the dorsal junction of the foot and leg, (3) foot length (FL) distance from the distal tip of the longest toe to the most posterior aspect of the heel, and (4) ball width (BW) linear distance from the most prominent aspect of the first MTP joint to the most prominent aspect of the fifth MTP joint Average and standard deviation (SD) values for each direct anthropometric measure are reported normalized to FL of the same foot To evaluate potential grading schemes, the extreme portions of the right foot length measures for this subject group were evaluated Extremes were defined on the smaller end of the range as all measures less than -1SD of the FL mean (SHRT) and on the higher end as all values greater than +1SD of the FL mean (LONG) FL data for the subjects centering around the mean within 1SD in each direction are referred to as CNTR Evaluation via regression analysis was made of the predictability of FL for the BG, BW, and SH measures in the SHRT, CNTR, and LONG groups

RESULTS

The average age of the subjects was 15 56 $\pm$ 0 65 years The subjects had an average height of 171 23 $\pm$ 18 73 cm and mean mass of 61 28 $\pm$ 10 31 kg Sixty-two percent of the subjects reported a history of injury Reports of ankle, foot, and knee injuries were 78 1%, 17%, and 15 6% respectively Multiple injury sites were reported by 15 6% of the subjects The most common type of injury was sprains reported in 64 1% of the cases, followed by ligamental injuries (18 8%), fractures (14 1%), and stress fractures (9 4%)

Direct anthropometric measures of FL and normalized values of BG, SH, and BW for the right and left extremities are reported in Table I No significant differences were found between right and left foot dimensions

Foot dimensions normalized to FL were examined (Table II) for the SHRT, CNTR, and LONG groups The trend indicated that as the FL increased from the lower extreme to the upper extreme group, the ratios decreased

Regression analysis of BG, BW, and SH to FL for the CNTR group indicated moderate correlations of 0 41, 0 44, and 0 63 for the respective dimensions The relationships for the extreme SHRT group fell to 0 15, 0 38, and -0 16 for BG, BW, and SH, respectively and 0 19, 0 21, and 0 56 for the LONG group

Table I Direct anthropometric measures normalized to foot length (FL) (Avg±SD)

Measure	Right	Left
FL (mm)	25.3 ± 1.32	25.4 ± 1.40
BG / FL	0.92 ± 0.04	0.92 ± 0.04
SH / FL	1.27 ± 0.04	1.26 ± 0.05
BW / FL	0.36 ± 0.02	0.36 ± 0.02

Table II Normalized values for SHRT, CNTR, and LONG groups (Avg ± SD)

Measure	SHRT	CNTR	LONG
FL (mm)	23.54±0.35	25.35±0.79	27.60±0.62
BG / FL	0.95±0.03	0.93±0.04	0.87±0.04
SH / FL	1.29±0.05	1.27±0.04	1.24±0.04
BW / FL	0.37±0.01	0.36±0.01	0.34±0.02

DISCUSSION

Sixty-one percent of the female adolescent athletes studied had an injury history, primarily ankle sprains The direct foot measurements were symmetrical and can be related to data of other populations to determine if last differentiation is required

Evaluation of the data in regards to last development indicates several points The comparison of ratio data in the extreme groups (SHRT vs LONG) shows that as foot length increases, girth and width measures decrease proportionately This finding suggests that developing a last with proportionately smaller width and girth dimensions for larger shoe sizes would provide an improved fit for this group Further investigation of the correlations between the various foot dimensions and FL however, indicate that the predictability of BW, BG, and SH measures by FL alone are moderate for the subjects centering around the average value of FL (CNTR) and become less predictable in the extreme groups

These data indicate that though a trend is seen for a proportionately smaller girth and width measures with increased foot length, foot length alone does not accurately predict the foot girth and width for a given size Moreover, at extremes the predictive qualities deteriorate Footwear development therefore must continue to provide adjustable fit systems throughout the size range of shoes, particularly at the extremes for this population Further evaluation of footprint and other anthropometric measures may prove useful in providing predictive sizing equations for the determination of optimal grading schemes in footwear development

REFERENCES

Bednarski, K N , Bunch, R P , and Cairns, M A (1987) Foot Morphology of women athletes Implications for last development B Jonsson, (ed) Biomechanics X-B, Human Kinetics Champaign, IL, 913-918

Milliron, M J and Betty, S D (1993) Foot profile of elite adolescent male basketball players 2nd World Congress of Biomechanics Proceedings, Amsterdam, Netherlands

Robinson, J R , Frederick, E C , and Cooper, L B (1984) Running participation and foot dimensions Medicine and Science in Sports and Exercise, 16(2), 200

The authors would like to acknowledge the assistance of C. Edington, S Betty, and R. Croce for their help in data collection and analysis.

THE EFFECTS OF NURSING TASKS ON SPINAL SHRINKAGE

Caboor D., Zinzen E., Van Roy P., Clarys J.P.
Department Experimental Anatomy, Vrije Universiteit Brussel, Laarbeeklaan 103, 1090 Brussels, Belgium

INTRODUCTION

The viscoelastic data of the spine are characterised by time dependent phenomena e.g.. creep, relaxation, hysteresis and strain-stress rate sensivity (Panjabi, 1977), mostly influenced by the water-imbibing capacity of the discus intervertebralis.

Throughout the day the vertebral column is subjected to compressive as well as other types of loading by gravity, changes in position, muscle activity, external forces, and external work (De Puky, 1935). The cumulation of different activities during daily work can produce a decrease of the vertebral column height. Reilly et al. (1984) found that the difference between the body height in the morning and the evening is 1% of the total body height, and Krag et al. (1990) found a 0.9% difference, with a mean value of 16,39 mm. Tyrell et al. (1985) reported a mean of 19 mm. The shrinkage mainly is achieved during the first hours of activity, and the study of Tyrell et al. (1985) indicates 54% of the loss of height within 1 hour, where the results of Leatt et al. (1986) leaded to the conclusion of 38.4% of the total shrinkage after 1 hour and a half.

The total body and the spine can be subdivided in different body regions and different height aspects. There is an abundance of literature describing the effects of compressive loading on the lumbar discus intervertebralis during different static postures, lifting technics and dynamic activities (Nachemson, 1981; Adams et al., 1983; Tyrell et al., 1985; White and Malone, 1990). However, the effects on the cervical spine have not been as extensively investigated. It seems interesting to verify to what extend and at what level the different height aspects and the different regions of the spine are separately influenced by a very variable daily activity such as nursing tasks in the hospital or patient care work.

The shrinkage and the possible degeneration of the discus intervertebralis depends on the frequency and intensity of the load during frequent dynamic and persistent static actions (Videman et al., 1990). Nursing personnel shows a high prevalence and a high incidence of Low Back Problems (LBP), due to lifting and transferring patients.

The first purpose of this study is an anthropometric approach of the effects of nursing tasks on the body height and the spine. A second aim deals with the localisation of significant changes of body height and significant spinal shrinkage. The third goal is to investigate if LBP in nursing personnel is related to spinal shrinkage and gender.

METHODS

Seventeen nurses, 4 male (2-LBP, 2+LBP) and 13 female (9-LBP, 4+LBP) subjects, were selected on a voluntary basis from 4 different Belgian hospitals. The history of LBP was based on a life-time prevalence. With the head in Frankfurter position, the stature, the C7 height, sitting height, and the height of the spina iliaca anterior superior (SIAS) and the spina iliaca posterior superior (SIPS) both at the left and right side, were measured twice at 6 AM before starting their job, and twice at the end of the normal daily work. Measurements were performed with an anthropometer (GPM) and a sitting height table (Holtain Limited, UK), both accurate within 1 mm. The measurements in the morning took place at about 1 hour 15 min (SD 30 min) after getting up and in the afternoon after an average of 9 hours (SD 30 min) work.

RESULTS

During the daily work, the mean change in stature measured 10.3 mm (SE 0.64 mm), the mean difference in sitting height was 8.09 mm (SE 0.66 mm) and the mean difference of C7 height measured 5.82 mm (SE 1.43 mm). Calculations indicated an average shrinkage of 4.56 mm (SE 1.54 mm) of the cervical spine and 3.71 mm (SE 1.84 mm) of the thoraco-lumbar spine. The results were checked on normal distribution, and differences in relation to LBP and gender were calculated using a 2-way ANOVA and a 1-way ANOVA with the Scheffe-F post-hoc test. No significant differences ($p<0.05$) were found. Using an ANOVA for Repeated Measures,

differences between the data of the morning and the afternoon were checked. Stature, sitting height, C7 height and the cervical spine showed a significant shrinkage during the daily work. The thoraco-lumbar spine as well as the SIPS and SIAS measurements did not indicate significant differences.

DISCUSSION

In our experiment the relative shrinkage, measured in total height is 0.6%, in sitting height 0.9%, in C7-height 0.4%, and in the cervical spine 1.8%. Taking into consideration the shrinkage of the first hour after getting up, our results confirm those of Reilly et al., 1984, Tyrell et al., 1985, Leatt et al., 1986 and Krag et al., 1990. In addition we notice that the changes of stature before and after the daily work are mostly influenced by the shrinkage of the cervical spine. Töndury (1974) and Penning (1978) suggest that morphology and function of the cervical discus intervertebralis change during life-time, characterised by a pseudo-degeneration of the fibers of the anulus fibrosus beginning at the age of nine. We wonder if, complementary to the hydration- and dehydration-process of the disci, this morphological aspect could be a reason why we found the highest shrinkage at the cervical level. The influence of the cervical part of the vertebral column on the spinal shrinkage might be an explication why we did not found any relation to LBP.

CONCLUSION

These results suggest that the change in stature during the daily work primarily is located in the vertebral column, and mostly is influenced by the shrinkage of the cervical spine. This can be one of the reasons why no relation between spinal shrinkage and LBP could be found, neither in male nor in female nurses.

REFERENCES

Adams, MA; Hutton, WC; The effect of posture on the fluid content of the lumbar intervertebral discs; Spine; 1983; 7; 665-671.

De Puky, P; The physiological oscillation of the length of the body; Acta orthop. Scand.; 1935; 6; 338-347.

Garg, A; Owen, BD; Carlson, B; An ergonomic evaluation of nursing assistants' job in a nursing home; Ergonomics; 1992; 35 (9); 979-995.

Krag, MH; Cohen, MD; Haugh, LD; Pope, MH; Body height changes during upright and recumbent postures; Spine; 1990; 15; 202-207.

Leatt, P; Reilly, T; Troup, JDC; Spinal loading during circuit weight-training and running; Br.J. Sports Med.; 1986; 20; 116-124.

Nachemson, A; Disc pressure measurements; Spine; 1981; 6; 314-318.

Panjabi, MM; Experimental determination of spinal motion behavior; Orthop. clin. North Am.; 1977; 8; 169-180.

Penning, L; Normal movements of the cervical spine; Amer. J. Roentgenol.; 1978; 130; 317-326.

Reilly, T; Tyrell, AR; Troup, JDC; Circadian variation in human stature; Chronobiol. Int.; 1984; 1; 121-126.

Töndury, G; The Cervical Spine; Huber, Bern; 1974.

Tyrell, AR; Reilly T; Troup, JDC; Circadian variation in stature and the effects of spinal loading; Spine; 1985; 10; 161-164.

Videman, T; Nurminnen, M; Troup, JDC; Lumbar spinal pathology in cadaveric material in relation to history of back pain, occupation and physical loadings; Spine; 1990; 15; 728-737.

White, TL; Malone, TR; Effects of running on intervertebral disc height; JOSPT; 1990; Oct; 139-146.

ACKNOWLEDGEMENTS

The authors would like to acknowledge the "Belgian Federal Services for Scientific, Technical and Cultural matters".

SENSITIVITY OF JOINT MOMENTS TO PEDAL ANGLE MEASUREMENT IN CYCLING

G E. Caldwell[†], L. Li[†], S D McCole[§], J M. Hagberg[§]

[†]Dept. of Exercise Science, University of Massachusetts, Amherst, MA, USA
[§]Dept of Medicine, University of Pittsburgh, Pittsburgh, PA, USA

INTRODUCTION

Kinetic analysis of cycling has given insights regarding patterns of pedal force application throughout the crank cycle Recording of the pedal orientation permits these force vectors to be transformed into a global coordinate system for analysis of vertical and horizontal force components These forces may be combined with kinematic data of lower limb motion to estimate the resultant moments using inverse dynamics analysis (Gregor et al., 1985, Redfield and Hull, 1986) A survey of the literature reveals there is general agreement that change in pedal orientation during the crank cycle approximates a sinusoid with a range of $\approx 55°$ However, there are a wide range of values of maximal pedal angle with respect to horizontal, ranging from -3° (toe down) to +10° (toe up) Discrepancies in the patterns of joint moments throughout the crank cycle are also found, particularly at the knee and hip Due to the importance of pedal loading to the calculation of joint moments, the variation in pedal angles may be responsible for these joint moment patterns. The purpose of this paper is to investigate the sensitivity of joint moment calculation to changes in the measured value of pedal orientation.

METHODS

Nine elite subjects rode their own bicycles mounted on a Velodyne ergometer Kinematic data were computed based on the motion of reflective markers on the crank, pedal and joint centers, collected at 50 Hz using standard planer cine techniques. A clip-in Look pedal instrumented with two piezoelectric load washers (Broker and Gregor, 1990) was used to measure pedal force data at 100 Hz with a 12-bit analog-to-digital convertor After appropriate bias adjustment and scaling to calibrated values, both the kinematic and force data were expressed as quintic splines and output at 1° increments for one complete crank revolution starting at top-dead-centre (TDC) This combined data set was used to calculate crank and pedal kinetics in global, pedal and crank reference systems (Coyle et al, 1991) Joint moments for the ankle, knee and hip were calculated from standard Newtonian equations. For this paper, four crank cycles of each subject cycling at a workload representing 80% of their maximum were used to calculate mean joint moment patterns The effect of pedal orientation was examined by altering the pedal angle data by a constant offset (± 5°) to represent the range of variation seen in the literature

RESULTS

The pedal orientation data for a typical trial, with all three constant offsets, are shown in Figure 1 The mean ankle moment pattern for 4 trials from the same subject are displayed in Figure 2, also for the three pedal offsets Note that the same basic pattern of dominant plantarflexor activity is evident for all three pedal orientations, with a change in peak moment of approximately 15%. However, this change in peak extensor moment is much greater at the knee joint (Figure 3), with an alteration of $\approx 40\%$. Note that the knee moment curve near BDC changes strongly from extensor to flexor in one

case, but stays near zero in another Interpretation would therefore change radically depending on pedal angle offset Figure 4 shows this interpretation problem to be magnified for the hip moment, because the pattern in mid-cycle in one case suggests strong extensor activity, and in another strong flexor activity

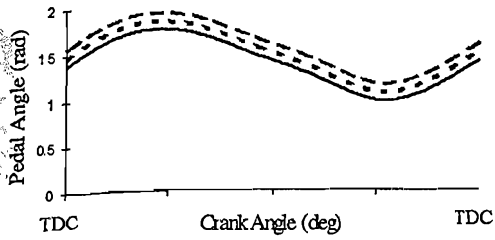

Figure 1: Pedal orientations, offsets 0 ± 5°.

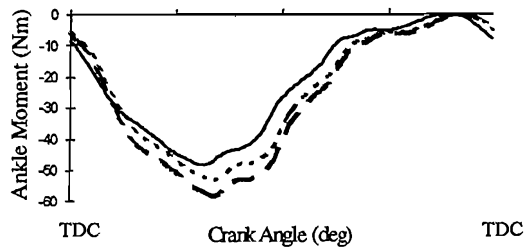

Figure 2: Ankle moments

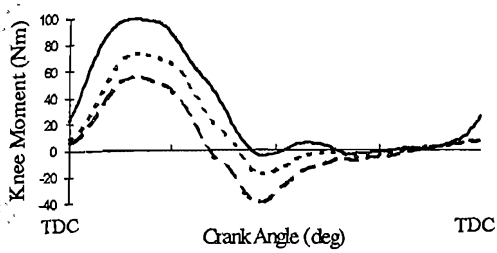

Figure 3: Knee moments

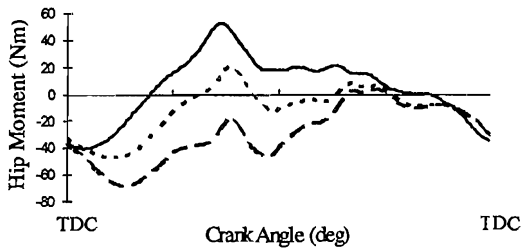

Figure 4: Hip moments

DISCUSSION

It is clear that a small change in pedal orientation data can effect dramatic changes in the calculations of joint moments, especially at the knee and hip. Changes in the resolution of the pedal force vector into horizontal and vertical components dictate the distal force moment terms in the calculation of ankle moment as well as ankle joint reaction forces. These in turn cause further changes as the calculation proceeds up the leg using the linked-segment method Due to the relatively vertical orientation of the leg near BDC, these changes have profound effects on knee and hip moments These results stress the importance of careful calibration of pedal measurements and the accurate synchronization of film or video data with digital force records.

REFERENCES

Broker, JP, & Gregor, RJ (1990) A dual piezoelectric force pedal for kinetic analysis of cycling. *Int. J. Sports Biomech.* 6 394-403

Coyle, EF, Feltner, ME, Kautz, SA, et al (1991) Physiological and biomechanical factors associated with elite endurance cycling performance *Med. Sci. Sp. Exc.* 23, 93-107

Gregor, RJ, Cavanagh, PR, & LaFortune, M (1985) Knee flexor moments during propulsion in cycling a creative solution to Lombard's paradox. *J. Biomech.* 18 307-316

Redfield, R, & Hull, ML (1986) On the relation between joint moments and pedalling rates at constant power in bicycling *J. Biomech.* 19 317-329

PHYSICAL WORK CAPACITY AND TOLERABLE WORKLOADS IN PARAPLEGIC PATIENTS

[1]Capodaglio, Paolo, [2]Pistarini, Caterina, [2]Fugazza, Gloria, [2]Achilli, Maria P , [2]Brignoli, Elvira, and [1]Bazzini, Giacomo C
[1]Ergonomics Unit, [2]Spinal Injuries Unit, Rehabilitation Center of Montescano, Clinica del Lavoro Foundation, Institute of Care and Research, Montescano (PV), Italy

INTRODUCTION

In the recent literature there is growing interest in the assessment of physical work capacity in paraplegics (DiCarlo & al , 1983, Knutsson & al , 1973, Nilsson & al , 1975) Little information of a systematic nature is available in the literature about the responses of paraplegic subjects to prolonged exertion within tolerable non-fatiguing limits (Hooker & Wells, 1988) The aims of this study were twofold to measure the cardiorespiratory fitness level of newly injured paraplegic patients performing arm exercise during primary rehabilitation and at discharge, comparing it with the fitness level of employed paraplegic patients, to determine the tolerable workload for prolonged physical activity in newly injured and employed paraplegics

METHODS

Four male subjects with paraplegia (mean height 176 cm, mean body weight 82 6 kg) with nearly complete traumatic D7-D9 lesions partecipated Two had sustained injury a mean of 5 2 months before the start of the study They had no decubitus ulcers or other major medical problems The other two were actively employed The first test was to be performed as soon as the subject was able to sit in a wheelchair All subjects were first familiarized with the technique for grading perceived exertion on a 10-point scale (Borg, 1982) and with the equipment, which consisted of an arm cranking ergometer (ACE) (Monark Rehab Trainer 881E) The arm cranking unit was secured to an adjustable table in order to keep the shoulder in line with the axis of the ACE The wheelchair was placed in such a position that the arm of the subject was in complete extension when the pedal was at its greatest distance Each subject performed a progressive resisted arm cranking exercise test at the velocity of 50 rpm The time course of a test was as follows after a three-minute warm-up at 0 Watt, increments of 12 5 Watt every 2 min were performed until subjects rated the perception of effort as "maximal" Respiratory and oxygen uptake variables were measured by a metabolic analyzer (EOS Spring, Jaeger) The following parameters were monitored every 30 seconds heart rate (HR), oxygen consumption (VO_2), ventilation (VE) and respiratory exchange ratio (RQ) The electrocardiogram was continuosly monitored during the testing sessions Each subject performed in different sessions a total of twelve 15-min endurance tests with the ACE at three constant loads corresponding to CR-3 ("moderate"), CR-4 and CR-5 ("heavy") subjective perceptions of effort obtained in the incremental test The order of load presentation was randomized The incremental test and the 12 endurance tests were repeated after a 4-week individualized aerobic arm training program The program consisted of a 20 to 30-minute session per day, during which the intensity of the exercise was chosen accordingly to the motivation and expectations of each patient

RESULTS

Individual cardiorespiratory fitness levels obtained from the incremental tests before training were VO_2=0 003 HR+0 15 and VO_2=0 015 HR-1 46 for the 2 newly injured patients, VO_2=0 013 HR-0 34 VO_2=0 01 HR-0 38 for the 2 employed subjects After patients completing the training program the fitness levels were VO_2=0 011 HR-0 52 and VO_2=0 017 HR-0 87 for the 2 newly injured patients The perception of exertion was found to be highly

correlated with heart rate ($r = 0\ 98$, $p < 0\ 001$) and workload ($r = 0\ 95$, $p < 0\ 001$) during both progressive resisted and endurance tests Regression analysis was performed to determine the individual iso-perception curves, that were represented by power functions, $Y = c \cdot X^n$, $(-1 < n < 0)$ The individual power output over time corresponding to each rating of subjective perception was calculated Improvement in endurance capacity, after the 4-week endurance training at "moderate-somewhat strong" intensity level, was monitored by the shifting of the "iso-curves" corresponding to a perception of "moderate" toward higher power output levels (Figure 1)

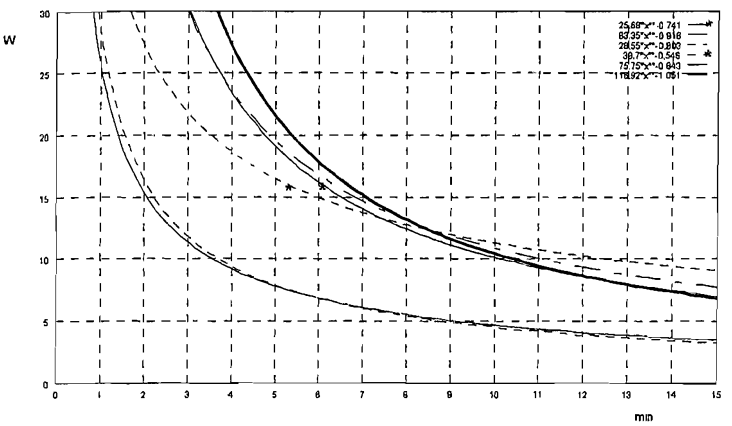

Figure 1. Individual iso-curves corresponding to a "moderate" effort before (2 curves on the left) and after (*) the 4-week training program in the 2 newly injured paraplegics The 2 curves on the right refer to the 2 employed paraplegics

DISCUSSION

In our study a 4-week endurance training program performed by newly injured paraplegics at "moderate" or "somewhat strong" levels of intensity led to a noticeable improvement in endurance capacity On the basis of our results, the individual "tolerance threshold" for prolonged arm cranking exercise may be defined by the "iso-curve" corresponding to a "moderate" effort on Borg's scale (CR-3) Physiological parameters remained constant at this level of perceptual intensity, with the respiratory exchange ratio (RQ) less than one If the subjects prolonged their performances at different workloads so as to exceed the corresponding time value identified by the CR-3 power function (Figure 1), an increase in the respiratory exchange ratio (RQ) value of more than one, as well as in the scoring of subjective perception of effort, was observed

REFERENCES

1 Borg G A category scale with ratio properties for intermodal and interindividual comparisons In Geisler HG and Petzold P, eds Psychophysical judgement and the process of perception Berlin VEB Deutscher Verlag der Wissenschaft, 1982 25-34

2 DiCarlo SE, Supp MD, Taylor HC Effect of Arm Ergometry Training on Physical Work Capacity of Individuals with spinal Cord Injuries Physical Therapy 1983,63(7) 1104-7

3 Hooker SP, Wells CL Effects of low- and moderate-intensity training in spinal cord-injured persons Med Sci Sports Exerc 1988,21(1) 18-22

4 Knutsson E, Lewenhaupt-Olsson E, Thorsen M Physical Work Capacity and Physical Conditioning in Paraplegic Patients Paraplegia 1973,11 205-6

5 Nilsson S, Staff D, Pruett E Physical work capacity and the effect of training on subjects with long standing paraplegia Scand J Rehab Med 1975,7 51-6

A COMPARISON OF THE ACCURACY OF SEVERAL HIP CENTRE LOCATION METHODS BY USING RSA TECHNIQUE

Cappozzo A.[1], Leardini A.[2], Larsen S.[3], Catani F.[2], Benedetti M.G.[2]
1-Istituto di Fisiologia Umana, Universitá degli Studi di Sassari, Sassari, Italy
2-Biomecanics Laboratory, Istituti Ortopedici Rizzoli, Bologna, Italy
3-Dept. Orthopaedics, University Hospital, Lund, Sweden

INTRODUCTION

The accurate 3-D location of the hip joint centre (HC) in a pelvic frame is a critical procedure in any movement analysis loboratory. A number of studies have proposed and tested different techniques to solve this problem. These techiques belong to two classes: 1) *functional approach* (1, 2) based on the assumption that the joint centre coincides with the pivot point of a 3-D movement between the adjacent segments; 2) *prediction approach*, i.e. regression equations based on statistical information acquired, mostly using imaging techniques, on a given population of subjects (3, 4). All of these techniques still deserve deeper investigations as concerns their accuracy. The present study aims at estimating the accuracy associated with the functional method as in Cappozzo (1) (where the HC is assumed to be the centre of the sphere described by markers located on the thigh during a flexion-extension followed by an ab-adduction of the hip), the prediction method proposed by Bell et al. (3), and the prediction method suggested by Davis et al. (4). Relevant regression equations and parameter definition were:

methods:	x	y	z
Bell et al.	$-0.19 \cdot D_{asis}$	$-0.30 \cdot D_{asis}$	$i \cdot 0.36 \cdot D_{asis}$
Davis et al.	$[-D_{hca}-D_{mrk}] \cdot \cos\beta + C \cdot \cos\theta \cdot \sin\beta$	$[-D_{hca}-D_{mrk}] \cdot \sin\beta + C \cdot \cos\theta \cdot \cos\beta$	$i \cdot [C \cdot \sin\theta - D_{asis}/2]$

where $i = 1$ for the right and $= -1$ for the left HC; Dasis is the distance between the anterior superior iliac spines's (ASIS); D_{hca} is the anterior/posterior component of the HC/ASIS distance; D_{mrk} distance between skin marker centroid and skin surface; $\theta = 28.4$ deg; $\beta = 18$ deg; $C = 0.115L - 0.0153$; L is the leg length in meter. The accuracy of the above listed methods was determined by comparing their results with the HC location obtained using the Roentgen Stereophotogrammetric Analysis (RSA), fruitfully utilized since 1974 for accurate 3D measurements from radiographs (5).

METHODS

Two adult healthy male volunteers partecipated in the experiments (Tab.1). Four spherical tantalum balls, diameter 0.8 mm, were stucked on the skin surface above the two anterior (ASIS) and posterior (PSIS) superior iliac spines. Two roentgen tubes exposed simultaneously the subject while standing in such a way that the calibration cage markers, the four skin markers and the femural head contours were visible in both films. Mathematical computations were performed for the reconstruction of the 3D position of each marker and HC using the relevant image coordinates. The image coordinates of the HC on each film were estimated as the centroids of the digitized femoral head image contours. The subject was then investigated in the movement analysis lab, equipped with the ELITE (by BTS, Milan) stereophotogrammetric system. Two rigid plates, mounting 3 retroreflective markers, were strapped to the pelvis and to the distal part of the thigh using elastic straps with velcro fasteners. The location of the 4 superior iliac spines with respect to the pelvic markers was obtained by calibration using the tecnique of the pointer (CAST protocol) as illustrated in (6). This permitted the determination of the pelvic anatomical frame shown in Fig.1 and the reconstruction of the thigh marker trajectories during movement in this frame.

RESULTS

The coordinates of the HC in the anatomical pelvic frame as obtained using RSA are given in table 1. The distance between the HC location as estimated using RSA and its estimates as obtained using the methods under analysis was calculated and considered to be a good measure of the relevant accuracy. Results are given in table 2 for each experiment using the functional approach (a, b, c) and each prediction technique.

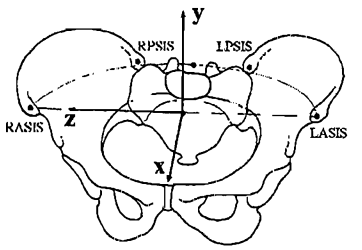

Figure 1. Pelvic anatomical frame

Table 1. Subjects characteristics and HC coordinates.

subj.	mass [kg]	stature [m]	age [years]	sex	right HC [mm]			left HC [mm]		
					x	y	z	x	y	z
#1	80	1.94	42	M	-61	-100	97	-61	-93	-104
#2	70	1.84	33	M	-43	-90	86	-45	-90	-84

Table 2. HC distances from the RSA estimation. Measurement unit is millimeter.

	Subject #1				Subject #2			
	Δx	Δy	Δz	Δ	Δx	Δy	Δz	Δ
Cappozzo-a	13	5	-3	13	-2	8	-7	10
Cappozzo-b	5	15	7	18	-4	14	-3	15
Cappozzo-c	6	13	11	18	4	6	5	9
Bell et al.	-17	-23	-20	35	3	-16	-2	17
Davis et al.	-19	15	-18	30	-21	5	1	22

DISCUSSION

Results obtained in the two subjects with the centre of the sphere method seem to be better than those obtained with the prediction methods, and more realistic than those presented up till now in the literature. Critical aspects of the centre of the sphere approach are the amplitude of rotations of the thigh with respect to the pelvis and the skin movement artefacts. If care is taken in maximizing the former and minimizing the latter quantity, then this approach may provid local HC coordinates with a maximum error within 2 cm. However, this technique may not be appropriate or even impossible to use with patients with limited hip mobility. For the sake of the accuracy, prediction methods require that the subject under analysis belong to the population consistent with that from which the regression parameters were obtained. This is the case for the subjects presented in this study. On the contrary errors may be larger than shown in table 2. As concerns the method proposed by Davis et al., the determination of the parameter D_{hca} was found unreliable (inter-experimentor 20% variation), and the HC coordinate estimates are very sensitive to this parameter.

REFERENCES

1) Cappozzo, A. (1984) Gait analysis methodology. *Hum Mov Sc* **3**, 27-54.
2) Blankevoord, L. et al. (1990) Helical axes of passive knee joint motions. *J. Biomechanics* **23**, 1219-1229.
3) Bell, A.L. et al. (1990) A comparison of the accuracy of several hip center location prediction methods. *J. Biomechanics* **23**, 617-621.
4) Davis, R.B. et al. (1991) A gait analysis data collection and reduction technique. *Hum Mov Sc* **10**, 575-587.
5) Selvik, G (1974) A roentgen-stereophotogrammetric method for the study of the kinematics of the skeletal system. Reprinted *Acta Orthop Scand* **60**(4), Supp232.)
6) Cappozzo, A. et al. (1994) Position and orientation in space of bones during movement: anatomical frame definition and determination. *Clin Biomec* (in press)

AN INVESTIGATION INTO CONJUGATE IMAGING TECHNIQUES FOR THE AUTOMATED REPRODUCTION OF THREE DIMENSIONAL COORDINATES

A.B.Carman and P.D. Milburn*.
Department of Biomedical Science, University of Wollongong, Australia.
*Department of Postgraduate Physiotherapy, University of Otago, New Zealand.

INTRODUCTION

Limitations are present in the accuracy and complexity of three dimensional (3D) human movement analysis due to the ability to identify and track individual points appearing in multiple camera images. Reduced external marker sets are often used, despite six to ten markers per 3D segment being recommended for accuracy in determining segmental based coordinate systems (1). The aim of the present study was to investigate the use of conjugate imaging techniques in the automated reproduction of 3D coordinates from multiple camera images, and to identify procedures which will enable the application of conjugate imaging techniques to the analysis of human motion.

METHODOLOGY

An important concept of conjugate imagery and epipolar geometry (Figure 1.) is that conjugate image points will always lie on conjugate epipolar lines regardless of camera orientation (2). With error in digitised camera image coordinates, several assumptions need to be made: i) a conjugate image point will lie at some finite distance from a conjugate epipolar line, ii) a conjugate image point will not necessarily be the closest image point to the conjugate epipolar line, and iii) an image point and its collinear line may be coincident with more than one set of multiple conjugate image points and their respective collinear lines With these assumptions, four criteria were established for testing the validity of conjugate image points The four criteria were 1) Conjugate Point Error (CPE), the perpendicular distance between the conjugate image point and the conjugate epipolar lin, 2) Lab Point Standard Error (LPSE), the standard error between the least squares lab point and paired conjugate image points, 3) Lab Point Error (LPE), the maximum radius over which a lab point may vary, and 4) Lab Point Paired Error (LPPE), the maximum distance between paired conjugate image points. The criterion values were established as part of the standard camera calibration procedure. An algorithm was then developed to systematically build up conjugate image points and then either combine or eliminated lab points based on criterion values.

RESULTS

The error in calculating lab points from paired conjugate image points was found to be dependent on the included angle between the first camera image point, the resulting lab point and the second camera image point. This error approached infinity as the angle approached 180 degrees. To enable comparisons of derived measures which use the error in the lab point produced by paired conjugate image points, such as LPSE, each paired error had to be normalised to 90 degrees. The normalised LPSE was reflective of the error, or "tightness", of the photographic and digitisation process. The CPE was dependent on the camera involved and represented the accuracy of the digitised points and camera calibration, hence a CPE was required for each camera. The present system accurately predicts 3D coordinates and conjugate image points for a 55 point marker system viewed in four cameras (digitisation error $< 0.2\%$, minimum lab point separation of 6 cm, and approximately even numbers of lab points visible in two and three camera images). With increased error in digitised coordinates, improved results could be obtained by increasing the number of cameras. This increased the number of lab points viewed in greater than three cameras and improved determination of the validity

of conjugate image points. The present system was capable of predicting 3D coordinate for a 55 point marker system viewed in eight cameras (digitisation error < 0.35%, minimum lab point separation 6 cm, and lab points visible in three and four camera images).

DISCUSSION

This study has shown the applicability of conjugate imaging techniques in the automated reproduction of 3D coordinates in human motion analysis. The capacity of the present system to accurately reproduce 3D coordinate data is dependent on the error of the digitisation process, the minimum distance between lab points and the number of lab points appearing in just one or two camera images. The present system did not appear to be limited by the maximum number of lab points or cameras (tested with 55 marker points and 8 cameras). When the magnitude of LPE approached the minimum lab point separation, as with increased digitisation error and closeness of markers, improved results could be obtained by increasing the number of cameras. Further investigation is being conducted into the relationship between the digitisation error, the lab point separation, the number of cameras and the ability of the present system to automatically reproduce 3D coordinates. The application of automated 3D coordinate reproduction in 3D tracking will lie as a starting point in an iterative algorithm similar to that described by Miller et al.(3).

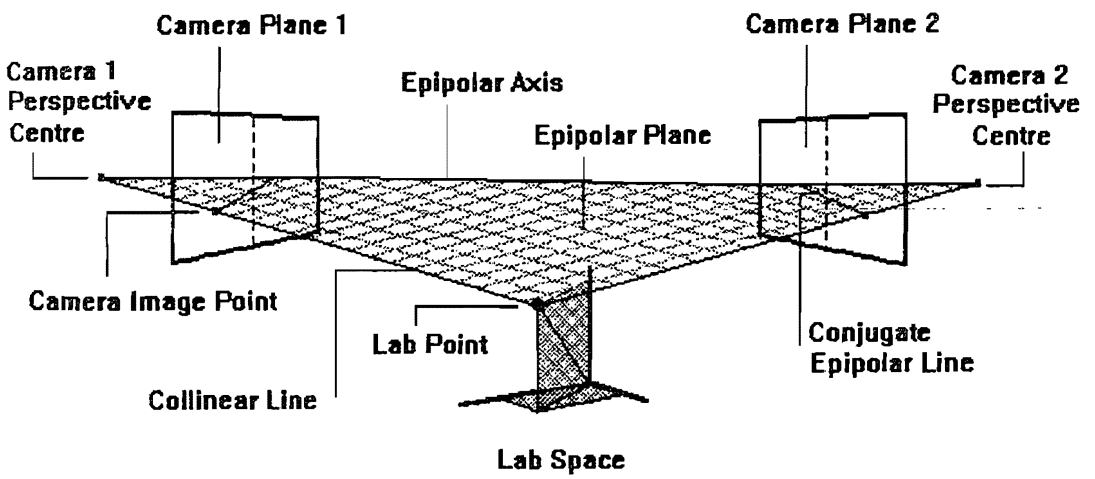

Figure 1. Conjugate imagery and epipolar geometry

REFERENCES

1. Hussain, M. (1977). Measurement of Spatial Motion Using Analytical Photogrammetric System. Michigan: University Microfilms.
2. Keating, T.J. (1977). Analytical Photogrammetry from Digitised Image Densities. Michigan: University Microfilms.
3. Miller, N.R. et al. (1980). A technique for obtaining spatial kinematic parameters of segments of biomechanical systems from cinematographic data. J Biom, 13(7), 535-548.

CONTRIBUTION OF MONO- AND BIARTICULAR MUSCLES TO BALLISTIC MOVEMENTS

CARPENTIER A., DUCHATEAU J. and HAINAUT K.

Laboratory of Biology, Université Libre de Bruxelles, Belgium

INTRODUCTION

During fast voluntary movements muscles with different histochemical and physiological profiles very often cooperate in synergy with the development of force and speed, but their respective contributions remain an exciting question. The Triceps surae is an interesting muscle because it consists of the Soleus (Sol), which contains mainly slow fibres and the gastrocnemii (Gasts), with about an equal amount of slow and fast fibres (Johnson et al, 1973), all distally linked by the same tendon. We have shown in a previous paper that during fast plantar flexions, the ratio Sol/Gasts Electromyographic (EMG) activities decreases with the increasing speed of movement (Carpentier et al, 1993). In the present work we compare the contributions of monoarticular Sol and biarticular Gasts during fast plantar flexions performed in two different positions.

METHODS

After expressing their informed consent, eight male subjects aged 18-28 years took part in this experiment. During the experimental session, the subjects lay on their backs with the left foot attached to a movable support, and performed plantar flexions at speeds increasing from 110°/sec to their maxima. Two articular knee positions (90° and 180°) were tested with the foot at 90°. The angular ankle motion was registered by way of a linear potentiometer and the angular speed was estimated from the first derivative of its output. Sol and Gasts EMG activities, recorded by way of surface electrodes over the motor point, were amplified (2,000 - 5,000), filtered (50 Hz - 5 KHz) and rectified before computer analysis. The integrated EMG activity was normalized with respect to its duration.

RESULTS

Our experimental results indicate that the maximal speed of plantar flexion is larger when the knee is flexed at 90° as compared to the extended position, respectively 425 ± 71 and 306 ± 60 °/s (mean $\pm$ SD). At maximal speeds of movement the relative EMG activities of Sol and Gasts are identical in the two knee angulations. At submaximal levels however, as the speed of movement increases, the linear increase in EMG appears to be larger in Gasts as compared to Sol at 90° flexion, while it is the opposite in the extended knee position. For example, the comparison of the Sol/Gasts EMG ratio at 120°/s and at maximal speed of movement shows a 45 % decrease at 90° knee flexion and a 102 % increase in the extended position (Figure 1).

DISCUSSION

The observation of a decrease in the maximal speed of the plantar flexion in the extended knee position as compared to 90° flexion is suprising since in the former position, the Gasts are slightly stretched and should thus be in their optimal length-velocity relationship. Decreased muscle activation cannot explain this observation since at the maximal speed of movement : (1) the Gasts EMG activity is larger in the extended knee position as compared to the 90° flexion; (2) the relative contribution of Gasts and Sol is not significantly different in the two articular angulations.

It is interesting to note that for submaximal speeds of movement the Sol/Gasts EMG ratio is larger at the 90° flexion of the knee, while it is the opposite in the extended position. This finding, which is mainly related to a modulation of the Sol EMG activity,

suggests that the neural Sol command adapts to the mechanical length-velocity efficiency of the Gasts in order to produce optimal torque during the movement.

In conclusion, these results extend previous observations (Duchateau et al, 1986; Le Bozec et al, 1980) to ballistic movements and further support the view favouring a specific control of muscles which act in synergy and thus optimally combine their contractile properties with respect to the programmed speed of movement in different articular positions.

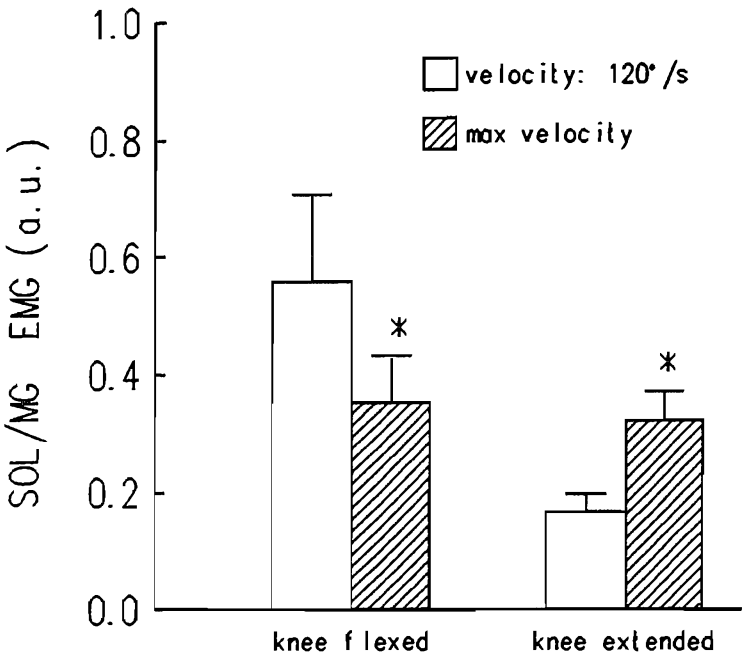

Figure 1 : Histograms showing the Sol/MG EMG ratio (mean ± SE) during plantar flexion at slow (120°/s) and fast (maximal) velocities for two knee angulations * Statistically different at $P < 0.05$

REFERENCES

- Carpentier, A., Duchateau, J. and Hainaut, K. (1993) The synergy of triceps surae muscles during fast movements. Proceedings of the XIVth Congress of ISB (Paris), 242-243.
- Duchateau, J., Le Bozec, S. and Hainaut, K. (1986) Contribution of slow and fast muscle to the triceps surae to a cyclic movement. Eur. J. Appl. Physiol. 55:476-481.
- Johnson, M.A., Polgar, J., Weightman, D. and Appleton, D. (1973) Data on the distribution of fibre types in thirty six human muscles. An autopsy study. J. Neurol. Sci. 18:111-129.
- Le Bozec, S., Maton, B. and Cnockaert, J.C. (1980) The synergy of elbow extensor muscles during dynamic work in man. . Elbow extension. Eur. J. Appl. Physiol. 44:255-269.

This work was supported by the Université Libre de Bruxelles and NATO (RG n°930261)

APPLICATION OF CONCEPTS VALIDATED FOR DENTAL IMPLANTOLOGY TO JOINT PROSTHETIC SYSTEMS DESIGN

F.Casolo, V Lorenzi, A Vallatta
D S T.M. - Politecnico di Milano, Milano, ITALY

INTRODUCTION

Today's strumentarium and procedure for the preparation of artoprostheses seat in the bone are, in most cases, very damaging for the tissue surrounding the implant The main sources of damages are the following -The bone during the workmanship or the polymerisation of the cement interface (if present) reaches a too high temperature over 50°C the tissue is permanently damaged. -Most of working tools make relevant damages to the network of blood vessels, pulling them out from their location in the intertrabecular spaces filled with marrow. -The over-stress of the bone surrounding the implant seat during workmanship also causes local necrosis of the tissue. -In some cases, the tools are not provided of a vent for the liquids collected in the cavity, thus they also induce over-pressure on the tissue over-pressure causes structural damages and ischemia in the bone tissue -Moreover, over-stress is also often originated after the implantation of the prosthesis, by the interference of the prosthesis with its seat, by the presence of bony debris at the implant interface or again by the liquids that can't find a vent during the stem positioning.

Out of these factors that mainly cause bone necrosis and its consequent reabsorption, big gaps are also generally evident in certain zones of the interfaces (even in presence of interference at other locations). These gaps are due to involuntary movements of the tools during the machining and to trabecular fractures caused, for instance, by inadequate sharpening of the tools; they also can compromise the primary stability of the implant and increase the tissue recovering times

A fibrous tissue membrane can originate from micro-movements of the prosthesis with respect to the bone.

Most of these damages are particularly evident in the trabecular tissue; this is probably one of the main reasons why some prosthetic stems have some links with the cortical bone

MATERIALS AND METHOD

In a recent research we studied how to solve very similar problems for dental endoprosthetic implants. We designed a new system which allows interface recovery without any woven bone production and reduces drastically the healing phase, achieving the "osteointegration" of the implant mostly by "primary bone recovery"

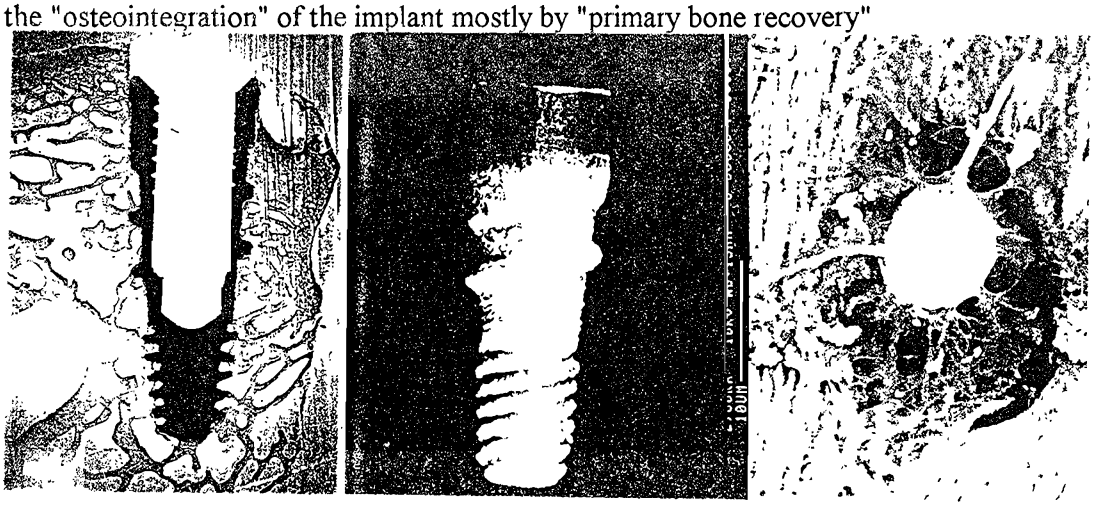

Fi a) histological section of the dental endoprosthesis, b) unscrewed implant, c) SEM image of the tissue surrounding the unscrewed implant

The key factor is a very precise congruence of the implant with its seat, obtained without over-stressing or overheating the tissue In fact, primary bone formation consequent to bone cutting can only fill few μm gaps The implant is a particularly shaped screw with a cylindrical neck, a conic core and an helix adequate to the spongeous bone The conic core assures an exact coupling with the seat; the cylindrical neck prevents the stress shielding of the spongy bone by the cortex. The most important and innovative part of the system is the precise strumentarium, whose main components are a stepped milling bone cutter, a conic reamer and a flow tapping tool. Histological sections of the implant, just after the surgery, show the precise congruence implant-seat, and the absence of damages to the trabecular structure (Fig 1a). SEM analysis of unscrewed implants demonstrated the presence of vital tissue at the interface just few days after the surgery The measure of the couple required to unscrew the implant shows a drastic shortening of the recovery phase (on animal tests)

The above described approach can be applied to joint replacement only if similar precision tools can be utilised, for example, if rasps are needed, it is impossible to obtain the high quality workmanship required for the "primary bone recovery" Therefore we start from joint prostheses characterised by axial symmetric stem An important goal that we are trying to achieve is to preserve as much bone as possible by minimising the stem size Also in this case, beside verifying the effect of surgical procedure, interference and gaps, it is important to analyse the stress pattern of the bone when the implant is loaded. For this aim F E method has been applied The parametric and axi-symmetric model of the stem with the bone allows a quite dense mesh, with relatively short run times, suitable for parameters optimization, it also allows to input physiological (not symmetric) loads The model parameters are. stem length diameter and tapering, pitch, thickness and depth of the thread, bone geometry and apparent density

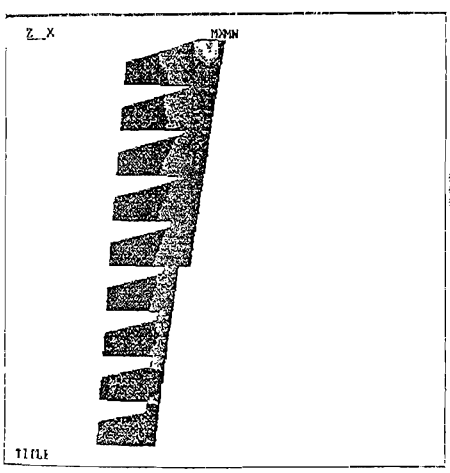

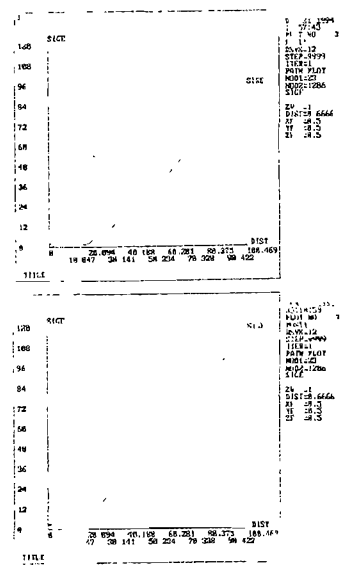

fig.2 equivalent stress in the proximal spongy bone

fig.3 equivalent stress along the cortex **a)**for threaded and **b)**for not threaded stem

Preliminary results show, for instance, that the presence of a thread with low pitch-depth ratio implies stress shielding, therefore, bone reabsoption near the core (fig 2 a) Moreover big transversal dimensions shift bone stress proximally (fig 2b) and the presence of a large thread seems to produce the same result with less material and relatively lower stiffness

References

Huiskes R et al (1982) *Finite Elements in Biom.* J Wiley & Sons, New York

Casolo F , Vrespa G X World Congress of Oral Implantologists, Sorrento 1990

KNEE JOINT TEST IN UNLOADED CONDITION

F. Casolo, M. Galli, A Vallatta and B. Zappa
D.S T.M Dept., Politecnico di Milano, Milano, Italy

INTRODUCTION

The evaluation of the knee movement without external load, can be useful for the diagnosis of knee pathologies or to evaluate the performance of artificial joints, in particular when other deambulation disorders can affect knee motion during gait analysis or when the subject is not jet allowed to walk.
Standard gait analyses are also affected by a number of artefacts which are incompatible with the precision required for those kind of diagnoses For both opto-electronic and goniometric methods, the main source of errors is the impact phase of the walking cycle In this phase the dynamic actions on the skin where the markers are placed, and on the goniometers lead to relevant movements with respect to leg bones.
To overcome those problems we choose to analyse a knee movement simple, repeatable, not including the impact on the ground and not requiring to the knee to support the body weigh. Even for the leg extension of a seated patient, the movement of the markers on the skin is not negligible, thus we tried to find some location where is possible to fasten a mechanical device on which markers are placed. Because of the geometry of the body segments in objects, where longitudinal -along the diaphysis- and transversal dimensions are very different (the second are very little), it is also important to locate at least one marker far from the longitudinal axis and then out of the body shape, this is another reason for using a mechanical device on which markers can be placed as required

MATERIAL AND METHODS

Our measures, obtained by means of an opto-electronic apparatus, concern the relative motion of tibia and femur, therefore we link to the only moving segment - the calf - a rigid frame, connected to the tibia (Fig 1).

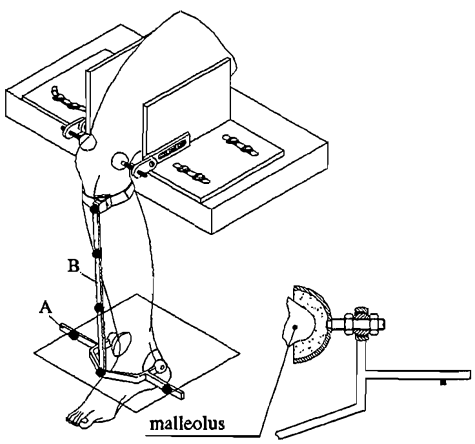

Fig 1 The rigid frame and the restraining system.

A special clamp, designed to hold both malleoli, is connected with a light transversal bar (A) in order to carry the "out of longitudinal axis" markers Another bar (B) is faced to the tibia and pressed on it by means of an elastic strip. The rigid connection of the structure to the malleoli is obtained by a material preformed with the bones shape as shown in Fig. 1b.
The femur is maintained in place by mean of another clamp faced on the lateral condyles and by fixing the pelvis at the iliac crests level The subject, seated in a standard posture, is asked to fully extend the knee and than to come back to the initial position of 90° flexion All subjects are tested five times for three conditions after the first five times,

the subject take a little walk, than came back to the special chair for the second set of measures, than, before the last set of measures, the apparatus holding the markers is removed an replaced. All tests proved a good repeatability - except for flexion angles near zero deg - and frame positioning is not a critical factor.

DISCUSSION

From the trajectory of the markers we compute the rotation matrices (R) of the moving segment with respect of the chair reference frame.

The representation of the results and their analysis require the choice of a set of angular parameters to be displayed. All sets of angular coordinates (e.g. Cardan, Euler, Rodriguez-Hamilton parameters, helical axis parameters, etc) can be calculated from the rotation matrix R. It is consequently also possible to pass from a system of angular coordinates to another one by means of R and to represent the same movement with different sets of graph. Some conventions must be avoided because presents singularities within the range of motion analysed, some other amplifies certain motion peculiarities and can be adopted to study special pathologies. It is generally convenient to adopt angular parameters having a clear physical meaning. Using one of the six Cardan sequences of rotation to analyse the knee in a physiological range of motion, all conventions characterized by the second rotation around the flexion axis -floating axis- should be avoided: for instance in these conditions , when flexion approaches to 90° little errors on this angle can origin drastic changes on the other two angular coordinates. All six Euler sequences must also be avoided because of singularities in the knee range of motion. We usually adopt a Cardan convention with the sequence of rotations around **y, z, x** axes and we define the three angles as flexo-extention, abdo-adduction, and intra-extra rotation. Most of tests (fig. 2b) show that intra-extra rotation diagrams during extension, can be quite different with respect to the ones relative to the flexion phase near full flexion, while they are very similar in the other interval. Knee geometry allows in fact both active and passive intra and extra-rotiation when the knee is near full flexion. Consequently nothing can be deduced comparing intra-extra rotation when flexion assumes high values. On the contrary we can obtain interesting results with our apparatus measuring active intra-extra rotation while flexion is constant.

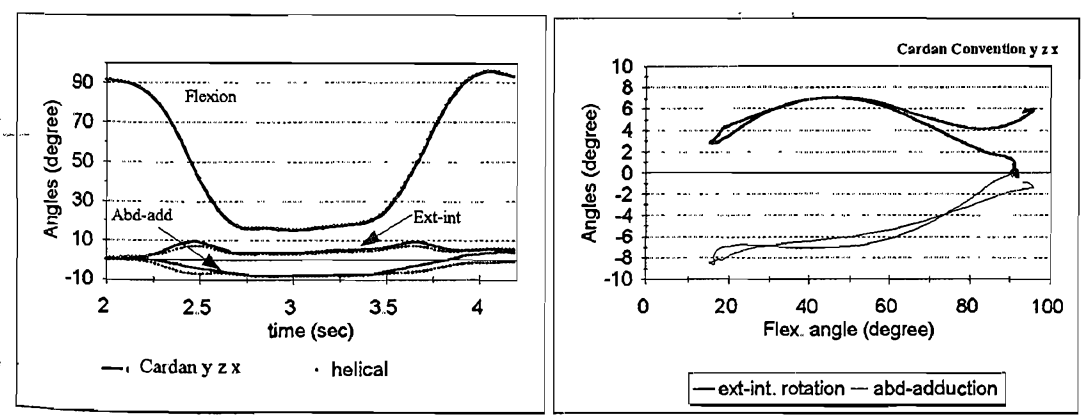

a b

Fig.2 a) Results of a flexion test vs time displayed by mean of Cardan and Helical convention - b) abdo-adduction and intra-extra rotation versus flex

REFERENCES

H.J. Woltring (1994), 3-D Attitude representation of human joints a standardization proposal, J. Biomechanics **27**, 1399-1414

EXAMINATION OF THE LANDING FROM A DROP

John H Challis

Applied Physiology Research Unit, School of Sport and Exercise Sciences, University of Birmingham, UK

INTRODUCTION

In a number of sporting activities it is necessary to control the landing from a drop There has been research into both the kinematics and kinetics of landing from a drop (e g McNitt-Gray et al , 1993, Devita and Skelly, 1992) It was the purpose of this investigation to examine the landing from a drop of a group of subjects, and to use a model to examine the strategy used by the subjects to perform the landing

METHODS

Eight female subjects participated in the study (mass 57 9 ± 7 6 kg, mean age 20 6 ± 1 9 years) All subjects were actively involved in gymnastics, were healthy, and gave informed consent The subjects were instructed to perform barefooted vertical drop landings from three different nominal heights (0 25, 0 44, and 0 80 m), they performed two trials from each height Their aim was to control the landing and return the body to upright standing posture They were free to select their strategy for controlling the landings For each subject the order of the nominal drop heights was randomised Prior to experimental testing subjects attended a practise session to familiarise themselves with the task required of them Subjects performed a self selected warm-up before both the familiarisation session and the test session

A Kistler (9281B12) piezoelectric force plate was used to collect ground reaction force data at a sample rate of 1000 Hz, for a time period of three second, with sampling being triggered by landing on the plate Kinematic data were obtained using a video based motion analysis system sampling at 50 Hz, these data were synchronised with the force data The data resulting from the force plate and video analysis system were combined to provide kinematic and kinetic descriptions of the landings, and to compute the true drop heights, as measured by the displacement of the centre of mass from the start of the drop until initial contact with the plate

A model of the landing from a drop was developed This model consisted of two masses separated by spring and damping elements, there was also a spring and damper between the lower mass and the ground (see figure 1a) In the model the lower mass represented the feet and shanks of the subjects, the lower damper and spring characterise the interaction between these segments and the force plate surface The other mass represented the remainder of the body, with spring and damper designed to represent the actions of the remainder of the body The model validity was assessed by determining model parameters for one trial and then simulating the next trial with the model and comparing model output which actual measures The parameters for the model also permitted calculation of other parameters which permitted characterisation of the landing, for example damping ratio, and damped frequency

RESULTS

From the nominal drop heights of 0 25 m, 0 44 m, and 0 80 m, the mean true drop heights were 0 217 m, 0 356 m, and 0 711 m With an increase in drop height there was an increase in maximum peak vertical ground reaction force, the mean peak vertical forces were 3 82, 4 86, 8 42 body weights The time to peak vertical ground reaction force decreased with increasing drop height, the mean times were 0 0546 s, 0 0507 s, and 0 0371 s

Model parameters were determined for each subject The accuracy of the model for simulated landings is demonstrated in figure 1b for a single subject, the graph shows the model produced vertical ground reaction force (8 8 % RMS difference between predicted and actual force)

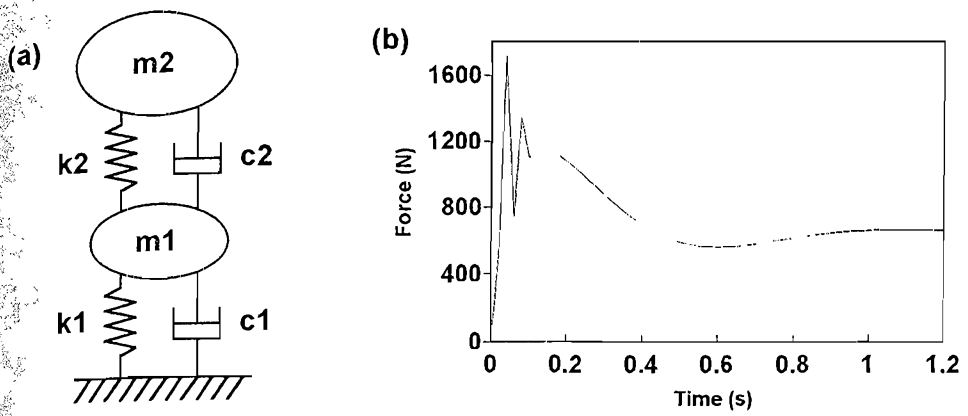

Figure 1 - (a) A schematic representation of the model (b) Graph showing model predicted vertical ground reaction force for a drop from a low height (0 217 m)

DISCUSSION

The results indicate the large forces the human body can experience as a consequence of a landing from a drop The results also indicate the obvious strategy used by the subjects of lowering their centre of mass when leaving the platform for dropping therefore the actual drop heights were always less than the nominal drop height

The parameter values for the lower damper (c1) and spring (k1) were different for each subject but consistent across trials As the force plate was assumed to be sufficiently rigid to assume c1 and k1 were not significantly influenced by it, these parameters represent the action of the foot in attenuating the initial force at impact They therefore represent the properties of the ball and arch of the foot, and the heel pad The upper damper (c2) and spring (k2) represent the combined actions of the muscles, predominantly of the legs, in controlling the landing In all cases the motion of this system could be described as overdamped in that the system permitted oscillatory motion With increasing drop height the stiffness of the spring remained constant but the degree of damping increased with drop height, therefore the damped frequency decreased with drop height

Despite the non-linear properties of the elements which comprise the musculo-skeletal system, the relatively simple model predicts with a reasonable degree of accuracy the ground reaction forces as a consequence of landing from a drop As such the model indicates a possible strategy used by subjects to control the landing from a drop The model can be used for predictive purposes, for example to estimate the forces a subject would experience when dropping from a given height

REFERENCES

Devita, P , and Skelly, W A (1992) Effect of landing stiffness on joint kinetics and energetics in the lower extremity **Medicine and Science in Sports and Exercise**, 24, 108-115

McNitt-Gray, J L , Yokoi, T , and Millward, C (1993) Landing strategy adjustments made by female gymnasts in response to drop height and mat composition **Journal of Applied Biomechanics**, 9, 173-190

OPTIMUM LENGTH OF MUSCLE CONTRACTION

Y.W. Chang, F.C. Su, H.W. Wu, K.N. An*

Institute of Biomedical Engineering, National Cheng Kung University
Tainan, TAIWAN.
*Orthopedic Biomechanics Laboratory, Mayo Clinic
Rochester, MN 55905, U.S.A.

INTRODUCTION

Muscles actuate movement by developing and transmitting forces to the skeleton. Understanding the characteristics of muscle contraction in vivo is important for designing the surgical procedure of tendon transfer and rehabilitation program. Mathematical modelling has been used for describing the muscle contraction. However, in vivo determination of the physiological and anatomical parameters is difficult but not impossible. The optimum muscle length and the associated joint position where the maximal muscle contraction force occurs are two of the important parameters for complete description of muscle model. The purpose of this study is to develop a method to determine these two parameters based on the physiologically and anatomically measurable data. Three major elbow flexors, biceps brachii (BIC), brachialis (BRA), and brachioradialis (BRD), were tested.

METHODS

Theory The basic rationale for solving the unknowns was that the external torque equaled to the summation of product of each elbow flexor force and its corresponding moment arm. The equation could be simplified as follows for the event of maximal voluntary contraction.

$$\tau = \sum_{i=1}^{3} (\hat{F}_{l_i} + \hat{F}_{pe_i}) * PCSA_i * \sigma_i * h_i$$

where τ was external torque. Normalized muscle forces due to active and passive length-tension relationship ($\hat{F}_l$ and $\hat{F}_{pe}$) were a function of muscle strain ($\varepsilon=(l-lo)/lo$; lo for optimum muscle length; l for muscle length). Physiological cross sectional area (PCSA) was adapted from literature. Moment arms (h) were calculated from biomechanical model of upper limb. Therefore, only optimum length and muscle stress (σ) remained unknown. Eight elbow joint positions were tested so as to provide eight equations for solving six unknowns. The determination of unknowns resulted in a sophisticated problem that had to be solved by using optimization approach due to the error of experimental measurement and the complexity of nonlinear equations. The objective function was mean square error.

Experiment Four male and four female normal subjects participated in the study. Mean age, weight, and height were 24.55±1.13 years, 55.44±4.58 kg, and 165.13±5.62 cm, respectively. None of these subjects had previous history of neuromusculoskeletal disorders in upper extremity. A Cybex isokinetic dynamometer was used to measure external torque applied at right elbow joint. Data were sampled at 2000 Hz by a 386 PC and IEEE488 A/D card. Each subject exerted maximal voluntary effort in 15, 30, 45, 60, 75, 90, 105, 120 degree of elbow flexion with 15 degree abduction of the shoulder. The duration of a sustainable effort was 2 seconds by a 2 minutes relaxation.

RESULTS

Average muscle stresses of male and female were 118 and 77 N/cm^2, respectively. Gender difference was significant ($p<0.001$). Muscle force could be predicted by product of the normalized muscle force ($\hat{F}_l + \hat{F}_{pe}$), PCSA, and muscle stress. The individual muscle moment was obtained by product of the muscle force and its moment arm. The predicted joint moment and measured external torque were shown in Figure 1.

Table 1: Optimum muscle length lo (cm) and the associated joint angle θ (degree).

	BIC	BRA	BRD
lo	13.52(0.76)	7.12(0.50)	16.69(1.83)
θ	102.20(6.94)	116.81(3.18)	76.75(13.07)
lo (An)	13.6(2.4)	9.0(2.9)	16.4(2.9)

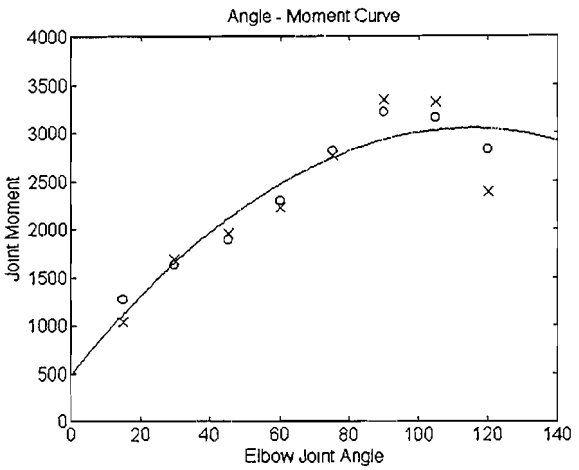

Figure 1: × for predicted moment; ○ for Cybex torque

DISCUSSION

Compared predicted optimum muscle length with muscle fiber length adapted from An et al (1981), the data were quite similar (Table 1). Also, the agreement between theoretically predicted and experimental moments was very good. However, for large elbow joint (120°), the discrepancy increased. This error may be due to some oversimplified assumptions, the experimental measuring error, and numerical error from optimization method. This study provided a method to predict the argued biomechanical parameters. The maximal muscle stresses of the three major elbow flexors were derived. Therefore, the limited capacity of human maximal muscle exertion was revealed quantitatively for male and female. The optimum lengths of the three major elbow flexors and their associated joint angle were significantly different. It implied these three muscles may dominate the muscle force at different range of motion. Additionally, the recruitment of a specific muscle in overall force production not only depended on its loading condition and constraints of the joint but also on its muscle fiber type and angle location of optimum length. In further analysis, EMG will be analyzed to determine the neuromuscular activation in submaximal isometric contraction and dynamic exercise both to confirm the muscle model and for clinical application.

REFERENCES

An, K. N. et al. (1981) J. Biomechanics **14**, 659-669.
Kaufman, K.R. et al. (1989) Neuroscience **40**, 781-792.

Acknowledgement This work was supported by NSC 83-0420-E-006-006, TAIWAN.

IN VIVO INTRA-MUSCULAR IMPLANTATIONS OF PHB/HV POLYESTERS IN SHEEPS. HISTOPATHOLOGIC AND BIODEGRADATION RESULTS.

[1,2]Chaput, C., [1]Rhalmi, S., [2]Yahia, L.H., [3]Selmani, A., [1]Rivard, C.-H.
[1]Department of Surgery, Ste-Justine Hospital, Montréal, Qc, CANADA; [2]Biomedical Engineering Institute, Ecole Polytechnique, Montréal, Qc, CANADA; [3]Chemical Engineering Department, Ecole Polytechnique, Montréal, Qc, CANADA.

INTRODUCTION

Poly(ß-hydroxybutyrate-ß-hydroxyvalerate) [PHB/HV] are microbial polyesters intra-cellularly produced as carbon/energy reserves for prokaryotic cells. They have been often compared to polypropylene in terms of physico-chemical (melting point, crystallinity level) and tensile properties, however PHB/HV polymers are reported as biodegradable materials (Brandl & al. 1990). They have been evaluated as degradable, biocompatible and natural thermoplastics for surgical devices. Drug delivery systems, sutures, bone plates and reconstructive devices have been proposed with PHB homopolymer (Holmes 1985, Brandl et al. 1990), but PHB membranes were also studied *In vivo* for guided tissue regeneration and thoraco-abdominal tissue reconstruction in animals (Malm & al. 1992, Boeree & al. 1992). PHB/HV polymers present improved physico-chemical (processibility, tactility) and accelerated hydrolytic degradability, and are now prefered for surgical implantable systems.

MATERIALS & METHOD

Three commercial PHB/HV (HV 7, 14 & 22%) copolymers were dissolved in chloroform (10% w/v) and cast on the glass surfaces of Petri dishes. The solvent was allowed to evaporate for at least 96 hrs, and all PHB/HV films were stored at room temperature. PHB/HV materials for implantations were sampled in rectangular film specimens. The specimen sizes were measured using a digimatic micrometric caliper. All specimens were sterilized by EtO. The PHB/HV films were implanted in dorsal muscular tissues of adult sheeps for 1, 5, 8, 11, 15, 20, 25, 30, 52, 66, 70 and 90 weeks. The animals were anesthezied using Acepromaycine^R and Thiopenthal^R 5.0%, surgically maintained using Halothane^R 1.5%. The dorsal region was incised on each side of the spine. The muscular tissues along and beside the spine were degaged, and three independant pounches were created. One PHB/HV specimen was disposed in each pounch and attached to the muscles by four permanent Prolene^R sutures. The pounches and incisions were closed with absorbable Dexon^R sutures. During the two days following surgery, the sheeps were admisnistrated with analgesics and antibiotics (Demerol^R/Permlong^R). Sacrifices were perfored by Euthanyl^R overdose, the muscular bundles and PHB/-HV specimens were excised. The samples were grossly dissected to degage the PHB/HV films. Specimens for histology were excised at 1, 5, 11, 20, 66, 70 and 90 wks and fixed in 10% formalin.The histological analysis was performed conventionally using paraffin embedding, thin slides (2-4µm) and Hematoxylin/Eosin staining. The tissues were enzymatically digested using collagenase (37°C, 1 week), then separated from the PHB/HV films in distilled water (density gradient). All PHB/HV specimens were washed using distilled water and ethanol, air-dried at 40°C, then stored at room temperature.

RESULTS & DISCUSSION

The mean weight and surface area of the PHB/HV specimens are 284.2+/-140.5g and 2715.5+/-591.1mm^2, respectively (N=30): HV7% 305.5+/-173.7g and 2439.1+/-280.9mm^2 (N=10); HV14% 288.5+/-139.9g and 2885.6+/-715.9mm^2 (N=10); HV22% 258.7+/-112.4g and 2821.7+/-636.2mm^2 (N=10). The PHB/HV specimens rapidly break up at the suture attachments, then lose its initial plane disposition inside the muscular fibrous tissues and start to fold up on itself. At 1 and 5 weeks, most PHB/HV films still remain intact in the muscles, then, for implantation periods of 5 wks and up, all PHB/HV specimens break up in film portions and debris. However, PHB/HV portions and debris did not travel through the muscular tissues, but remain concentrated at the same site. For all implantation periods, PHB/HV materials are rapidly infiltrated and surrounded by muscular tissues and membranes. Implantations from 5 to 30 wks demonstrate a thin fibrous capsule infiltrating the PHB/HV portions and surrounding the

PHB/HV materials. For 66 to 90 wks implantations, the PHB/HV debris were individually surrounded by thin fibrous capsules, packed together and surrounded from the muscular tissues by a thick membrane. No abscess formation and tissue necrosis was observed in the tissues adjacent to the PHB/HV specimens. The caspule thickness and cellular activity at the implant surface were evaluated by histology: inflammatory cells (macrophages, neutrophiles) were observed in the fibrous capsules at 1 and 11 wks.

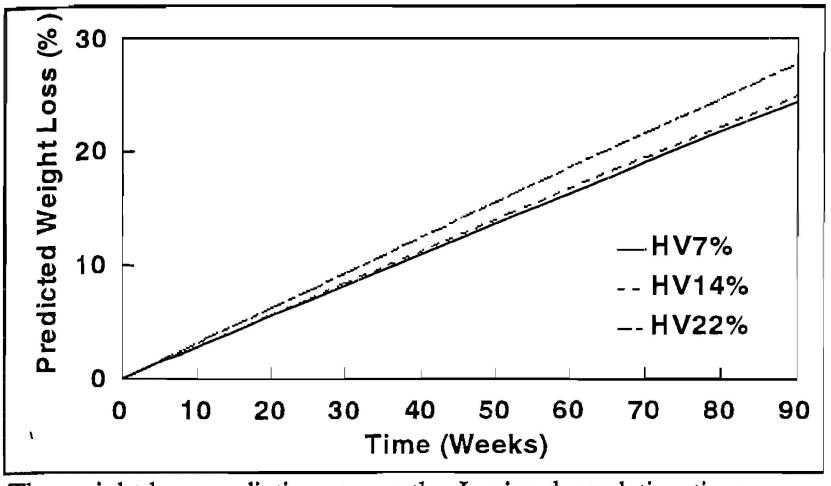

Figure 1: The weight loss prediction versus the *In vivo* degradation time.

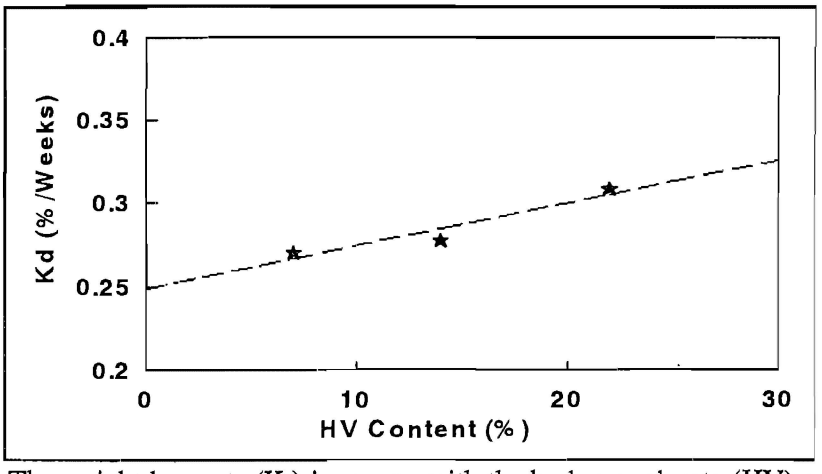

Figure 2: The weight loss rate (K_d) increases with the hydroxyvalerate (HV) content.

The PHB/HV materials present extremely variable and low weight losses during the intra-muscular implantations in sheeps. Most PHB/HV implants still remain intact at 70 and 90 wks. The weight loss rate, as determined by correlation analysis with the time, ranges from 0.27 to 0.31%/wks over the *In vivo* period, and seems to increase with the HV content. Physico-chemical and microstructural analyses (GPC, DSC, NMR, SEM) will inform us on the real *In vivo* degradation effects and kinetics. Although the weight loss was highly irregular and variable *In vivo*, the results suggest that PHB/HV materials chemically and/or enzymatically degrade, but present extremely low dissolution even for long-term implantations (years).

REFERENCES

1. Brandl H., Gross R.A., Lenz R.W., Fuller R.C. In: "Advances in Biochemical Eng." Vol. 41, A. Fiechter (ed), Springer-Verlag Berlin Heidelberg 1990, pp77-93.
2. Holmes A.J. (1985) Phys. Technol., 16:32-36.
3. Malm T., Bowald S., Karacagil S., Bylock A., Busch C. (1992) Scand. J. Thor. Cardiovasc. Surg., 26:9-14.
4. Boeree N.R. Dove J., Cooper J.J., Knowles J., Hastings G.W. (1992) Biomaterials, 14:793-796.

STIFFNESS AND STRENGTH CHANGES IN A SHEEP FRACTURE HEALING MODEL: THE IMPLICATIONS IN CLINICAL FRACTURE ASSESSMENT

Mellick J.Chehade, Namal Nawana, Mark J. Pearcy, Anthony P. Pohl

Department of Orthopaedics and Trauma, Royal Adelaide Hospital and University of Adelaide. School of Engineering, Flinders University of South Australia, Adelaide, Australia

INTRODUCTION

Current evaluation of fracture healing relies on manual stability testing, radiology and the empirical passage of time. Kenwright (1985) estimated that this assessment is accurate in 90% of long bone fractures to ± 3 weeks. Techniques such as vibrational analysis, wave propagation analysis and strain gauge instrumentation of fracture fixation devices have been investigated with the aim of objectively assessing the mechanical properties of healing long bone fractures. These techniques are indicators of fracture *stiffness*. In clinical practice, our main objective is to assess fracture *strength*. In assessing refracture risk with stiffness monitoring, a workable correlation between stiffness and strength must be assumed. The aim of this study was to examine time related stiffness and strength changes in a healing fracture and to test the validity of this assumed correlation between stiffness and strength.

METHODS

An osteotomy of the left tibia of 40 merino wethers (after the application of an external fixator) was used as the fracture model. The sheep were then able to ambulate freely on the fractured limb. Eight sheep were randomly assigned to each of 5 groups destined for culling at 2, 4, 6, 8 or 10 weeks. After culling both tibiae were excised, the right acting as a control. The bending stiffness and strength of the excised tibiae were determined in the mediolateral plane with four-point mechanical bending tests. Stiffness was calculated from the slope of the bending moment/displacement curves, both at low loads, LLS, (150N) and at failure loads, FLS, (to 2250N). The ultimate strength was determined from the highest load value. Stiffness and strength values where expressed as healing ratios relative to the non-osteotomised control bones: the "low load stiffness healing ratio", LLSHR; the "failure load stiffness healing ratio", FLSHR, and the "strength healing ratio", SHR. These were all correlated against fracture healing time. The two stiffness measurements were then correlated against strength.

RESULTS

Of the 40 sheep, 24 tibial pairs survived fracture whilst being excised from the tibia and were suitable for analysis. A wide range of stiffness and strength results was obtained within each time group tested with marked overlapping of the 95% confidence limits between the groups (Fig. 1). The mean bending stiffness of the control tibiae (13.9Nm/mm) was found to be significantly higher when tested to failure than when tested under low loads (9.9Nm/mm); p = 5.6E-09.

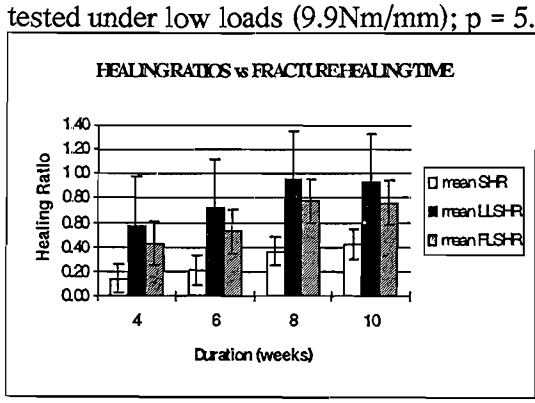

Fig 1

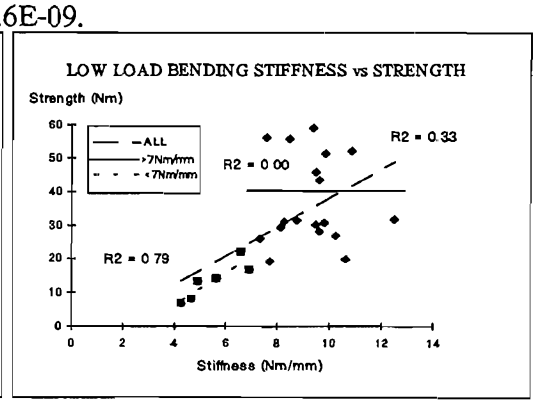

Fig 2

The mean FLSHR (0.68) was found to be significantly lower than the mean LLSHR (0.85); p=3.1E-06. At 8 weeks mean LLSHR, FLSHR and SHR were 0.95, 0.78, and 0.36 respectively. In the 10 week period of this study, 5 sheep showed LLSHR values greater than 1.0 (1.09 -1.27) whereas thegreatest FLSHR in the same period was only 0.99. With small loads, the overall correlation between stiffness and strength is poor (R^2=0.33). On further analysis of this data, however, a strong correlation is observed in the early stages of fracture healing (R^2=0.79 for stiffness <7Nm/mm). Thereafter the correlation breaks down (Fig. 2).

With the high "fail" loading forces, a much stronger correlation with strength is observed (R^2=0.64). Similarly, this correlation is stronger at low stiffness values (R^2=0.80 where stiffness <7Nm/mm compared with R^2=0.20 where stiffness >7Nm/mm). When the stiffness and strength *healing ratios* are correlated, where LLSHR ≥0.99 the SR ≥0.24 but with values as high as 0.62 (Fig.3). Where FLSHR ≥0.99 the SR is ≥0.33 (Fig. 4).

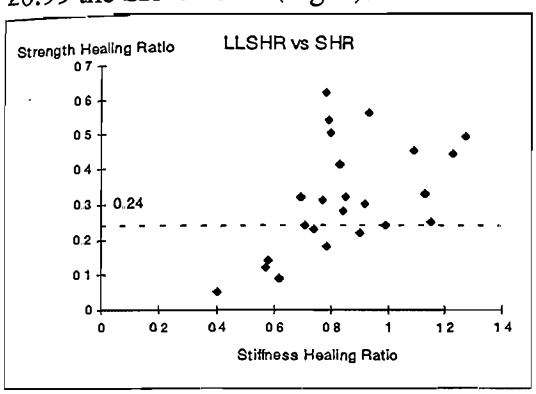

Fig. 3

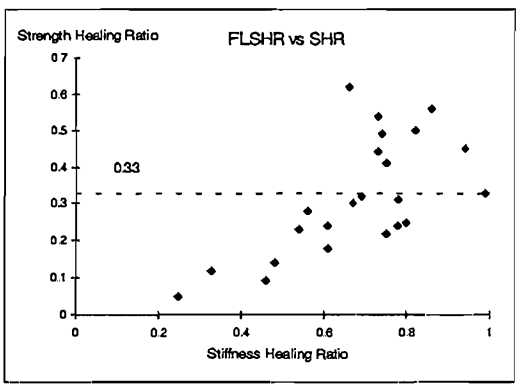

Fig. 4

CONCLUSIONS

Because of the non-linear stiffness characteristics, studies looking to correlate stiffness as determined by direct mechanical tests with indirect stiffness assessments such as with vibrational analysis, will need to take into account test loading conditions.

In this sheep fracture healing model, the wide variations in the relative stiffness and strength values at any given point in time highlight the poor predictive value of the empirical passage of time as an indicator of fracture healing.

The clinical implications of these findings are several. Stiffness monitoring can be used to quantify strength in the early stages of fracture healing. By being able to show a return to prefracture stiffness, a *minimum* strength value may be confidently predicted. In this study it is 24% under low loads and 33% under "fail" loads. The stiffness measured under higher loads better reflects the ultimate strength characteristics of the healing bone. This implies that clinical stiffness monitoring should ideally be performed under heavy loading conditions.

If this 24% of prefracture strength is sufficient to support non strenuous, normal daily activities, then stiffness monitoring may be used to assess a clinical healing "baseline". It will not, however, predict which fractures have regained the greater strength characteristics required for the heavier loads associated with manual labour or professional sporting occupations. Thus any assessment of refracture risk based on stiffness monitoring techniques will be inherently limited.

REFERENCES

Kenwright J. (1985) Biomechanical measurement of fracture repair. In: Whittle M, Harris JD, eds. *Biomechanical Measurement in Orthopaedic Practice*. Oxford, Oxford University Press, 3-9.

GAIT OF NORMAL SUBJECTS IN SPECIALISED ACTIVITIES OF DAILY LIVING

Chen Xiaon, State Key Laboratory of Mechanical Transport, Chongqing University, Peoples Republic of China

Paul J P, Bioengineering Unit, University of Strathclyde, Glasgow, Scotland.

INTRODUCTION. Although there exists a substantial literature on the kinematics of normal walking at uniform speed in a straight line on a level surface (Eberhart et al, 1947) and many other investigations have acquired data in the sagittal plane, the numbers offering a full 6 quantity, 3 dimensional analysis are considerably smaller. Activities other than straight line walking include the negotiation of stairs or ramps (Morrison 1967, Paul and Poulson (1972). Studies of locomotion in a nonlinear path have included Harrison and Nicol (1984) where athletic young subjects jumped, walked and ran in straight line locomotion and also in undertaking a right angle turn. This research programme relates to knee joint loading while carrying a load in one hand while walking in straight lines, circular arcs and sharp right angle turns.

There has always been an interest in the fatigue strength of knee joint implants due to fatigue failures in service and wear since it is reported that massive bone osteolysis is triggered by the presence of wear particles of UHMWP. Standards for design and testing of implants require knowledge of load cycles and their frequency. The current investigation explores the protocols for kinetic analysis of gait while carrying loads and turning while walking. Shopping, carrying children, and using public transport involves one-sided load carrying and negotiation of obstacles obstacles and taking avoiding action in crowded pavements, passages and corridors.

MATERIALS AND METHODS. The preliminary stage of the investigation involves two adult male volunteers in the age range 30 to 40 years. Test subjects wore brief shorts, having bare legs and wearing normal footwear. Subjects were of normal body mass/stature ratio with no history of skeletal, articular or muscular dysfunction. The three dimensional trajectories of markers on anatomical landmarks were registered by a VICON Movement Analysis System in association with ground to foot force records from three Kistler Force Platforms, subjected to regular checks according to the CAMARC quality assurance protocol. This paper reports the ground to foot records obtained while carrying a 10kg suitcase in one hand and negotiating an arc of 2m radius or turning sharply through a right angle. The same procedures were undertaken unloaded. Subjects walked at their self-assessed normal fast and slow speeds.

RESULTS. The figures show the X Z and Z components of ground to foot force (forwards, upwards and outwards respectively on the foot). Loading and fast speed give highest vertical forces. The forces of the two shear force curves interchange in the sharp turning activity. These specimen load curves indicate significant loading of the knee considered in a second paper. Slow speed of walking in both cases leads to a 3 peak Fy curve.

REFERENCES

Eberhart H D Ed. (1949) Fundamental studies of human locomotion. Univ of California, Berkeley.

Harrison D W and Nicol A C (1988) Knee joint loads during running and turning activities, in, Biomechanics in Sport. Inst Mech Eng, London, 13-18.

Morrison J B (1969) The function of the knee joint in various activities. Biomed Eng **4,** 573-580.

Paul J P and Poulson J (1974) The analysis of forces transmitted by joints in the human body, in, Experimental Stress Analysis, CISM, Udine, Italy.

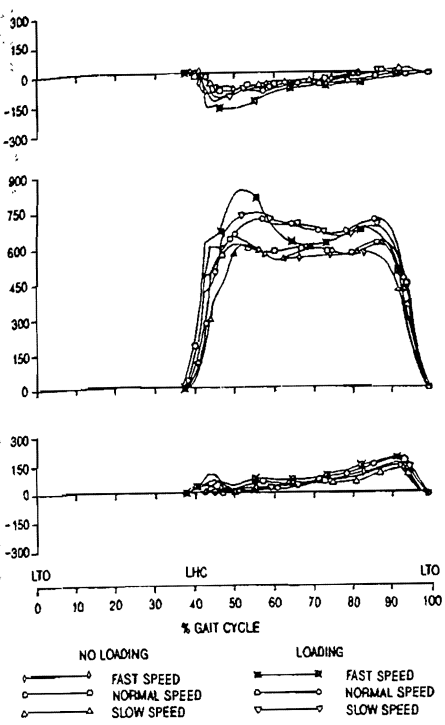

RIGHT ANGLE TURN WHILST WALKING (TURN LEFT SUBJECT No1)
REACTION FORCES OF GROUND TO LEFT FOOT

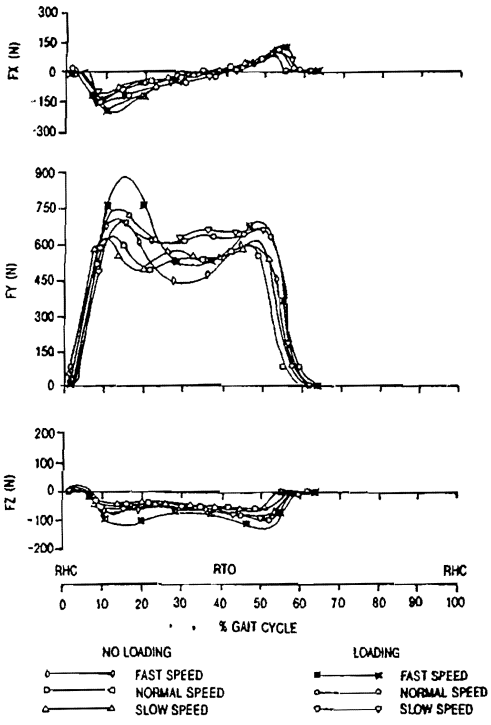

RIGHT ANGLE TURN WHILST WALKING (TURN LEFT SUBJECT No1)
REACTION FORCES OF GROUND TO RIGHT FOOT

THE USE OF OPTIMIZATION METHOD IN PREDICTING THE ANTHROPOMETRIC DATA OF THE BIOMECHANICAL MODEL

Cheng-Kung Cheng[1], Horng-Chang Chen[2] and Chia-Ou Chang[2]
[1]Center for Biomedical Engineering and [2]Institute of Applied Mechanics
National Taiwan University, Taipei, Taiwan, R O C

INTRODUCTION

Many biomechanical models have used the kinematic, kinetic and anthropometric data combined with equations of motion to calculate the joint resultant forces and moments (Crowninshield and Brand, 1981) Once the joint resultant forces and moments were calculated, the reduction method or optimization method was then applied in the prediction of the joint force distributions (Cheng, 1988). The anthropometric data included the mass, center of mass, moment of inertia of the musculoskeletal segments (Plagenhoef et al., 1983) Lack of the complete anthropometric data results in the estimation error of the model predictions The present anthropometric data used for the biomechanical model are based on Caucasian data In order to have the anthropometric data of the local populations and to overcome the problem of the individual difference, the optimization techniques were used with a two-dimensional eight-link biomechanical model to predict the anthropometric data (mass ratios (M), centers of mass (CM) and coefficients of moment inertia (CMI) of link segments) of the individual

METHOD

A two-dimensional biomechanical model of eight link segments, including hand, forearm, arm, head, trunk, thigh, lower leg and foot was developed The Elite motion analysis system was used to record and analyze the kinematic data of the biomechanical model The Kistler force platforms were used to measure the ground reaction forces of the foot Optimization techniques in minimizing the error between the estimated data from the biomechanical model and measured data from the force plateforms were applied as the cost function The estimated data and measured data included the ground reaction forces and application point of the ground reaction forces The optimization algorithm used is Adaptive Simulated Annealing (ASA) which was developed by Ingber (1993) The rational equality and inequality constraints were applied in the optimization calculations The initial anthropometric data (initial values) used for the optimization calculation were adopted from the literature published Caucasian data To verify the mathematical model, a custom-made three links' metal structure with known dimensions was developed to simulate the body leg Since the distribution of M, CM and CMI of the metal structure are known, we can use it to verify the mathematical model Eight volunteered subjects were also studied to test the reproducibility and to have preliminary data of the local populations The subjects were asked to perform symmetrical free motion from standing to half squatting

RESULTS

The estimated anthropometric data of the custom-made three links' structure were well verified with the known (calculated) anthropometric data in using above mentioned optimization methods The averaged estimated error of all the anthropometric parameters is 3 36% In the reproducibility study, two of eight subjects were studied twice to evaluate the reproducibility The results showed that the average errors of the mass ratio, center of

mass and coefficient of the mass moment of inertia are 1 13%, 2 69% and 4 41%, respectively The results of eight link segments in eight subjects showed that high individual difference was seen due to different body shapes of eight subjects The average difference of all anthropometric parameters between the literature data and individual predicted data were ranged from -10% to 11% as shown on the Figure 1 However, the average data of the eight subjects showed only about 4% difference with the Caucasian data

DISCUSSION

According to the above results, the present method has demonstrated a good prediction of the human anthropometric data of the biomechanical model The method can predict different anthropometric data for the different individuals The results also implied that global distributions of the human anthropometric data are similar between different race In conclusion, the present method has been verified as a possible method to predict the individual anthropometric data for the musculoskeletal biomechanical modelling

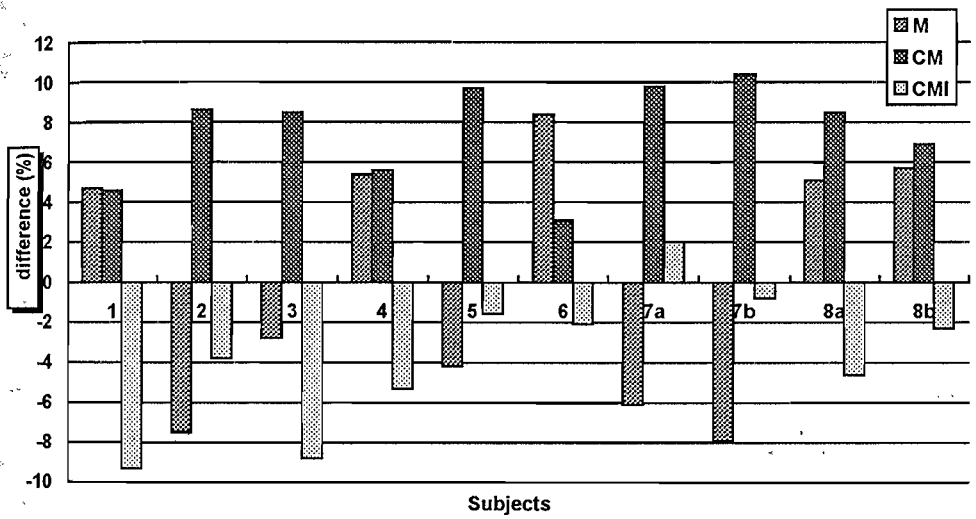

Figure 1 Average difference of all anthropometric data between the literature data and individual predicted data

REFERENCES

1 Crowninshield, R D and Brand, R A (1981) The prediction of forces in joint structures distribution of intersegmental resultants In Exercise and Sports Sciences Reviews, D I Miller, Editor The Franklin Institute Press, Vol 9, pp 159-181
2 Cheng, C K (1988) A Mathematical model for predicting bony contact forces and muscle forces at the knee during human gait Ph D thesis, The University of Iowa
3 Plagenhoef, S , Evans, F G and Abdelnour, T (1983) Anatomical data for analyzing human, Research Quarterly for Exercise and Sport, 54(2) 169-178
4 Ingber, L (1993) Simulated annealing practice versus theory Math Comput Modelling, 18 29-57

ANALYSIS OF 3-D SHOULDER MOMENTS DURING DOOR OPENING AND CLOSING

P. L. Cheng & A. C. Nicol

Bioengineering Unit, University of Strathclyde, Glasgow, Scotland

INTRODUCTION

Door opening and closing is one of the primary activities of daily living, and can be characterised as pushing and pulling. Although pushing and pulling strengths have been intensively investigated, most previous results are isokinetic and limited to the hand loads (Ayoub & McDaniel 1974, Snook 1978). Little attention has been focused on the shoulder moments during real pulling and pushing activities such as door opening and closing. In real activities, not only the hand loads but also the inertial and gravitational loads will influence the shoulder moments. The purpose of this study is to investigate how much shoulder moment is required during the door opening activity and how the hand loads, inertial and gravitational effects contribute to the shoulder moments.

METHODS

A simplified door was made for use in the motion analysis laboratory. The door was instrumented with a six-component strain gauged force transducer, which was fitted between the door and a cylindrical handle of diameter 0.03m. During the activities the forces acting on the hand by the door handle were recorded by the A-D converter of a Vicon motion analysis system. The handle was 0.75m from the hinged left side of the door with a holding height of 0.9 to 1.3m from the ground. A viscous door closer was used as a resistance element.

The subject stood with his right hand holding the handle and the arm fully extended. In order to allow the door to be fully opened without body movement, the frontal plane of the subject's body formed an angle of 30 to 45 degrees to the door. The whole activity involved pulling (opening) the door to the widest opening and then pushing it back to the original (closed) position without stopping between the pulling and pushing. The coordinates of sixteen markers, affixed to the trunk, arm and transducer, together with the force transducer signals were collected simultaneously by a six-camera Vicon motion analysis system at 50Hz sampling frequency. Four subjects were tested and each subject was measured three times.

The kinematics data were filtered by a FIR filter at the selected cut-off frequency for each data sequence using the residual analysis method (Winter 1990). The shoulder joint moments were calculated using the inverse dynamics method. The hand loads measured by the transducer, the inertial forces and torques and the gravitational forces of the arm were all considered in the calculations.

RESULTS

The three-dimensional shoulder moments expressed in the trunk coordinate system are given in Fig.1 to Fig. 4, where Mx is the adduction-abduction moment about the posterior-anterior axis (directed forward), My is the inward-outward moment about the vertical axis (directed upward), and Mz is the flexion-extension moment about the transverse axis (directed from left to right). The resultant moment (Mr) and its components on the three axes of the trunk coordinate system are given in Fig.1. The contributions of the hand loads, the inertial forces and moments of the arm, and the gravitational forces of the arm on the three orthogonal components of the shoulder moment are given in Fig.2 to Fig. 4, respectively.

It can be seen that the major moment acting on the shoulder joint is the flexion moment, which is mainly caused by the gravitational effect of the arm. The peak resultant and flexion moments occurred at the starting and end point of the activity with the arm

fully extended. The contribution of hand loads and the inertial effects (Fig.2, 3) result in a decrease of the resultant and flexion moments at the beginning of the pulling phase (opening door), but the hand loads cause increased resultant and flexion moments in the pushing phase (closing door). The second major moment on the shoulder joint is the abduction moment (-Mx) mostly due to the gravitational effect. It was also found that the inward-outward rotational moment (My) and its three sources of contributions are all at a low magnitude.

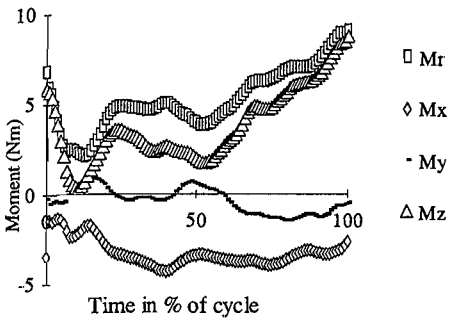

Fig.1 3-D shoulder moments

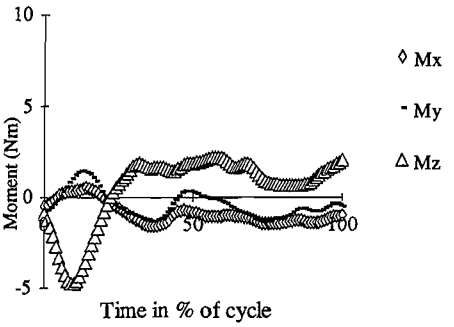

Fig. 2 Shoulder moments by hand loads

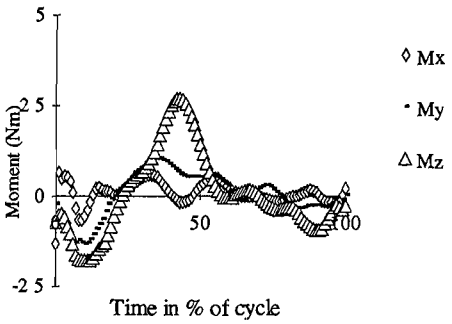

Fig. 3 Shoulder moments by inertial effects

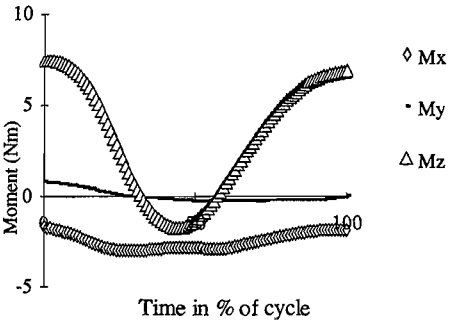

Fig. 4 Shoulder moments by gravity

DISCUSSIONS

The results shows that the gravitational forces on the arm are the major contributors to the shoulder moment, especially during pushing a door and at the starting and end points of the activity, at where the maximum shoulder moment occurred. The resistance of the door, represented by the hand loads, reached a maximum value of 70% of the moment due to the gravitational effects at the corresponding point. In the pulling phase the extension moment (-Mz) due to the hand loads was balanced by the flexion moment due to the weight of the arm. If the door is opened by pushing then the hand loads, the inertial effects and gravitational effects will combine to produce a larger shoulder moment. The maximum abduction moment reached 85% of the resultant moment at the corresponding point, therefore its contribution to the shoulder moment must not be neglected in the biomechanical analysis of the activity.

CONCLUSIONS

Detailed information of the 3-D shoulder moment has been obtained and show that gravitational effects are dominant. It is recommended that full three-dimensional analysis is required for the pushing and pulling actions, and that gravitational effects should not be neglected.

REFERENCES

Ayoub, M. M. & McDaniel, J. W. (1974), *AIIE, Tr.* **6**, 185-195.

Snook, S. H. (1978), *Ergonomics*, **21**, 963-985.

Winter, D. A. (1990), *Biomechanics and Motor Control of Human Movement*, John Wiley & Sons, Inc. New York.

MOTION PATTERNS OF THE HEAD IN THOROUGHBRED HORSES DURING DIFFERENT GAITS

T.K. Cheung and K.N. Thompson
Maxwell Gluck Equine Research Center
University of Kentucky

Lexington, USA

INTRODUCTION

Studies of equine kinematics have been generally concentrated on the limbs. Less attention has been paid to the movements of the head and neck. These segments of the body compose a significant percentage of weight (head = 4.5%, neck = 5.5%) of the horse (Leach and Crawford, 1983), and their movements will undoubtedly influence gait patterns and energy exchange with other segments of the body in each gait cycle. The head and neck movements are therefore an integral part of equine locomotion. The change in movement patterns of the head was observed for horses with various degrees of lameness (Girtler and Floss, 1983). Recently, head and withers excursions were reported for horses before and after an induced carpal lameness (Peloso et al, 1993). Data of these studies showed that the heads of normal horses rose and fell twice in a sinusoidal manner within a stride cycle for both the walk and the trot. Given limited data reported in the literature, the purpose of this study was to further investigate the characteristics of head movements in normal Thoroughbred horses exercising at different gaits and to relate these movements to the metacarpophalangeal (fetlock) joint. The fetlock joint was chosen because of its clinical and biomechanical importance in equine locomotion study.

MATERIALS AND METHODS

Eight horses, five geldings and three mares between 10 to 15 years of age were used and trained to exercise comfortably on treadmills. The weight of the horses ranged from 450 to 550 kg. Reflective markers were placed at the nose, mid-metacarpal bone, fetlock joint and mid-proximal phalanx of the left forelimb. The horses were then walked, trotted, cantered, and galloped on a horizontal treadmill at 1.9, 4.0, 7.0 and 9.5 m/s respectively. The horses' movements were recorded two-dimensionally at 200 frames per second (Motion Analysis, Santa Rosa, USA). The lead forelimb was used at the canter and gallop. The fetlock joint angle was calculated in terms of the dorsal angle of the joint. Velocity of the head was taken as the time derivative of the head displacement. Stride characteristics of the left forelimb were identified with the fetlock joint angles as reported in the literature (Adrian et al., 1977; Ratzlaff et al., 1993).

RESULTS AND DISCUSSION

Fig. 1 showed that amplitude of head displacement was the least at the trot (9.4 ± 1.3 cm), while the amplitude was of relatively the same order between the walk (19.7 ± 3.0 cm), the canter (21.4 ± 3.2 cm) and the gallop (22.0 ± 2.5 cm). The frequency characteristics also varied between gaits as shown in Fig. 2. Head movement in the canter and gallop followed a sinusoidal pattern with a single cycle, while the walk and trot were with two cycles as reported by Girtler and Floss (1983) and Peloso et al. (1993). Different frequency of rise and fall of the head appeared to be a function of symmetry of gait. The head dropped to its lowest position at approximately the mid-stance of each of the support forelimbs in the walk and trot. In the canter and gallop, the head fell to its lowest position before the stance of the lead forelimb and then rose at its maximum velocity during mid-stance, at which time the fetlock joint experienced maximum extension. Maximum upward velocity of the head was observed at the second

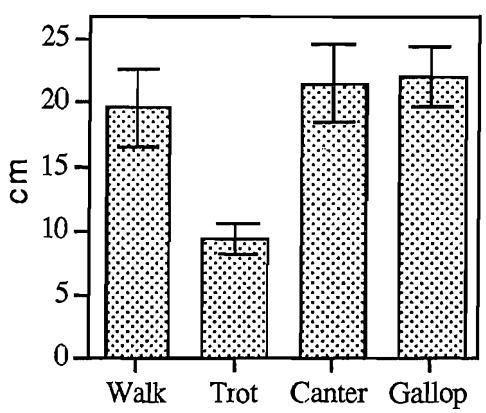

Fig. 1 Head displacements of test horses at different gaits (mean±SD).

peak extension of the fetlock joint during the stance of the forelimb in the walk. For the trot, the head moved upward at its highest speed after fetlock joint flexion was initiated during the stance of the forelimb. Similar to the displacement, the magnitude of velocity was lowest in the trot (66.7±12.9 cm/s) and highest in the gallop (135.0±23.8 cm/s). The velocity for the walk and canter were 100.0±6.3 and 103.0±24.4 cm/s respectively. Results obtained in this study have shown the head movement patterns in vertical direction in different gaits in relation to the fetlock joint activity. Further work is necessary to fully describe the coordination between the head and other segments of the body.

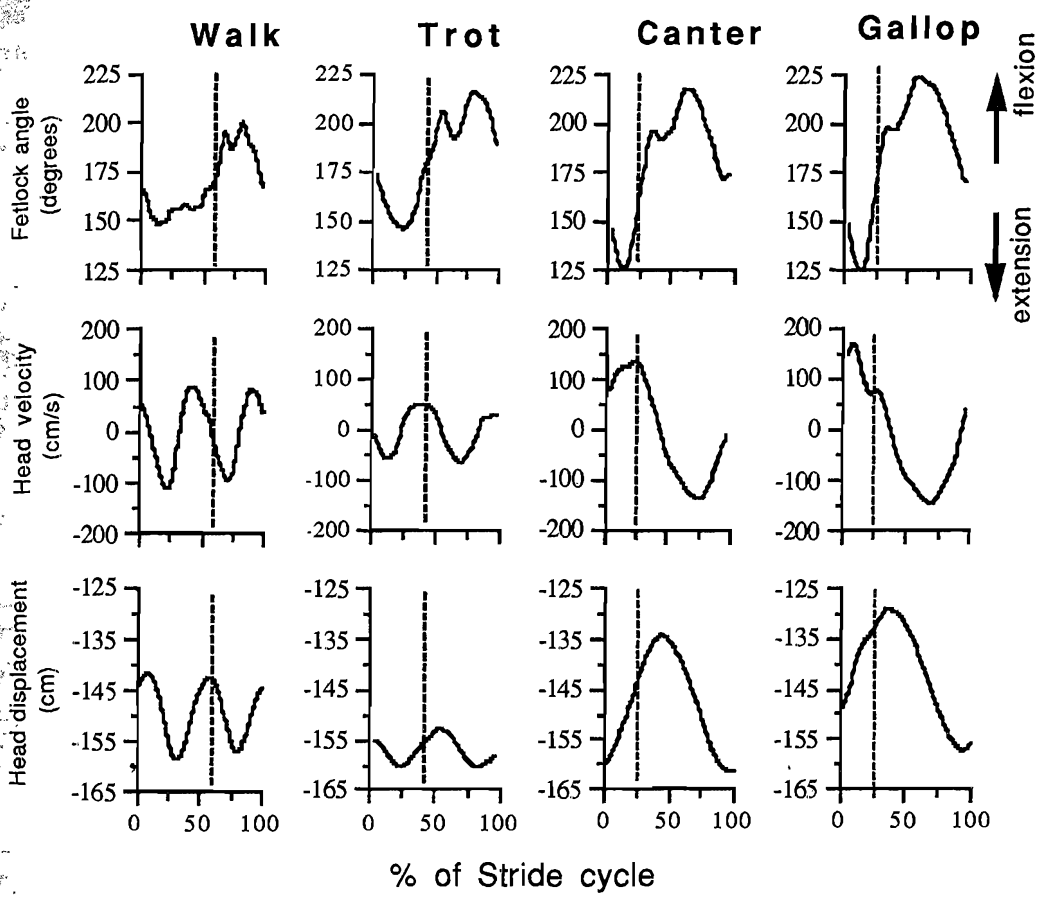

Fig. 2 Fetlock angles, head displacements and velocities in a stride cycle of the walk, the trot, the canter and the gallop of representative trials. (The left and the right of the dotted line shown in each graph represented the stance and swing phases respectively.)

REFERENCES

Adrian, M., Grant, B., Ratzlaff, M., Ray, J. and Boulton, C. (1977) Electrogoniometric analysis of equine metacarpophalangeal joint lameness. *Am. J. Vet. Res.*, **38**, 431-435.

Girtler, D. and Floss FN. (1984) Zur Bewegung gesunder und bewegungsgestörter Pfrede. *Arch. Tierärztl. Fortbild.*, **8**, 132-139.

Leach, D.H. and Crawford, W.H. (1993) Guidelines for the future of equine locomotion research. *Equine Vet. J.*, **15**, 103-110.

Peloso, J.G., Stick, J.A., Soutas-Little, R.W., Caron, J.C., DeCamp, C.E. and Leach, D.H. (1993) computer-assisted three-dimensional gait analysis of amphotericin-induced carpal lameness in horses. *Am. J. Vet. Res.*, **54**, 1535-1543.

Ratzlaff, M.H, Wilson, P.D., Hyde, M.L., Balch, O.K. and Grant, B.D. (1993) Relationships between locomotor forces, hoof position and joint motion during the support phase of the stride of galloping horses. *Acta Anat.*, **146**, 200-204.

LOWER EXTREMITY JOINT LOADING DURING IMPACT IN RUNNING

G.K. Cole, B.M. Nigg, K.G.M. Gerritsen, and A.J. van den Bogert

Human Performance Laboratory, University of Calgary, Calgary, Canada

INTRODUCTION

Repetitive impact loading has been shown to produce cartilage degeneration in an animal model (e.g. Yang et al., 1989). Similar loading characteristics have been observed in the ground reaction force during heel-toe running leading to the assumption that runners may be at risk to the development of osteoarthrosis in the joints of the lower extremity. However, runners as a group do not show a higher incidence of osteoarthrosis (Konradsen et al., 1990), which raises the question of whether the joint loading conditions in the animal studies are the same as those in human running. These internal loading conditions may differ since it is reasonable to assume that factors such as skeletal alignment and muscular activity, which influence joint loading, will differ between an active movement like running and the controlled conditions of the animal experiments. The purpose of this study was to estimate the sagittal plane contact forces in the ankle, knee, and hip joints during the impact phase in heel-toe running.

METHODS

A 2-D, forward dynamics model was used to provide estimates of joint contact forces. The model consisted of four rigid segments (foot, leg, thigh, trunk) connected by hinge joints. Body mass and segment lengths were obtained from a male subject. Eight functional muscle groups were included in the model: soleus, gastrocnemius, tibialis anterior, vasti, rectus femoris, hamstrings, gluteals, and iliopsoas. The force producing characteristics of each muscle group were represented by a Hill-type model.

The mass of each body segment was fractioned between soft and skeletal tissue based on cadaveric information. Each soft tissue mass was modelled as a point mass placed between the contractile and series elastic elements of the Hill model. The trunk segment was sectioned into skeletal and non-rigid parts, the two sections attached to one another by a linear spring. The mass fraction of the non-rigid part and the spring constant were selected to provide a good agreement between the predicted and experimental vertical ground reaction force peaks (figure 1a). The predicted vertical ground reaction force was calculated using a non-linear viscoelastic relation between force and surface deformation beneath the foot that was obtained from in-vivo impact tests of the shoe/heelpad system (Aerts and De Clercq, 1993). The horizontal ground reaction force was modelled as Coulomb friction.

Initial segment positions and velocities, as well as initial muscle forces, were required for the simulation model. Kinematic and ground reaction force measurements were collected of the subject running at 4.0 m/s. Inverse dynamics were used to calculate the resultant moments at the ankle, knee and hip joints at the time of heelstrike. Multiple sets of initial muscle forces (i.e. different co-contraction) were generated that satisfied the resultant joint moments. Simulations using different combinations of initial muscle forces were carrried out using the DADS software (version 7.5, CADSI, Coralville, IA). The movement was simulated over a 50 ms time period.

RESULTS

Results are presented here for one arbitrary set of initial muscle forces and are normalized to body weight. There was initial force in each of the joints due to muscular contraction. The force in the ankle joint exhibited an initial decrease over the first 10 ms of contact followed by a sharp increase until 32 ms of contact, the time of the impact peak in the vertical ground reaction force (figure 1b). The forces in the knee and hip joints, however, remained nearly constant from the time of heelstrike to the time of the impact peak in the ground reaction force (figures 1c and 1d, respectively). Although the

magnitude of the contact force in each joint varied depending on the amount of muscular co-contraction that was assumed, the trends observed in the joint contact forces were independent of the initial co-contraction. In addition, the predicted kinematics were in good agreement with the experimentally measured kinematics of the subject. .

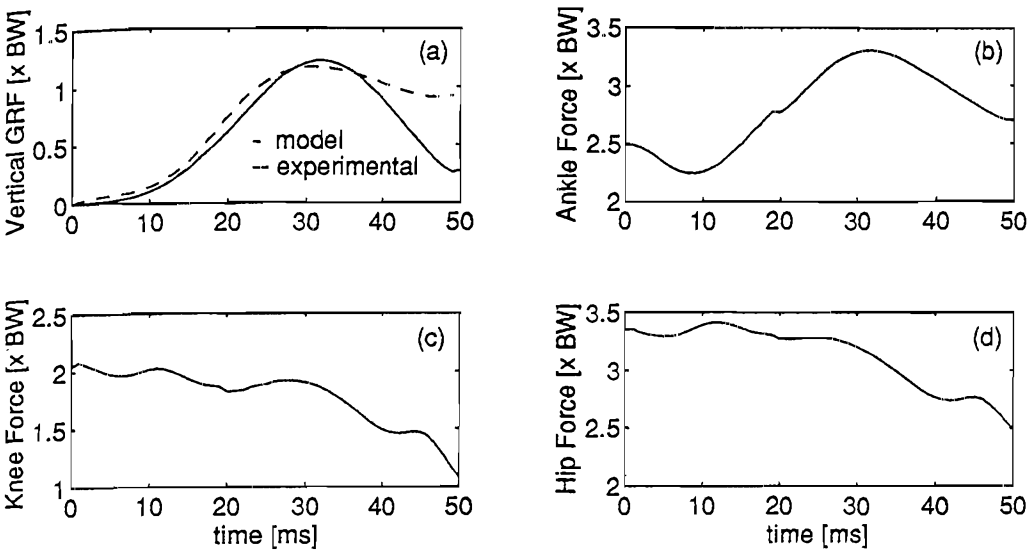

Figure 1: Model predictions of (a) the vertical ground reaction force and the contact forces at (b) the ankle joint, (c) the knee joint, and (d) the hip joint during the impact phase in running for one subject. Each joint force shown is the "compressive" component acting at the joint.

DISCUSSION

The main result of this study is that unlike the vertical ground reaction force, the contact forces in the knee and hip joints did not increase at a high rate during the impact phase of running. This result is due to the influence of the hamstrings muscle group on the joint force. At heelstrike, a flexion moment exists at the knee joint and an extensor moment exists at the hip joint, both moments satisfied to a large part by force in the hamstrings. The hamstrings "preload" each joint prior to heel contact. Following heelstrike, these muscles shorten quickly and their force decreases sharply, offsetting the increase in joint force due to the impact condition. The above result was largely independent of the assumptions made in the model and was also shown to be insensitive to the selection of model parameters.

Clinically, this study provides a possible explanation for the discrepancy between the observations of cartilage degeneration in an animal model (e.g. Yang et al., 1989) and the observed incidence of osteoarthrosis in runners (Konradsen et al., 1990). It has been shown that the degenerative changes in the cartilage of animal models are more sensitive to the rate of applied impact load than the magnitude (Yang et al., 1989). The muscular forces acting in the lower extremity have the potential to substantially reduce the rate of loading in the knee and hip joints during the impact phase in running. It may be speculated that this muscular control mechanism is responsible for limiting the harmful effects of the impact in running on the joints of the lower extremity. This study was limited to a single subject, and studies are ongoing to determine if this mechanism can be observed in other runners.

REFERENCES

Aerts, P. and De Clercq, D. (1993) Deformation characteristics of the heel region of the shod foot during a simulated heel strike. J. Sport Sciences, 11, 449-461.

Konradsen, L., Bert Hansen, E.M. and Sondergaard, L. (1990) Long distance running and osteoarthrosis. Am. J. Sports Med., 18, 379-381.

Yang, K.H. et al. (1989) Differential effect of load magnitude and rate on initiation and progression of osteoarthrosis. Trans Orthop Res Soc, 14, 148.

BALANCE RELATED POSTURAL ADJUSTMENTS WHEN LIFTING AN OBJECT OF KNOWN WEIGHT

Dianne A.C.M. Commissaris, Huub M. Toussaint

Faculty of Human Movement Sciences, Vrije Universiteit

Amsterdam, The Netherlands

INTRODUCTION

The maintenance of balance during goal-directed action is an essential requirement for most, if not all, daily activities. The maintenance of balance and control of posture have been mainly investigated in static postural tasks, e.g., standing (Bouisset and Zattara, 1987) and, less extensively, in dynamic tasks like locomotion (Nashner and Forssberg, 1986). In those studies, an *expected* perturbation of balance proved to elicit *anticipatory postural adjustments*, defined as actively initiated movements which predictively counteract disturbances to balance that are associated with the expected perturbation. The goal of the present study is to examine whether in a complex dynamic action, i.e. lifting an object of known weight, anticipatory postural adjustments occur, and if so, how these adjustments are functionally related to lifting technique. Picking up a large load, positioned just within reach in front of the subject, will cause a forward and downward shift of the centre of gravity (*CoG*) and will thus present the subject with an expected perturbation of balance.

METHODS

Eight male subjects were asked to lift a barbell (20% of body mass, positioned 0.35 m in front of the subject), straight up to acromion height, using either a backlift or a leglift technique. Speed of movement was imposed by an acoustic metronome. Before picking up the barbell, subjects performed several unloaded movement cycles to attune to the desired lifting speed. Kinematics and ground reaction forces were recorded during the last two movement cycles. By means of an inverse dynamic analysis, the following biomechanical parameters were calculated (Toussaint *et al.*, in press): the instantaneous horizontal momentum of the *CoG* of the body and load ($\mathbf{p}_{hor}$); the instantaneous angular momentum of the body and load ($\mathbf{h}$); the horizontal positions of *CoG* and centre of pressure (*CoP*), expressed as a percentage of the base of support (CoG_{rel} and CoP_{rel}, with heels defined as 0%). To investigate the presence and nature of anticipatory postural adjustments, the biomechanical parameters of the last unloaded downward phase (II) were compared to those of the previous unloaded downward phase (I). The barbell was picked up following downward phase II.

RESULTS

Comparison of downward phase II to downward phase I revealed distinct anticipatory postural adjustments in both lifting techniques. In the last part of phase II, a pronounced increase of the backward directed $\mathbf{p}_{hor}$, an increase in $\mathbf{h}$ and a forward shift of the CoP_{rel} were observed (upper panels and lower left panel of Figure 1). The anticipatory postural adjustments proved to be specific to lifting technique. In the leglift the backward directed change in $\mathbf{p}_{hor}$ was larger, as was the positive increase in $\mathbf{h}$. The CoG_{rel} shifted backward in the leglift, whereas in the backlift it moved slightly forward (lower right panel of Figure 1).

DISCUSSION

The anticipatory postural adjustments found can be understood from the mechanical consideration that a load lifted in front of the body induces a forward and downward shift of the *CoG* and a clockwise rotation of the body. The increase in the

backward directed $\mathbf{p}_{hor}$ and in **h** were aimed at counteracting the expected addition of the load. Thus, the anticipatory postural adjustments indeed predictively counteracted expected disturbances to balance. Although lifting speed and load mass were similar for both techniques, suggesting a similar perturbation to balance, the postural adjustments showed clear differences between both techniques. As, compared to the backlift, the CoG_{rel} is positioned more forward at the end of phase II in the leglift, addition of the load will imply a greater risk for imbalance. The larger increase in the backward directed $\mathbf{p}_{hor}$ and the backward shift of the CoG_{rel} can be regarded as leglift-specific anticipatory postural adjustments aimed at minimizing the risk for loss of balance. In conclusion, the lifting movements to be performed apparently were specified in advance, before contact with the load was made (see also Gordon *et al.*, 1993). The movement specifications also incorporated the interaction between the expected perturbation and the mechanical requirements of the lifting technique.

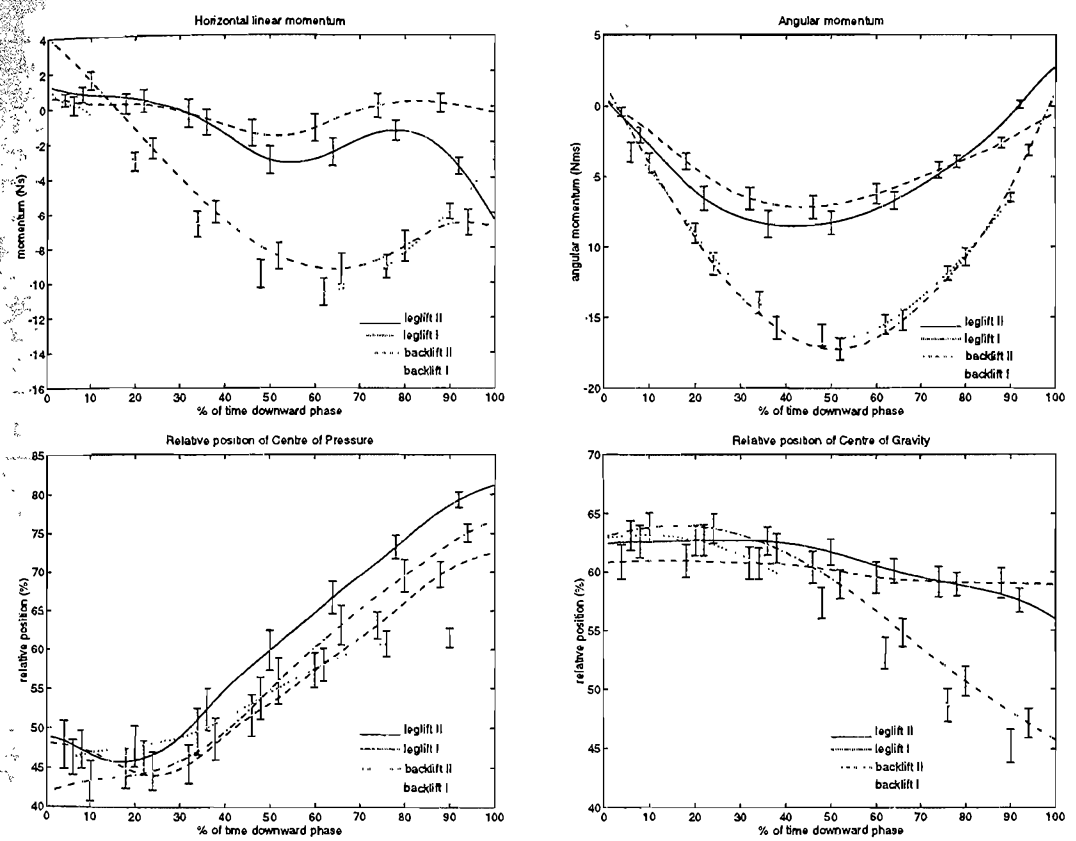

Figure 1 Means and standard error of four biomechanical parameters during downward phase II and I (expressed as a percentage of the movement time), for the leglift (29 trials) and the backlift (32 trials)

REFERENCES

Bouisset, S. and Zattara, M. (1987) Biomechanical study of the programming of anticipatory postural adjustments associated with voluntary movement. *J. Biomechanics* **20**, 735-742.

Gordon, A.M., Westling, G., Cole, G.J. and Johansson, R.S. (1993) Memory representations underlying motor commands used during manipulation of common and novel objects. *J. Neurophysiol.* **69**, 1789-1796.

Nashner, L.M. and Forssberg, H. (1986) Phase-dependent organization of postural adjustments associated with arm movements while walking. *J. Neurophysiol.* **55**, 1382-1394.

Toussaint, H.M., Commissaris, D A.C.M., Dieën, J.H. van, Reijnen, J.S., Praet, S.F.E. and Beek, P.J. et al. (in press) Controlling the ground reaction force during lifting. *J. Motor Behavior* (to appear in September 1995)

SOME ASPECTS OF TWO DIFFERENT ANTHROPOMETRICAL MODELS AND THEIR APPLICATION IN MOTION ANALYSIS.

S.C Correa[1], U Glitsch[2], M.Paris[2] and W.Baumann[2]

1 - Federal University Rio de Janeiro, Rio de Janeiro, Brazil

2 - Institute of Biomechanics, German Sport University, Cologne, Germany

INTRODUCTION

Motion analysis usually requires the values of mass and inertia parameters of the different segments in order to determine the physical properties of the segments There are a lot of equations to calculate these human body parameters Dempster's equations (1955) or these equations as presented by Winter (1979) are still today used by a lot of researchers, first because their input data are only height and weight, what makes it very attractive when the number of subjects is very great, and second because it does not involve an anterior training of the researcher in anthropometrical measurements. Zatsiorsky et al (1984) determined by radioisotope methods on a sample of 100 living subjects the regression equations with the same arguments as Dempster. The aim of this paper is to compare the results of both procedures in relation to mass, length, estimation of center of gravity, and moments of inertia at the different segments, and describe some problems in their application in motion analysis

METHODOLOGY

From the running kinematics we have performed a 3D analysis The analysis was based on a 14 segments model represented by 17 markers points (estimation of joint centers) For the Zatsiorsky's model we have combined the described three parts of the trunk in one segment and for Winter's model the head was considered as a part of the trunk For each subject, anthropometric data were obtained using tables provided by Dempster (as described by Winter,1979), and using the regression equations described by Zatsiorsky (1984) The segments' length calculated by the equations have been compared with the anatomical length as defined by both authors Then we have applied both models to the motion analysis.

RESULTS AND DISCUSSION

The segments' definition specially for trunk and thigh is very different between both models For example, the difference between the trunk in both models for a 1.78 m man is of the magnitude of 171 mm and between both thighs this is of 100 mm In Table 1 is listed for both methods the percentual differences between the measured length (as defined by both authors) and the results obtained from the equations, for one man with a height of 1 78m We observed that the difference between the measured and the calculated value for the upper arm in Zatsiorsky's model was very great (29%). The reason is that for Zatsiorsky there's a difference between what he calls "the biomechanical lengths of segments" and the anthropometrical lengths. And for the upper arm he (Zatsiorsky et al.,1990) describes a coefficient of 0 73 that should be multiplied by the measured value in order to find the biomechanical value It means that in reality the upper arm has also a different definition for both authors

One subject had been specially analyzed in order to observe the behavior of the regression equations in relation to a subject with 100 kg and that was out the range described by Zatsiorsky (1983) for the use of the regression equations . We have observed that the differences between the measured and the calculated values could be of more than 20% for several segments It shows that it is highly recommended to use the regression equations only for subjects that correspond to the values of weight (73 + 9 1 kg) and height (174 1 + 6 2 cm) of the sample that has been used to calculate the equations.

The results with the percentual differences in the anthropometrical data between Winter's Model and Zatziorsky's for a man with 71,5 kg and 1 78m are described in the Table 2. The percentual differences in the center of gravity estimation are very similar to the differences in length. We have noticed in the comparison between the two models that most of the differences in mass, length, center of estimation and moment of inertia of the segments are due to the different definitions of the segments. The segments in

which we have observed a greater difference in lengths between the models are the same in which we can also see a greater difference in the others parameters

A problem linked to the applicability of these both models to a motion analysis is how to relate the calculated anthropometrical data to the digitized joint's center that sometimes, as for the thigh in the Zatsiorsky's model, represents a distance of more than 100 mm, between the defined distal extremity of the segment and the estimated joint center In order to overcome these problems one of the solutions is to use other arguments, beyond height and weight for the adjust Another problem is how to correct the center of gravity of the foot when usually the models describe this position only in the sole. This is possible through a simple assumption for the center of gravity, considering the foot as a triangle formed by heel, front foot extremity and ankle joint

TABLE 1 Percentual differences between the measured segments' lengths (as defined by both authors) and the results obtained from the equations of both models, for one man with a height of 1 78m (% in relation to the measured)

SEGMENTS	WINTER(%)	ZATSIORSKY(%)
FOOT	1 4	- 11.6
SHANK	8.9	- 5 6
THIGH	-0 4	1 7
HAND	-7 1	-14 4
FOREARM	-0 7	-13.8
UPPER ARM	3.6	-29 4
TRUNK	1 9	-1 6

TABLE 2 Percentual differences in the anthropometrical data between Winter's and Zatsiorsky's model for one man with 71 5 kg and 1 78 m (Winter in relation to Zatsiorsky).

	MASS (%)	LENGTH (%)	MOMENT OF INERTIA (about the frontal axis %)
FOOT	6	13	66
SHANK	8	11	61
THIGH	-30	-17	-30
HAND	-2	8	0
FOREARM	-0 8	7 5	40
UPPER ARM	3	36	109
TRUNK*	33	20	174

*Trunk means for Winter Trunk + neck+ head

REFERENCES

Dempster, W T (1955) Space requirements of the seated operator In *WADC Technical Report*, pp 55-159 Wright Patterson Air Force Base, OH

Winter, D A (1979) *Biomechanics of Human Movement.* John Wiley & Sons, New York

Zatsiorsky, V (1984) *Biomechanik des menschlichen Bewegungs-apparates*, Sportverlag, Berlin

Zatsiorsky,V , Seluyanov, V and Chugunova, L (1990) In vivo body segment inertial parameters determination using a gamma-scanner method In *Biomechanics of Human Motion* (Edited by Berne, N and Cappozzo, A), pp 186 - 202, Bertec Corporation, Worthington, Ohio

THE EFFECT OF TRICEPS SURAE LENGTH ON MAXIMAL PLANTAR FLEXOR TORQUE AND ELECTROMYOGRAPHIC ACTIVITY IN MAN

Andrew G. Cresswell, Wolfgang N. Löscher and Alf Thorstensson

Department of Neuroscience, Karolinska Institute, Stockholm, Sweden.

INTRODUCTION

Plantar flexor torque production by the triceps surae is complex, as changes in ankle and/or knee angle may change the length - tension relationships of the soleus (SOL) and gastrocnemius (GA) muscles independently. This independence can be used experimentally, i.e., reducing the force producing capability of GA by shortening its length via knee flexion, while maintaining the length and force capability of SOL constant. A question arises as to how the central nervous system activates GA for a maximal voluntary plantar flexion effort (MVC) with the knee flexed as compared to straight. The purpose of this study was therefore to determine the relative contribution of GA to isometric plantar flexor torque production, and to investigate the activation of the GA muscle at standardised insufficient lengths.

METHODS

Subjects (n=10) lay prone with their right foot secured to a force instrumented foot-plate. Adjustments made under the thigh and trunk created internal knee angles of 60, 90, 120, 150 and 180°. A 6 s isometric maximal voluntary contraction was performed at each of the five knee angles. A supramaximal voltage stimulus was delivered to the triceps surae 5 s into each contraction to provide a torque twitch. An additional measurement at each knee angle, with the subject relaxed, provided a resting torque twitch. Surface and intra-muscular EMG was recorded from the lateral and medial heads of GA and from the lateral aspect of SOL. Maximal voluntary plantar flexor torque at each knee angle was measured as the mean torque value for the period between 2-4 s. Resting twitch amplitudes were computed for all knee angles. The superimposed twitch amplitude was normalised to the resting twitch amplitude at the same knee angle. For each trial the mean rectified EMG amplitude was calculated for the period between 2-4 s and normalised to the highest EMG activity that occurred for the same period in the 180° (straight) knee position.

RESULTS

The MVC, and the absolute and normalised resting twitch amplitudes (normalised to the resting twitch amplitude at 180°) showed significant sigmoidal decreases with decreasing knee angle (Fig. 1*A*). At the 60° knee angle the mean plantar flexor torque of the MVC was 40% less than that at 180°. The mean of the resting twitch at the 60° knee angle was 42% less than that at 180°. The MVC superimposed twitch amplitudes showed no significant change with decreasing knee angle (mean 16% of the resting twitch). A significant decline in GA MVC EMG, but not SOL, occurred with decreasing GA length. The MVC EMG amplitude of GA being significantly less at 120°, 90° and 60° as compared to the 180° knee angle (Fig. 1*B*).

DISCUSSION

From the results, the contribution of GA to plantar flexor torque can be estimated for the straight leg position. Earlier studies have shown the possible plantar flexor torque contribution from synergistic muscles of the triceps surae to be approx. 20 - 30% (Murray *et al.*, 1976). Therefore, assuming that the amount of GA shortening was sufficient to exclude any significant force production, the torque contribution at the straight leg position can be calculated to be at least 40% from GA, and maximally 30% from SOL. However, some uncertainty remains regarding whether the torque produced by GA at the 60° position is truly zero. The decrease in torque production we observed

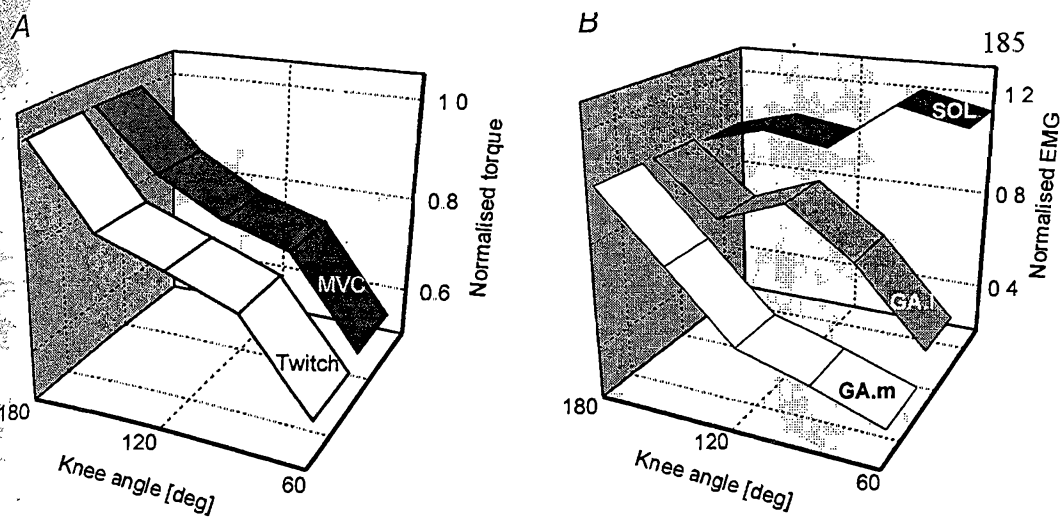

Fig1. *A*) Mean maximum voluntary plantar flexor torque and peak torque of the resting twitch and *B*) mean of the maximal voluntary EMG amplitudes of SOL, and the lateral and medial heads of GA (GA.l and GA.m, respectively) at different knee angles. See Methods for normalisation procedures.

with decreasing GA length is likely a result of changes in contractile behaviour and/or neuromuscular transmission and not reduced voluntary effort. This is supported by the close matching of the supramaximal resting twitch and voluntary torque curves, particularly at the 60° position.

A substantial decrease in EMG amplitude, despite maximum effort, was observed in the shortened GA, while the EMG of SOL, which never underwent a length change, did not alter. This result may be explained by i) the electrode configuration with respect to the recording volume alters during GA shortening; ii) the activity of GA spinal motoneurons is reduced at shortened lengths; and iii) action potential transmission/propagation along a shortened GA is impaired. Electrode configuration changes seem unlikely, as the intra-muscular EMG showed similar results. A reduced GA motoneuron activity is feasible as feedback to neurons at the spinal and/or even subcortical and cortical level from receptors sensing muscle length could be occurring The level of spinal and supraspinal 'drive' was assessed by the superimposed supra-maximal stimulation (Belanger and McComas, 1981). No significant difference for the increase of the superimposed maximal twitch was found with changing knee angle, thereby indicating that the 'drive' to the triceps surae was similar for all MVC's. Therefore, the decline of GA amplitude is unlikely to result from a reduced voluntary effort. In an attempt to resolve whether neuromuscular transmission - propagation is diminished in a shortened muscle we additionally recorded supra-maximal M-wave amplitudes in GA and SOL in six subjects. It appeared that the M-wave of GA decreased with knee flexion in four of the six subjects, while SOL remained unchanged for all. However, it was not always possible to reliably record GA M-waves at the 90° and 60° knee positions. At the present time it seems that the decrease of GA EMG activity with decreasing muscle length is brought about by impaired action potential transmission/propagation and/or reflex changes on the GA motoneuron pool.

REFERENCES

Murray, M. P. Guten, J. M. Baldwin, J.M. and Gardner G.M. (1976) A comparison of plantarflexion torque with and without the triceps surae. *Acta Orthop Scand* **47**:122-124

Belanger, A. Y. and McComas, A. J. (1981) Extent of motor unit activation during effort. *J. Appl Physiol.* **515**:1131-1135

PERFORMANCE OF SHORT POSTERIOR SPINAL FIXATORS USED IN THE STABILISATION OF SEVERE LUMBAR ANTERIOR COLUMN INJURIES

Cripton PA, Jain GM, Nolte LP, Berlemann U

M.E. Müller Institute for Biomechanics, University of Bern, Switzerland

INTRODUCTION

Posterior lumbar spinal fixators are commonly used for the stabilisation of slightly and moderately unstable lumbar spine segments. There is not currently a consensus regarding the suitability of these fixators for the treatment of highly unstable spinal injuries such as vertebral body burst fractures. The efficacy of these devices may depend in part on the stresses occurring in the device components and the effect of cross stabilisation of the longitudinal rods on the kinematic stabilisation provided. The objectives of this study were to estimate and measure the forces and moments occurring in these devices (Studies A and B) and to experimentally evaluate the effect of cross-bracing on their stabilising potential (Study C). Results for severe anterior column injuries and for intact specimens are compared.

MATERIALS AND METHODS

STUDY A Internal fixator components (i.e. pedicle screws, longitudinal rods and the interconnecting clamps) of a monosegmental instrumented fusion were idealised as beams and the forces and moments therein were estimated using planar beam bending equations. Material properties of the interconnecting hard and soft tissues were modelled by linear and rotational springs. An injury parameter (IP) was defined which was a function of the spring constants. The IP was varied between 0 (complete tissue removal) and 1 (intact tissue). Fixator and tissue stresses were analysed for axial compression, flexion and extension loading.

STUDY B Three fresh human lumbar cadaveric functional spinal units were instrumented with AO Dick internal fixators (Synthes, Paoli, USA). The longitudinal rods of the fixators had six strain gauges mounted on their surfaces. Prior to testing the rods were calibrated as six-degree of freedom load cells (accuracy 5% of measured load). The forces and moments in the rods were measured for intact specimens and subsequent to removal of the intervertebral tissue. Intradiscal pressure was also measured during testing. The specimens were subjected to flexion/extension, torsion and lateral bending moments of 8 Nm.

STUDY C Five fresh human three lumbar segment cadaveric specimens were instrumented with SOCON fixators (Aesculap AG, Tuttlingen Germany). Specimens were subjected to flexion/extension, lateral bending and torsional moments of 10 Nm. Each specimen was tested intact, subsequent to fixator implantation and 1000 sinusoidal flexion/compression cycles (0.4 to 10 Nm / 10-250 N), and after a vertebrectomy of the middle vertebra. All stabilised specimens were tested with and without cross-bracing. The resulting kinematics were measured using an optoelectronic motion analysis system (Northern Digital, Waterloo, Canada).

RESULTS

STUDY A Internal forces and moments in the longitudinal rod increased exponentially as the injury parameter approached 0 (vertebrectomy or removal of disc). The maximum force and moment occurring in one longitudinal rod under simultaneous flexion/compression loading were 500 N and 25 Nm respectively.

STUDY B After tissue removal the moments in the longitudinal rods were observed to increase for all loading cases. In flexion the average bending moment in one rod was observed to increase from 0.33 to 3.98 Nm (1100%). In lateral bending a 17% increase in the bending moment from 0.64 to 0.75 Nm was measured. In torsion an increase, in the torsional moment, of 625% from 0.48 to 3.48 Nm was recorded. In the instrumented intact specimens the disc supported significant percentages of the torsional and flexion/extension applied moments.

STUDY C In the intact specimen the fixator reduced the measured motion for all loading cases but the addition of the cross brace had no significant effect. The vertebrectomy destabilised the specimens in all three loading situations. In this case adding the cross-brace to the fixator only increased the stability significantly under torsional loading. The average torsional range of motion (ROM) decreased by 26% from 23.6° to 17.4° when the cross-brace was attached.

DISCUSSION

The maximum bending moment some longitudinal rods can be subjected to and still allow an infinite service life has previously been reported [1] to range between 6 and 18 Nm. Our experimental and theoretical results suggest these devices may be over-stressed or operating with very low factors of safety with respect to infinite service life requirements when used to stabilise severe anterior column injuries. This situation may lead to *in vivo* failure of device components, as has been previously reported [2], or to loss of correction height due to clamp failure or loosening at the screw bone interface. Cross-bracing of the short segment fixators failed to significantly improve the stability of non-injured specimens. It may only be biomechanically beneficial to cross-brace fixators used to stabilise highly unstable segments. However, in these cases both the resulting component stresses and the ROM allowed suggest that additional anterior stabilising procedures may be necessary clinically.

REFERENCES

[1] Duffield *et al.*, Spine **18**: 1695-1703 (1993).
[2] Ebelke *et al.*, Spine **16**: S428-S432 (1991)

ERRORS IN STRESS-SHIELDING EVALUATION OF CEMENTLESS HIP STEMS

Luca Cristofolini [1,2], Brian P. McNamara [1,3], Angelo Cappello [2], Aldo Toni [1]

[1] Biomaterials Technology Lab, Rizzoli Orthopaedic Institute, Bologna, Italy
[2] Engineering Faculty, University of Bologna, Italy
[3] Bioeng. Res. Centre, Mechanical Engineering Dept., Trinity College, Dublin 2, Ireland

INTRODUCTION

Hip stems need to be tested *in-vitro* to investigate the load transfer and evaluate stress-shielding effects. However, there is no agreement on the loads to be simulated, the strain measurement locations, or the testing procedure in general (Colgan *et al.*, 1994). Stress-shielding tests are normally performed despite the fact that a methodological analysis is far from complete. The effect of experimental variables have been investigated only partially and only in few cases (Rohlmann *et al.*, 1982; Finlay *et al.*, 1991).

We performed a sensitivity analysis on some experimental variables. In particular the problem of consistently reproducing the same loading condition on the intact and the implanted femur was investigated. Further, the difference between measuring bone strains for an uncemented stem immediately post-operatively (pure press-fit) and at later times, as bone growth takes place (progressing stem-bone bonding) was evaluated.

MATERIALS AND METHODS

Using a set of reference axes, six composite femurs (Pacific Res. Labs, Vashon Island, WA, USA) were potted distally and prepared with 20 strain gauges. The femurs were first tested intact, with a hip joint force only, and also with an abducting force. Based on Cristofolini *et al.* (1994 and 1995), a cantilever system was designed to apply the abducting and the hip joint forces at controlled angles and ratios. The femurs underwent standard surgery to implant an uncemented CrCo stem (An.C.A., Cremascoli, Italy), which was inserted in load control using a materials testing machine (Harman *et al.*, 1995). They were then loaded with the same systems of forces as the intact femurs. A 3D Finite Element (F.E.) model supported the sensitivity analysis (McNamara *et al.*).

After the test on the press fitted femurs, the stems were inserted once more filling the gaps with PMMA bone cement in some femurs and epoxy glue in others, in an attempt to simulate the condition when bone formation commences, passing from press-fitted to partially bonded stem (a cement layer to simulate bone filling the gaps) and subsequently to fully bonded interface (glued to simulate complete osseointegration).

	Hip joint force error			Abducting force error			Strain gauge position error		
Femur aspect	1mm ant/post	1mm lat/med	±1° abduct	1mm ant/post	1mm lat/med	±1° abduct	1mm along the femur	1mm around the femur	5° misalign
Ant/Post	-20/+20%	1/ 6%	4/ 18%	-11/+14%	-8/+9%	1/ 9%	<±.1%	-34/+204%	29/ 90%
Lat/Med	-1/+1.4%	1.6/ 2%	3/ 11%	-.1/+.8%	.7/ 2.6%	.5/ 5%	<±.2%	<±1%	-.5/+14%

Table 1- Errors on the axial strains on the four aspects of the femur due to experimental inaccuracies, as evaluated from a sensitivity analysis with the F.E. model. Mispositioning of the force application points and misalignments are in the first 6 columns; errors in strain gauge application are in the last 3 columns.

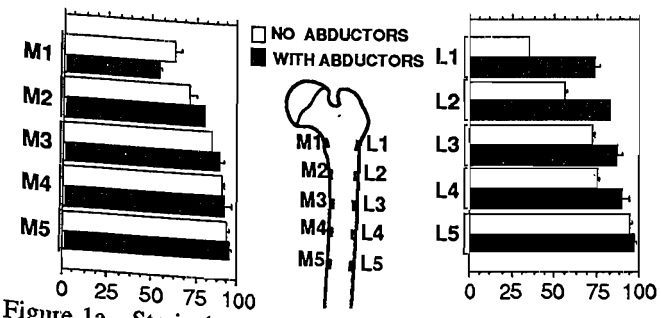

Figure 1a - Strain (mean±STD) in the femurs with uncemented CrCo stem as percentage of the strains in the intact, on the medial and lateral side: without and with the abductors simulated.

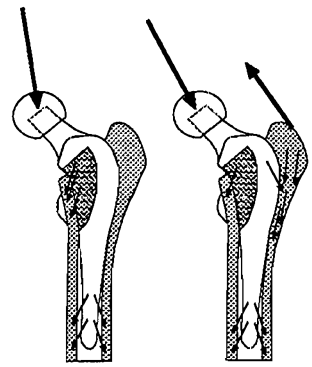

Figure 1b - Load transfer without (left) and with the abductors (right).

RESULTS

Table 1 reports the sensitivity analysis performed using the F.E. model, based on inaccuracies estimated from repeated testing (over 250 runs). The strains measured in the

intact femur were compared with those in the implanted for the same loading condition. Fig. 1a compares the stress-shielding for the CrCo stem when evaluated without and with the abductors simulated. Fig. 2 represents the stress-shielding (abductors simulated) due to the same stem (i) press-fitted, (ii) with a thin layer of bone cement and (iii) glued. The F.E. predicted strain magnitudes and distribution agreed with the experimental results.

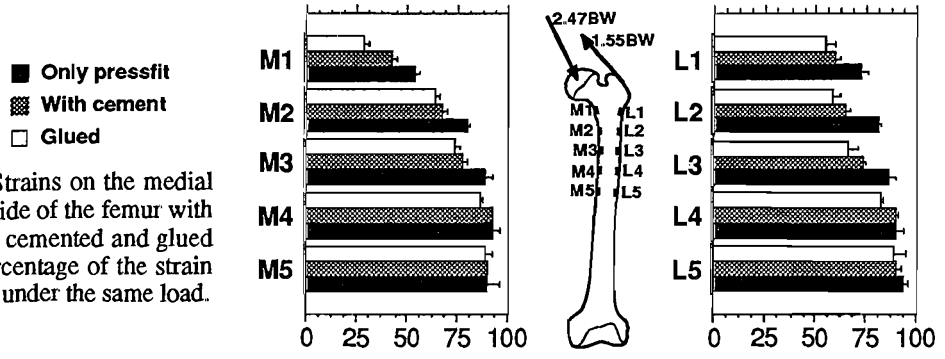

Figure 2 - Strains on the medial and lateral side of the femur with press-fitted, cemented and glued stem, as percentage of the strain in the intact under the same load.

DISCUSSION

The data in Table 1 highlight how errors due to inaccuracy of force application are not increased by the inclusion of the abductors in the set-up. This is due to the larger moments generated by these muscles, corresponding to longer lever arms that "forgive" some inaccuracy in the force positioning. The errors induced by gauge mispositioning make unreliable the anterior and posterior locations (too close to the neutral axis).

The load transfer mechanism shown in Fig. 1b accounts for the general stress-shielding overestimation (Fig. 1a) when the abductors are neglected, as their presence contributes to direct transfer of the load to the femur in the proximal lateral region.

The bone strains below the distal tip of the stem in the implanted femur should be 100% of the intact, but this does not happen exactly (most distal gauges Fig. 1a and 2). This is due to the head offset restoration within a few millimetres of the physiological position due to the always existing surgical inaccuracy. This causes a change in the bending moment if the same system of forces is applied. An alternative solution is to apply the same resultant moment (rather than the same force values), adjusting the moment arms and keeping constant the resultant force and the angles. This problem has received little attention in the literature and is not even mentioned in many investigations.

Fig. 2 shows the difference between the bone strains recorded immediately post-operatively (pure press-fit) and after the bone starts to in-grow, progressing from partial stem-bone bonding (press-fit with cement layer) to complete bonding (press-fit with glue). When the stem is bonded to the bone, the construct forms a stiffer structure which experiences reduced strains. In the pure press-fit situation instead, the stem has a certain degree of rigid body motion in the femur, and thus the femur has more freedom to bend. This interpretation was also confirmed by the F.E. analysis.

REFERENCES

1. Colgan, D., Trench, P., Slemon, D., McTague, D., Finlay, J.B., O'Donnel, P., Little, E.G. (1994) A review of joint and muscle load simulation relevant to in-vitro stress analysis of the hip. *Strain* **30(2)**: 47-61.
2. Rohlmann, A., Mossner, U., Bergmann, G., Kolbel, R. (1982) Finite-element-analysis and experimental investigation of stresses in a femur. *J.Biomed.Eng.***7**:241-246.
3. Finlay, J.B., Chess D.G., Hardie W.R., Rorabeck C.H., Bourne R.B. (1991) An evaluation of three different loading configurations for the in-vitro testing of femoral strains in total hip arthroplasty. *J. Orthop. Res.* **9**: 749-759.
4. Cristofolini, L., McNamara, B.P., Cappello, A., Toni, A. (1994) A new protocol for stress shielding tests of hip prostheses. In *Abstracts 2nd World Congress Biomechanics* (Edited Blankervoort L., Koolos J.G.M.)p338. Stichting World Biomechanics Nijmegen
5. McNamara, B.P, Viceconti, M., Cristofolini, L., Toni, A., Taylor, D. (in press) Experimental and numerical pre-clinical evaluation relating to total hip arthroplasty. In *Recent advances in computer methods in biomechanics and biomedical engineering*(Eds: Middleton, J., Pande, G.N., Williams, K.R.) Books & Journals International, Swansea.
6. Harman, M.K., Toni, A., Cristofolini, L., Viceconti, M.(1995) Initial stability of uncemented hip stems. *Medical Engineering & Physics* **17(3)**: 163-171.
7. Cristofolini, L, Viceconti,M., Toni,A., Giunti,A.(1995) Influence of thigh muscles on the axial strains in a proximal femur during early stance in gait. *J.Biomech.* **28**: 617-624.

METHODOLOGY FOR THE KINEMATIC ANALYSIS OF THE RUNNING

[1]Cunha, Sergio A , [2]Brenzikofer, René, and [3]Lima Filho, Euclydes C
[1]Departmento de Educação Física, Universidade Estadual Paulista, Bauru, Brasil, [2]Instituto de Física "Gleb Wataghin", Universidade Estadual de Campinas, Campinas, Brasil, [3]Instituto de Matemática, Estatística e Ciência da Computação, Universidade Estadual de Campinas, Campinas, Brasil

INTRODUCTION

In order to analyze human movement in a quantitative way, the human eye is not always the most adequate instrument It is necessary to keep the sequence of images of the analized phenomenon for a certain time, which is not possible for our vision Through videographic register techniques, we can obtain discrete information about movement, which can be stored, becoming avaiable for analysis To these discrete data, we associate a continuous function to improve their representation Thus, we have developed a complete and precise quantitative description method of human movement In this work, we have measured the kinematic variables of a subject's lower limbs while running and have detected patterns and rhythms of this movement

Therefore, the aim of this study is to develop a method sensitive to the quantitative analysis of the kinematics of human movement

METHODS

The methodology developed consists of a sequence of technical procedures It begins with the shooting of parts of a subject's run using one VHS video camera Next, we digitalize each sequence of images frame-to-frame, transfering this information to the computer Then, we measure the angular position of the lower limbs in relation to the vertical, and the horizontal and vertical position of the knee joint as a function of time We also correct the scale and perspective effects due to monocular filming with a camera which followed the subject's run with a rotation movement on a fixed tripod A continuous function is adjusted to the discrete data obtained in the measuring using a trigonometric polynomial (Fourier series), whose parameters are adjusted by least squares fit. In this work, we have decided to do the adjustment using six harmonics Finally, we evaluate the quality of this adjustment by observing the behavior of residues (distance between measured point and adjusted function)

RESULTS AND DISCUSSION

With the adjustment of the best function to the set of data referring to each part of the run we thus have the position of each limb as a function of time The first derivative of this function represents velocity and the second derivative represents acceleration. Having the position-as-function-of-time variable we can superpose all the runs shot, in order to find out the pattern of that movement. For this, we need to normalize the time variable, using the complete stride cycle as unit. This detected pattern refers to the subject's speed rate between 2 9 and 4 2 m/s. We can also determine the rhythm chosen by the subject to perform the run by measuring the time spent between two consecutive touches of the same foot on the ground. Besides, with the kinematic data and inertia parameters, we can approach Dynamics using, for instance, Newton's or Lagrange's formalism.

Another way to present the movement graphically is to use the angle-angle diagram. Instead of plotting the angular variable against time, we develop a graph of the searched angle, with regard to vertical, as a function of the total adjacent articulation angle

Therefore, it is possible to relate the analysis so developed with real movement and interpret the phenomenon observed. The methodology presented here provides technical and methodological support for future research

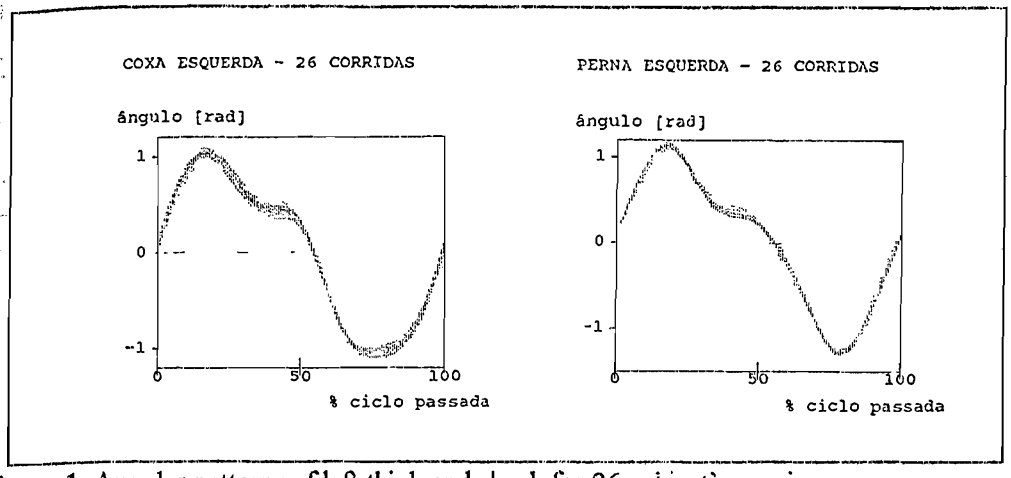

Figure 1 Angular patterns of left thigh and shank for 26 subject's running

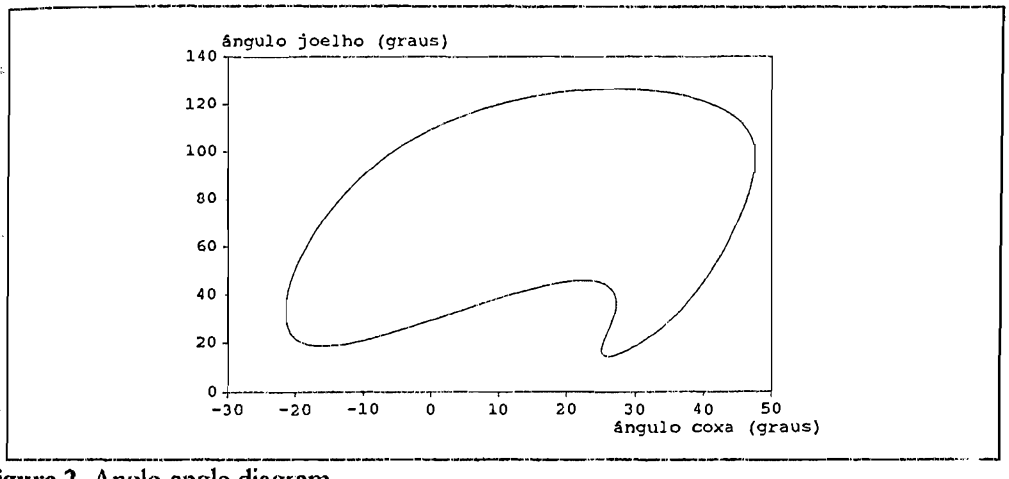

Figure 2. Angle-angle diagram

REFERENCES

1. BRENZIKOFER,R (1992) O formalismo de Lagrange, um exemplo de aplicação. In. IV Congresso Brasileiro de Biomecânica, São Paulo.
2. CAVANAGH,P.R., GRIEVE,D W.(1973) The graphical display of angular movement of the body British Journal of Sports Medicine, London, 7,129-133
3. CAVANAGH,P R (1990) Biomechanics of distance running. Champaign:Human Kinetics Books.
4. ENOKA,R M.(1988) Neuromechanical basis of kinesiology. Champaign:Human Kinetics Books.
5. MUÑOZ,M.E.S , BRENZIKOFER,R.(1992) Obtenção das coordenadas de articulações humanas em imagens digitalizadas In:1ª Mostra de Trabalhos da Unicamp em Computação de Imagens Campinas.
6. SYMON,K R (1982) Mecânica. 4.ed Rio de Janeiro: Campus
7. WINTER,D.A , SIDWALL,H.G., HOBSON,D.A (1974) Measurement and reduction of noise in kinematics of locomotion. Journal of Biomechanics, 7, 157-159.
8. WINTER,D.A.(1979) Biomechanics of human movement. New York.John Wiley and Sons

Supported by FUNDUNESP, CAPES, FAPESP, FAEP and CNPq

THE PHYSICAL MODEL OF THE ANAL SPHINCTER MUSCLES GROUP

Anna M DĄBROWSKA-TKACZYK[1], Leszek STEFAŃSKI[2]
[1] Divission of Strength of Materials and Computational Mechanics, Department of Engineering Mechanics, Faculty of Mechanical Engineering Silessian Technical University, Gliwice, [2] The Department of the Alimentary Tract Surgery the Silessian Academii of Medicine, Katowice, POLAND

INTRODUCTION

Biomechanical investigations of musculoskeletal system most often concern to the human system of motion, where the voluntary skeletal muscles are the activators, cotrolled by the nervous system. The voluntary muscles act also in the organs, where cooperate with tissues of different physical properties and biomechanical characterystics As an example may be anal closing group of muscles The main functions in this group perform external sphincter and anal elevator - the voluntary muscles, involuntary, smooth internal sphincter, all of them surrounded by connective tissue Based on the morphological investigations [3], physical properties of tissues [2] and their biomechanical characteristics [1,2] the physical model was made This model is the first step to further mathematical modelling and analysis of this organ

THE PHYSICAL MODEL

Investigations of cooperation of muscles consist on to determine the muscles forces as the functions of the time The physical model of the anal closig muscle system (fig 1) consists of the internal sphincter, having form of flattened pipe with fibres place parallely to long axis, surrounded by three layers of external sphincter fit close and lie together The all layers of external sphincter are circumferentially arranged and tonically active where the whole system is in the rest The middle layer, consists of two parts, is connected, at the back, to rigid (tail bone) and flexible (anococcygeal ligament) elements,

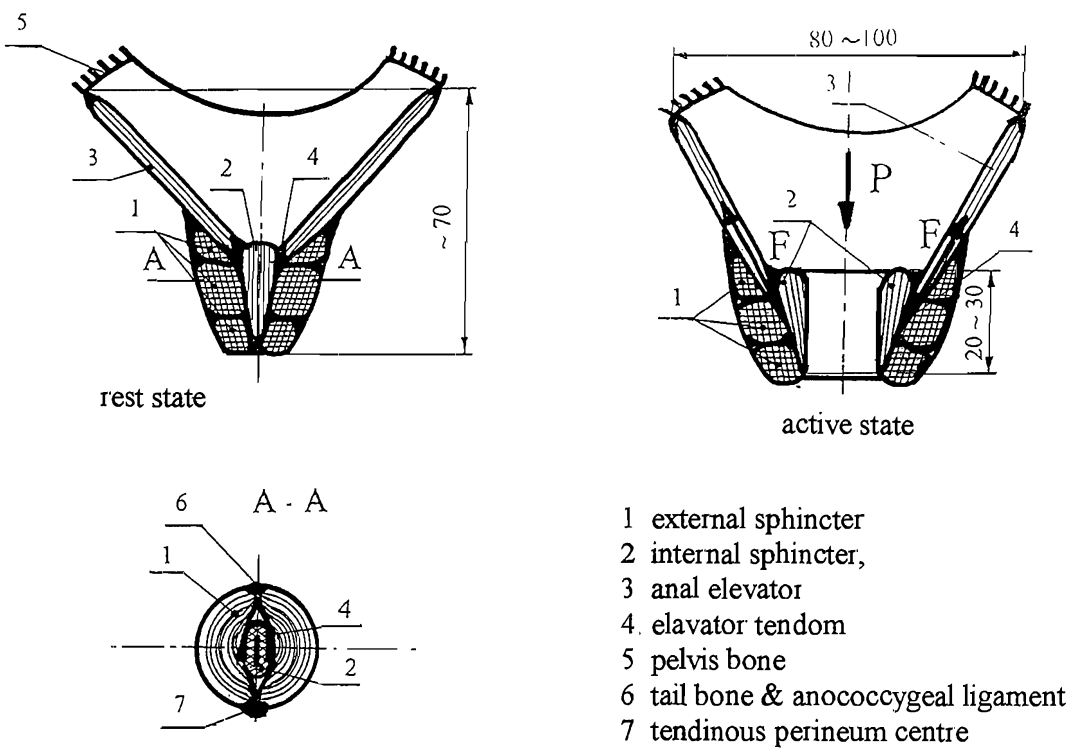

Fig 1 The physical model of the anal sphincter muscle group

but in the front side both parts are attached to tendinous perineum centre The other two layers of the external sphincter are connected to the soft tissue Between both sphinters (internal and external) penetrates anal elavator tendom at the part of circumference, converts, going up, to its muscle fibres lie in form of sheat, connected on circumference to rigid body - upper edge of pelvis bone

The experiences in modelling of the skeletal muscle cooperation in human motion systems show that the determination of parameters of model structure is not less important then the properly building of model

The model of the anal closing muscle group consists of following elements (tissues) voluntary striated muscles, smooth muscle, connective tissue, ligaments and bones Each of them differ from others in fhysical properties in passive state such stiffness, guantity of strain, relaxation of the strength, quantity of histeresis of the curve $\sigma(\varepsilon)$ [2] The striated and smooth sphincters muscles have also different biomechanical characteristics [1,2] in the active state

DISCUSSION

The problem of the anal closing group muscles cooperation during performing theirs normal functions may be consider in two categories on the medical and biomechanical points of view For surgeon physicians there are essential the rules of physiology of this organ activity, the functions of particurall muscles and nerves, the reasons of the pathological phenomena, as also investigations and determination ways of substitution or assisting the functions of demaged muscle and nerves by healthy elements On the other side this system can be consider as some kind of biomechanism controlled by nervous system, made of tissues of different characteristics Essential question in this case is evaluation the forces value, as a time functions, and rules of control The following features shoud be take into attention

- cooperation voluntary striated muscles and smooth muscles,
- the manner of connection muscles and other tissues elements in the system (insertions to the rigid elements (bones) and flexible (ligaments),
- existance oh the circumferentially arranged external sphincter,
- tonically active state of external sphincter during rest of the system and relaxed state of this muscle when the system is active,
- active state of the anal elevator muscle during active state of the system

The features and properties presented above compose some parameters of physical model structure, necessary to determine the mathematical model The results of modelling should give new informations into knowlege of this system and should be useful for physicians Determination the control criteria, based of analysis of different variants of innervation [3] is the separate problem which will be considered in further researches

REFERENCES

1 Dąbrowska-Tkaczyk A M (1994) The review of skeletal muscles models Proc III-th Int Scient Conf "Achievements in the mechanical and material engineering , Gliwice, 85-95

2 Fung Y C (1981) Biomechanics Mechanics properties of living tissues , Springer-Verlag, New York

3 Stefański L , Aleksandrowicz R , Jaworski J M (1995) The clinical aspects of the anal sphincter muscle topography and nervation changeability ,Folia Morphologica, Poznań (in print)

VALIDATION OF A LUMBAR BACK MODEL

Karl Daggfeldt, Qiang-min Huang and Alf Thorstensson

Department of Neuroscience, Karolinska Institute, Stockholm, Sweden

INTRODUCTION

In order to asses loads on different parts of the back, without invasive measures, a mathematical representation is needed. As the anatomical and physiological knowledge of the trunk increases more detailed and realistic mechanical models develop (e. g. McGill and Norman, 1986). The aim of this study was to incorporate new findings of variations in muscle lever arm lengths with changing spinal curvature (Tveit *et al.* 1994) and intra-abdominal pressure (Cresswell *et al.* 1992) into a mechanical model of the lumbar spine and to validate the model by comparing the maximal isometric strength produced voluntarily with that calculated by the model.

METHODS

One subject, age 31 years, height 195 cm and weight 92 kg, was used in this preliminary study. The lumbar back extensor muscles were modelled as 48 fascicles according to the anatomical descriptions of Bogduk *et al.* (1992) for the erector spinae and multifidus muscles and standard anatomical textbooks for quadratus lumborum. Magnetic resonance imaging was used to measure lever arm lengths, muscle cross sectional areas and muscle lengths at three different degrees of flexion-extension in the lumbar spine. Inbetween values were obtained by means of linear interpolation. Degree of flexion-extension was measured as the angle in the sagittal plane between the upper surfaces of S1 and L1, named the angle of lumbar lordosis. Attachments of fascicles with a lumbar origin were measured on sagittal images of the lumbar spine. The fascicles were modelled to run in straight lines between their origins and insertions. The fascicles with a thoracic origin, which transmit their force to the lumbar region via the erector spinae aponeurosis (ESA), were modelled with a line of pull between the ESA on the L3/L4 and L4/L5 transverse images. Cross sectional areas of the lumbar erector spinae, multifidus and quadratus lumborum were measured on the transverse images. Division into individual fascicles and the cross sectional area of the thoracal erector spinae were assumed to be proportional to cross sectional areas reported by Bogduk *et al.* (1992). Lever arm lengths for the L5/S1 level were measured as the shortest distance in the sagittal plane from the centre of the disk to the line of pull for the individual muscle fascicles. The influence on the extensor muscle torque production by the changing muscle geometry with a changing lumbar curvature was taken into account. The muscle tension versus length relationship was modelled as a fixed maximal value for lengths greater than the optimal length for active force production and as a sinus function for lengths shorter than this optimal length, decreasing to zero for half the optimal length. The maximal specific muscle tension and the degree of lumbar flexion for optimal muscle length were varied to make the calculated maximal strength fit the measured maximal strength (in a least squares sense).

Maximal voluntary static muscle strength around L5/S1 was measured in eight positions from maximal lumbar flexion to maximal lumbar extension. At the same time intra-abdominal pressure (IAP) was recorded with a pressure transducer inserted through the esophagus to the stomach. For the IAP torque generation, the pressure at the L5/S1 level was assumed to act on an area surrounded by the abdominal wall, the pelvis and the spine.

RESULTS

By adjusting the two unfixed parameters, it was possible to create a strength curve in good agreement with the measured maximal strength (fig 1). The maximal muscle tension became 34 N/cm^2 which corresponds well with in vitro measurements from the literature. The lumbar curvature for optimal active force production by the back extensor muscles became that of maximal flexion (an angle of lumbar lordosis of -10°). IAP was shown to make a considerable relative contribution to the torque production (10-21%), especially in the more flexed positions (fig 1).

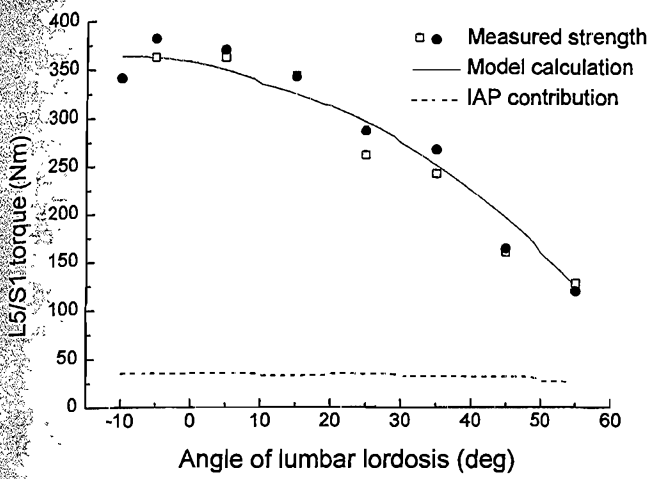

Figure 1. Maximal torque around L5/S1 at different angles of lumbar lordosis either calculated by the model or measured on two consecutive trials. The torque contribution from the intra-abdominal pressure calculated from the values measured during the maximal contractions is also shown.

DISCUSSION

The model was validated in the sense that it gave realistic values of the maximal specific muscle tension. Further validation of the optimal length calculation can be obtained by measuring sarcomere lengths of the back extensors for different curvatures (cf. Lieber *et al.* 1994). The IAP was considered to be created entirely by the diaphragm and the transversus abdominis (cf. Cresswell *et al.* 1992). It is possible that also the oblique abdominal muscle contribute which would counteract the back extensor torque. The ESA is thicker medially where the lever arm length is the longest and might therefore transmit more force there. Since the force transmission was modelled to be even along the ESA in the transverse plane, the torque contribution from the erector spinae muscles of thoracic origin could be somewhat underestimated. Further electromyografic and anatomical studies might resolve these questions. The model will yield lower compressive forces on the back for greater lumbar extension since the muscle lever arm lengths increased with an increased lordosis. Also the IAP will decrease the compressive loading both by a direct unloading of the spine and by contributions to the back extensor torque, which for a given external load will reduce the need for back extensor muscle force.

REFERENCES

Bogduk N., Macintosh, J. E. and Pearcy, M. J. (1992) A universal model of the lumbar back muscles in the upright position. *Spine* **17**:897-913.

Cresswell, A. G., Grundström, H. and Thorstensson, A. (1992) Observations on intra-abdominal pressure and patterns of abdominal intra-muscular activity in man. *Acta Physiol. Scand.* **144**:409-418.

Lieber, R. L., Loren, G. J. and Fridén J. (1994) In vivo measurement of human wrist extensor muscle sarcomere length changes. *J. Neurophysiol.* **71**:874-881.

McGill, S. M. and Norman, R. W. (1986) Partitioning of the L4-L5 dynamic moment into disc, ligamentous, and muscular components during lifting. *Spine* **11**, 666-677.

Tveit, P., Daggfeldt, K., Hetland, S. and Thorstensson, A. (1994) Erector spinae lever arm length variations with changing spinal curvature. *Spine* **19**:199-204.

ENERGY COST AND SPRING-MASS MODEL IN HUMAN RUNNING

G. Dalleau, A. Belli, M.Bourdin, J.-R. Lacour
Laboratoire de Physiologie - GIP Exercice, Univ. Lyon I, France

INTRODUCTION

From a mechanical point of view, a running man has often been considered as a bouncing ball (Cavagna 1964). During the braking phase of contact, a part of mechanical energy is stored in elastic elements of leg extensor muscles. The recovery of this stored elastic energy, during the propulsive phase, minimizes the muscle energy expenditure. One can then assume that the leg behaves like a spring which supports the total body mass (McMahon 1990, Alexander 1988) (*see figure 1*). Taylor (1985) has already shown that the less energy consuming hopping frequency in man was the resonant frequency of the spring-mass system. In running, however, Cavanagh et al. (1982) observed that the free chosen step length for a given velocity was not the most economical one. Several studies have been carried out to determine the optimal step frequency which permits a subject to run with a minimal metabolic cost. But to the best of our knowledge, relationship between energy cost of running and resonant frequency has never been studied.

The purpose of this study was then to investigate whether the inter-individual energy cost variability could be inferred by the differences between the free chosen step frequency and the resonant frequency determined by the mass-spring model.

METHODS

Eight distance runners (mass 71.2 ± 5.1 kg, height 1.78 ± 0.07 m) volunteered to participate in this study. They ran on a treadmill at a velocity corresponding to 90% of their maximal aerobic velocity (5.1 ± 0.33 m.s^{-1}).

During running, the vertical position (z) and the horizontal velocity (v) of the body of the runner were monitored using a kinematic arm (Belli 1992) linked to the subject with a belt fastened around his waist. The subjects were also equipped with pressure transducer soles in order to assess their contact phase and their step frequency (F_{step}).

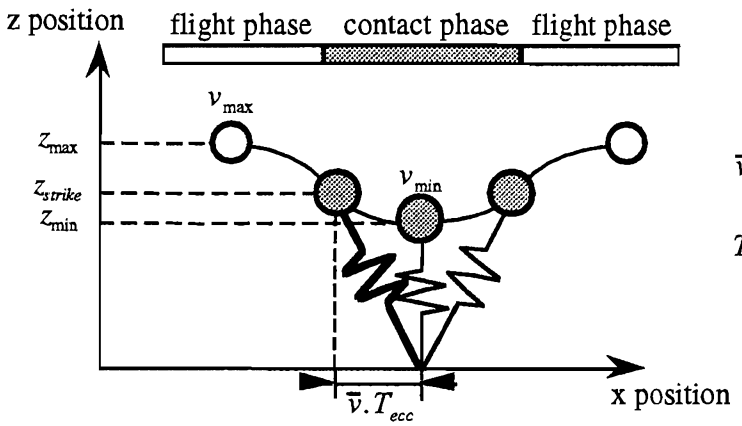

Figure 1 : *The spring-mass system bouncing forward*

Resonant frequency determination :

In such system, the resonant frequency F_R is calculated as : $F_R = \frac{1}{2\pi}\sqrt{\frac{K}{M}}$

where K is the stiffness of the spring and M is the body mass.

Knowing body displacements and assuming that during the eccentric phase the mechanical work is stored as elastic energy in the spring, the stiffness of the spring K could be calculated by the equation : $K = 2.(W_M).(\Delta r)^{-2}$

where Δr is the compression of the spring ($\Delta r = \sqrt{z_{strike}^2 + \bar{v}^2.T_{ecc}^2} - z_{min}$), W_M is the mechanical work ($W_M = 9.81 \cdot M \cdot (z_{max} - z_{min}) + 0.5 \cdot M \cdot (v_{max}^2 - v_{min}^2)$).

Energy cost of running determination : Net oxygen uptake (ml $O_2.kg^{-1}.s^{-1}$) was determined with open circuit method and was divided by the running velocity ($m.s^{-1}$) in order to calculate the energy cost of running (C_r).

RESULTS

Data analysis was focused on the strong leg, *i.e.* the leg performing the highest mechanical work. In that case, a significant relationship was obtained between relative frequency differences $\Delta F\%$ ($\Delta F\% = |F_{step} - F_R| . F_R^{-1}.100$) and C_r (figure 2), the farther the step frequency from the resonant frequency the higher the energy cost of running. C_r was inversely related to stiffness (figure 3).

These relationships were not obtained on the other leg.

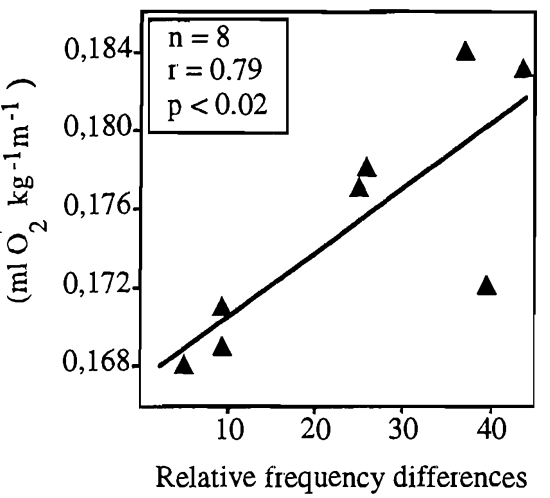

Figure 2 : *Relationship between relative frequency differences and energy cost of running*

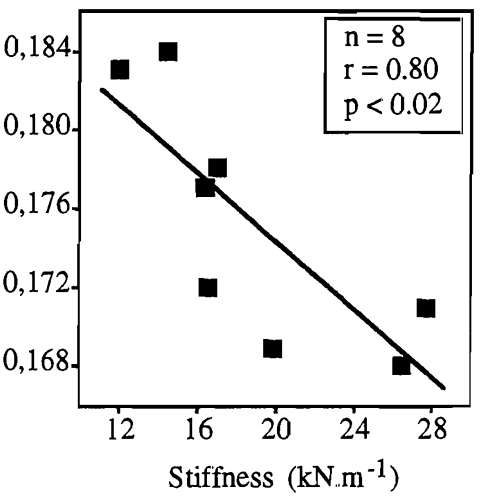

Figure 3 : *Relationship between stiffness and energy cost of running*

DISCUSSION

The relationship obtained between C_r and $\Delta F\%$ shows that the spring-mass model provides a good approach for studying the energy cost of running. Our results support the assumption that the resonant frequency is the frequency which requires the lowest energy to drive a mass spring system.

The stiffness values calculated in this study are in agreement with the data of the literature (McMahon, 1990). Assuming that a high stiffness is related to a good stretch shortening cycle utilization, the relationship between high stiffness and low C_r further support the validity of the spring-mass model.

The lack of correlation obtained on the "weak" leg could be explained by functional differences between legs (Cavanagh, 1990). Furthermore, the significant relationships obtained on the strong leg let us assume that only this leg was able to take advantage of the best utilization of stretch-shortening cycle.

REFERENCES

Alexander, R. M. (1988). In *Biomechanics XI A*, pp 17-25.

Belli A., Rey, S., Bonnefoy, R. and Lacour, J.-R. (1992). *Ergonomics* **27**, 285-287.

Cavagna, G. A., Saibene, F. P., and Margaria, R.(1964). *J. appl. Physiol.* **19**, 249-256.

Cavanagh, P. R. (1990). *Med. Sci. Sports Exerc.* **22**, 546-557.

Cavanagh, P.R., and Williams, K. R. (1982). *Med. Sci. Sports Exercise* **14**, 30-35.

McMahon, T. A. and Cheng, G. C. (1990). *J. Biomechanics* **23**, 65-78.

Taylor C.R. (1985). *J. exp. Biol.* **115**, 253-262.

SOFTWARE ENVIRONMENT FOR THE DEVELOPMENT AND TEST OF NEUROPROSTHESES TO RESTORE FREE STANCE AND STEPPING IN PARAPLEGICS

W.J. Daunicht, S. Swoboda, R. Steiner, V. Hömberg
Neurologisches Therapiecentrum,
Institut an der Heinrich-Heine-Universität Düsseldorf, Germany

INTRODUCTION

We define a neuroprosthesis as a closed loop system that is capable of restoring some body function that has been lost due to lesions of the nervous system. In the past a number of open loop systems have been designed to generate stepping movements of the legs using functional neuromuscular stimulation in order to restore locomotion with the aid of crutches. In our group we develop a closed loop control system aimed at the stabilization of stance and stepping without crutches. To assure stability and security of such a control system, a substantial part of the development has to be carried out with computer simulations. We therefore built a software model of the human body to provide an environment sufficient to develop and test such a closed loop neuroprosthesis.

MODEL

In order to deal with disturbances resulting from active movements of the upper limbs and the head, the model comprises the whole body with 17 rigid body segments and 42 degrees of freedom in 3 dimensions (Hatze 1981). As the modeling of the mechanical environment of the body is crucial, ground reaction forces occurring during movements are calculated on the basis of constraints (Steiner 1993). Then the model supports the simulation of available technical sensors, such as goniometers, accelerometers and sensors of pressure between foot and ground.

Of course, the muscle properties constitute another essential part of the closed loop; therefore we included simulations of 86 muscles of the lower limb (Fig.1).

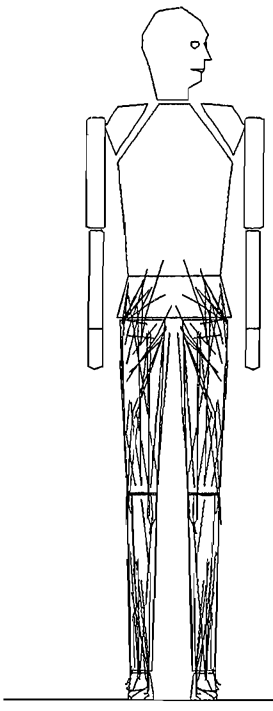

Figure 1: Scheme of simulated human body with 17 rigid body segments and 42 degrees of freedom. Paths of 86 leg muscles included in the model are shown as polygons.

The muscle model is based on a polygon approximation of the path of the muscle centroids described in segmental coordinate systems in order to calculate torques from muscle forces (Delp 1990). The forces resulting from stimulating inputs are obtained from a single-input single-output model of the muscle dynamics (Zajac 1989). The inputs of the whole model are therefore stimulation trajectories, the outputs are trajectories of generalized coordinates (mainly joint angles) as well as sensory signals.

DISCUSSION

Because of the inherent mechanical instability and the extreme complexity such a model is impossible to verify as a whole and difficult to assess. We therefore use a qualitative three-level procedure to evaluate our simulation. The first level is the animated presentation of the generalized coordinates. The animation results in 3-dimensional movies of whole body movements, e.g in the presence of gravity and closed loop control. The second level is the animation of movements resulting from open loop activation of individual muscles in the absence of gravity, thereby eliminating the need for stabilizing closed loops. Thirdly, the time functions of physical variables, such as forces, torques, angles etc. can be displayed as desired.

With these tools we can demonstrate, that the results of our simulations are qualitatively consistent with what one might expect, and validate the model on a coarse level. A precise comparison of time functions of physical variables from simulations and experiments does not seem useful, as the accumulation of errors in the identification of all the ca. 2000 model parameters seems to prevent significant results on a fine level anyway.

However, as closed loop systems are designed to compensate for parameter deviations, a model validated on a coarse level seems to be sufficient to develop and test control loops. Simulation using a model with reduced complexity, but incorporating rigid body dynamics, ground reaction forces, three types of sensors and muscle models, have been carried out (Beckmann 1992). It could be shown, that a control system can be achieved that assures stability in a wide range of postures and is insensitive to changes of up to 30% in parameters such as body mass or maximal muscle forces.

In conclusion, according to our simulation results a model of the complexity as outlined above seems to be not only necessary, but also sufficient as environment for the development of closed loop neuroprostheses in paraplegic patients.

Acknowledgements: This work was supported by DFG grant Da 199/2-2.

REFERENCES

J. Beckmann, W.J. Daunicht, and V. Hömberg. Control of a paraplegic patient model by neuroprothetic networks. In I. Aleksander and J. Taylor, editors, *Artificial neural networks*, volume II, pages 471–474. Elsevier, Amsterdam, 1992.

S.L. Delp. *Surgery simulation: A computer graphics system to analyze and design musculoskeletal reconstructions of the lower limb.* PhD thesis, Stanford University, 1990.

H. Hatze. *A comprehensive model for the human motion simulation and its application to the take-off phase of the long jump.* J. Biomech., 14:135–142, 1981.

R. Steiner and W.J. Daunicht. Spatial simulation of human body motions during collisions and contact with hard surfaces. In *I.S.B. XIVth Congress Abstr.*, volume II, 1286–1287, 1993.

F.E. Zajac. *Muscle and tendon: properties, models, scaling, and application to biomechanics and motor control.* Crit. Rev. Biomed. Eng., 17:359–411, 1989.

DEVELOPMENT OF A DEVICE TO MEASURE PLANTAR PRESSURE AND SHEAR

BL Davis and JE Perry

Department of Biomedical Engineering,
The Cleveland Clinic Foundation, Cleveland , OH

INTRODUCTION

The principle mechanical factors leading to plantar ulceration in the diabetic foot are not fully understood. Although excessively high shear or pressure has been shown to coincide with sites of ulceration (Boulton et al., 1983, Pollard and LeQuesne, 1983) there are many cases where patients develop plantar ulcers and yet do not have loading patterns that are thought to be hazardous. Davis (1993) has described three loading situations, dependent on the interaction of shear and pressure, that could potentially lead to ulceration. To date any investigation of the combined effects of shear and pressure has been hampered by the fact that no equipment has been available to simultaneously measure both shear and vertical stresses under the foot.

METHODS

We have constructed a device consisting of an array of 16 transducers that is capable of simultaneously measuring both shear and pressure under the region of the forefoot. Each transducer (Fig. 1) has two components: 1) a 9cm aluminum tube, approximately 1mm wall thickness, with 8 strain gages and 2) an S-shaped cantilever cap with 4 strain gages (2 gages placed on opposing faces of the S backbone). The surface area of each cap measures 2.5cm x 2.5cm. Shear components of stress are measured using the gages on the column while vertical forces are acquired from the cantilever. The 16 transducers are arranged in a 4 x 4 array with a 1.5mm gap between adjacent transducers. Each transducer was statically calibrated with a weight and pulley arrangement.

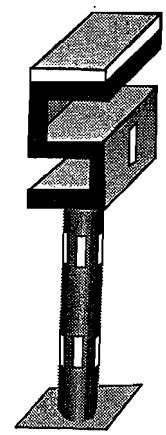

Fig 1 The transducer

Thirty-two multiplexors were used in the hardware implementation and a straight data acquisition method, using subroutines and facilities that came with the board, was employed. Although this method required extensive hardware, the software implementation was more reliable, device errors were prevented and the integrity of the data was improved relative to other techniques that were investigated. Data acquisition takes place over a period of 2 seconds at a sampling frequency of 38Hz.

RESULTS

Three ascending and three descending calibration trials were carried out for each transducer. Shear calibration was performed in the anterior-posterior (AP), medial-lateral (ML), and combined AP-ML directions along with investigating the effects of torsion and compression on shear. Compressive loading and the effects of a torsional force were also analyzed. Calibration plots for those scenarios involving possible cross-talk show good linearity, minimal hysteresis, and good agreement between applied and measured loads (Fig 2). For all 16 transducers, forces in all three directions (vertical, AP, ML) can be measured with accuracies to within 4 % of the true value.

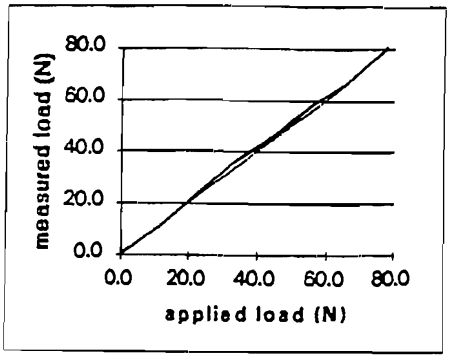

(a)

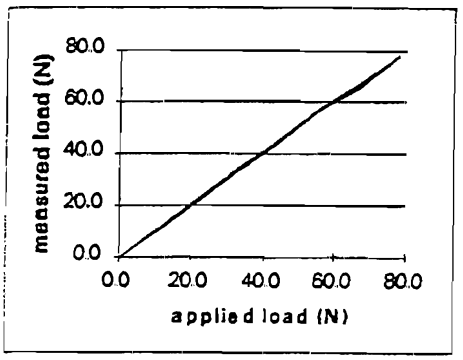

(b)

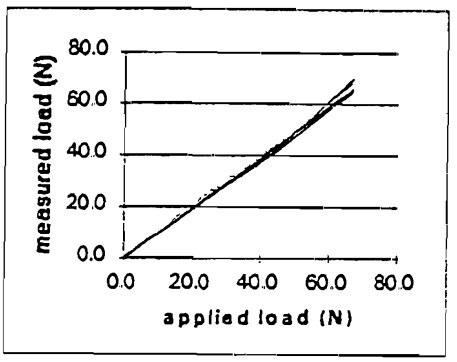

(c)

Fig. 2. Calibration plots for a representative transducer in the (a) combined ML-AP direction along with the effects of (b) torsion and (c) compression on shear measurements. Data correspond to 3 trials of loading (solid line) and 3 trials of unloading (dashed line).

DISCUSSION

With the device that has been constructed we have demonstrated, for the first time, that loading under the feet can be simultaneously measured in all three dimensions The ability to quantify loading under the foot in this manner has the potential to fill a large void in the scientific literature and to have significant clinical implications. The device has been constructed so that different materials can be capped onto each transducer, in order to examine the shear/pressure properties of materials commonly used in therapeutic footwear. One limitation of the current device is the large transducer area of 6.25cm^2. We are currently developing a larger device consisting of 96 transducers, each with a surface area one-fourth as large as the current design

REFERENCES

Boulton AJM, Hardisty CA, Betts RP, Franks CI, Worth RC, Ward JD and Duckworth T (1983) Dynamic foot pressure and other studies as diagnostic and management aids in diabetic neuropathy *Diabetes Care*, 6:26-33

Davis BL (1992) Foot ulceration: hypothesis concerning shear and vertical forces acting on adjacent regions of skin. *Medical Hypothesis*, 40:44-47

Pollard JP and LeQuesne LP (1983) Method of healing diabetic forefoot ulcers. *Brit. Med. J.*, 286:436-437

ACKNOWLEDGEMENTS

Funding provided by NIH-NIAMS and Thorlo, Inc.